Universitat Autònoma de Barcelona

Departament de Genètica i Microbiologia
Facultat de Biociències

MICROBIAL FUEL CELL PERFORMANCE:
DESIGN, OPERATION AND BIOLOGICAL FACTORS

Naroa Uría Moltó
2012

Universitat Autònoma de Barcelona

Departament de Genètica i Microbiologia
Facultat de Biociències

MICROBIAL FUEL CELL PERFORMANCE:
DESIGN, OPERATION AND BIOLOGICAL FACTORS

Tesis Doctoral presentada por Naroa Uría Moltó para optar al Grado de Doctor en Microbiología por la *Universitat Autònoma de Barcelona*.

Con el visto bueno del director de la Tesis Doctoral,

Dr. Jordi Mas Gordi

A mis padres y Xavi

Dig that hole, forget the sun
And when at last the work is done
Don't sit down
It's time to dig another one

(*Pink Floyd*, *"Breathe"*)

CONTENTS

ABBREVIATIONS AND UNITS

ABBREVIATIONS

Symbol	Meaning
ACNQ	2-amino-3-carboxy-1,4-naphtoquinone
AEM	Anion Exchange Membrane
Ag/AgCl	Silver/Silver Chloride Electrode
BES	Bioelectrochemical System
BOD	Biological Oxygen Demand
BPM	Bipolar Membrane
CH_4	Methane
CLSM	Confocal Laser Scanning Microscopy
Co	Coenzyme
CO	Carbon monoxide
CO_2	Carbon dioxide
CoTMPP	Cobalttetramethoxyphenylporphyn
DAPI	4´-6´-diamidino-2-phenylindole
DET	Direct Electron Transfer
DGGE	Denaturing Gradient Gel Electrophoresis
D_{si}	Simpson Index
E^o	Potential
E_{KA}	Half-saturation potential
EDTA	Ethylenediaminetetraacetic acid
EET	Extracellular Electron Transfer
E_p	Peak potential
Fe	Iron

Symbol	Meaning
$Fe(CN)_6$	Ferricyanide
FMN	Flavin mononucleotide
H_2	Hydrogen
H_4MPT	Tetrahydromethanopterine
I	Intensity
IV (curve)	Intensity Voltage curve, Polarization curve
KNO_3	Potassium nitrate
MEC	Microbial Electrolysis Cell
MFC	Microbial Fuel Cell
MCD	Maximum Current Density
MPD	Maximum Power Density
NaCl	Sodium Chloride
OCT	Open Circuit Time
OCV	Open Circuit Potential
OD	Optical Density
P	Power
PBS	Phosphate Buffer Saline
PEM	Proton Exchange Membrane
PQQ	Pyrroloquinoline quinone
Pt	Platinum
Pyr-FePc	Pyrolysed iron(II) phthalocyanine
R_{ext}	External Resistance
RVC	Reticulated Vitreous Carbon
SEM	Scanning Electron Microscopy
SHE	Standard Hydrogen Electrode
Soln	Solution
THF	Tetrahydrofolate
TSB	Trypticase Soy Broth

Symbol	Meaning
V_{cell}	Cell Voltage
vs.	Versus
υ	Scan rate
wt	Weight

UNITS

Symbol	Meaning
A	Amperes
Å	Angstroms
$A \cdot m^{-2}$	Amperes per square meter
C	Coulombs
ºC	Degree Celsius
$cells \cdot mL^{-1}$	Cells per milliliter
cm	Centimeters
cm^2	Square centimeters
g	Relative centrifugal force
g	Grams
h	Hours
L	Liters
M	Molar concentration
mA	MilliAmperes
$mA \cdot cm^{-2}$	MilliAmperes per square centimeter
mg	Milligrams
min	Minutes

Symbol	Meaning
mL	Milliliters
mm	Millimeter
mM	MilliMolar
mol·e^{-}	Electron mols
mV	MilliVolts
mV·s^{-1}	MilliVolts per second
ng	Nanograms
nm	Nanometers
rpm	Revolutions per minute
s	Seconds
cfu	Colony forming units
cfu·mL^{-1}	Colony forming units per milliliter
V	Volts
W	Watts
µA	MicroAmpere
µA·cm^{-2}	MicroAmpere per square centimeter
µg·mL^{-1}	Micrograms per milliliter
µm	Micrometers
µM	MicroMolar
µL	MicroLiter
µW	MicroWatts
µW·cm^{-2}	MicroWatts per square centimeter
Ω	Ohms
KΩ	KiloOhms

Summary / Resum / Laburpena / Resumen

SUMMARY

A Microbial Fuel Cell (MFC) is a bioelectrochemical system, in which bacteria oxidize organic matter and transfer the electrons through their electron transport chains onto an electrode surface producing electricity. The efficiency of the system depends on the metabolic activity of the microorganisms growing at the anode but also on a large number of factors related to the design and operation of the MFC. The purpose of this work is to contribute to the analysis and control of some of these factors as well as to throw some light on the role of different electron transfer mechanisms in MFC operation. To achieve this goal different experiments using the electrogenic bacterium *Shewanella oneidensis* MR-1 have been carried out.

First of all, this works analyses the role of several design factors in MFC performance. This part of the research focuses on the effect of different abiotic catalysts (Fe-based soluble catalysts and platinum-based surface catalysts) as well as the cathode to anode ratio required for unhindered power output. The results indicate that soluble catalysts such as ferricyanide operating with carbon cathodes allow much higher power values, and therefore need smaller cathode/anode ratios than platinum-based cathodes. In the long term, however, MFCs containing soluble iron catalysts show a progressive degradation of fuel cell performance make them unfit for applications requiring extended operations. In recent years, the search for a suitable catalyst at the cathode has led researchers to explore the possible use of biocathodes. In this work, we demonstrate the capacity of *Shewanella oneidensis* MR-1 to catalyse the cathode reaction both under aerobic and anaerobic conditions, being able to sustain the current provided by bacteria present in the anode. *Shewanella oneidensis* MR-1 biocathodes show the best performance when oxygen is used as the electron acceptor, with results clearly comparable to those obtained with platinum cathodes indicating the efficiency of this bacterium in the catalysis of oxygen reduction.

The potential of anode bacteria for current production does not only depend on the levels of microbial activity and on the removal of cathodic limitations but seems to be also affected by factors related to the operation of the system as it has been observed with the anode potential or the external resistance. In addition to these, we have shown the importance of continuous MFC

operation as another important factor to take into account for some applications. Periods of circuit interruption produce an alteration of the normal current output in the form of defined current peaks that appear when closing the circuit after a short period of current interruption and that decay slowly back to the original stable values. In depth analysis of this response demonstrates the capacity of *Shewanella oneidensis* MR-1 to store charge when no electron acceptors are present.

Finally, a series of experiments were designed using different anode coatings to help determine the contribution of the different electron transfer mechanisms to current production in MFCs harbouring complex microbial communities. The MFC with a naked anode shows that direct electron transfer mechanisms are responsible for most of the current generated. The microbial community formed agrees with the electron transfer pathways available. So, this MFC presents species able of direct and mediated electron transfer as *Shewanella, Aeromonas, Pseudomonas* or *Propionibacterium*. The MFC sustained by shuttle-dependent electron transfer follows in importance being responsible for as much as 40% of current output. This reactor shows a great quantity of different redox species in the anolyte bulk, some of them not related to mediators currently described in the literature. Finally, in the MFC with a nafion-coated anode, the only chemical species able to diffuse to the anode surface is hydrogen. In this case, current production is sustained by the interaction between some organisms, such as *Comamonas, Alicycliphilus, Diaphorobacter* or the archaea *Methanosaeta* and the anode. Oxidation of acetate by these microorganisms results in hydrogen production that is therefore oxidised at the anode surface after crossing the nafion barrier. Current production by this mechanism would account for not more than 5% of the total current evolved in an unrestricted MFC.

RESUM

Una pila microbiana de combustible és un sistema bioelectroquímic en el qual els bacteris oxiden matèria orgànica transfereixen els electrons a través de la seva cadena respiratòria cap a la superfície d'un elèctrode produint electricitat. L'eficiència d'aquest sistema depèn de la seva activitat metabòlica dels microorganismes de l'ànode, però també d'un gran nombre de factors relacionats amb el disseny i l'operació de la pila microbiana. L'objectiu d'aquesta tesi és contribuir a l'anàlisi i control d'alguns d'aquests factors, així com a ajudar a determinar el paper dels diferents mecanismes de transferència d'electrons en el funcionament d'una pila microbiana. Per a assolir aquest objectiu s'han dut a terme diferents experiments mitjançant l'ús del bacteri electrogènic *Shewanella oneidensis* MR-1.

En primer lloc, aquest treball analitza el efecte en el rendiment de una pila microbiana de diversos factors relacionats amb el disseny. Aquesta part del estudi es centra en el efecte de diferents catalitzadors abiòtics (catalitzadors solubles amb ferro catalitzadors de superfície amb platí) així com també la relació entre les àrees del càtode i ànode que es necessiten per a què no estigui afectat la potència. Els resultats revelen que els catalitzadors solubles com el ferricianur permeten l'obtenció de potències molt més grans, i per tant, necessiten una menor relació entre les àrees de càtode i ànode que en el cas de les piles que fan servir càtodes de platí. No obstant això, a llarg termini, les piles que contenen catalitzadors solubles de ferro mostren una degradació progressiva del rendiment de la cel·la de combustible que les fa poc adequades per a aplicacions que requereixen operacions de llarga durada. Recentment, en la cerca de catalitzadors adequats per al seu ús en el càtode ha dirigit als investigadors a explorar el possible ús de biocàtodes. En aquesta tesi es demostra la capacitat de *Shewanella oneidensis* MR-1 per a catalitzar la reacció del càtode tant en condicions aeròbiques com anaeròbiques, sent capaç de mantenir el corrent proporcionat per les bactèries presents a l'ànode. Els biocàtodes formats per *Shewanella oneidensis* MR-1 mostren un millor rendiment quan es fa servir oxigen com a acceptor d'electrons, amb resultats comparables als obtinguts amb càtodes de platí, cosa que indica l'eficiència d'aquest bacteri per a catalitzar la reducció de l'oxigen.

El potencial dels bacteris que es troben a l'ànode per a la producció de corrent no només depèn dels nivells d'activitat microbiana ni de la supressió de les limitacions de la reacció del càtode, sinó que sembla que està afectada també per factors relacionats amb el funcionament del sistema com s'ha observat amb el potencial de l'ànode o la resistència externa. A més d'aquests factors, nosaltres mostrem l' importància d'una operació ininterrompuda en una pila microbiana com un altre factor rellevant per a algunes aplicacions. Períodes d'interrupció del circuit produeixen una alteració en els valors de corrent en forma de pics definits, que apareixen quan el circuit és tancat després d'un període d'interrupció i que cauen lentament fins a arribar valors normals de corrent. Mitjançant anàlisis més exhaustius d'aquest fenomen es demostra la capacitat de *Shewanella oneidensis* MR-1 per a emmagatzemar càrrega elèctrica en absència d'acceptors d'electrons.

Finalment, es van dissenyar una sèrie d'experiments cobrint els ànodes de diferents formes. Així, s´ajuda a determinar la contribució en la producció de corrent dels diferents mecanismes de transferència d'electrons en piles amb comunitats microbianes complexes. La pila amb l'ànode descobert mostra que els mecanismes de transferència directa són responsables de la major part del corrent generat. La comunitat microbiana formada es troba relacionada amb la via de transferència d'electrons disponible. D'aquesta manera, aquesta pila presenta espècies microbianes capaces de transferir electrons tant de forma directa com mitjançant mediadors com ara *Shewanella, Aeromonas, Pseudomonas* o *Propionibacterium*. Els mecanismes de transferència mitjançant mediadors el segueixen en importància, sent els responsables del 40% del corrent produït. Aquesta pila amb el corrent dependent de la producció de mediadors mostra una gran quantitat d'espècies redox en l´anolit, algunes d'elles no relacionades amb mediadors ja descrits. Finalment, a la pila amb l'elèctrode cobert de nafion l'única espècie química capaç d'arribar a la superfície de l'ànode és l'hidrogen. En aquest cas, la producció de corrent es manté gràcies a la relació entre alguns organismes com *Comamonas, Alicycliphilus, Diaphorobacter* o la archaea *Methanosaeta* i l'ànode. L´oxidació d´acetat per aquests microorganismes produeix hidrogen que s´oxida en l'ànode després de creuar el nafion. El corrent generat mitjançant aquest mecanisme no suposa més del 5% del total del corrent generat en una pila sense restriccions.

LABURPENA

"Microbial Fuel Cell (MFC)" bat sistema bioelektokimiko da non bakteriek materia organikoa oxiditzen duten eta beren arnas katearen bidez elektrodo batera elektroiak trasmititzen dituzten, elektrizitatea sortuz. Sistema honen eraginkortasuna anodoan hazten diren mikroorganismoen aktibitate metabolikoaren menpe dago, baina MFC-en diseinuak eta funtzionamenduak zerikusia dute ere. Tesi honen helburua da faktore horietako batzuk analisia eta kontrola laguntzea. Gainera MFC baten funtzinamenduan, elektroien transferentzia mekanismo desberdinek duten funtzioa zehaztu nahi izan dugu. Helburu hori lortzeko esperimentu desberdinak egin dira *Shewanella oneidensis* MR-1 bakteria electrogenikoa erabiliz.

Lehenik eta behin, MFC baten errendimenduan diseinuarekin lotutako hainbat faktoreren papera aztertzen du lan honek. Ikerketaren zati hau, katalizadore abiotiko desberdinetan (burdinez katalizatzaile disolbagarriak eta platinozko katalizatzaileak) eta baita, lortutako potentzia kaltetuta ez dadin, katodo eta anodo arlo arteko harremanean ere oinarritzen da. Emaitzek erakusten dutenez katalizatzaile disolbagarriek, ferricyanide adibidez, potentziak askoz handiagoak lortzen dituzte eta, horregatik, platinozko katodoekin pilek baino erlazio txikiagoa izan behar dute anodo eta katodoen artean. Hala ere, epe luzera, burdina katalizatzaile disolbagarriak dituzten pilek erreginaren errendimenduan beherapena pairatzen dute eta horregatik ez dira aproposenak iraupen handiko lanetarako . Berriki, katodoarentzako katalizatzaile egokien bilaketan, ikertzaileek biokatodoen erabilpena aztertu dute. Bai kondizio aerobikoetan bai kondizio anaerobikoetan katodoaren erreakzioa katalizatzeko *Shewanella oneidensis* MR-1-en kapazitatea erakusten da tesi honetan. *Shewanella oneidensis* MR -1 biokatodoek errendimendu hobe erakusten dute oxigenoa elektroi hartzaile bezala erabiltzean. Emaitza hauek platinozko katodoekin lortutakoak alderagarriak dira, eta bakteria honen oxigenoaren murrizketa katalizatzeko eraginkortasuna islatzen dute.
Anodoan dauden bakterien kapazitatea korronte sortzeko ez dago bakarrik mikrobioen aktibitate mailaren eta katodoaren erreakzioaren menpe, baizik eta sistemako funtzionamenduarekin erlazionatuta dauden faktoreak ere eragina dute. Hau anodoaren potentzialarekin edo kanpoko erresistentziarekin ikusten da jada. Faktore hauetaz gain, MFC-en eragiketa etengabearen

garrantzia erakusten dugu. Zirkuitu etenaldi epeek korrente baloreetan aldaketak ekoizten dituzte. Aldaketa hauek agertzen dira zirkuitua ixten dugunean etenaldi epe baten ondoren eta motel erortzen dira korrente balore arruntak lortu arte. Fenomeno honen azterketa sakonaren bidez, *Shewanella oneidensis* MR-1-en gaitasuna karga elektrikoa gordetzeko erakusten da elektroi hartzailerik ez dagoenean.

Azkenik, korrente ekoizpenean elektroi transferentzi mekanismo desberdinen eragina zehazteko, esperimentu batzuk diseinatu egin ziren anodoak estaliz era desberdinak erabiltzen mikrobioen komunitate konplexuekin MFC-an. Anodo estalgabetua duen pilak zuzeneko transferentzia mekanismoak korrente gehienaren arduradunak direla islatzen du. Sortutako mibrobioen komunitatea elektroi transferentzia bidearekin harremanetan dago. Honela, pila honek zuzen eta bitartekoen bidez elektroi trasmititzeko gaitasuna duten microbioen espezieak aurkezten ditu, besteak beste, *Shewanella, Aeromonas, Pseudomonas* edo *Propionibacterium*. Elektroi transferitzeko mekanismoak bitartekoen bidez garrantziaz hurrengoak dira korrontearen % 40a sortzen baitituzte. Pila honek, korrontea bitartekoen menpe dagoena, redox espezie asko erakusten ditu anolitoan. Gainera, horietako batzuek ez daukate zerikusirik literaturan aipatutako bitartekeriekin. Azkenik, nafion estalita elektrodoa daukan MFC-an hidrogenoa espezie kimiko bakarra anodora iristeko gai izan da. Kasu honetan, korronte produkzioa sortzen da organismo batzuen (*Comamonas, Alicycliphilus, Diaphorobacter* edo archaea *Methanosaeta*) eta anodoren arteko harreman bati esker. Organismo hauek azetatoa oxidatzen dute, eta hidrogenoa ekoizten dute. Geroztik, hidrogenoa oxidatzen da anodoan nafion gurutzatu ondoren. Hidrogenoaren bidez korrontea bakarrik murrizte gabe MFC-aren korrontearen %5 izan da.

RESUMEN

Una pila microbiana de combustible es un sistema bioelectroquímico en el cual las bacterias oxidan materia orgánica y transfieren los electrones a través de su cadena respiratoria a un electrodo produciendo electricidad. La eficiencia de este sistema depende de la actividad metabólica de los microorganismos creciendo en el ánodo, pero también de un gran número de factores relacionados con el diseño y la operación de la pila microbiana. El objetivo de esta tesis es contribuir al análisis y control de algunos de estos factores, así como ayudar a determinar el papel de los diferentes mecanismos de transferencia de electrones en el funcionamiento de estos dispositivos. Para conseguir este objetivo se han llevado a cabo diferentes experimentos usando la bacteria electrogénica *Shewanella oneidensis* MR-1.

En primer lugar, este trabajo analiza el papel de varios factores relacionados con el diseño en el rendimiento de una pila microbiana. Esta parte del estudio se centra en el efecto de diferentes catalizadores abióticos (catalizadores solubles con hierro y catalizadores de superficie con platino) así como en la relación entre las áreas del cátodo y ánodo necesarias para que no se vea afectada la potencia obtenida. Los resultados revelan que catalizadores solubles como el ferricianuro permiten potencias mucho mayores, y por tanto necesitan una menor relación entre las áreas de cátodo y ánodo que en el caso de las pilas con cátodos de platino. No obstante, a largo plazo, las pilas con catalizadores solubles de hierro muestran un descenso progresivo del rendimiento de la celda de combustible que las hace poco adecuadas para aplicaciones que requieren operaciones de larga duración. Recientemente, la búsqueda de catalizadores adecuados para el cátodo ha llevado a los investigadores a explorar el posible uso de biocátodos. En esta tesis se demuestra la capacidad de *Shewanella oneidensis* MR-1 para catalizar la reacción del cátodo tanto en condiciones aeróbicas como anaeróbicas, siendo capaz de aceptar la corriente proporcionada por las bacterias presentes en el ánodo. Los biocátodos formados por *Shewanella oneidensis* MR-1 muestran un mejor rendimiento cuando se usa oxígeno como aceptor de electrones, con resultados comparables a los obtenidos con cátodos de platino, lo que indica la eficiencia de esta bacteria para catalizar la reducción del oxígeno.

El potencial de las bacterias que se encuentran en el ánodo para la producción de corriente no sólo depende de los niveles de actividad microbiana y de la supresión de las limitaciones de la reacción del cátodo, sino que es afectada también por factores relacionados con el funcionamiento del sistema como el potencial del ánodo o la resistencia externa. Además de estos factores, nosotros mostramos la importancia de una operación ininterrumpida como otro factor relevante para determinadas aplicaciones. Periodos de interrupción del circuito producen una alteración en los valores de corriente en forma de picos, que aparecen cuando el circuito es cerrado tras un periodo de interrupción y que caen lentamente hasta alcanzar valores normales de corriente. Mediante análisis más exhaustivos de este fenómeno se demuestra la capacidad de *Shewanella oneidensis* MR-1 para almacenar carga eléctrica en ausencia de aceptores de electrones.

Finalmente, se diseñaron una serie de experimentos cubriendo los ánodos de diferentes maneras para ayudar a determinar la contribución en la producción de corriente de los diferentes mecanismos de transferencia de electrones en pilas con comunidades microbianas complejas. La pila con el ánodo descubierto muestra que los mecanismos de transferencia directa son responsables de la mayor parte de la corriente generada. La comunidad microbiana formada se encuentra relacionada con la vía de transferencia de electrones disponible. De esta manera, esta pila presenta especies microbianas capaces de transferir electrones tanto de forma directa como mediante mediadores como por ejemplo *Shewanella, Aeromonas, Pseudomonas* o *Propionibacterium.* Los mecanismos de transferencia mediante mediadores le siguen en importancia, siendo los responsables del 40% de la corriente producida. Esta pila cuya corriente depende de la producción de mediadores muestra una gran cantidad de especies redox en el anolito, algunas de ellas no relacionadas con mediadores ya descritos. Por último, en la pila con el electrodo cubierto de nafion, la única especie química capaz de llegar a la superficie del ánodo es el hidrógeno. En este caso, la producción de corriente es sostenida gracias a la relación entre algunos organismos como *Comamonas, Alicycliphilus, Diaphorobacter* o la archaea *Methanosaeta* y el ánodo. La oxidación de acetato mediante estos microorganismos resulta en la producción de hidrógeno, el cual es oxidado en la superficie del ánodo tras cruzar el nafion. La producción de corriente mediante este mecanismo no supone más del 5% de la corriente producida mediante una pila sin restricciones.

General Introduction

GENERAL INTRODUCTION

THE MICROBIAL FUEL CELL (MFC) CONCEPT

In 1911, Potter demonstrates for first time the capacity of microbial cultures to transfer reducing equivalents from reduced organic compounds to an electrode therefore, producing electricity [1,2]. However until 1960, this microbial capacity was not incorporated into a fuel cell design and the first Microbial Fuel Cell (MFC) emerged [3,4]. Since then, Microbial Fuel Cell term has been used to refer to a large number of systems that produce electricity using microorganisms [5,6].

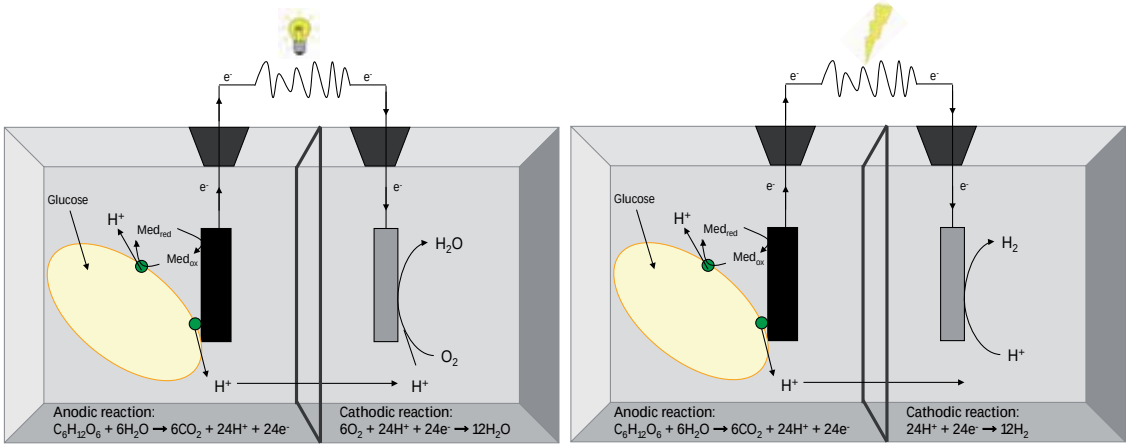

Figure 1. Microbial Fuel Cell (A) and Microbial Electrolysis Cell (MEC) (B) diagrams.

A MFC can be defined as a system in which microorganisms function as catalysts to convert chemical energy into electrical energy. Conceptually, a MFC often consist of two compartments, the anode and the cathode chambers separated by a proton exchange membrane (PEM). Microbes in the anode chamber oxidize reduced substrates and generate electrons and protons in the process. Unlike in an aerobic metabolism, the electrons are absorbed by the anode, acting as an artificial electron acceptor, and are transported to the cathode through an external circuit. After

crossing the PEM, the protons enter the cathode chamber where they combine with oxygen to form water (Figure 1A). Electric current generation is made possible by keeping microbes separated from oxygen or any other terminal electron acceptor other than the anode and this requires an anaerobic anodic chamber [7].

More recently, it has been demonstrated that, adding power to the system, hydrogen can be produced at the cathode. In this case, the system is called Microbial Electrolysis Cell (MEC) (Figure 1B). So, MFCs and MECs are grouped together as Bioelectrochemical Systems (BES) referring to an electrochemical system in which whole cell biocatalysts perform oxidation and/or reduction at electrodes [8,9].

MICROBIOLOGICAL ASPECTS

For a better understanding that how bacteria are able to produce electricity is necessary to know how bacteria capture and process energy. Bacteria oxidize substrates and electrons are transferred to respiratory enzymes by NADH (reduced form of nicotinamida adenine dinucleotide). These electrons flow down a respiratory chain moving protons across an internal membrane. The protons flow back into the cell through the enzyme ATPase creating ATP. The electrons are finally released to a soluble terminal electron acceptor. If electrons exit the respiratory chain at some reduction potential less than this of the oxygen then bacteria obtain less energy (Figure 2) [10].

Often soluble electron acceptors are depleted in the microbial environment, thus microorganisms turn to fermentation or use non-soluble electron acceptors transferring electrons outside the cell to a solid acceptor [11]. The capacity of microorganisms to produce electricity has been related to this ability to transfer electrons onto natural extracellular electron acceptors. This process is called extracellular electron transfer (EET) [9], and the microorganisms able to carry it out are exoelectrogens [5]. Extracellular electron transfer has been studied in microorganisms able to respire insoluble metals, as Fe(III) and Mn(IV), or humic substances too large to enter the cells

[8,12]. The difference between microbial electricity production and natural biogeochemical processes, such as Fe(III) reduction, is that electrons are transferred to an electrode rather than a natural electron acceptor [13].

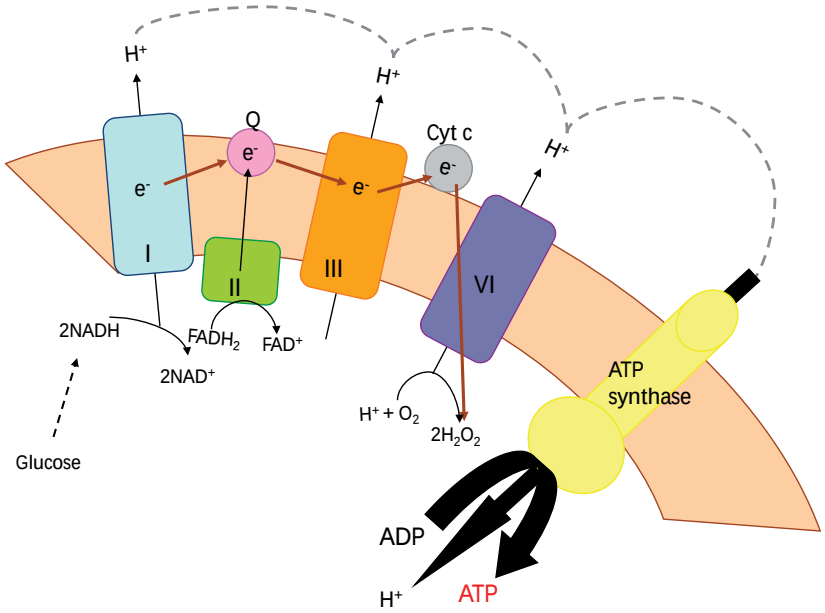

Figure 2. Electron transport chain. I. NADH dehydrogenase, II. Succinate dehydrogenase, III.Cytochrome reductase, IV. Cytochrome oxidase.

Electricigens

The term electricigen is used to distinguish those microorganisms capable of obtaining energy for growth from electron transfer to the anode, from other bacteria associated with the electrodes but not contributing to electricity production [13].

Our knowledge about the diversity of bacteria capable of exoelectrogenic activity is steadily increasing. A diverse range of microorganisms has been found in association with electrodes in MFC systems, especially when an environmental inoculum is used [14,15,16]. A large number of publications have characterized the microbial communities developed in MFCs operating with different inoculum, substrates or operation modes such as different external resistance, electrode potential or hydraulic retention time [17,18,19,20,21]. So, community analysis performed on electrochemically active biofilm growing in MFCs suggests a far greater diversity of electricigens that was previously suspected [5,16].

Electron transfer mechanisms

Electricigens has been described to be able to extracellular electron transfer by different mechanisms (Figure 3). These processes are not mutually exclusive and microorganisms may be capable of using several mechanisms simultaneously.

Indirect electron transfer by reduced metabolic products

A fermentative microorganism converts glucose to reduced metabolic products such as, alcohols, acids, or even hydrogen, which can be abiotically oxidized at the anode producing electrons and protons. However, these systems are not efficient for electricity production since only part of the electrons available in the organic fuel are recovered as electricity, thus results in the accumulation of organic products in the anode chamber [13]. Several organisms, which have been reported to generate current through this mechanism, are among other *Clostridium, Alcaligenes* or *Enterococcus* [21,22,23].

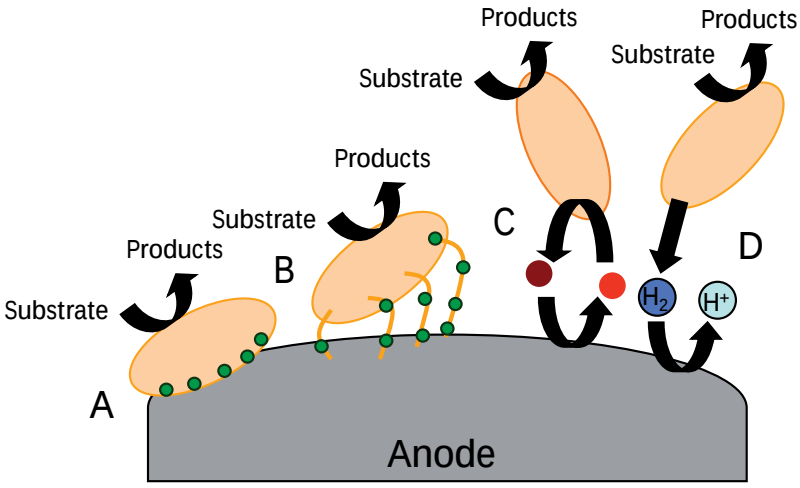

Figure 3. Electron transfer mechanisms. Direct electron transfer by membrane bound proteins (A) and nanowires (B). Mediated electron transfer by electron shuttles (C) and fermentation end products (D).

Mediated electron transfer (MET)

Mediators or electron shuttles are soluble molecules, which can be reversibly oxidized and reduced. Artificial mediators, such as thionine, benzylviologen, 2,6-dichlorophenol, 2-hydroxy-1,4-naphthoquinone and various phenazines, iron chelates and neutral red, offer the possibility for microorganisms to generate reduced products that are more electrochemically active than most fermentation products. These mediators can accept electrons from cellular electron carriers and then, transfer these electrons to the electrode [13]. However, they are usually considered as pollutants and cannot be considered for large scale or environmental applications. Artificial mediators are important in MFCs that use microorganisms such as *Escherichia coli*, *Proteus* and *Bacillus* [24,25,26].

In some cases, electricigens might produce their own mediators to promote extracellular electron transfer. Additionally, these electron shuttles can be used for other bacteria different from the producers [22]. This mechanism has the advantage of not requiring direct contact with the

electrode enabling long-range electrical interaction between the microorganisms and the electrode. Since the synthesis of electron shuttles is a process energetically expensive for the microorganism, microbial mediators must be recycled many times in order to recover the energy invested [13] and, therefore, their occurrence is usually limited to systems with low diffusivity.

In some studies, the production of electron shuttles by bacteria is the only mechanism explaining to current production, although few redox mediators have been identified with certainty [27]. The production of mediators by bacteria was firstly proposed in *Shewanella oneidensis* [28]. First, it was proposed that quinones mediated extracellular electron transfer [27,28], however flavins have been recently identified as the main endogenous redox shuttles in this bacterium [29,30]. Other microorganisms with capacity for electron shuttle production have been reported. For example *Pseudomonas* produces phenazines. Among them, phenazine-1-carboxamide (PCN) and pyocyanin enable extracellular electron transfer to the electrode [31]. Beside these bacteria, *Geothrix fermentans* and *Propionibacterium freudenreichii* has been observed to secrete quinones and 1,4-dihydroxy-2-naphthoic acid respectively [32,33], while *Lactobacillus plantarum, Streptococcus lactis* and *Erwinia dissolvens* have been found to produce ferric quelate compounds [34].

Direct electron transfer to electrodes (DET)

Direct electron transfer requires the physical contact between the cell and the anode. This mechanism can involve membrane-bound electron carriers and conductive appendages called “nanowires” [5].

Membrane-associated electron transfer is carried out by components of the respiratory chain [22]. It has been demonstrated that redox active proteins, such as *c*-type cytochromes and iron-sulphur proteins, are localized at the outer-membrane and can act as direct conduits for electron flow to solid-phase electron acceptors [35]. Bacteria known to develop this electron transfer mechanism are *Geobacter* spp. [36], *Aeromonas hydrophila* [37], *Rhodoferax ferrireducens* [38], *Shewanella* spp. [39] and *Desulfobulbus propionicus* [40].

Multihaem *c*-type cytochromes are the major electron carrier proteins used by *Geobacter sulfurreducens* and *Shewanella oneidensis*. These bacteria are the best known electricigen bacteria in BES studies, since sequencing of their genomes has allowed an in depth genomic analyses. The findings show that both species can employ similar strategies indicating that the combination of cytochromes and conductive nanowires is a general strategy for extracellular electron transfer toward Fe(III)-oxides [8].

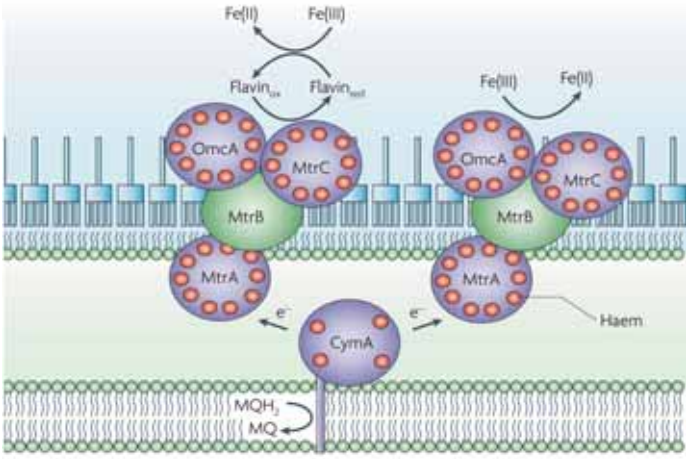

Figure 4. Representation of the multiheme *c*-type cytochromes involved in *Shewanella oneidensis* MR-1 EET (Image extracted from ref. 46).

Forty-two genes have been identified encoding *c*-type cytochromes in *Shewanella* genome, fourteen of which contained four or more hemes [41], thus heme-centered proteins play a critical role in *Shewanella* EET mechanisms. Initial genetic analyses suggested that EET was facilited by a specific cytochrome, *Cym*A that moves electrons from the quinone pool to other decaheme *c*-type cytochromes (*Mtr*C and *Omc*A) [27,41,42]. More recent analyses with knockout mutants have shown additional proteins that are involved in electron transfer to an electrode including the

previously mentioned *Cym*A, *Mtr*C and *Omc*A with *Mtr*A, *Mtr*B and *Gsp*G [43]. It is proposed that *Mtr*A, *Mtr*B and *Mtr*C form a complex in which *Mtr*C is an extracellular element that mediates extracellular electron transfer; *Mtr*B is a trans outer membrane β-barrel protein that serves as a sheath within which *Mtr*A and *Mtr*C exchange electrons [44]. Transport of these cytochromes to their extracellular location seems to require the action of protein *Gsp*G, typical of type II secretion systems [45] (Figure 4).

In the case of *Geobacter sulfurreducens,* with over one hundred *c*-type cytochromes coded in its genome, a high expression of the outer membrane *Omc*S and *Omc*E has been observed when growing on an electrode. Experimental deletion of these genes has been observed to greatly decrease current production [47,48]. These results suggested that *Omc*S and *Omc*E are involved in electron transfer to solid acceptors. Later works reported that *Omc*B and a multicopper protein, *Omp*B, were also outer-membrane surface proteins that functioned as terminal reductases for iron (III)-oxides [49,50] (Figure 5).

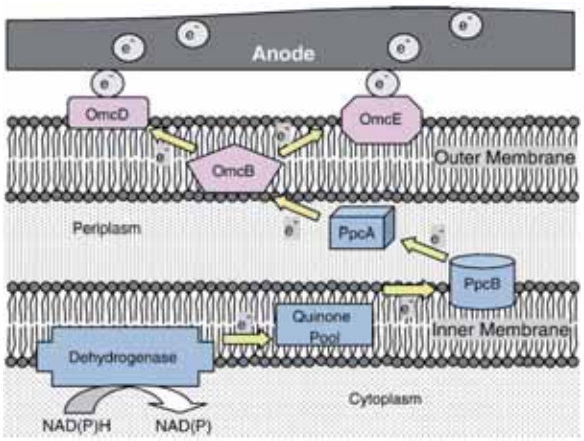

Figure 5. Components of electron transport chain proposed to the electron transport from *Geobacter* to the anode (Image extracted from ref. 7).

Although it is undeniable that cytochromes play an essential role in electron transfer to solid acceptors, the pathways for electron transport from the inner membrane to the outer-membrane remain undefined both in *Shewanella* and *Geobacter* [27]. Additionally, electron transfer via *c*-type cytochromes is not the only mechanism developed by these bacteria for direct electron transfer.

Gorby and co-workers reported the production of appendages by *Geobacter* and *Shewanella* species, which were termed "nanowires" [51]. Nanowires are pili or pilus-like structures, which are conductive due to the presence of decaheme surface proteins normally involved in iron reduction [52]. They allow electron transfer across the multilayer biofilms on anodes putting in contact the anode and the cells or the cells with other [53]. So, cell-to-cell electron transfer by forming a pilus network has been reported to transfer electrons through about 50 μm of anode biofilm (Figure 6) [54,55].

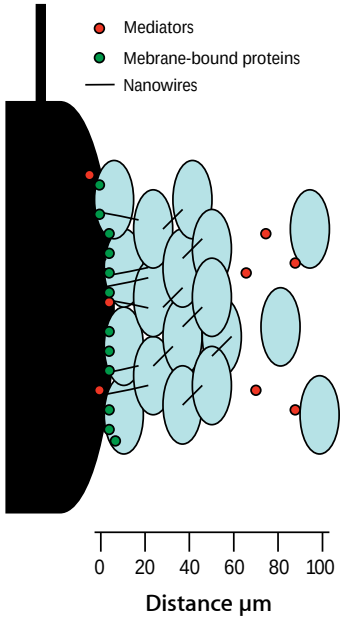

Figure 6. Working range of different direct and indirect electron transfer mechanisms in an anode biofilm supposing 100 μm of thickness (Image adapted from ref. 55).

The nanowires mediated electron transfer proposed for *Geobacter sulfurreducens* seems to have slightly different characteristics in *Shewanella oneidensis* [56]. Although filamentous structures observed in *Shewanella* have been suggested to be nanowires, they have a diameter of about 100 nm, much wider than the pili present in *Geobacter* with 3-5 nm diameter. So, while *Geobacter* appendages seem to be single strands, those of *Shewanella* might be formed by bundles of conductive wires bound together [52,57]. Mutation studies have also demonstrated the role of these appendages in electron transfer, showing that deletion of *pil*A (*Geobacter sulfurreducens*) and *pil*S (*Shewanella oneidensis*), involved in pili development, reduces the power output obtained in MFCs [44,48].

Methods for the study of electron transfer mechanisms

Electrochemists use various voltammetric techniques to characterize electrochemical reactions at the electrode surface. Some of these have been adapted to characterize electrogenic bacteria. These include cyclic voltammetry, low-scan cyclic voltammetry, differential pulse voltammetry and chronoamperometry [58,59].

The most commonly used is cyclic voltammetry, which allows the study and characterization of both direct and indirect electron transfer interactions between microorganisms and anodes [59,60,61,62,63], as well as to determine the redox potentials of the species involved [59]. So, voltammetries have been employed to interpret the anodic electron transfer process at different stages of microbial growth and metabolic activity [58].

Cyclic voltammetry consists basically in the study of current as a function of applied potential. So, the electrode potential is ramped linearly until reaching a set potential then, the potential ramp is reversed back to the starting voltage. For this, a three electrode configurations is needed in which the working electrode, that is the electrode on which the reaction of interest takes place, is used in conjunction with a reference electrode and an auxiliary electrode. The application of a known potential is carried out by using a reference electrode. This is an electrode, which has a stable and well-known potential (e.g., SHE is a hydrogen electrode with a potential of 0 V, while Ag/AgCl

reference electrode has a potential of +0.197 V). The auxiliary electrode (e.g., platinum wire), often also called the counter electrode, functions as a cathode providing the circuit over which current is measured. A potentiostat is used to generate voltage scan. The rate of change of potential with time is referred to as the scan rate (υ). In MFC studies, low scans are usually employed (1-10 mV/s), so that at each applied potential all proteins involved in the pathway are oxidized and reduced multiple times [63].

Biocathodes

While most of the research carried out on the biological components of MFCs has dealt with microorganisms growing at the anode and with their role of catalysing electron flow from reduced organic compounds to the anode, microorganisms have also been observed that have the ability to take electrons from a cathode in the same way that they can transfer them to an anode. Thus, in the search for a suitable catalyst for the cathode of MFCs research in the use of biocathodes has recently become a rather exciting topic.

As found for the anodic communities, cathodic communities can harbour high species diversity. Direct and indirect mechanisms have been also described to play a role in electron transfer from the cathode to the microorganisms, although these are much less studied that the anodic electron transfer processes. Although, *Geobacter* and *Shewanella* cytochromes have been reported to be able of direct electron uptake from the cathode in the presence of different final electron acceptors [64], recent studies with *Geobacter sulfurreducens* have showed different electrochemical response of this bacterium according to the electrode potential. Thus, different *c*-type cytochromes would be selected to meet the availability and potential of the terminal electron acceptor [65,66], which is not surprising due to the great diversity of cytochromes coded in its genome. Other bacteria perform mediated electron transfer by excreting redox-active compounds. This has been observed for example in *Acinetobacter calcoaceticus*, which secretes pyrroloquinoline quinine (PQQ) for extracellular electron transfer in microbial cathodic oxygen reduction [67].

The use of biocathodes has several advantages over abiotic cathodes. For example microorganisms can act as catalysts and no noble metals are needed additionally they are auto replicating and sustainable.

MICROBIAL FUEL CELL APPLICATIONS

Electricity generation

The fact that MFCs are able to generate electricity was recognized long time ago but power output has been usually to low to power practical applications. One feasible way to improve this problem is to store the electricity in rechargeable devices as capacitors, and use stored electricity [68,69]. Researchers have described MFCs as a suitable option to supply energy to Gastrobots by self-feeding the biomass collecting by themselves [70,71]. Additionally, MFCs are suitable for powering small telemetry systems and wireless sensors (Figure 7) [72].

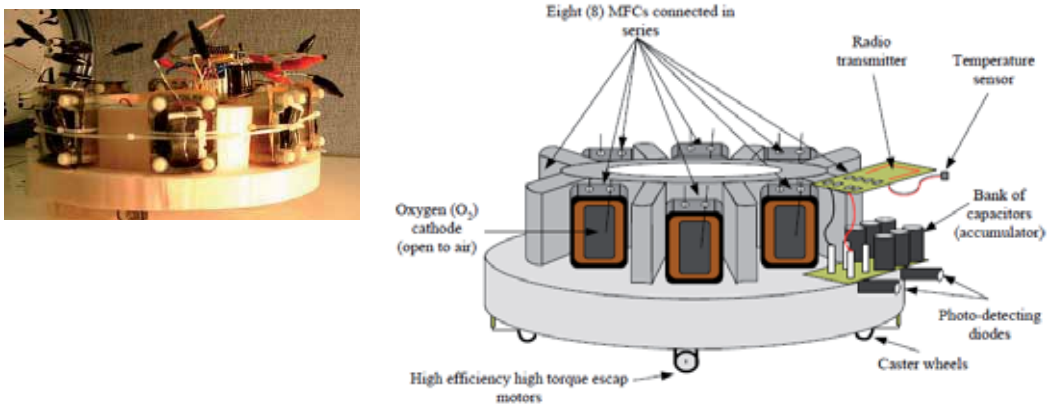

Figure 7. EcoBot II fully assembled with the wireless transmitter and temperature sensor on top. Schematic diagram of EcoBot II with labelled parts (Image extracted from ref. 75).

In recent years, besides the development and optimization of electricity production of these devices, the number of practical applications has increased [73]. However, many of these applications are not currently feasible and require significant improvements for their use in terms of efficiency, cost of materials, physical architecture and chemical limitations among others [14,74].

Wastewater Treatment

In 2004, Liu *et al.* demonstrated the possibility to produce electricity in a MFC from domestic wastewater while at the same time accomplishing biological wastewater treatment [76]. Bacteria are able to couple degradation of a great diversity of substrates to electricity production [18,77]. Many types of industrial wastewater from food-processing industries [17] or agricultural wastewaters [78] among others [79,80] containing large amounts of organic matter are good candidates for treatment with MFC technology.

Figure 8. Pilot-scale microbial fuel cell (Image extracted from ref. 83).

The anodic environmental requires anaerobic conditions thus avoiding the energy that is required to provide strong aeration in aerobic treatments. Oxygen, on the contrary, is normally used at the cathode, but using air-cathodes no aeration of the wastewater is needed saving costs [81], in addition recovery of energy might reduce the total cost of the treatment. Despite its advantages, for this application of MFCs to be feasible, the construction and operation costs must be reduced [81,90]. Moreover, MFCs for the large scale wastewater treatment still face problems of scale up and slow rates of substrate degradation (Figure 8) [14].

Sediment MFC

A MFC able to produce electricity from the organic matter in aquatic sediments was described at first time by Reimers *et al*. [5,84]. These systems are being studied for powering electronic devices in remote locations, as sensors for oceanography or environmental monitoring (Figure 9) [73,85].

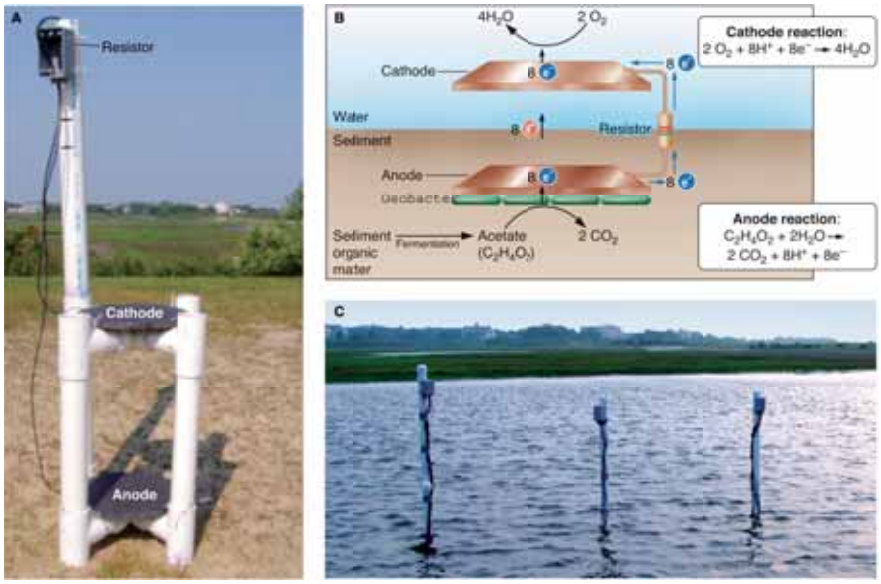

Figure 9. Sediment fuel cell images (A,C) and diagram of sediment fuel cell reactions (B) (Image extracted from ref. 86).

These types of sensors do not have access to conventional power sources and, thus, require battery replacement on periodic bases. Seawater sediment MFCs however, uses the natural voltage gradients and organic matter present in the natural environments. Anode is placed in the anoxic marine sediment while cathode is located on the oxygen-rich seawater eliminating the need for the use of a PEM to power generation. Moreover, the high conductivity of the water allows a good performance [14,73,85].

Bioremediation

Remediation can include both, degradation of organic pollutants at the anode as well as reduction of inorganic chemicals at the cathode [87]. Anaerobic bacteria in a MFC can oxidize a great variety of substrates and electron donors. The treatment of contaminants such as petroleum hydrocarbons [88,89], selenite [90], sulfide [91] or phenol [92] among others have been carried out by oxidative biodegradation in a MFC with the consequent production of current. *Geobacter* species, for example, have been shown to be important in anaerobic degradation of petroleum components by linking the oxidation of the contaminant to the reduction of Fe(III). So, placing an electrode in the polluted soil the rate of bioremediation is greatly increased [14,88]. In the same way, oxidized contaminants such as nitrate [93,94], perchlorate [95], uranium [96] or nitrobenzene [97], can be reduced at the cathode by microorganisms, which use the anode as electron donor.

In spite of the extensive research being carried out, the use of MFC technology for bioremediation has still a long way to go, as research is being carried out only at laboratory-scale and under controlled conditions [98]. In order to make such processes able to compete with existing remediation technologies, major engineering challenges towards field application include the identification of suitable and sustainable electrode materials, site-specific design, and operation criteria [98].

Sensors

Microbial cells can also be used in the design and construction of a wide variety of sensors [99]. MFCs have the potential to be a direct, quantitative sensor for microbial respiration [100]. Electrical current obtained by an MFC is a direct measure for metabolic activity of electrogenic bacteria [101]. MFCs have been studied as BOD biosensors for a long time [102,103,104]. MFC technologies have been also employed to monitor target chemicals like glucose [105], lactate [106] or acetate [107]. Additionally, since current generation is correlated with substrate concentration, current has been used as a measure of contaminant concentration or toxicity [108].

MICROBIAL FUEL CELL PERFORMANCE

Power output

The performance of a MFC is quantified in terms of power output. Power is calculated as $P=I \cdot V_{cell}$. Normally, the V_{cell} is measured across a fixed external resistor (R_{ext}), while current intensity is calculated from Ohm´s law ($I=V_{cell}/R_{ext}$).

The maximum power output is obtained from polarization curves (Figure 10) [109]. Polarization curves show how well MFCs is able to maintain a voltage as current demand is increased. At a current intensity of zero, voltage displays a maximum value usually referred to as OCV (open circuit voltage). Voltage decreases with increasing current output and eventually becomes zero when the MFC is no longer able to sustain more current [59].

The cell voltage produced at any specific current is considered to be the result of voltage losses due to overpotentials, which are potential losses owing to electron transfer resistances and internal resistances better explained later [5,22].

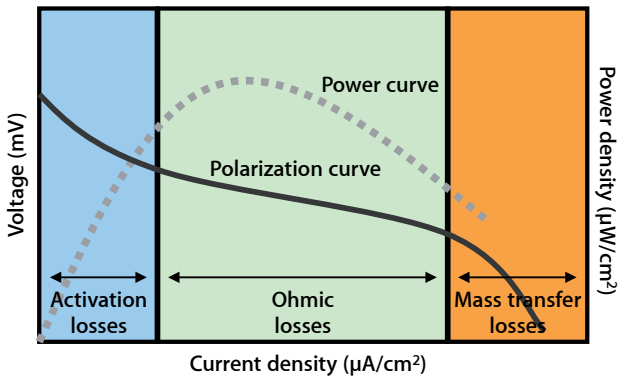

Figure 10. Representation of different characteristics regions of a polarization curve, also called IV curve.

A power curve, which describes the power as the function of the current, can be calculated from the polarization curve (Figure 10). In OCV conditions, as no current flows for the circuit, no power is produced. After this, the power increases with current until reaching the maximum power point. Beyond this point, the power drops due to the increasing internal resistance and electrode overpotentials [5].

MFC Overpotentials

For a redox reaction to be place spontaneously, the electron donor must have a redox potential lower than the electron acceptor (Figure 11). This difference in potential is proportional to the amount of energy generated from the reaction. In a MFC, oxidation of an electron donor at the anode is coupled to the reduction of an electron acceptor with a higher electrode potential at the cathode [110].

The anode potential is set by the respiratory enzymes of the bacteria while cathode potential is determined by the catholyte and the oxidant [111]. However, in practice, the actual voltage output of an MFC is less than the predicted thermodynamic ideal voltage due to irreversible losses occurring as overpotentials. An overpotential is the difference between the equilibrium potential of an electrode with zero net current and its operating potential with a net current flow, which represents the extra energy needed to force the electrode reactions [59].

The main three physical components of the MFC are the anode, cathode, and if present, the membrane, however, many parameters involved in microbial fuel cell operation and design, affect these overpotentials [5].

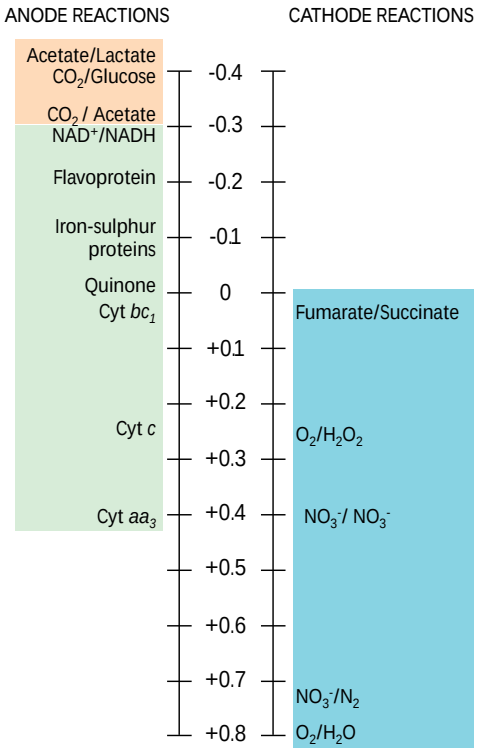

Figure 11. Potentials of different oxidation/reduction process occurring in the anode and cathode.

Bacterial metabolic losses

Catalysts generally increase the rate of a reaction without being changed by receiving energy from the reaction they catalyze. Microorganisms obtain energy from the oxidation of the substrate to support their growth; therefore, they are not considered true catalysts since they are responsible of a certain energy loss. Bacteria oxidize low potential substrates to transfer the electrons obtained to an electron acceptor that, in the case of MFCs, is the anode. The energy gain for the bacteria is higher the higher the anode potential is. However, this produces a decrease of the MFC voltage, reducing the performance (Figure 12). For this reason, the potential of the anode must be maintained as low as possible, although too low anode potentials can make other process like fermentation more beneficial in terms of energy production, inhibiting electron transport to the electrode [109,112].

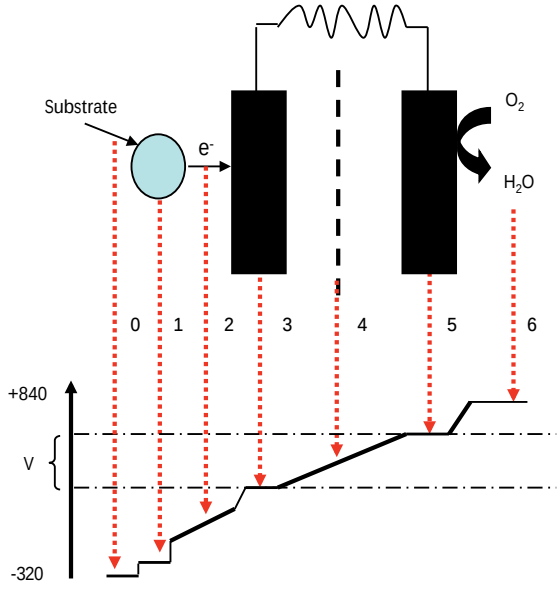

Figure 12. Potential losses. 0. Bacterial metabolic losses. 1. Electron transfer losses. 2. Electrolyte resistance. 3. Losses at the anode. 4. MFC and PEM resistance. 5. Losses at the cathode. 6. Acceptor reduction losses. V. Useful potential difference (Image adapted from ref. 22).

Activation losses

Current production in MFCs depends to a large extent on the kinetics of oxidation and reduction at the electrode surface. The reactions kinetics are limited by activation energy barriers in the electron transfer from the cell electron carrier to the anode surface or from the cathode to the reduced species (Figure 12). Additional losses as a result of bacteria deriving energy from substrate oxidation to growth are also inevitable [5].

Activation overpotentials are affected by different anode and cathode parameters. Parameters affecting the anode include the area, roughness and texture of the electrode, the electrochemical characteristic of the material used, the anode potential, and the mechanism and kinetics of electron transfer [22]. It has been hypothesized that electrogenic microorganisms can reduce the overpotentials and then, increase the energy gain by optimizing their electron transfer strategies [111]. So, the closer the interaction between bacteria and the electrode, the lower the losses. On the other hand, the magnitude of cathodic activation overpotential depends on the reduction kinetics. Kinetic performance can be improved by using improved catalysts at the cathode, increasing the reaction interface area, temperature, or the concentration of oxidant [110].

Ohmic losses

Ohmic losses, also called internal resistance, are due to limitations in charge (electrons and protons) transport, mainly as a consequence of the resistance from the electrodes, electrolytes, presence of diffusion barriers (nafion) or distance between anode and cathode (Figure 12) [110].

Optimization of different abiotic factors as an increase of electrolyte conductivity, PEM surface, pH control, a reduction of electrode spacing or PEM resistivity, can reduce these losses [110].

Mass transfer losses

They are losses related to limitations in the transport of reactants to or from the electrode surface (Figure 12) [5]. These limitations appear when diffusional transport is not sufficient to cope with the rates at which reactants are consumed or produced at the electron surface. Mass transfer losses usually appear when operating at high current output and can be relieved to some extent by applying turbulence at the electrode surface. Experimental data suggest that mass transport limitations due to oxidant transport in the cathode compartment are typically much more severe than transport limitations in the anode compartment due to the poor solubility and slow reduction kinetics of oxygen. Hence, when determining mass transport losses in fuel cell systems, only the limiting concentration for the oxidant is considered.

Mass transport losses occur at high current density, and the magnitude increases with increasing current density [5]. So, high substrate or oxidant concentrations can reduce these losses. Beside a good stirring of the MFC chambers and an increase of substrate or oxidant concentrations, electrode material and cathode compartment geometry can also minimize mass transport limitations and performance losses [110].

AN OVERVIEW OF FACTORS AFFECTING POWER OUTPUT

Design factors

Anode

Anodic materials must be conductive, biocompatible, must have high specific surface area, high porosity and rugosity, and must be chemically stable in the reactor solution [5,109]. Metal anodes are normally made of noncorrosive stainless steel mesh avoiding the use of other metals with toxic effects on microorganisms. However, the most versatile and extensively used material is carbon (Figure 13B), available as fibrous material (carbon fiber, paper, foam or cloth), as compact graphite

plates, rods or granules, although other more compact forms of carbon have been also used (reticulated vitreous carbon (RVC)) [5,109,113].

In all types of anode materials, an increase of power output is observed as the surface area of the electrodes increases [22,114]. The highest specific surface areas and porosities for anodes have been obtained using graphite brush anodes, which consist of graphite fibers wound around a conductive metal core (Figure 3A) [113].

Anode overpotentials can be also decrease by modifying the electrode surface in order to improve the electrochemical characteristics of the electrode and enhance bacterial adhesion [115-121]. For example, anodes have been chemically modified with redox active sites as quinones or quinoid groups [115], or by biding mediators (anthraquinone-1,6-dissulfonic acid (AQDS), or 1,4-naphthoquinone (NQ)) [118] or metals such as Mn^{+4}, Fe^{+3} or Ni^{+2} [117,118]. With ammonia treatment of carbon cloth anodes very high power values could be also reached [116]. Current generation has also been improved by the use of electrocatalytic materials like platinum combined with polyaniline or fluorinated polyanilines [119,120], and tugsten carbide [121].

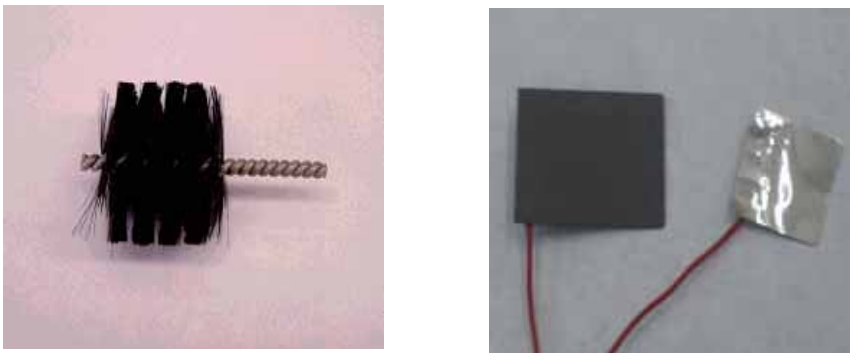

Figure 13. Graphite brush (Image extracted from ref. 113) (A), carbon paper (B) and platinum electrodes (C).

Cathode

The performance of the cathode is normally an important limitation in a MFC [110]. To reduce these, great efforts have been made to improve cathode reaction by the use of catalysts like nobel metals (platinum), liquid chemicals (ferricyanide) or microorganisms (biocathodes). The concentration of these catalysts or the area of the electrode strongly affects power output.

Oxygen is the most widely used electron acceptor due to its high oxidation potential, availability, low cost, sustainability, and the lack of a chemical waste product. However, the poor kinetics of oxygen reduction reaction at neutral pH and low temperatures [122], make selection of the cathode to be critical due to the need for a catalyst. So, the choice of the cathode material greatly affects performance and it is changed depending on the application [109].

Reduction of oxygen is usually catalyzed by a precious metal catalyst [74]. Platinum is the best known oxygen reduction catalyst (Figure 13C) [123]. However, although platinum based oxygen electrodes provide useful benchmarks on the performance of the system, they are not practical for all applications due to their high cost [122], tendency to poisoning by the formation of a platinum oxide layer at the surface [7,109], and sensitivity to biological and chemical fouling. Lead dioxide (PbO_2) has been also studied as cathode catalysts with power output recoveries four times higher than platinum. However, the toxicity of this metal limits its use in MFCs for some applications [110,124]. Inexpensive materials such as transition metal porphyrines and phthalocyanines have been studied in MFCs to replace platinum as oxygen reduction catalysts with good current levels [122,125].

Other materials, such as carbon paper, carbon cloth or graphite, can also be used but, in this case, a liquid catalyst is required. The most commonly used chemical catholyte in MFCs is ferricyanide. It has reduction kinetics faster than oxygen on the cathode, and a relatively high redox potential (0.358 V), its concentration in the solution is not limited by low solubility and it does not require the use of precious metals on the cathode such as platinum [110].

Tests using ferricyanide show much greater power generation than those with oxygen, this is probably related to high open circuit potential and greater mass transfer efficiency than dissolved oxygen. Oxygen is predicted to have a higher cathode potential than ferricyanide however, in practice, the potentials achieved using oxygen are much lower than theoretical values due to the high overpotentials of the oxygen reduction, while cathode potential achieved with ferricyanide as catalyst is quite close to that calculated for standard conditions [5,123,126].

Other catholytes, that have been also used, are iron-chelates or permanganate resulting in improved electricity generation [127,128]. However, liquid catalysts are not suitable for sustainable electricity generation since, due to the very slow re-oxidation rate by oxygen, they need to be replaced [10,110]. In addition, the long term performance of the system can be affected by diffusion across the membrane [109].

Proton Exchange Membrane

MFC designs normally require the separation of the anode and the cathode chambers by a proton exchange membrane (PEM). Nafion 117 (Dupont Co., USA) is the most popular because it is highly selective for protons [7,109].

However, a number of problems exist associated to its use, such as oxygen leakage from cathode to the anode, substrate loss into the cathode, transport of other ions than protons as ferricyanide, and biofouling [129].

As an alternative strategy, the use of anion exchange membranes (AEM), bipolar membranes (BPM), ultracentrifugation membranes or cation exchange membranes with less expensive and more durable materials have been proposed and studied in MFCs [130-133] however, nafion is still now the best option [7,109].

Internal resistance

This is dependent on both the resistance of the electrolyte between the electrodes and the resistance of the membrane (PEM). Internal resistance can be decreased by reducing the separation between anode and cathode electrodes, improving proton migration through the PEM, by an adequate mixing, increasing the PEM area or even by removing this membrane [22].

So, MFC architecture has an important effect on internal resistance. MFCs are constructed using a great variety of configurations depending of the goals of the research. Figure 14 shows an example of the great variety of different designs developed for discontinuous and continuous operation. A typical MFC consists of an anodic chamber and a cathodic chamber separated by a PEM (two-chamber MFC). However, single-chamber MFCs have been designed eliminating the need for the cathodic chamber [7].

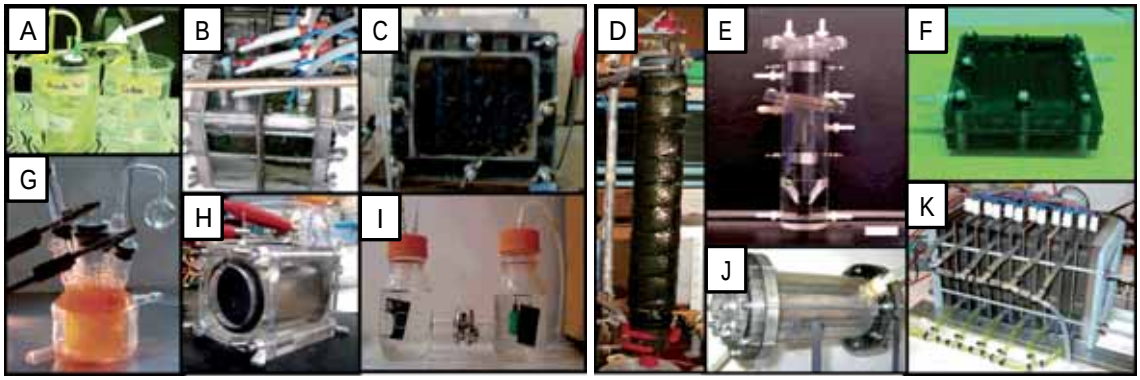

Figure 14. Types of MFCs used in studies: (A) easily constructed system containing a salt bridge (shown by arrow) [134]; (B) MFCs where the chambers are separated by the membrane and held together by bolts [31]; (C) same as B but with a continuous flow-through anode (granular graphite matrix) and close anode-cathode placement [135]; (D) upflow, tubular type MFC with inner graphite bed anode and outer cathode [141]; (E) upflow, tubular type MFC with anode below and cathode above, the membrane is inclinated [136]; (F) flat plate design where a channel is cut in the blocks so that liquid can flow in a serpentine pattern across the electrode [137]; (G) photoheterotrophic type MFC [138]; (H) single-chamber, air-cathode system in a simple "tube" arrangement [142]; (I) two-chamber H-type system showing anode and cathode chambers [139]; (J) single-chamber system with an inner concentric air cathode surrounded by a chamber containing graphite rods as anode [76]; (K) stacked MFC [140] (Figure extracted from ref. 109).

Two-chamber MFCs are normally used in laboratories although seldom in real world applications since their complex designs are difficult to scale-up. Although they can be operated in either batch or continuous mode, they typically run in batch mode [7]. The compartments can take various practical shapes. A widely used and inexpensive design is a two-chamber MFC built in a traditional "H" shape. This consists in two vessels joined by a tube that separates both, anode and cathode chambers by a proton exchange membrane (PEM) or more simply, by a salt bridge [7,109]. This configuration can be used to study basic parameters as the study of new materials or microbial communities, but it typically produces low power densities due to high internal resistance [7,109], caused by the reduced PEM area and the distance between the electrodes.

So, several architectures have been designed to reduce this resistance. Single-chamber MFCs have more simple designs and cost savings [7]. In this configuration, instead of submerging and placing it in a chamber separate from the anode, the cathode is placed in direct contact with air, either in the presence or in the absence of PEM [109,142]. Another variation is the design of MFCs operating in continuous flow, as for example cylindrical reactors with a concentric inner tube that acts as an air-cathode [143] or with a inner anode consisting of granular media with the cathode on the outside [141]. Additionally, Stacked-MFCs, which are formed by several MFCs connected in series or in parallel, have been designed to enhance voltage or current output [7].

Chemical factors

Electricity generation in a MFC is based on the metabolic activity of the microorganisms. For this reason these systems have to run under conditions optimal for growth of the microorganisms utilised. Thus, MFCs are usually operated at ambient temperature, atmospheric pressure and at neutral pH.

Proton availability and pH

The proton availability to the cathode is a limiting factor in current production. By increasing ionic strength by adding NaCl to MFCs, it is possible to improve the performance thanks to an increase of the ionic conductivity [144].

Moreover since the membrane constitutes a diffusional barrier, proton transport through the membrane is slower than production at the anode resulting in a pH difference. The use of a buffer compensates the slow proton transport rate and improves proton availability for the cathodic reaction [145].

Temperature

MFC performance can also be affected by temperature as a result of its effect on bacterial kinetics, oxygen reaction rates catalyzed by platinum on the cathode, and the rate of mass transfer of protons through the liquid. MFC studies are normally conducted at elevated temperatures of 30-37°C since high temperature can accelerate chemical and biological reactions. However, in experiments in which the reactor operates at different temperatures, only a slight reduction in power density (9%) was observed when the temperature was reduced from 32 to 20°C, which could reduce the operating costs above all in applications such as wastewater treatment [144].

Gradient formation within the biofilm

Gradients in the concentration of substrate, local potential and proton accumulation, can be formed in an electrochemical active biofilm and affect the performance of a MFC (Figure 15) [45]. Low concentration of substrate can result in limitation of electron donor in some sections of the biofilm, meanwhile protons produced during substrate oxidation can accumulate in the biofilm forming a pH gradient [146].

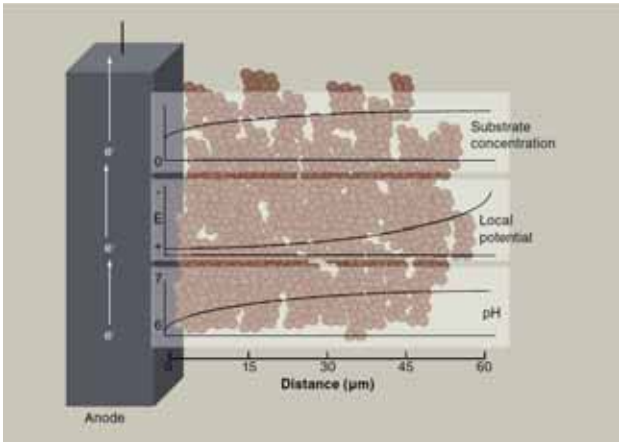

Figure 15. Gradient formation in an electrogenic biofilm [Figure extracted from ref. 45].

Additionally, gradient potentials are expected across the thickness of the biofilm due to the electron conduction through the conductive matrix that forms the biofilm [147].

Microbiological Aspects

The microbial component plays an important role in the overall performance of a MFC. Factors such as cell concentration, microbial activity with regard to the oxidation of the substrate or the rates of electron transfer influence power output and therefore, must be taken into account.

Inoculum

Although in MFC research a great number of microorganisms have been isolated, in general substantially lower power outputs are normally with pure cultures, likely due to a number of synergistic interactions that occurs in the original mixed cultures [45,148]. In these MFCs, which are

sustained by pure cultures, a relation between the bacterial concentration and power has been studied with power increasing as a function of bacterial concentration [114].

In MFCs working with complex communities, biological optimization implies the selection of suitable bacterial consortia and the bacterial adaptation to the optimized reactor conditions [22]. More studies, which differentiate between community members that use the electrode as electron donor and those who are effective colonizers of the anode material but do not contribute to current production [45], could help to select electricigens.

Microbial Activity

The rate at which substrate is oxidized and electrons are released onto the anode depends on the activity level of the organism. Factors affecting microbial activity such as temperature, the concentration of limiting substrates or even the presence of inhibitory substances are likely to affect the output of a MFC [22,58].

Electron scavengers

Coulombic efficiency, as the percentage of electrons recovered as electrical current according to the theoretical maximum number of electrons obtained from the anodic organic substrate, is a good parameter to determine the efficiency of a MFC in current production [14,109]. This efficiency is in great extent dependent on the microorganisms, which oxidize the substrate. An incomplete oxidation of the substrate produces a loss of energy in the form of unoxidized substrates [14]. Additionally, different metabolisms oxidize the substrate without using the electrode as electron acceptor. So, in MFCs using mixed cultures, electrogenic bacteria compete for the substrate with other functional groups such as fermenters, acetogens and methanogens. Operational factors as electrode potential or external resistance have been demonstrated to affect on competition among the different metabolisms [149].

Electron transfer mechanisms

Microorganisms are not naturally designed to dispense energy to power a fuel cell and, although the mechanisms by which microorganisms oxidize the anodic substrates and transfer the electrons to the anode are very important for power output, little is known about them.

From the standpoint of current production is not clear what is the best anodic electron transfer mechanism for MFCs. Every pathway has advantages and disadvantages in terms of coulombic efficiency or energy gain for the microorganisms [112] and there is a high diversity of opinions between the publish studies about which one is the best related to power output.

A kinetic analysis used to study the extracellular potential losses suffered by microorganisms as a consequence of the EET different processes was used to hypothesize about these different mechanisms in terms of MFC performance. Direct electron transfer was reported to have the minimal EET losses due to the proximity of the cell and the electrode, however it also produces limited current density due to the fact that this pathway is only possible for the first layer of the biofilm. Soluble electron shuttle production allows the presence of higher biomass of electricigens, but it is also limited by the slow diffusion of redox species, especially at low concentrations. Electron-shuttle concentration gradients associated with electron shuttle diffusion can lead to EET losses higher than 100 mV. Electron transfer through biofilm matrix via nanowires, and bound cytochromes seems to be the more favourable process. This mechanism offers the possibility of obtaining high current densities at low anode potential losses [58].

However, a greater understanding of these mechanisms is required in order to find means to efficiently divert electrons from the metabolism to a fuel cell anode [58,112]. More information about these processes may also lead to other improvements, most notably in the design and/or anode materials and genetic engineering of the bacteria to enhance the connections between electricigens and anodes. For this reason, research activities in this field have enormously increased in recent years [62,63].

Operational factors

Anode potential

The capability of microorganisms to generate current at the anode depends to a great extent on the anode potential [111]. This is defined by the potential of the respiratory enzymes or electron carriers used by the bacteria to carry out the electron transfer. However, this potential is also affected by the reduction potential of the cathode and by the overpotentials of the anode explained previously.

When the MFC circuit is opened and therefore, there is not current flow, anode potential becomes more negative due to the accumulation of reduced redox components. When the circuit is connected, the anode potential increases because of the oxidation of these redox species. Several works have shown that the capacity of bacteria to transfer electrons to an anode is influenced by the anode potential in the same way that microbial growth rate depends on the substrate concentration. Consequently, the anode half-saturation potential (E_{KA}) has been used to define the anode potential at which current density is half of the maximum current generation [150]. Thus, the amount of power provided by the MFC increases as the more negative anode potential is maintained at a set resistance. This indicates that for a given current the anode reaction suffers less overpotentials [74,109,150].

High anode potentials promote bacterial activity and growth since bacteria can use the respiratory chain in an oxidative metabolism. However, low anode potentials are most useful to produce high current densities due to the fact that they allow higher potential difference between anode and cathode. Additionally, too low anode potentials can turn the bacteria into fermentative metabolism reducing the coulombic efficiency [22,149,151].

External resistance

This factor is related to the potential of the anode. MFCs normally are operated under a fixed external resistance that allows the current flow through the system. Some studies have reported the effect of external resistance in the performance and the bacterial community structure formed on the anode [19,149]. Low external resistance generates high current densities that increase the anode potential. On the contrary, high resistances maintain low anode potentials due to the reduced current flow [22]. Additionally, high resistances can lead microorganisms to reduce other electron acceptors present in the medium when complex substrates such as wastewater reducing the power output [145].

Batch vs. Continuous operation

It has been observed that MFCs operated in batch mode favour the development of microorganisms producers of electron shuttles. Continuous systems however select biofilm-forming species that can either use the electrode directly or transfer electrons through the biofilm matrix using mobile redox species [21,152]. Thus, these operation systems can change the performance of the MFC in function of the electron transfer pathway selected.

AIMS AND OUTLINE OF THE THESIS

In a MFC the electricity produced is directly related to the activity of the microorganisms. However, it has been demonstrated that a great variety of factors other than microbial metabolism affect power output. So, the research objective of this study is the analysis and optimization of several of the factors involved in the performance of a MFC including design, operation and biological factors.

Very often the performance of a MFC becomes limited by the inability of the cathode to transfer electrons to final acceptors at a rate high enough to compensate biological production of electrical charge in the anode compartment. For this reason, the first objective (Chapter 1) is the comparison of different catalysts, both solid and liquids, in terms of power output and long time stability. Additionally, the appropriate area ratio cathode/anode was determined according to each type of catalyst. While catalysts as soluble iron or solid platinum can be used for small scale applications, they cannot be used in large scale industrial facilities due to their effects as pollutants or their extremely high price. This has led us to study the possibility of using microorganisms as cathode catalysts. In Chapter 2, the electrogenic bacterium *Shewanella oneidensis* MR-1 is used as a catalyst in the cathode with the aim of determining its capacity to sustain power production in MFCs using different final electron acceptors. In Chapter 3 we explore how discontinuous operation affects the temporal patterns of current output in MFCs of *Shewanella oneidensis* MR-1. In this chapter, we also intend to demonstrate whether biofilms of *Shewanella oneidensis* MR-1 have ability to store charge during periods of circuit interruption. Finally, inoculation of MFCs with complex communities has been observed to produce values of power output higher than MFCs based on pure cultures, the difference being probably related to the synergetic relations existing within the microbial community. Chapter 4 attempts to study how the existence of different mechanisms of electron transfer and different microbial groups in the community result in differences in power output of the MFCs.

REFERENCES

(1) Potter, M.C. On the difference of potential due to that vital activity of microorganisms. *Proc. Univ. Durham Phil. Soc.* 1910, 3, 245-249.

(2) Potter, M.C. Electrical effects accompanying the decomposition of organic compounds. *Proc. R. Soc. Lond. B.* 1911, 84, 260-276.

(3) Berk, R.S.; Canfield, J.H. Bioelectrochemical energy conversions. *Appl. Microbiol*. 1964, 12, 10-12.

(4) Van Hees, W. A bacterial methane fuel cell. *J. Electrochem. Soc*. 1965, 112(3), 258-262.

(5) Logan, B.E. Microbial Fuel Cells. John Wiley & Sons, NY (2008).

(6) Ieropoulos, I. A; Greenman, J.; Melhuish, C.; Hart, J. Comparative study of three types of microbial fuel cell. *Enzyme Microb. Technol.* 2005, 37, 238-245.

(7) Zhuwei, D.; Li, H.; Gu, T. A state of the art review on microbial fuel cells: a promising technology for wastewater treatment and bioenergy. *Biotechnol. Adv.* 2007, 25, 464-482.

(8) Rabaey, K.; Rodríguez, J.; Blackall, L.L.; Keller, J.; Gross, P.; Batstone, D.; Verstraete, W.; Nealson, K.H. Microbial ecology meets electrochemistry: electricity-driven and driving communities. *ISME J.* 2007, 1, 9-18.

(9) Rabaey, K. Bioelectrochemicall systems: a new approach towards environmental and industrial biotechnology. In: *Bioelectrochemical Systems: from extracellular electron transfer to biotechnological application*. Rabaey, K.; Angenent, L.; Schröder, U:; Kelle, J., Eds. IWA Publishing:London 2010. pp 1.

(10) Logan, B.E.; Regan, J.M. Microbial fuel cells: challenges and applications. *Environ. Sci. Technol*. 2006, 40(17), 5172-5180.

(11) Hernandez, M.E.; Newman, D.K. Extracellular electron transfer. *Cell. Mol. Life Sci.* 2001, 58, 1562-1571.

(12) Fredrickson, J.K.; Zachara, J.M. Electron transfer at the microbe-mineral interface: a grand challenge in biogeochemistry. *Geobiology*. 2008, 6, 245-253.

(13) Lovley, D.R. Bug juice: harvesting electricity with microorganisms. *Nat. Rev. Microbiol*. 2006, 4, 497-508.

(14) Franks, A.E.; Nevin, K.P. Microbial Fuel Cells, a current review. *Energies*. 2010, 3, 899-919.

(15) Phung, N.T.; Lee, J.; Kang, K.H.; Chang, I.S.; Gadd, G.M.; Kim, B.H. Analysis of microbial diversity in oligotrophic microbial fuel cells using 16S rDNA sequences. *FEMS* Microbiol. Lett. 2004, 233, 77-82.

(16) Logan, B.E.; Regan, J.M. Electricity-producing bacterial communities in microbial fuel cells. *TRENDS in Microbiol*. 2006, 14(12), 512-518.

(17) Patil, S.A.; Suraski, V.P.; Koul, S.; Ijmulwar, S.; Vivek, A.; Shouche, Y.S.; Kapadnis, B.P. Electricity generation using chocolate industry wastewater and its treatment in activated sludge. *Bioresource Technol*. 2009, 100(21), 5132-5139.

(18) Pant, D.; Van Bogaert, G.; Diels, L.; Vanbroekhoven, K. A review of the substrates used in microbial fuel cells (MFCs) for sustainable energy production. *Bioresourc. Technol*. 2009, 101, 1533-1543.

(19) Lyon, D.Y.; Buret, F.; Vogel, T.M.; Monier, J. Is resistance futile? Changing external resistance does not improve microbial fuel cell performance. *Bioelectrochemistry*. 2010, 78, 2-7.

(20) Torres, C.; Krajmalnik-Brown, R.; Parameswaran, P.; Marcus, A.K.; Wanger, G.; Gorby, Y.A.; Rittmann, B.E. Secting anode-respiring bacteria based on anode potential: phylogenetic, electrochemical, and microscopic characterization. *Environ. Sci. Technol*. 2009, 43, 9519-9524.

(21) Rabaey, K.; Boon, N.; Siciliano, D.; Verhaege, M.; Verstraete, W. Biofuel cells select for microbial consortia that self-mediate electron transfer. *Appl. Environ. Microbiol*. 2004, 70, 5373-5382.

(22) Rabaey, K.; Verstraete, W. Microbial fuel cells: novel biotechnology for energy generation. *TRENDS Biotechnol*. 2005, 23(6), 291-298.

(23) Karube, I.; Matsunaga, T.; Tsuru, S. Biochemical fuel cellutilizing immobilized cell of *Clostridium butryicum*. *Biotechnol. Bioeng*. 1977, 19, 1727-1733.

(24) Benetto, H.P.; Delaney, G.M.; Mason, J.R.; Roller, S.D.; Stirling, J.L.; Thurston, C.F. The sucrose fuel cell: efficient conversion using a microbial catalyst. *Biotechnol. Lett*. 1985, 7, 699-704.

(25) Park, D.H.; Zeikus, J.G. Electricity generation in microbial fuel cells using neutral red as an electronophore. *Appl. Environ. Microbiol.* 2000, 66(4), 1292-1297.

(26) Roller, S.D.; Bennetto, H.P.; Delaney, G.M.; Mason, J.R.; Stirling, J.L.; Thurston, C.F. Electron-transfer coupling in microbial fuel cells: 1. comparison of redox-mediator reduction rates and respiratory rates of bacteria. *J. Chem. Technol. Biot*. 1984, 34(1), 3-12.

(27) Marsili, E. et al., Shuttling via soluble compounds. In: *Bioelectrochemical Systems: from extracellular electron transfer to biotechnological application*. Rabaey, K.; Angenent, L.; Schröder, U.; Kelle, J., Eds. IWA Publishing:London 2010. pp 59.

(28) Newman, D.K.; Kolter, R. A role for excreted quinones in extracelular electron transfer. *Nature*. 2000, 405, 94-97.

(29) von Canstein, H.; Ogawa, J.; Shimizu, S.; Lloyd, J.R. Secretion of flavins by *Shewanella* species and their role in extracellular electron transfer. *Appl. Environ. Microbiol*. 2008, 74(3), 615-623.

(30) Marsili, E.; Baron, D.B.; Shikhare, I.D.; Coursolle, D.; Gralnick, J.A.; Bond, D.R. *Shewanella* secretes flavins that mediate extracellular electron transfer. *PNAS*. 2008, 105(10), 3968-3973.

(31) Rabaey, K.; Boon, N.; Hofte, M.; Verstraete, W. Microbial phenazine production enhances electron transfer in biofuel cells. *Environ. Sci. Technol*. 2005, 39(9), 3401-3408.

(32) Nevin, K.P.; Lovley, D.R. Mechanisms for accessing insoluble Fe(III) oxide during dissimilatory Fe(III) reduction B *Geothrix fermentans*. *Appl. Environ. Microbiol*. 2002, 68(5), 2294-2299.

(33) Wang, Y.F.; Masuda, M.; Tsujimura, S.; Kano, K. Electrochemical regulation of the end-product profile in *Propionibacterium freudenreichii* ET-3 with an endogenous mediator. *Biotech. Bioeng*. 2008, 101, 579-586.

(34) Vega, C.A.; Fernandez, I. Mediating effect of ferric chelate compounds in microbial fuel cells with *Lactobacillus plantarum, Streptococcus lactis* and *Erwinia dissolvens*. *Bioelectrochem. Bioenerg.* 1987, 17, 217-222.

(35) Bretschger, O. et al. A survey of direct electron transfer from microbed to electronically active surfaces. In: *Bioelectrochemical Systems: from extracellular electron transfer to biotechnological application*. Rabaey, K.; Angenent, L.; Schröder, U:; Kelle, J., Eds. IWA Publishing:London 2010. pp 81.

(36) Bond, D.R.; Lovley, D.R. Electricity production by Geobacter sulfurreducens attached to electrodes. *Appl. Environ. Microbiol*. 2003, 69, 1548-1555.

(37) Pham, A.C.; Jung, S.J.; Phung, N.T.; Lee, J.; Chang, I.S.; Kim, B.H.; Yi, H.; Chun, J. A novel electrochemically active and Fe(III)-reducing bacterium phylogenetically related to *Aeromonas hydrophila*, isolated from a microbial fuel cell. *FEMS Microbiol. Lett*. 2003, 223, 129-134.

(38) Chaudhuri, S.K.; Lovley, D.R. Electricity generation by direct oxidation of glucose in mediatorless microbial fuel cells. *Nat. Biotechnol*. 2003, 21, 1229-1232.

(39) Newton, G.J.; Mori, S.; Nakamura, R.; Hashimoto, K.; Watanabe, K. Analyses of current-generation mechanisms of *Shewanella loihica* PV-4 in microbial fuel cells in comparison with *Shewanella oneidensis* MR-1. *Appl. Microbiol. Enviro*n. 2009, 75(24), 7674-7681.

(40) Holmes, D.E.; Bond, D.R., Lovley, D.R. Electron transfer by *Desulfobulbus propionicus* to Fe(III) and graphite electrodes. *Appl. Microbiol. Enviro*n. 2004, 70(2), 1234-1237.

(41) Mowat, C.G.; Chapman, S.K. Multi-hemo cytochromes – new structures, new chemistry. *Dalton Trans*. 2005, 3381-3389.

(42) Myers, C.R.; Myers, J.M. Role for outer membrane cytochromes *Omc*A and *Omc*B of *Shewanella putrefaciens* MR-1 in reduction of manganese dioxide. *Appl. Environ. Microbiol*. 2001, 67(1), 260-269.

(43) Bretschger, O., Obraztsova, A.; Sturm, C.A.; Chang, I.S.; Gorby, Y.A.; Reed, S.B.; Culley, D.E.; Reardon, C.L.; Barua, S.; Romine, M.F.; Zhou, J.; Beliaev, A.S.; Bouhenni, R.; Saffarini, D.; Mansfeld, F.; Kim, B.H.; Fredrickson, J.K.; Nealson, K.H. Current production and metal oxide reduction by *Shewanella oneidensis* MR-1 wild type and mutants. *Appl. Environ. Microbiol*. 2007, 73, 7003–7012.

(44) Hartshorne, R.S.; Reardon, C.L.; Ross, D. Nuesterd, J.; Clarkea, T.A.; Gatesa, A.J.; Millsa, P.C.; Fredricksonb, J.K.; Zacharab, J.M.; Shib, L.; Beliaevb, A.S.; Marshallb, M.J.; Tienc, M.; Brantleyd, S.; Butta, J.N.; Richardsona, D.J. Characterization of an electron conduit between bacteria and the extracellular environment. *Proc. Natl. Acad. Sci. USA*. 2009, 106(52), 22169-22174.

(45) Franks, A.E.; Malvankar, N.; Nevin, K.P. Bacterial biofilms: the powerhouse of a microbial fuel cell. *Biofuels*. 2010, 1(4), 589-604.

(46) Fredrickson, J.K; Romine, M.F.; Alexander S.; Beliaev, A.S.; Auchtung, J.M.; Driscoll, M.E.; Gardner, T.S.; Nealson, K.H.; Osterman, A.L.; Pinchuk, G.; Reed, J.L.; Rodionov, D.A.; Rodrigues, J.L.M.; Saffarini, D.A.; Serres, M.H.; Spormann, A.M.; Zhulin, I.B.; Tiedje, J.M. Towards environmental systems biology of *Shewanella*. *Nature*. 2008, 6, 592-603.

(47) Holmes, D.E.; Chaudhuri, S.K.; Nevin, K.P.; Metha, T.; Methe, B.A.; Liu, A.; Ward, J.E.; Woodard, T.L.; Webster, J.; Lovley, D.R. Microarray and genetic analysis of electron transfer to electrodes in *Geobacter sulfurreducens*. *Environ. Microbiol*. 2006, 8, 1805-1815.

(48) Metha, T.; Coppi, M.V.; Childers, S.E.; Lovley, D.R. Outer membrane *c*-type cytochromes required for Fe(III) and Mn(IV) oxide reduction in *Geobacter sulfurreducens*. *Appl. Environ. Microbiol*. 2005, 71, 8634-8641.

(49) Leang, C.; Coppi, M.V.; Lovley, D.R. *Omc*B, a *c*-type polyheme cytochrome, involved in Fe(III) reduction in *Geobacter sulfurreducens*. *J. Bacteriol*. 2003, 185, 2096-2103.

(50) Quian, X.; Reguera, G.; Mester, T.; Lovley, D.R. Evidence that *Omc*B and *Omp*B of *Geobacter sulfurreducens* are outer membrane surface proteins. *FEMS Microbiol. Lett*. 2007, 277(1), 21-27.

(51) Gorby, Y.A.; Beveridge, T.J. Composition, reactivity, and regulation of extracellular metal-reducing structures (nanowires) produced by dissimilatory metal reducing bacteria. 2005. Warrenton, VA.

(52) Gorby, Y.A.; Yanina, S.; McLean, J.S.; Rosso, K.M.; Moyles, D.; Dohnalkova, A.; Beveridge, T.J.; Chang, I.S.; Kim, B.H.; Kim, K.S.; Culley, D.E.; Reed, S.B.; Romine, M.F.; Saffarini, D.A.; Hill, E.A.; Shi, L.; Elias, D.A.; Kennedy, D.W.; Pinchuk, G.; Watanabe, K.; Ishii, S.; Logan, B.; Nealson, K.H.; Fredrickson, J.K. Electrically conductive bacterial nanowires produced by *Shewanella oneidensis* strain MR-1 and other microorganisms. *Proc. Natl. Acad. Sci. U A*. 2006, 103(30), 11358-11363.

(53) Reguera, G.; McCarthy, K.D.; Mehta, T.; Nicoll, J.S.; Tuominen, M.T.; Lovley, D.R. Extracellular electron transfer via microbiol nanowires. *Nature*. 2005, 435, 1098-1101.

(54) Reguera, G.; Nevin, K.P.; Nicoll, J.S.; Covalla, T.L.; Woodard, T.L.; Lovley, D.R. Biofilm and nanowire production leads to increased current in *Geobacter sulfurreducens* fuel cells. *Appl. Environ. Microbiol*. 2006, 72, 7345-7348.

(55) Aelterman, P.; et al. Microbial Fuel Cells as an engineered ecosystem. In *Bioenergy*; Wall, J.D., Harwood, C.S., Demain, A. Eds.; ASM Press: Washington, DC 2008; pp 307.

(56) El-Naggar, M.Y.; Wanger, G.; Leung, K.M.; Yuzvinsky, T.D.; Southam, G.; Yang, J.; Lau, W.M.; Nealson, K.H.; Gorby, Y.A. Electrical transport along bacterial nanowires from *Shewanella oneidensis* MR-1. *PNAS*. 2010, 107(42), 18127-18131.

(57) Reguera, G.; McCarthy, K.D.; Metha, T.; Nicoll, J.S.; Tuominen, M.T.; Lovley, D.R. Extracellular electron transfer via microbiol nanowires. *Nature*. 2005, 435, 1098-1101.

(58) Torres, C.I.; Marcus, A.K.; Lee, H-S.; Parameswaran, P.; Krajmalnik-Brown, R.; Rittmann, B.E. A kinetic perspective on extracellular electron transfer by anode-respiring bacteria. *FEMS Microbiol. Rev*. 2010, 34, 3-17.

(59) Zhao, F.; Robert, C.; Slade, T.; Varcoe, J.R. Techniques for the study and development of microbial fuel cells: an electrochemical perspective. *Chem. Soc. Rev*. 2009, 38, 1926-1939.

(60) Fricke, K.; Harnisch, F.; Schröder, U. On the use of cyclic voltammetry for the study of anodic electron transfer in microbial fuel cells. *Energ. Environ. Sci*. 2008, 1, 144-147.

(61) Marsili, E.; Rollefson, J.B.; Baron, D.B.; Hozalski, R.M.; Bond, D.R. Microbial biofilm voltammetry: direct electrochemical characterization of catalytic electrode-attached biofilms. *Appl. Environ. Microbiol*. 2008, 74(23), 7329-7337.

(62) Carmona-Martinez, A.A.; Harnisch, F.; Fitzgerald, L.A.; Biffinger, J.C.; Ringeisen, B.R.; Schröder, U. Cyclic voltammetrix analysis of the electron transfer of *Shewanella oneidensis* MR-1 and nanofilament and cytochrome knock-out mutants. *Bioelectrochemistry*. 2011, 81, 74-80.

(63) Baron, D.; LaBelle, E.; Coursolle, D.; Gralnick, J.A.; Bond, D.R. Electrochemical measurement of electron transfer kinetics by *Shewanella oneidensis* MR-1. *J. Biol. Chem*. 2009, 284, 28865-28873.

(64) Huang, L.; Regan, J.M.; Quan, X. Electron transfer mechanisms, new applications, and performance of biocathode microbial fuel cells. *Bioresource Technol*. 2011, 102, 316-323.

(65) Rosenbaum, M.; Aulenta, F.; Villano, M.; Angenent, L.T. Cathodes as electron donors for microbial metabolism: which extracellular electron transfer mechanisms are involved. *Bioresource Technol*. 2011, 102, 324-333.

(66) Wei, J.; Liang, P.; Cao, X.; Huang, X. A new insight into potential regulation on growth and power generation of *Geobacter sulfurreducens* in microbial fuel cells based on energy point. *Environ. Sci. Technol*. 2010, 44, 3187-3191.

(67) Freguia, S.; Tsujimura, S.; Kano, K. Electron transfer pathways in microbiol oxygen biocathodes. *Electronchim. Acta.* 2010, 55, 813-818.

(68) Ieropoulos, I.; Greenman, J.; Melhuish, C. Imitation metabolism: energy autonomy in biologically inspired robots. *Proceedings of the 2nd international symposium of imitation of animals and artifacts*; 2003, 191-4.

(69) Liang, P.; Wu, W.; Wei, J.; Yuan, L.; Xia, X.; Huang, X. Alternate charging and discharging of capacitor to enhance the elctron production of bioelectrochemical systems. *Environ. Sci. Technol*. 2011, 45, 6647-6653.

(70) Ieropoulos, I.; Melhuish, C.; Greenman, J. Eco-Bot-II: an artificial agent with a natural metabolism. *Adv. Robot Syst.* 2005, 2, 295-300.

(71) Wilkinson, S. "Gastrobots" – benefits and challenges of microbial fuel cells in food powered robot applications. *Auton. Robot*. 2000, 9, 99-111.

(72) Shantaram, A.; Beyenal, H., Veluchamy, R.R.A.; Lewandowski, Z. Wireless sensors powered by microbial fuel cells. *Environ. Sci. Technol*. 2005, 39, 5037-5042.

(73) Lovley, D.R. Microbial fuel cells: novel microbial physiologies and engineering approaches. *Curr. Opin. Biotech*. 2006, 17, 327-332.

(74) Logan, B.E. Exoelectrogenic bacteria that power microbial fuel cell. *Nat. Rev. Microbiol*. 2009, 7, 375-381.

(75) Ieropoulos, I.; Melhuish, C.; Greenman, J.; Horsfield, I.; Hart, J. Energy autonomy in robots through Microbial Fuel Cells. In *CiteSeerX - Scientific Literature Digital Library and Search Engine*, The Pennsylvania State University, USA, 2004.

(76) Liu, H.; Ramnarayanan, R.; Logan, B.E. Production of electricity during wastewater treatment using a single chamber microbial fuel cell. *Environ. Sci. Technol*. 2004, 38, 2281-2285.

(77) Kiely, P.D.; Regan, J.M.; Logan, B.E. The electric picnic: synergistic requirements for exoelectrogenic microbial communities. *Curr. Opin. Biotech*. 2011, 22, 378-385.

(78) Gálvez, A.; Greenman, J.; Ieropoulos, I. Landfill leachate treatment with microbial fuel cells; scale-up through plurality. *Bioresourc. Technol*. 2009, 100, 5132-5139.

(79) You, S.J.; Zhao, Q.L.; Jiang, J.Q. Biological wastewater treatment and simultaneous generating electricity from organic wastewater by microbial fuel cell. *Huang Jing Ke Xue*. 2006, 27, 1786-1790.

(80) Feng, Y.; Wang, X.; Logan, B.; Lee, H.; Brewery wastewater treatment using air-cathode microbial fuel cells. *App. Microbiol. Biotechnol*. 2008, 78, 873-880.

(81) Logan, B.E. Simultaneous wastewater treatment and biological electricity generation. *Water Sci. Technol*. 2005, 52(1-2), 21-37.

(82) Angenent, L.T.; Karim, K.; Al-Dahhan, M.H.; Wrenn, B.A.; Domínguez-Espinosa, R. Production of bioenergy and biochemical from industrial and agricultural wastewater. *TRENDS Biotechnol*. 2004, 22(9), 477-485.

(83) Wrighton, K.C.; Coates, J.D. Microbial fuel cells: plug-in and power-on microbiology. *Microbe*. 2009, 4(6), 281-287.

(84) Reimers, C.E.; Tender, L.M.; Fertig, S.; Wang, W. Harvesting energy from the marine sediment-water interface. *Environ. Sci. Technol*. 2001, 35(1), 192-195.

(85) DeLong, E.F.; Chandler, P. Power from the deep. *Nat. Biotechnology*. 2002, 20, 788-789.

(86) Lovley, D.R. Microbial energizers: fuel cells that keep on going. *Microbe*. 2006, 1(7), 323-329.

(87) He, Z.; Largus, T.; Angenent, T. Application of bacterial biocathodes in microbial fuel cells. *Electroanal*. 2006, 18, 2009-2015.

(88) Anderson, R.T.; Rooney-Varga, J.; Gaw, C,V.; Lovley, D.R. Anaerobic benzene oxidation in the Fe(III)-reduction zone of petroleum-contaminated aquifers. *Environ. Sci. Technol*. 1998, 32, 1222-1229.

(89) Morris, J.M.; Jin, S.; Crimi, B.; Pruden, A. Microbial fuel cell in enhancing anaerobic biodegradation of diesel. *Chem. Eng. J*. 2009, 146, 161-167.

(90) Catal, T.; Bermek, H.; Liu, H. Removal of selenite from wastewater using microbial fuel cells. *Biotechnol. Lett*. 2009, 31, 1211-1216.

(91) Rabaey, K.; Van de Sompel, K.; Maignien, L.; Boon, N.; Aelterman, P.; Clauwaert, P.; De Schamphelaire, L.; Pham, H.T.; Vermeulen, J.; Verhaege, M.; Lens, P.; Verstraete, W. Microbial fuel cells for sulphide removal. *Environ. Sci. Technol*. 2006, 40, 5218-5224.

(92) Luo, H.; Liu, G.; Zhang, R.; Jin, S. Phenol degradation in microbial fuel cells. *Chem. Eng. J*. 2009, 147, 259-264.

(93) Gregory, K.B.; Bond, D.R.; Lovley, D.R. Graphite electrodes as electron donors for anaerobic respiration. *Environ. Microbiol.* 2004, 6(6):596-604.

(94) Clauwaert, P.; Rabaey, K.; Aelterman, P.; De Schamphelaire, L.; Pham, T. H.; Boeckx, P.; Boon, N.; Verstraete, W. 2007. Biological denitrification in Microbial Fuel cells. *Environ. Sci. Technol*. 2007, 41:3354-3360.

(95) Thrash, J.C.; Van Trump, J.I.; Weber, K.A.; Miller, E.; Achenbach, L.A.; Coates, J.D. Electrochemical stimulation of microbial perchlorate reduction. *Environ. Sci. Technol*. 2007, 41(5), 1740-1746.

(96) Holmes, D.E.; Finneran, K.T.; O´Neil, R.A.; Lovley, D.R. Enrichment of members of the family Geobacteraceae associated with stimulation of dissimilatory metal reduction in uranium-contaminated aquifer sediments. *Appl. Environ. Microbiol*. 2002, 68(5), 2300-2306.

(97) Li, J.; Liu, G.; Zhang, R.; Luo, Y.; Zhang, C.; Li, M. Electricity generation by two types of microbial fuel cells using nitrobenzene as the anodic or cathodic reactants. *Bioresource Technol*. 2010, 101, 4013-4020.

(98) Aulenta, F. *et al*. Bioelectrochemical systems (BES) for subsurface remediation. In: *Bioelectrochemical Systems: from extracellular electron transfer to biotechnological application*. Rabaey, K.; Angenent, L.; Schröder, U:; Kelle, J., Eds. IWA Publishing:London 2010. pp 305.

(99) Su, L.; Jia, W.; Hou, C.; Lei, Y. Microbial biosensors: a review. *Biosens. Bioelectron*. 2011, 26, 1788-1799.

(100) Tront, J.M.; Fortner, J.D.; Plötze, M.; Hughes, J.B.; Puzrin, A.M. Microbial fuel cell biosensor for in situ assessment of microbial activity. *Biosens. Bioelectron*. 2008, 24, 586-590.

(101) Stein, N.E.; Hamelers, H.V.M. Buisman, C.N.J. Influence of membrane type, current and potential on the response to chemical toxicants of a microbial fuel cell based biosensor. *Sensor. Actuat. B: Chem*. 2012, 163, 1-7.

(102) Karube, I.; Matsunga, T.; Mitsuda, S.; Suzuki, S. Microbial electrode BOD sensors. *Biotechnol. Bioeng*. 1977, 19, 1535-1547.

(103) Kim, B.H.; Chang, I.S.; Gil, G.C.; Park, H.S.; Kim, H.J. Novel BOD (biological oxygen demand) sensor using mediator-less microbial fuel cell. *Biotechnol Letter*. 2003, 25, 541-545.

(104) Zhang, Y.; Angelidaki, I. Submersible microbial fuel cell sensor for monitoring microbial activity and BOD in groundwater: focusing on impact of anodic biofilm on sensor applicability. *Biotechnol. Bioeng*. 2011, 108(10), 2339-2347.

(105) Kumlanghan, A.; Liu, J.; Thavarungkul, P.; Kanatharana, P.; Mattiasson, B. Microbial fuel cell-based biosensor for fast analysis of biodegradable organic matter. *Biosens. Bioelectron*. 2007, 22, 2939-2944.

(106) Kim, H.J.; Hyun, M.S.; Chang, I.S.; Kim, B.H. Microbial fuel cell type lactate biosensor using a metal-reducing bacterium, *Shewanella putrefaciens. J. Microbiol. Biotechnol*. 1999, 9, 365-367.

(107) Tront, J.M.; Fortner, J.D.; Plotze, M.; Hughes, J.B.; Puzrin, A.M. Microbial fuel cell biosensor for *in situ* assessment of microbial activity. *Biosens. Bioelectron*. 2008, 24, 586-590.

(108) Dávila, D.; Esquivel, J.P.; Sabaté, N.; Mas, J. Silicon-based microfabricated microbial fuel cell toxicity sensor. *Biosens. Bioelectron*. 2011, 26, 2426-2430.

(109) Logan, B.E.; Hamelers, B.; Rozendal, R.; Schröder, U.; Keller, J.; Freguia, S.; Aelterman, P.; Verstraete, W.; Rabaey, K. Microbial Fuel Cells: methodology and technology. *Environ. Sci. Technol*. 2006, 40(17), 5181-5192.

(110) Rismani-Yazdi, H.; Carver, S.M.; Christy, A.D.; Tuovinen, O.H. Cathodic limitations inmicrobial fuel cells: an overview. *J. Power Sources*. 2008, 180, 683-694.

(111) Pham, T.H.; Aelterman, P.; Verstraete, W. Bianode performance in bioelectrochemical systems: recent improvements and prospects. *TRENDS Biotechnol*. 2009, 27(3), 168-178.

(112) Schröder, U. Anodic electron transfer mechanisms in microbial fuel cells and their energy efficiency. *Phys. Chem. Chem. Phys.* 2007, 9, 2619-2629.

(113) Logan, B.; Cheng, S.; Watson, V.; Estadt, G. Graphite fiber brush anodes for increased power production in air-cathode microbial fuel cells. *Environ. Sci. Technol*. 2007, 41, 3341-3346.

(114) Dávila, D, Esquivel, J.P.; Vigués, N.; Sánchez, O.; Garrido, L.; Tomás, N.; Sabaté, N.; del Campo, F.J.; Muñoz, F..J.; Mas, J. Development and optimization of microbiol fuel cells. *J. New Mat. Elect. Syst*. 2008, 11, 99-103.

(115) Scott, K.; Rimbu, G.A.; Katuri, K.P.; Prasad, K.K.; Head, I.M. Application of modified carbon anodes in microbial fuel cells. *Process Saf. Environ. Prot*. 2007, 85, 481–488.

(116) Cheng, S.; Logan, B.E. Ammonia treatment of carbon cloth anodes to enhance power generation of microbial fuel cells. *Electrochem. Commun*. 2007, 9, 492-496.

(117) Park, D.H.; Zeikus, J.G. Improved fuel cell and electrode designs for producing electricity from microbial degradation. *Biotechnol. Bioeng*. 2003, 81, 348-355.

(118) Lowy, D. A.; Tender, L. M.; Zeikus, J. G.; Park, D. H.; Lovley, D.R. Harvesting energy from the marine sediment-water interface. II - Kinetic activity of anode materials. *Biosens. Bioelectron*. 2006, 21, 2058-2063.

(119) Schröder, U.; Nieβen, J.; Scholz, F. A generation of microbial fuel cell with current output boosted by more than one order of magnitude. *Angew. Chem. Int. Ed*. 2003, 42, 2880-2883.

(120) Niessen, J.; Schröder, U.; Rosenbaum, M.; Scholz, F. Fluorinated polyanilines as superior materials for electrocatalytic anodes in bacterial fuel cells. *Electrochem. Commun*. 2004, 6, 571-575.

(121) Rosenbaum, M.; Zhao, F.; Schröder, U.; Scholz, F. Interfacing electrocatalysis and biocatalysis with tungsten carbide: a high-performance, noble-metal-free microbial fuel cell. *Angew. Chem*. 2006, 118, 1-4.

(122) Yu, E.H.; Cheng, S.; Scott, K.; Logan, B.E. Microbial fuel cell performance with non-Pt cathode catalysts. *Journal of Power Sources*. 2007, 171, 275-281.

(123) Zhao, F.; Harnisch, F.; Schröder, U.; Scholz, F.; Bogdanoff, P.; Herrmann, I. Challenges and constraints of using oxygen cathodes in microbial fuel cells. *Environ. Sci. Technol*. 2006, 40(17), 5193-5199.

(124) Morris, J.M.; Jin, S.; Wang, J.; Zhu, C.; Urynowicz, M.A. Lead dioxide as an alternative catalyst to platinum in microbial fuel cells. *Electrochem. Commun*. 2007, 9(7), 1730-1734.

(125) Zhao, F.; Harnisch, F.; Schroder, U.; Scholz, F.; Bogdanoff, P.; Herrmann, I. Application of pyrolysed iron (II)phthalocyanine and CoTMPP based oxygen reduction catalysts as cathode materials in microbial fuel cells. *Electrochem. Commun.* 2005, 7, 1405–10.

(126) Oh, S.; Min, B.; Logan, B.E. Cathode performance as a factor in electricity generation in microbial fuel cells. *Environ. Sci. Technol*. 2004, 38(18), 4900-4904.

(127) Aelterman, P.; Versichele, M.; Genettello, E.; Verbeken, K.; Verstraete, W. Microbial fuel cells operated with iron-chelated air cathodes. *Electrochim. Acta*. 2009, 54, 5754-5760.

(128) You, S.; Zhao, Q.; Zhang, J.; Jiang, J.; Zhao, S. A microbial fuel cell using permanganate as the cathodic electron acceptor. *J. Power Sources*. 2006, 162, 1409-1415.

(129) Chae, K.J.; Choi, M.; Ajayi, F.F.; Park, W.; Chang, I.S.; Kim, I.S. Mass transport through a proton exchange membrane (nafion) in microbial fuel cells. *Energ. Fuels*. 2008, 22, 169-176.

(130) Harnisch, F.; Schröder, U:; Scholz, F. The suitability of monopolar and bipolar ion exchange membranes as separators for biological fuel cells. *Environ. Sci. Technol.* 2008, 42(5), 1740–1746.

(131) Rozendal, R.A.; Hamelers, H.V.M.; Molenkamp, R.J.; Buisman, C.J.N. Performance of single chamber biocatalyzed electrolysis with different types of ion exchage membranes. *Water Res*. 2007, 41, 1984-1994.

(132) Kim, J.R.; Cheng, S.; Oh, S.-E.; Logan, B.E. Power generation using different cation, anion, and ultrafiltration membranes in microbial fuel cells. *Environ. Sci. Technol*. 2007, 41, 1004-1009.

(133) Heijne, A.T.; Hamelers, H.V.M.; de Wilde, V.; Rozendal, R.A.; Buisman, C.J.N. A bipolar membrane combined with ferric iron reduction as an efficient cathode system in microbial fuel cells. *Environ. Sci. Technol*. 2006, 40, 5200-5205.

(134) Min, B.; Cheng, S.; Logan, B.E. Electricity generation using membrane and salt bridge microbial fuel cells. *Water Res.* 2005, 39, 1675-1686.

(135) Rabaey, K.; Ossieur, W.; Verhaege, M.; Verstraete, W. Continuous microbial fuel cells convert carbohydrates to electricity. *Water Sci. Technol*. 2005, 52, 515-523.

(136) He, Z.; Minteer, S.D.; Angenent, L.T. Electricity generation from artificial wastewater using an upflow microbial fuel cell. *Environ. Sci. Technol*. 2005, 39, 5262-5267.

(137) Min, B.; Logan, B.E. Continuous electricity generation fromdomestic wastewater and organic substrates in a flat plate microbial fuel cell. *Environ. Sci. Technol*. 2004, 38, 5809-5814.

(138) Rosenbaum, M.; Schröder, U.; Scholz, F. In situ electrooxidation of photobiological hydrogen in a photobioelectrochemical fuel cell based on Rhodobacter sphaeroides. *Environ. Sci. Technol*. 2005, 39, 6328-6333.

(139) Logan, B.E.; Murano, C.; Scott, K.; Gray, N.D.; Head, I.M. Electricity generation from cysteine in a microbial fuel cell. *Water Res*. 2005, 39, 942-952.

(140) Aelterman, P.; Rabaey, K.; Pham, T.H.; Boon, N.; Verstraete, W. Continuous electricity generation at high voltages and currents using stacked microbial fuel cells. *Environ. Sci. Technol*. 2006, 40, 3388-3394.

(141) Rabaey, K.; Clauwaert, P.; Aelterman, P.; Verstraete, W. Tubular microbial fuel cells for efficient electricity generation. *Environ. Sci. Technol*. 2005, 39, 8077-8082.

(142) Liu, H.; Logan, B.E. Electricity generation using air-cathode single chamber microbial fuel cell in the presence and absence of a proton exchange membrane. *Environ. Sci. Technol*. 2004, 38, 4040-4046.

(143) Liu, H.; Ramnarayanan, R.; Logan, B.E. Production of electricity during wastewater treatment using a single chamber microbial fuel cell. *Environ. Sci. Technol*. 2004, 38, 2281-2285.

(144) Liu, H.; Cheng, S.; Logan, B.E. Power generation in fed-batch microbial fuel cells as a function of ionic strenght, temperature, and reactor configuration. *Environ. Sci. Technol*. 2005, 39, 5488-5493.

(145) Gil, G.C.; Chang, I.S.; Kim, B.H.; Kim, M.; Jang, J.K.; Park, H.S.; Kim, H.J. Operational parameters affecting the performance of a mediator-less microbial fuel cell. *Biosens. Bioelectron*. 2003 18:327.

(146) Franks, A.E.; Nevin, K.P.; Jia, H.; Izallalen, M.; Woodard, T.L.; Lovley, D.R. Novel strategy for 3D real-time imaging of microbial fuel cell communities: monitoring the inhibitory effects of proton accumulation within the anode biofilm. *Energ. Environ. Sci.* 2009, 2(1), 113-119.

(147) Franks, A.E.; Nevin, K.P.; Glaven, R.H.; Lovley, D.R. Microtoming coupled to microarray analysis to evaluate the spatial metabolic status of *Geobacter sulfurreducens biofilms. ISME J.* 2010, 4(4), 509, 519.

(148) Parameswaran, P.; Torres, C.I.; Lee, H.; Krajmalnik-Brown, R.; Rittmann, B.E. Syntrophic interactions among anode respiring bacteria (ARB) and non-ARB in biofilm anode: electron balances. *Biotechnol. Bioeng*. 2009, 103(3), 513-523.

(149) Jung, S.; Regan, J.M. Influence of external resistance on electrogenesis, methanogeneis, and anode prokaryotic communities in microbial fuel cells. *Appl. Environ. Microbiol*. 2011, 77(2), 564-571.

(150) Marcus, A.K.; Torres, C.I.; Rittmann, B. Conduction-based modeling of the biofilm anode of a microbial fuel cell. *Biotechnol. Bioeng.* 2007, 98, 1171–1182.

(151) Wagner, R.C.; Call, D.F.; Logan, B.E. Optimal set anode potentials vary in bioelectrochemical systems. *Environ. Sci. Technol.* 2010, 44(16), 6036-6041.

(152) Pham, H. T.; Boon, N.; Aelterman, P.; Clauwaert,P.; De Schamphelaire, L.; van Oostveldt, P.; Verbeken, K.; Rabaey, K.; Verstraete, W. High shear enrichment improves the performance of the anodophilic microbial consortium in a microbial fuel cell. *Microb. Biotechnol*. 2008, 1, 487-496.

Chapter 1

Effect of the cathode/anode ratio and the choice of cathode catalys on the performance of microbial fuel cell transducers for the determination of microbial activity.

Partially published in Proceedia Engineering
Totally published in Sensor and Actuators B: Chemical

CHAPTER 1.

EFFECT OF THE CATHODE/ANODE RATIO AND THE CHOICE OF CATHODE CATALYST ON THE PERFORMANCE OF MICROBIAL FUEL CELL TRANSDUCERS FOR THE DETERMINATION OF MICROBIAL ACTIVITY

ABSTRACT

Microbial activity can be measured using sensors based on microbial fuel cell technology. In these sensors, microorganisms in contact with the anode generate a current proportional to their metabolic activity. Proper operation of such a device requires that activity at the anode is not impaired by the ability of the cathode to transfer current to the cathodic electron acceptor. Therefore, we have determined the minimum cathode to anode ratio required for unhindered performance of the microbial fuel cell. Our results indicate that for the same level of biological activity, the optimal cathode/anode ratios depend on the type of cathode being used. Thus, while carbon paper/ferricyanide cathodes require ratios of 4, platinum cathodes need much higher ratios of about 27. Cyclic voltammetry measurements indicate that platinum cathodes have a much slower dynamic behaviour than cathodes based on carbon paper/ferricyanide. While these results indicate that carbon paper/ferricyanide cathodes provide the most current for the same cathode area, extended experiments carried over a period of several days indicate a progressive degradation of fuel cell performance in cells using iron catalysts. Overall, our conclusion is that soluble iron-based catalysts provide much higher power output than solid phase platinum catalysts, but at the expense of a reduced life span, which limits their use for applications, requiring extended operation.

INTRODUCTION

During recent years, a number of different sensor types using impedance spectroscopy, fluorescence or optical density have been proposed for the detection and quantification of microbial biomass in liquid samples. In some instances, the models proposed have actually been commercialized. However, efficient systems for the quantification of bacterial activity have not yet been described.

Microbial Fuel Cells (MFCs) provide a viable transducing mechanism for the determination of microbial activity in liquid samples. In some specific instances, the principle has been used for specific applications such as detection of toxicity [1,2,3]. Utilization of MFCs as sensing devices requires however their ability to respond to changes in the level of biological activity present in the anode compartment. The problem is that power output, and therefore signal output of a MFC is also dependent on several other factors. Between them, the surface area of the proton exchange membrane (PEM) and the relative sizes of the anode and cathode seem to play an important role [4]. The power values obtained are usually normalized in order to make the efficiency of power production by different MFCs comparable. In many studies, this normalization is carried using the surface area of the anode, assuming that bacterial activity limits power output. However, recent reports demonstrating that tripling the surface area of the cathode increased power density by 22% [4,5] indicate otherwise.

Additionally, the choice of the cathode material is another factor to consider depending on the application [6]. For oxygen reduction different cathode materials have been proposed. Platinum is the best known [7]. However, due to its high cost [8], tendency to poisoning by the formation of platinum oxide layer at the surface [6,9,10], and sensitivity to biological and chemical fouling [11,12], platinum based electrodes are not useful for all applications. For this reason, different and cheaper alternatives to noble metal catalyst have been studied such as pyrolysed iron(II) phthalocyanine (Pyr-FePc) and cobalttetramethoxyphenylporphyn (CoTMPP) applied on graphite cathodes [13,9].

Other materials such as carbon paper or graphite can also be used with a soluble catalyst, which accelerates the poor oxygen reaction on these electrode materials. The couple ferric/ferrous iron is a good electron mediator for oxygen reduction for three reasons: fast reaction at carbon electrodes [14,15], high standard potential (+0.77 V vs. SHE), and possible biological oxidation of ferrous iron to ferric iron with oxygen as the electron acceptor up [16,15].

Ferricyanide is the catalyst most extensively used due to its high solubility in water and the fact that replaces the use of precious metal in the cathode. Moreover it has a standard potential of 0.361 V that, due to the short polarization of the cathode, is quite close to the real potential achieved [15,17,18]. So, despite the fact that oxygen reduction has a standard potential supposedly higher than ferricyanide reduction [18] in practice this is not true and a higher energy yield is obtained with ferricyanide. Nevertheless, ferricyanide has some disadvantages that have drawn the attention to the use of alternative ferric iron catalysts such as sulphate or iron chloride [9]. Ferricyanide is commonly used as a catalyst in MFC cathodes, but due to the very slow re-oxidation rate by oxygen, it is not regarded as sustainable [6,9]. On the other hand, other ferric iron sources precipitate at neutral pH. To avoid this precipitation the use of chelating agents is required such as ethylenediaminetetraacetic acid (EDTA) [19,20,9].

In this study, we attempt to determine the optimal cathode/anode ratio for both solid surface and soluble catalysts as well as to compare the performance and stability of different types of catalysts when used in the cathode compartment of MFC transducers for prolonged periods of several days.

EXPERIMENTAL PROCEDURE

Bacterial strains and their cultivation

Shewanella oneidensis strain MR1 (ATCC 7005500) was grown aerobically in 100 mL of Trypticase Soy Broth (TSB) at 27ºC. After 36 hours of aerobic growth, the cells were harvested by centrifugation (10100 *g* x 15 min, 4ºC) using a 5804R Eppendorf centrifuge. For subsequent

adaptation to anaerobic conditions, the resulting pellet was resuspended in 1 L of AB minimal medium ($[NH_4]SO_4$ 2 g, Na_2HPO_4 7.31 g, KH_2PO_4 7.85 g, NaCl 3 g, Na_2SO_4 0.011 g, $MgCl_2 \cdot 6H_2O$ 0.2 g, CaCl 3.625 mg, $FeCl_3 \cdot 6H_2O$ 0.2 mg). After inoculation the medium was supplemented with lactate (0.02 M) as the carbon source and fumarate (0.1 M) as electron acceptor, and further incubated with agitation at room temperature for 48 hours. After this period the culture was centrifuged and inoculated in AB minimal medium with lactate (0.02 M), so the culture was ready for inoculation into a fuel cell.

Microbial Fuel Cell design and measurements

Fuel cell architecture and assembly

In this study, a two-chamber fuel cell was used. The cell was built using two solid (4x11x11 cm) methacrylate blocks (Figure 1). The interior of each block had been machined to form an inner cylindrical reactor with a volume of 130 mL. The top of the blocks was drilled to provide ports for inoculation and sampling as well as electrical connections for both the anode and the cathode.

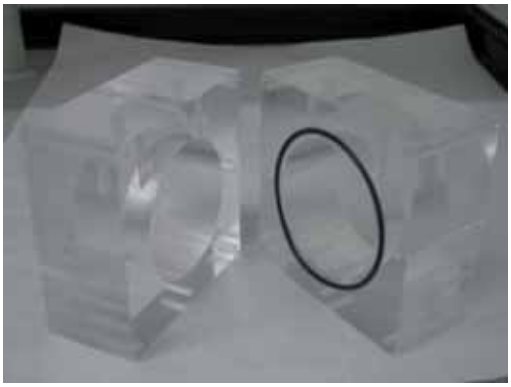

Figure 1. Methacrylate blocks used to MFCs construction.

The two methacrylate blocks were assembled around a proton exchange membrane (PEM) and held in place by means of stainless steel screws. The membrane employed was Nafion®117 (Ion power, Inc.) with a thickness of 183 µm and effective area of 38.46 cm^2. The reactor was made watertight using a rubber gasket (76x3 mm) between both methacrylate blocks, which exerted pressure on the membrane.

Electrodes

In the anode chamber, carbon paper electrodes (B2120 Toray Carbon Paper Designation TGPH-120, plain, no wet proofing; E-Tek, Inc.) with a thickness of 0.35 mm were used in all cases (Figure 2D). This material is very common in MFC because it has a high conductivity (electrical resistivity of 80 mΩ·cm through plane) and is well suited for bacterial growth [18].

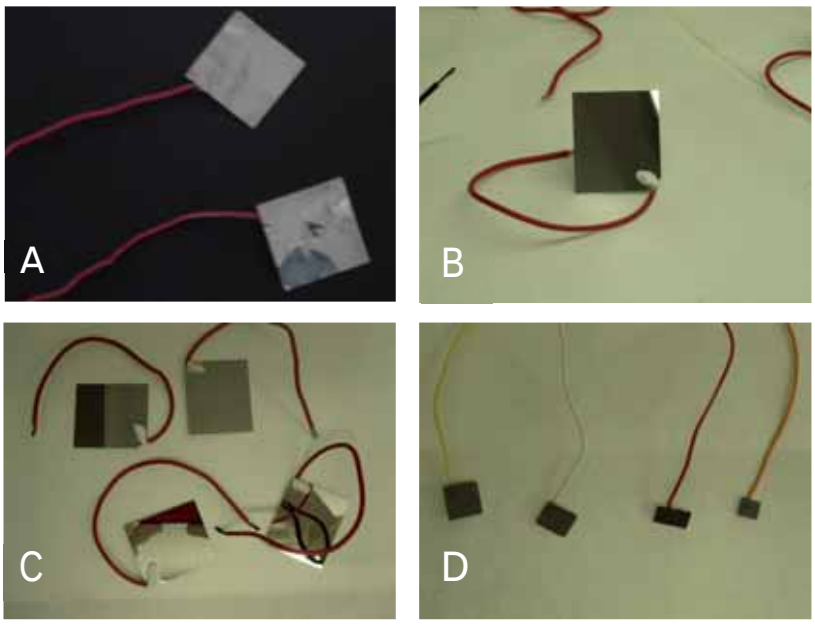

Figure 2. Electrode materials used in this study: platinum foil (A), black platinum-silicon wafer (B), platinum-silicon wafers (C), carbon paper (D).

In the cathode chamber, different electrode materials were employed. On the one hand, four metal or metal coated cathodes were used: commercial platinum foil (Figure 2A), black platinum (Figure 2B), silicon wafers coated with platinum (Figure 2C), and a heavy duty commercial stainless steel scourer woven from a single strand of stainless steel. Platinum foil was obtained from a commercial source (Goodfellow Cambridge Limited), with a purity of 99.95% and a thickness of 0.1 mm. The silicon wafers with platinum were produced by thin-film technology using 4" double side polished silicon wafers. A first titanium layer of 150 Å was deposited as adhesion promoter, followed by 1500 Å platinum layer deposited in both sides. The metallization was performed in a single process using electron beam evaporation. Black platinum was obtained using the same procedure but modifying parameters that provide a metal layer with higher rugosity.

On the other hand, carbon paper electrode with a size of 12 cm^2 was used. The main difference when this material is employed for the cathode is that a catalyst is usually necessary in order to accelerate the reduction of oxygen. In our case, we used three different liquid catalysts: ferricyanide (0.05 M $K_3[Fe(CN)_6]$ in a 0.1 M phosphate buffer), EDTA chelated iron sulphate (0.5 M $Fe_2(SO_4)_3$, 0.1 M EDTA) and EDTA chelated iron chloride (0.5 M $FeCl_3$, 0.1 M EDTA).

Each electrode was welded to the wire using conducting silver loaded epoxy (RS Components) with all exposed surfaces of the wire covered with epoxy as well. The weldings were covered with a non corrosive silicone rubber coating (RS Components).

Microbial Fuel Cell operation and characterization

Once the fuel cells were assembled the two chambers were filled through the sampling ports. Inoculation of the fuel cells was made at a final concentration of approximately 10^8 cells·mL^{-1} in AB minimal medium. Lactate (0.02 M), used as the carbon source was added only once right before inoculation. Both, anode and cathode were stirred slowly (250 rpm). The cathode was pumped with air and nitrogen was injected into the anode headspace to avoid oxygen inputs. After inoculation the electrodes were connected to a source meter and current output was monitored. The measurements were made with 2 source meter units (Keithley®2612) connected to a personal

computer that allow simultaneous monitoring of up to 4 independent fuel cells. Data collection was automatized using a custom made program developed with LabView 8.5 (Nationals Instruments).

For MFC characterization, IV curves were built at selected times. IV curves were performed by imposing different output current values between the cell electrodes and measuring the resulting voltage. So, current initially set to 0 µA, was increased stepwise with an interval of time between steps of 3 minutes. For each current step, the device measured the output voltage. The curve ended when the voltage reached 0. The power was calculated as the product of the values of voltage and current.

Electrochemical characterization of the cathodes

Cyclic voltammetries were performed on a potentiostat/galvanostat model FRA2 Micro-Autolab Type II. The electrochemical cell was kept at 25ºC and maintained in a Faraday cage to avoid external noise. An Ag/AgCl electrode (Metrohm, Switzerland), and a platinum-ring electrode (Metrohm, Switzerland) were used as reference and auxiliary electrode respectively. The system was operated through a PC using GPES software.

Platinum/oxygen and carbon paper/ferricyanide electrodes were compared by cyclic voltammetry at a scan rate of 20 $mV \cdot s^{-1}$. For the platinum-oxygen system, the electrochemical cell was filled with oxygen saturated 0.5 M potassium nitrate and using a platinised silicon wafer as the working electrode. In the case of carbon paper-Fe system, a working electrode of carbon paper was submerged in 1 mM potassium hexacyanoferrate (II) dissolved in the 0.5 M potassium nitrate.

Cyclic voltammetries of the platinum and black platinum silicon wafer cathodes were performed at different scan rates (2 $mV \cdot s^{-1}$ to 500 $mV \cdot s^{-1}$) in 1 mM potassium hexacyanoferrate (II) dissolved in 0.5 M potassium nitrate. Before performing the voltammetry, the solution was flushed with nitrogen to remove the oxygen.

Experimental design

Impact of the ratio cathode/anode on the power output of MFCs with soluble and solid catalysts

To study the effect of the ratio cathode/anode four identical fuel cells were inoculated with *Shewanella oneidensis* MR-1 at a final concentration of 10^8 cfu·mL^{-1} in AB minimal medium, supplemented with 0.02 M lactate as anolyte.

As a model of soluble catalyst, ferricyanide was used to study the influence of cathode/anode relation. We compared four different anode sizes (1.5 cm^2, 3 cm^2, 6 cm^2 and 12 cm^2) while maintaining a constant cathode of 12 cm^2. The cathode had phosphate buffer (0.1 M) with 0.05 M ferricyanide.

For solid catalysts the experiment was repeated using a 13.55 cm^2 platinum-coated silicon wafer as the cathode in all cells while using 0.1 M buffer phosphate as catholyte. Four reactors were assembled with different anode sizes of 0.25, 0.5, 0.75 and 1 cm^2. The anode sizes were much smaller than in the previous experiment as preliminary trials indicated that solid catalysts used at the cathode surface reach power densities an order of magnitude lower than soluble catalysts.

Characterization of the MFCs was executed at start up, before detectable growth occurred, by means of one initial (t = 0) IV curve. At the time of inoculation, since all the MFCs shared the same inoculum, differences between them could be only attributed to the ratios cathode/anode used. The maximum power density obtained for each cathode/anode ratio in this curve, was represented as a function of the ratio.

Our experimental set up allows the simultaneous study of 4 microbial fuel cells. In this experiment we decided to use the 4 cells to study 4 different cathode/anode ratios instead of running replicate experiments. The variability of the experimental results was thus determined in separate experiments in which identical fuel cells were inoculated with the same culture giving relative standard errors inferior to 10%. The relative standard errors increased up to 40-50% when fuel cells

were filled with different inocula. Therefore, whenever possible we have attempted to run comparison experiments using the same inoculum.

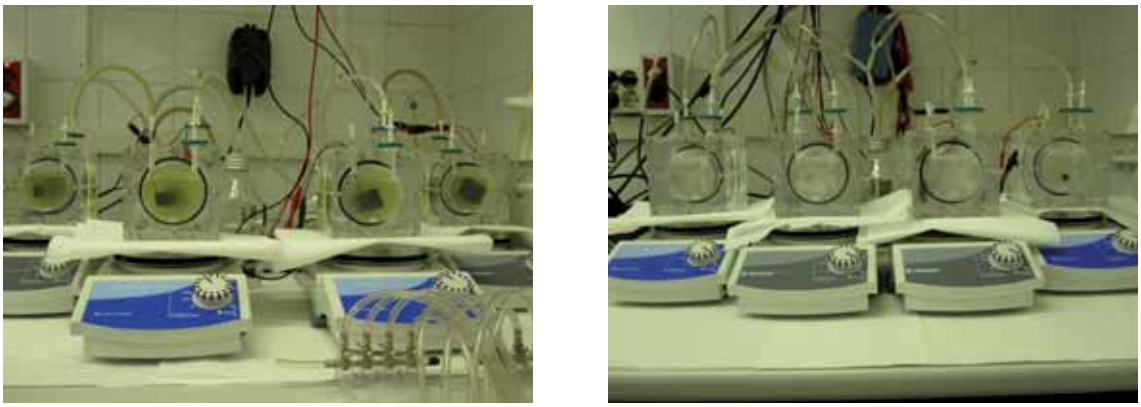

Figure 3. Images of the experimental setup using Fe-based soluble catalysts (A) and Pt-based catalysts (B).

Long term performance of different solid and soluble catalysts

To analyze the extent to what long term performance of the cathode was affected by the type of material being used we constructed several MFCs with different solid catalysts such as a commercial platinum foil (6.25 cm^2), platinum-coated silicon (13.55 cm^2), black platinum silicon (13.55 cm^2), and stainless steel (529.5 cm^2), and liquid catalysts such as ferricyanide, EDTA chelated iron sulphate and EDTA chelated iron chloride.

As in the previous experiment, the anode composition was the same in all MFCs and contained a culture of *Shewanella oneidensis* MR-1 at a concentration of about 10^8 $cfu \cdot mL^{-1}$ in AB minimal medium, supplemented with 0.02 M lactate. The anode size was 0.5 cm^2 in the case of MFCs with solid catalysts, and 3 cm^2 in the case of MFCs with liquid catalysts.

In the MFCs with solid catalyst, the cathode contained 0.1 M phosphate buffer and one of the electrodes mentioned above. Fuel cells with carbon paper electrode had ferricyanide, EDTA chelated iron sulphate and EDTA chelated iron chloride as soluble catalysts, all at a concentration of 0.05 M. Both, anode and cathode were stirred slowly (250 rpm). The cathode was pumped with air and nitrogen was injected into the anode headspace to avoid oxygen inputs.

The fuel cells were run for 5 to 7 days. During this period they were monitored by carrying out IV curves preceded by a 1 hour stabilization period during which the cell circuit was open and voltage was allowed to stabilize.

RESULTS AND DISCUSSION

Impact of the ratio cathode/anode on the power output with solid and soluble catalysts

Power output in microbial fuel cells depends on the properties of the anode as electron acceptor for the microbial populations as well as on the properties of the cathode as a catalyst for oxygen reduction. But it also depends to a rather large extent on the abundance and level of activity of the microbial components. It turns out that when comparing different electrode materials, growth of the biological components is strongly affected by the material used. Thus in fuel cells containing cathodes of different sizes or catalytic performances, growth can range from virtually non existent to exuberant. When comparing these cells, the bulk of the differences observed would be caused by the large difference in biomass found between both cells despite the fact that both used exactly the same inoculum. In order to avoid this problem, only the results corresponding to the IV curve obtained right after the inoculation were used in this experiment. That way it is sure that biomass concentration is the same and that the results obtained depends only on the cathode/anode ratio.

Soluble catalysts

In the study carried out using soluble iron ferricyanide as a catalyst the IV curves (Figure 3A) indicate very similar values of open circuit voltage (OCV), between 300 and 400 mV with a

maximum difference of about 76 mV. The observed voltage drop when increasing current output was more pronounced the smaller was the anode surface. The IV plots also indicate that maximum current and power values increased when increasing the anode area (0.125 mA and 5.35 µW for 1.5 cm^2 anode, 0.27 mA and 10.32 µW for 3 cm^2 anode, 0.4 mA and 17.45 µW for 6 cm^2 anode and, 0.68 mA and 28.82 µW for 12 cm^2 anode).

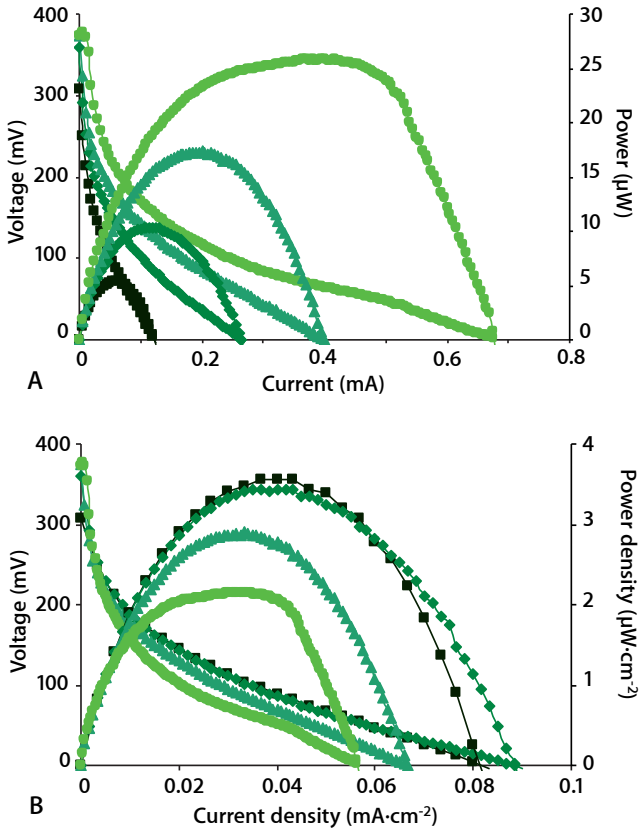

Figure 3. Initial IV curves made at the time of inoculation (A) without normalized values and (B) with values normalized by the anode area (Ratios cathode/anode, ■ : 8, ◆ : 4, ▲ : 2, ● : 1).

Normalizing power and current values to the area of the anode (Figure 3B) shows that the MFCs with the highest performance (higher current and power output per surface unit) are those with smaller anodes. Increasing the anode size to ratios cathode/anode below 4 causes a clear decrease in the normalized power and current values.

Plotting normalized maximum power density against the ratio cathode/anode (Figure 4) again indicates this fact. The results show that attempts to increase power output by maximizing power production in the anode (through increasing the size of the anode or the concentration of bacteria) in fuel cells that use soluble mediators are severely hampered by the performance of the cathode. This can be attributed to the appearance of mass transfer problems at the surface of the cathode [21].

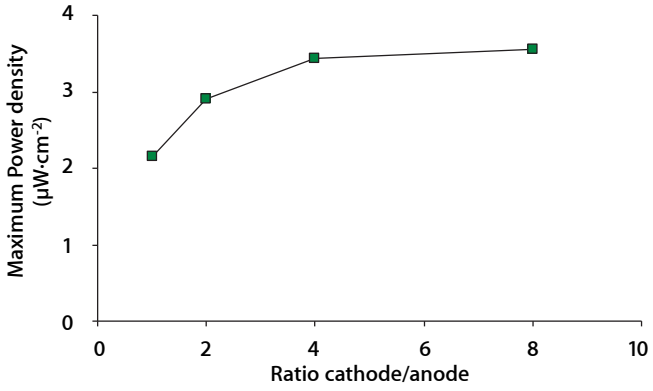

Figure 4. Relation between maximum power density values of initial IV curves obtained for the different anode sizes MFCs with liquid catalyst and the ratio cathode/anode.

Solid catalysts

When the study was performed using platinum as a cathode catalyst the IV curves (Figure 5) showed open circuit voltages between 200 and 300 mV in the four cells. As in the previous experiment, maximum current and power outputs tended to increase when increasing anode size (Figure 5A).

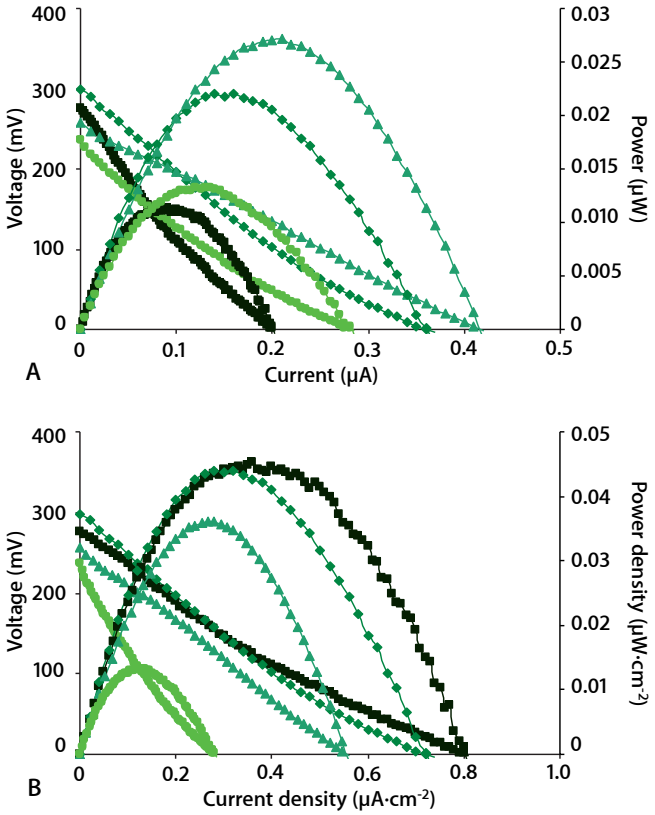

Figure 5. Initial IV curves made at the time of inoculation (A) without normalized values and (B) with values normalized by the anode area (Ratios cathode/anode, ■ : 54.6, ◆ : 27.3, ▲ : 18.2, ● : 13.65).

Also as in the previous experiment, current and power values normalized to the anode surface show that maximum values are obtained with the small anode areas (Figure 5B). However, plotting maximum values of normalized power output against the ratio cathode/anode (Figure 6) indicates that the cathode becomes limiting at ratios below 30.

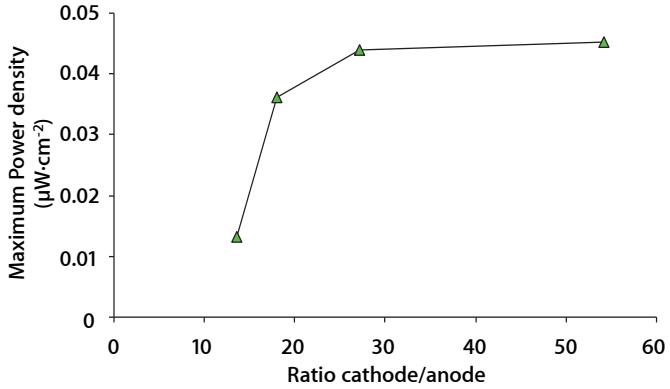

Figure 6. Relation between maximum power density values of initial IV curves obtained for the different anode sizes MFCs with solid catalyst, and the ratio cathode/anode.

Long term performance of different solid and soluble catalysts

Once we established the optimal cathode/anode ratio for both solid and soluble catalysts, we proceeded to evaluate the ability of different soluble and solid catalysts to operate at the cathode of a microbial fuel cell for extended periods of time.

As stated in materials and methods, several solid (solid platinum, silicon oxide covered with platinum and black platinum, and stainless steel) as well as soluble (ferricyanide, EDTA chelated iron sulphate and EDTA chelated iron chloride) catalysts were used.

For each catalyst, after inoculating the fuel cells, maximum power output as a function of time was estimated from individual IV curves taken at different times. Maximum power was then normalized to the area of the cathode and the results, expressed as maximum power densities, have been plotted in Figure 7 and 9.

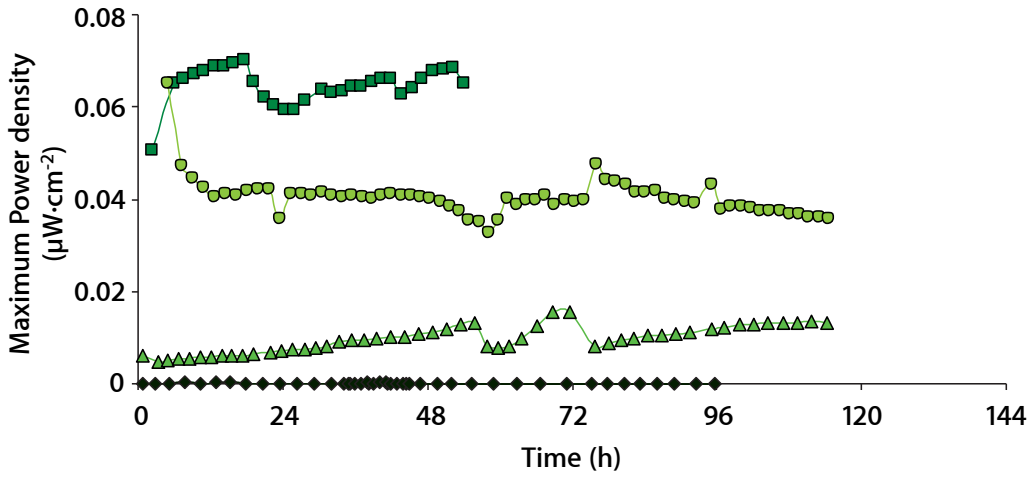

Figure 7. Evolution of the maximum power density, obtained in the IV curves made all along the experiment, in MFC transducers using platinum (■), black platinum (●), silicon wafer-based platinum (▲), and stainless steel (♦) as cathode catalysts.

Figure 7 shows the variation with time of maximum power output in fuel cells containing 4 different solid catalysts. The results indicate that, except for the case of the platinum covered silicon wafer that seems to increase with time, the rest of the materials (black platinum covered silicon, solid platinum and stainless steel) are quite stable, being able to provide a low but sustained power output at values that range between a maximum average of 0.065 $\mu W \cdot cm^{-2}$ in the case of solid platinum, and a minimum average of 0.0001 $\mu W \cdot cm^{-2}$ in the case of stainless steel. Also, the power densities obtained were extremely dependent on the type of material used. The highest power density was obtained with solid platinum foil. Because platinum foil is prohibitively

expensive for mass production, other materials were tested. Thin layers of platinum deposited on top of wafers of silicon oxide might provide an inexpensive alternative. As a control we used stainless steel. Not surprisingly, stainless steel provided the lowest, by far, power density. Platinum-covered silicon oxide wafers were unable to match the power output of solid platinum, a fact for which we have no clear cut answer but which might be related to the extreme smoothness of the silicon chip surface. To increase the roughness of the electrode, some of the silicon oxide wafers were coated with a thin layer of black platinum, in which the coating metal surface presents a much higher roughness. Black platinum coated electrodes had a power density much higher than smooth surface platinum.

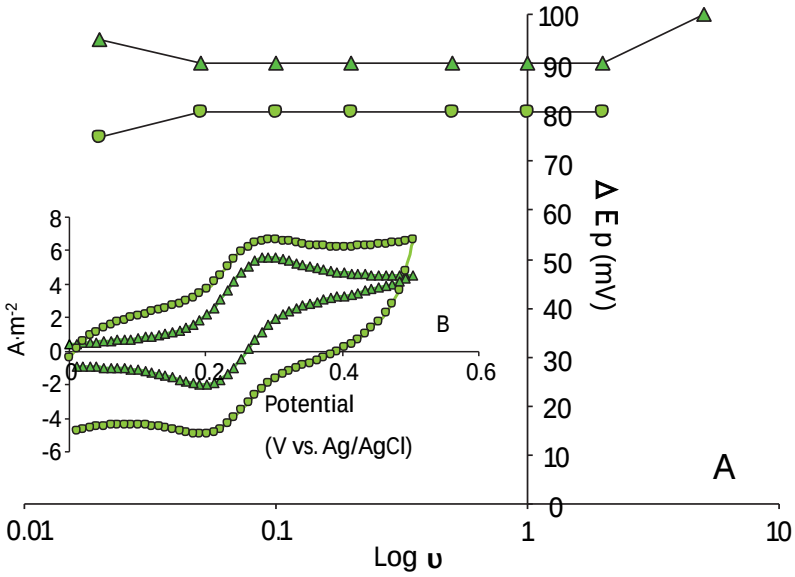

Figure 8.A. Variation of oxidation and reduction peak separation of silicon wafer –based platinum (▲) and black platinum (●) cyclic voltammograms at different potential scan rates. B. Cyclic voltammograms of silicon wafer–based platinum (▲) and black platinum (●) at potential scan rate of 50 $mV \cdot s^{-1}$.

In an attempt to explain the different behaviour of platinum and black platinum we ran cyclic voltammetries of both electrode types. Voltammetry can be used for testing the performance of the electrodes. By analysing the variation of peak position as a function of scan rate it is possible to gain an estimate for the electron transfer rate constants [22]. So, Figure 8A shows the separation of cathodic and anodic peak potential of each voltammogram, made at different scan rates in the range between 2 $mV \cdot s^{-1}$ and 500 $mV \cdot s^{-1}$ for black platinum and silicon wafer-based platinum electrodes in ferrocyanide. The difference between redox peaks with the increase of scan rate is very stable in both cases.

However, this distance is smaller for black platinum indicating improved catalytic activity. Additionally, as seen in the voltammograms obtained with a scan rate equal to 50 $mV \cdot s^{-1}$ (Figure 8B), black platinum obtained higher redox peak currents and higher graphic amplitude due to their higher capacitance. It should be noted that many electrode materials used in MFCs cannot produce reversible electrochemical reactions even for the classic reversible redox couple $Fe(CN)_6^{-3}$ /$Fe(CN)_6^{-4}$. The main reason for this is that the heterogeneous processes of electrode reactions can be significantly affected by the microstructure, roughness and function groups present on the electrode surface [23]. Thus, these voltammetries confirm black platinum as a viable alternative in the cathode of MFCs due to its higher roughness and better catalytic and charge-transfer capacity.

When long term experiments were attempted using soluble catalysts, the observations were quite different. Figure 9 shows the results obtained during 7 days of continuous operation. A common pattern observed in the three soluble catalysts used was a progressive increase in power density that probably reflects the development of biological populations in the anode compartment. This rapid increase could not be observed in the solid catalyst experiments because maximum power output was about one order of magnitude lower, and thus, did not allow the bacteria to fully express their maximum power production.

The increase in power output observed when using soluble catalysts was followed by a progressive decrease, above all in the case of the ferricyanide cell. We first attributed this decrease to lactate depletion. However, a quick calculation shows a coulombic yield of 1003 C from the oxidation of

0.02 M lactate to acetate (4 mol e^-/mol lactate). If we take into account a coulombic efficiency of 50% as reported for pure cultures of *Shewanella oneidensis* MR-1 [24], the amount of charge released should be about 500 C. The amount of charge produced by our cells up to the inflection point is only 64 C, much less than the amount released if all lactate had been consumed.

The drop could also be related to a lowering of the Fe^{3+}/Fe^{2+} ratio due to an insufficient reoxidation of these iron chelates by oxygen. For this reason, the drop would occur first in the cells with higher current values, but again the amount of oxidized iron available is more than sufficient to accept all the electrons released during the oxidation of 0.02 M lactate.

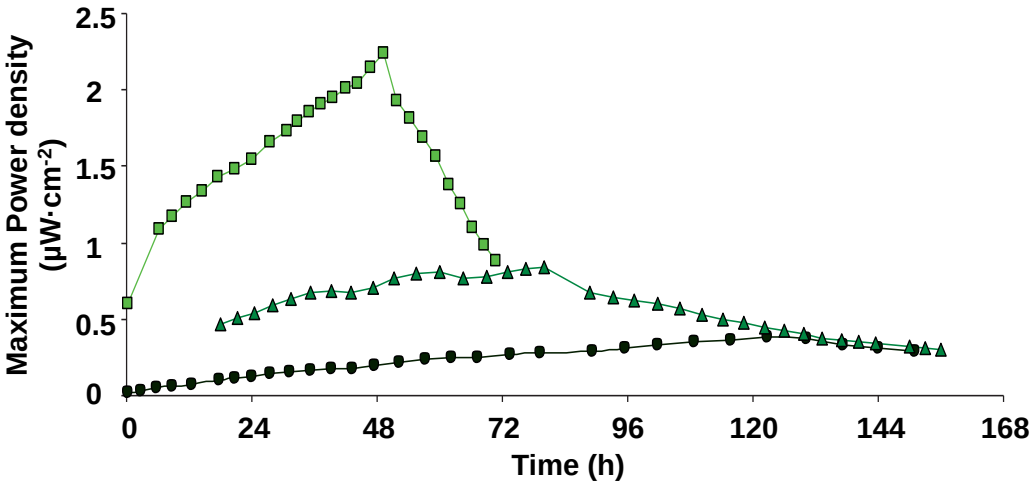

Figure 9. Evolution of the maximum power density, obtained in the IV curves made all along the experiment, in MFC transducers using liquid catalysts: Ferricyanide (■), EDTA-iron sulphate (▲) and EDTA-iron chloride (●).

We observed that the fall in maximum power density coincided with the onset of iron diffusion through the proton exchange membrane. The cation exchange membrane could not maintain the low catholyte pH required to keep ferric iron soluble. Cation exchange membranes transport

cations other than protons, which can cause a pH rise in the cathodic compartment [25,15]. This pH rise caused extensive iron precipitation that damaged the membrane [15]. Diffusion of iron through the membrane can also cause a decrease in fuel cell performance because bacteria use this iron as electron acceptor instead of electrode.

The data collected in this experiment show maximum power densities (0.38, 0.83 and 2.24 $\mu W \cdot cm^{-2}$) much higher than the maximum obtained with solid platinum foil (0.07 $\mu W \cdot cm^{-2}$). This difference of 10-20 times in power output when changing from a Pt-oxygen cathode (solid platinum, silicon oxide covered with platinum and black platinum) to a carbon paper-Fe (ferricyanide, EDTA chelated iron sulphate and EDTA chelated iron chloride) is much higher than reported increases of 1.5 to 1.8 times in similar experiments [5,4]. To confirm this data, we carried out a separate electrochemical study running cyclic voltammetries of Pt-oxygen and carbon paper-Fe systems. The results confirm the experimental observations made in the MFCs.

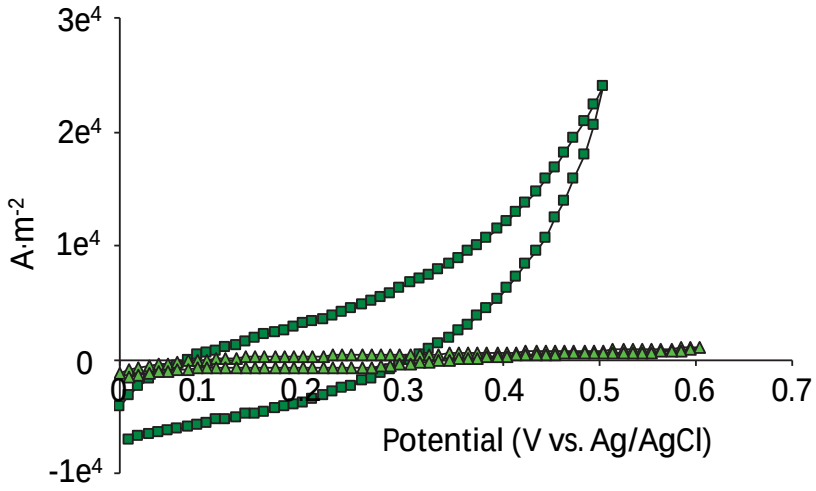

Figure 10. Cyclic voltammograms of oxygen reduction on silicon wafer based platinum (▲) and ferric reduction (■) on carbon paper electrode at a potential scan rate of 0.2 $V \cdot s^{-1}$.

So, in Figure 10 is possible to observe the maximum values obtained by the carbon paper-Fe system are on the order of 20 fold higher ($2.4e^4$ $A{\cdot}m^{-2}$) than the obtained by the Pt-oxygen system ($2.4e^3$ $A{\cdot}m^{-2}$).

The discrepancy between our 10-20 fold increase and the 1.5-1.8 fold increase reported by Oh *et al*. [5,4] is probably related to the fact that this authors use platinised carbon paper instead a platinum. It is likely that platinised carbon paper has a much higher roughness and therefore, a much higher effective area than our platinum electrodes. The large difference observed, thus, is not a result of much higher electron transfer efficiency when using ferricyanide, but of a much lower transfer rate of our solid catalysts due to their smooth surface.

The higher power values observed when using soluble catalysts, such as ferricyanide or iron-chelating catholytes versus solid surface catalysts is both a function of the different potentials of the chemicals (lower activation energy) as well as the higher mass transfer efficiency [5]. Activation losses at the cathode have been identified as the dominant limitation in MFCs [11,12], particularly due to low proton availability [10,12]. Concentration overpotentials are associated with the concentration gradient of the reagents and products in the proximity of the electrode. Inefficient mass transfer through diffusion and convection of substrate or removal of products may limit the maximal current production at an electrode [26].

Besides, the formation of mixed potentials and the flow of internal currents have been reported in the case of platinum based electrodes, due to the permeation of fuel from the anode. Fuel crossover through the separator membrane into the cathode compartment may considerably decrease the electrode performance due to the formation of mixed potentials and the flow of internal currents causing a depolarization even at open circuit [27,28].

Another factor that may play a role in the order of magnitude difference observed between solid surface catalysts and soluble catalysts might be related to the fact that during the first part of the experiment, iron acts as an electron acceptor rather than as a shuttle/catalyst for oxygen reduction. As soon as the pool of oxidized iron falls below a certain level, the cathode reaction becomes

limited by the kinetics of oxygen reduction by iron, which is clearly slower than the kinetics of iron reduction at the cathode surface [7]. As soon as the MFC shifts from iron reduction to oxygen reduction, an additional factor comes into play. Whereas iron reduction and thus its redox potential are independent of the proton concentration, the oxygen reduction reactions involve the consumption of one proton per transferred electron, no matter whether the reaction proceeds to water or to hydrogen peroxide. The consequence is a thermodynamically controlled shift of the polarization curve toward more negative values, which, depending on the nature and thus pH dependence of the anodic reaction, significantly reduces the MFC potential and power output [7].

CONCLUSIONS

In order for the anode to provide its full signal range when used as a sensing element, the performance of the device cannot be limited by the cathode. The area ratio cathode/anode above, which the cathode ceases to be limiting, depends on the type of catalyst used. For soluble cathode catalyst, ratios above 3 to 4 are enough to guarantee full performance of the anode. When solid cathode catalysts are used ratios above 27 must be used to ensure the same performance.

As a rule, fuel cells with liquid catalysts in the cathode provide much higher power densities than cells using solid surface catalysts. Our results seem to indicate that this is probably related to the fact that during the first days of operation of the MFC, iron acts as an electron acceptor rather than as a mediator for oxygen reduction.

The different solid surface catalysts tested provide a relatively low but very stable signal making them suitable for applications requiring extended operation, but in which high sensitivity is not needed. Transducers using liquid catalysts provide an alternative when higher output is required, but at the expense of a limited operation span.

Acknowledgements

This work was supported by grants CSD2006-00044 TRAGUA (CONSOLIDER-INGENIO2010) and CTQ2009-14390-C02-02 from the Spanish Ministry of Education and Science to JM.

REFERENCES

(1) Dávila, D.; Esquivel, J.P.; Sabaté, N.; Mas, J. Silicon-based microfabricated microbial fuel cell toxicity sensor. *Biosens. Bioelectron*. 2011, 26, 2426-2430.

(2) Kim, M.; Hyun, M.S.; Gadd, G.M.; Kim. H.J. A novel biomonitoring system using microbial fuel cell. *Environ. Monit*. 2007, 9, 1323-1328.

(3) Tront, J.M.; Fortner, J.D.; Plötze, M.; Hughes, J.B.; Puzrin, A.M. Microbial fuel cell biosensor for in situ assessment of microbial activity. *Biosens. Bioelectron*. 2008, 24, 586-590.

(4) Oh, S.E.; Logan, B.E. Proton exchange membrane and electrode surface areas as a factor that affect power generation in microbial fuel cells, *Appl. Microbiol. Biotechnol*. 2006, 70, 162-169.

(5) Oh, S.E.; Min, B.; Logan, B.E. Cathode performance as a factor in electricity generation in microbial fuel cells, *Environ. Sci. Technol*. 2004, 38, 4900-4904.

(6) Logan, B.E.; Hamelers, B.; Rozendal, R.; Schröder, U.; Keller, J.; Freguia, S.; Aelterman, P.; Verstraete, W.; Rabaey, K. Microbial Fuel Cell: Methodology and Technology. *Environ. Sci.Technol*. 2006, 40, 5181-5192.

(7) Zhao, F.; Harnisch, F.; Schröder, U.; Scholz, F.; Bogdanoff, P.; Herrmann, I. Challenges and constraints of using oxygen cathodes in microbial fuel cells. *Environ. Sci.Technol*. 2006, 40, 5193-5199.

(8) Yu, E.H.; Cheng, S.; Scott, K.; Logan, B.E. Microbial fuel cell performance with non-Pt cathode catalysts. *J. Power Sources.* 2007, 171, 275-281.

(9) Aelterman, P.; Versichele, M.; Genettello, E.; Verbeken, K.; Verstraete, W. Microbial fuel cells operated with iron-chelated air cathodes. *Electrochim. Acta*. 2009, 54, 5754-5760.

(10) Zhuwei, D. ; Li, H.; Gu, T. A state of the art review on microbial fuel cells: a promising technology for wastewater treatment and bioenergy. *Biotechnol. Adv*. 2007, 25, 464-482.

(11) Rismani-Yazdi, H.; Carver, S.M.; Christy, A.D.; Tuovinen, O.H. Cathodic limitations in microbial fuel cells: An overview. *J. Power Sources*. 2008,180, 683-694.

(12) Erable, B.; Etcheverry, L.; Bergel, A. Increased power from a two-chamber microbial fuel cell with a low-pH air-cathode compartment. *Electrochem. Commun*. 2009, 11, 619-622.

(13) Zhao, F.; Harnisch, F.; Schroder, U.; Scholz, F.; Bogdanoff, P.; Herrmann, I. Application of pyrolysed iron (II)phthalocyanine and CoTMPP based oxygen reduction catalysts as cathode materials in microbial fuel cells. *Electrochem. Commun*. 2005, 7, 1405–1410.

(14) Taylor, R.J.; Humffray, A.A. Electrochemical studies on glassy carbon electrodes. I. Electron transfer kinetics, *J. Electroanal. Chem*. 1973, 42, 347-354.

(15) Heijne, A. ter; Hamelers, H.V.M.; de Wilde, V.; Rozendal, R.R.; Buisman, C.J.N. A bipolar membrane combined with ferric iron reduction as an efficien cathode system in microbial fuel cells. *Environ. Sci. Technol*. 2006, 40, 5200-5205.

(16) Rohwerder, T.; Gehrke, T.; Kinzler, K.; Sand, W. Bioleaching review part A: Progress in bioleaching: fundamentals and mechanisms of bacterial metal sulfide oxidation. *Appl. Microbiol. Biotechnol*. 2003, 63, 239-248.

(17) You, S.; Zhao, Q.; Zhang, J.; Jiang, J.; Zhao, S. A microbial fuel cell using permanganate as the cathodic electron acceptor. *J. Power Sources.* 2007, 162, 1409-1415.

(18) Logan, B.E. Microbial Fuel Cells. John Wiley & Sons, New York (2008).

(19) Zumdahl, S.S. Chemical Principles. Houghton Mifflin Company, Boston (1998).

(20) Santana-Casiano, M.; González-Dávila, M.; Rodríguez, M.J.; Millero, F.J. The effect of organic compounds in the oxidation kinetics of Fe(II). *Mar. Chem*. 2000, 70, 211-222.

(21) Dávila, D.; Esquivel, J.P.; Vigués, N.; Sánchez, O.; Garrido, L.; Tomás, N.; Sabaté, N.; del Campo, F.J.; Muñoz, F.J.; Mas, J. Development and optimization of microbial fuel cells. *J. Mater. Electrochem. Syst.* 2008, 11, 99-103.

(22) D. Andrienko. Cyclic Voltammetry. 2008. Available in: http://www.mpip-mainz.mpg.de/~andrienk/journal_club/cyclic_voltammetry.pdf.

(23) Zhao, F.; Slade, R.C.T.; Varcoe, J.R. Techniques for the study and development of microbial fuel cells: and electrochemical perspective. *Chem. Soc. Rev*. 2009, 38, 1926-1939.

(24) Lanthier, M.; Gregory, K.B.; Lovley. D.R. Growth with high planktonic biomass in *Shewanella oneidensis* fuel cell. *FEMS Microbiol. Lett*. 2008, 278, 29-35.

(25) Rozendal, R.A., Hamelers, H.V.M.; Buisman, C.J.M. Effects of membrane cation transport on pH and microbial fuel cell performance. *Environ. Sci. Technol*. 2006, 40, 5206-5211.

(26) Clauwaert, P.; Aelterman, P.; Pham, T.H.; de Schamphelaire, L.; Carballa, M.; Rabaey, K.; Verstraete, W. Minimizing losses in bio-electrochemical systems: the road to applications. *Appl. Microbiol. Biotechnol*. 2008, 79, 901-913.

(27) Bockris, J.O.M.; Khan, U.M. Surface Electrochemistry, A Molecular Level Approach. Plenum Press, New York, London (1993).

(28) Harnisch, F.; Wirth, S.; Schröder, U. Effects of substrate and metabolite crossover on the cathodic oxygen reduction reaction in microbial fuel cells: Platinum vs. iron(II) phthalocyanine based electrodes. *Electrochem. Commun*. 2009, 11, 2253-2256.

Chapter 2

Performance of *Shewanella oneidensis* MR-1 as a cathode catalyst in microbial fuel cells containing different electron acceptors.

CHAPTER 2.

PERFORMANCE OF ***Shewanella oneidensis*** MR-1 AS A CATHODE CATALYST IN MICROBIAL FUEL CELLS CONTAINING DIFFERENT ELECTRON ACCEPTORS

ABSTRACT

In recent years, the search for a suitable catalyst at the cathode has led researchers to explore the possible use of biocathodes. The electrogenic bacterium *Shewanella oneidensis* MR-1 is an electrogenic bacterium with a great versatility for anaerobic respiration. In this work, the capacity of this bacterium to catalyze the reduction of different electron acceptors such as oxygen, nitrate and fumarate, is studied. Cyclic voltammetries indicate that different proteins were involved in the electron uptake according to the terminal electrode acceptor. Biological oxygen reduction showed the best performance, while nitrate was observed to produce less current that expected by a complete nitrate reduction. Additionally, MFC with fumarate as terminal electron acceptor indicated that this was not a suitable electron acceptor to electricity production.

INTRODUCTION

Development of practical applications derived from Microbial Fuel Cell (MFC) technology is often faced with the need to use expensive catalysts at the cathode surface in order to allow a fast enough oxygen reduction rate. Platinum is one of the best known catalysts, however its high cost [1] and tendency to poisoning [2] does not make it suitable for commercial applications. Carbon paper or graphite electrodes have also been used in combination with soluble catalysts that accelerate the oxygen reaction at the electrode. Ferricyanide is commonly used although it has some disadvantages. Due to the very slow re-oxidation rate by oxygen, it acts more often as an electron acceptor than as an electron shuttle and, as a consequence, it must be replaced. Therefore, it can not be regarded as sustainable [1].

The use of microorganisms as cathode catalysts has been recently studied. In this type of cathode, bacteria receive electrons from the electrode through their electron transport chain and use them to reduce an external electron acceptor. Direct electron transfer from electrodes was first observed in *Geobacter* species in potentiostat-poised half cells [3]. Since then, different papers have described the capacity of complex communities to reduce different electron acceptors as oxygen or nitrate in a MFC cathode [4,5]. Biocathodes have several advantages over abiotic cathodes. They have a lower cost, longer sustainability and the possibility to couple cathode activity to the removal of unwanted compounds [6].

Shewanella oneidensis MR-1 has been widely studied for its ability to use an anode as electron acceptor under anoxic conditions. The major criteria in the selection of this bacterium for it use in biocathodes is its capacity to reduce more than ten terminal electron acceptors as Mn(III), Fe(III), Cr(VI), U(VI), fumarate, nitrate, trimethylamine N-oxide, dimethyl sulfoxide, sulphite, thiosulfate or elemental sulphur [7]. This versatility indicates the existence of a complex and versatile electron transport system with a high number of electron transport components with several quinones [8,9] and *c*- and *b*-cytochromes [9,10]. However, its ability to collect electrons from a cathode and transfer them to a soluble electron acceptor has also been reported [11].

Freguia *et al*. [11] demonstrated the capacity of this electrogenic bacterium to use the electrode as electron donor by externally fixing the anode potential at -200 mV. In this study, oxygen was used as the final electron acceptor, although the mechanisms involved in this reduction, whether direct or mediated electron transfer, has not been established. A recent paper has studied the reduction capacity of the genus *Shewanella* using a MFC cathode as electron donor in a chrome bioremediation process [12]. These authors compare different *Shewanella* strains using fumarate and chrome as electron acceptors, and obtained differences in efficiency and power output related to the strain, which relate to the great variety of electron pathways that are available in this genus.

In our study, we have constructed complete MFCs using *Shewanella oneidensis* MR-1 in both anode and cathode compartments. These MFCs have been used to compare the ability of *Shewanella* biocathodes to operate using different electron acceptors. Additionally, electrochemical analyses have been run in order to detect changes in the electrochemical make up of *Shewanella* as a consequence of growth in the presence of different electron acceptors.

EXPERIMENTAL PROCEDURE

Bacterial strains and their cultivation

Shewanella oneidensis strain MR-1 (ATCC 7005500) was grown aerobically in 1 L of Trypticase Soy Broth (TSB) at 27°C. After 24 h of aerobic growth, the cells were harvested by centrifugation (10.000 *g* x 15 min, 4°C) using a 5804R Eppendorf centrifuge. The resulting pellets were resuspended in 1 L of phosphate buffer (0.1 M). 100 mL of this suspension were inoculated in both chambers anode and cathode of the four cells.

Microbial fuel cell design

In this study, four two-chamber fuel cells were used. MFCs were built using two cylindrical glass vessels with a volume of 1 L. The vessels were closed at the top by a lid equipped ports for inoculation and sampling as well as for instrumentation and gas supply.

The two reactors set in an H-configuration were separated by a Nafion®117 (Ion power, Inc.) proton exchange membrane (PEM) with a thickness of 183 μm and an effective area of 11.34 cm^2. The union was sealed with a stainless steel clamp.

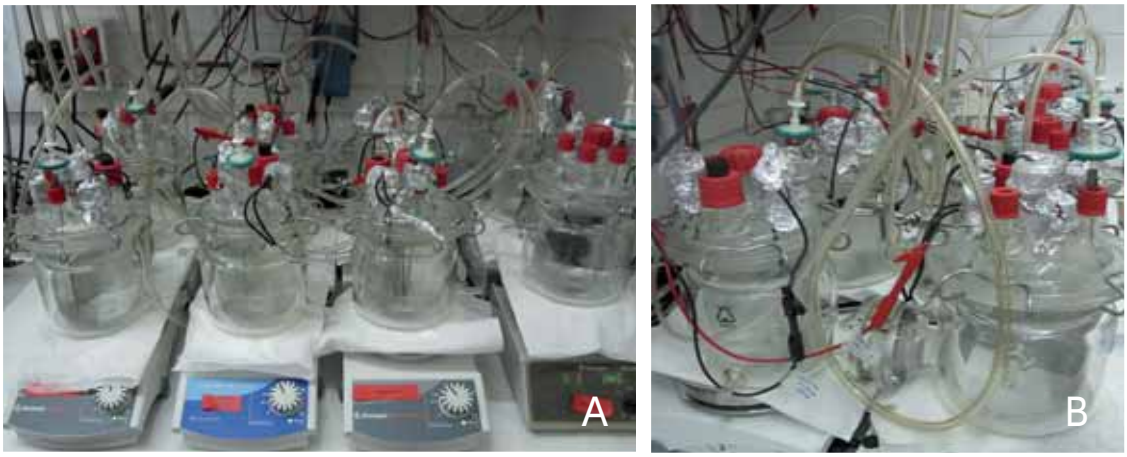

Figure 1. A,B. Experimental setup.

In all cases anode and cathode chambers contained 0.1 M phosphate buffer inoculated with *Shewanella oneidensis* MR-1 bacterium at a final concentration of $4.7e^5 \pm 5.30e^4$ cells·mL^{-1}. Both anode and cathode were made of carbon paper (B2120 Toray Carbon Paper Designation TGPH-120, plain, no wet proofing; E-Tek, Inc.) with a thickness of 0.35 mm and an area of 10 cm^2.

Anode conditions were the same in all cases using lactate (20 mM) as the sole carbon source. The chambers were sparged with nitrogen to maintain anaerobic conditions. The cathode chambers did not contain a carbon source but were supplied with different electron acceptors. The aerobic cathode (MFC-oxygen) was sparged with air, while the anaerobic cathodes containing 10 mM nitrate (MFC-nitrate) or 10 mM fumarate (MFC-fumarate) as electron acceptors were sparged with nitrogen. Both, anode and cathode chambers were stirred at 250 rpm using magnetic stirrers.

Microbial fuel cell operation and characterization

Voltage across a 50 KΩ external resistance was continuously monitored, using a digital multimeter data acquisition system (HP 34970A, Agilent, USA).

Polarization curves were performed periodically by connecting anode and cathode to a source meter (Keithley®2612) controlled by a personal computer running a custom made program developed with LabView 8.5 to automate data collection. Curves were performed by imposing different output current values during 3 minutes and, measuring the resulting voltage. The curve ended when the voltage reached 0, and power was calculated as the product of the values of voltage and current. Power and current values were normalized to the area of the anode.

Electrochemical characterization

Anode potentials were recorded against an Ag/AgCl reference electrode using a potentiostat/galvanostat model FRA2 Micro-Autolab Type II. The measures were performed in open circuit conditions, disconnecting the electrode of the external resistance to avoid current flow.

Cyclic voltammetries were performed with the same potentiostat/galvanostat. An Ag/AgCl electrode and a platinum coated silicon wafer electrode were used as reference and auxiliary

electrode respectively. Cyclic voltammetric analyses were run between -0.2 V and 0.8 V vs. Ag/AgCl (-0.4 to 0.6 vs. SHE) at a scan rate of 1 mV s^{-1}.

Cathode biofilms were analyzed at the end of the experiment after removing the electrodes from the reactor, and washing them several times in phosphate buffer to eliminate redox mediators from the biofilm. These electrodes were then used as the working electrode of an electrochemical cell containing 100 mL of oxygen free phosphate buffer. In order to analyze the possible presence of redox shuttles in the catholyte, the cathode solution (100 mL) was filtered through 0.22 µm filter (Millex®GP, Millipore) to remove bacteria, and introduced into an electrochemical cell. In this case, a carbon paper electrode with an area of 0.5 cm^2 was used as the working electrode.

For the sake of comparison, current values were normalized to the area of working electrodes used. Also, in this case, potentials were expressed vs. SHE.

Biomass determination

Concentration of bacteria in the anolyte chamber was monitored at different times using spectrophotometry and fluorescence microscopy.

Optical density at 550 nm was measured using a SmartSpecTMPlus spectrophotometer (BIO-RAD Laboratories, USA) using phosphate buffer as a blank.

For fluorescence microscopy counts, samples were fixed with formaldehyde (0.4% final concentration)(Sigma, USA) and filtered through 0.2 µm pore size GTBP filters (Millipore, USA). Bacteria were stained using the bacterial viability test Live/Dead®BacLight™ Bacterial Viability Kit (Invitrogen) by following the protocol detailed by the supplier. The filters were mounted on glass slides using immersion oil and were observed in a Zeiss AXIO Imager A1 fluorescence microscope (Zeiss, Germany).

Biofilm morphology and viability

Scanning Electron Microscopy (SEM) and Fluorescence microscopy images were obtained from the biofilm formed in all MFCs. Before staining, the electrodes were washed in phosphate buffer and cut with a size of 0.5 cm^2.

Scanning electron micrographs were taken using an EVO®MA 10 microscope (Zeiss, Germany) after the electrodes fragments was coated with gold.

Viability of cells in the biofilm was also determined using the bacterial viability test Live/Dead®BacLight™ Bacterial Viability Kit (Invitrogen) by following the protocol detailed by the supplier. Images were acquired with a Zeiss AXIO Imager A1 fluorescence microscope (Zeiss, Germany).

RESULTS AND DISCUSSION

After seven days of operation, similar biomass levels were measured in the four anode compartments with an average of $5.36e^5 \pm 5.93e^4$ cells·mL^{-1} indicating no differences in initial culture adaptation to the anodic MFC conditions (Figure 2). Similar values of anode open circuit potential (-0.269 ± 0.008 V vs. SHE) were reached along the experiment in all cases indicating that the differences in the electron acceptor used in the cathode did not affect the anode overpotentials.

In the cathode side, the type of electron acceptor used had a significant influence in the performance of the MFCs right from the beginning. Voltage recorded over a 50 KΩ external resistor showed a better performance of the oxygen MFC with initial values of 100 mV. The initial voltage generated in the fumarate MFC was lower than 35 mV, while the nitrate MFC needed 1 day to produce a measurable current.

These initial differences are probably the consequence of large cathode overpotentials caused by the lack of adaptation of the organisms to the different cathode conditions. The inoculum of *Shewanella* was identical in all MFC, but it was grown under aerobic conditions. Previous adaptation of the organism to each electron acceptor before inoculation, would probably have reduced these activation losses.

After 4 days of operation, stable values were established that lasted until the end of the experiment. While oxygen and nitrate showed stable operating voltages of 276.76 ± 31.21 and 37.7 ± 9.7 mV respectively, the fumarate containing MFC had much lower values (6.9 ± 2.25 mV). The high values observed in the operating voltages of the oxygen and nitrate MFCs seem to agree with the higher cell numbers observed after 7 days of operation (Figure 2).

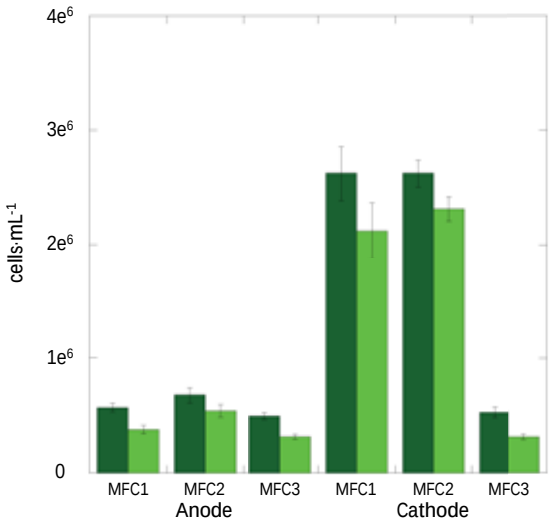

Figure 2. Biomass levels measured using viability test Live/Dead®BacLight™ Bacterial Viability Kit and fluorescence microscope, in the anode and cathode suspension of each MFC after 7 days of operation (■ : total cells, ■ : viable cells).

Images obtained by fluorescence microscopy and SEM also showed a thicker biofilm attached to these cathodes (Figure 3). The supply of electron acceptor could be an important factor for the performance of the MFC. However, concentrations at the start of the experiment were not limiting and a second feed at the end of the experiment showed no significant changes in the potentials registered, indicating no restrictions on electron acceptor for bacterial respiration in any of the cathodes.

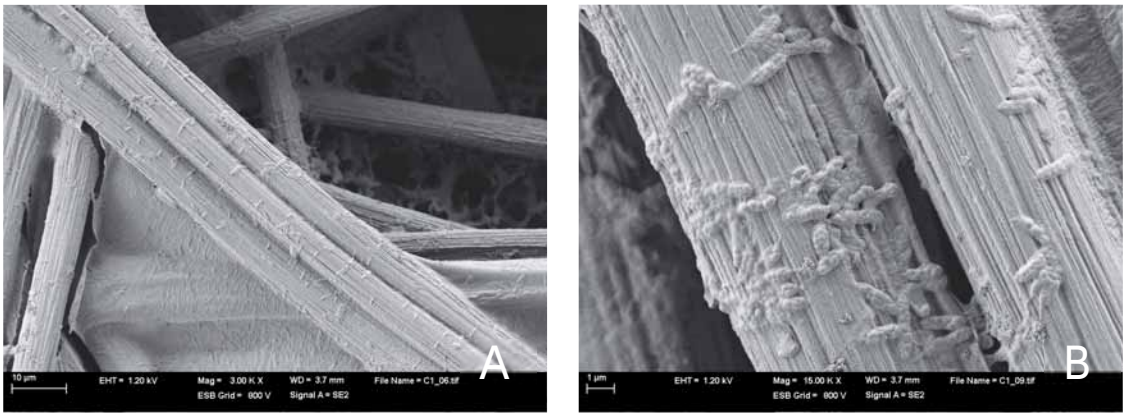

Figure 3. A,B. SEM images of the cathode of the MFC with oxygen as final electron acceptor.

Polarization and power curves were carried out to study the effect of the different final electron acceptors on the performance of MFCs with *Shewanella oneidensis* MR-1 biocathodes. Curves collected at day 7 for each MFC are shown in Figure 4. Additionally, Table 1 collects values of the OCV, maximum current density (MCD) and maximum power density (MPD) obtained between day 4, when voltage stabilized and day 7 when the experiment ended.

Oxygen is the widely used electron acceptor in cathodes due to its high redox potential (+0.82 V) and relatively low cost [13]. However, slow oxygen reduction rates on graphite electrodes make

necessary the use of catalysts or artificial electron mediators [13]. The use of bacteria as catalysts of the reaction improves the performance of the MFC and avoids the use of noble metals.

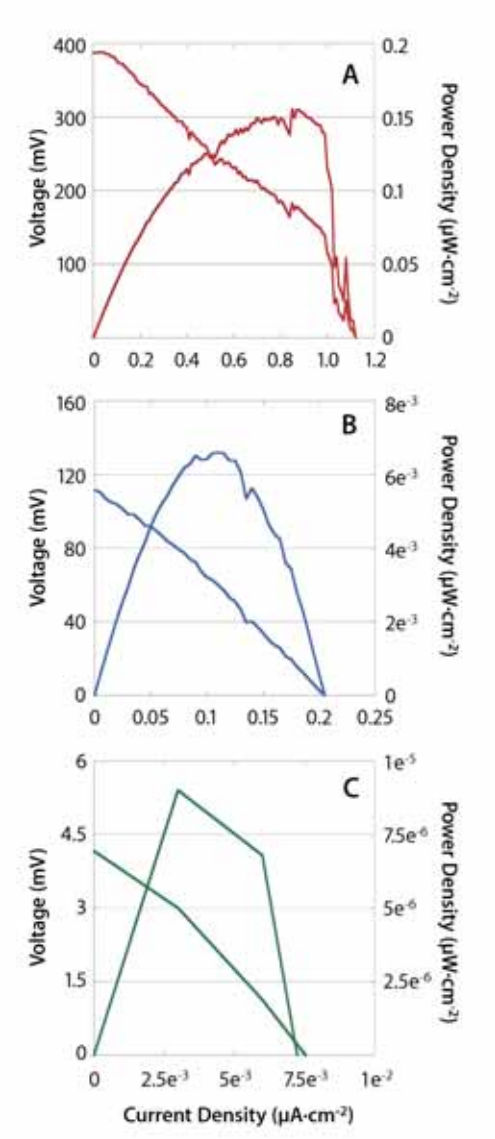

Figure 4. IV curves of oxygen-MFC (A), nitrate-MFC (B) and fumarate-MFC (C) performed at day 7.

The MFC with an aerobic biocathode had the best performance during all the experiment with open circuit voltages of about 393.62 ± 4.08 mV. During the experiment, power and current output increased steadily, reaching a maximum of 0.16 ± 0.02 $\mu W \cdot cm^{-2}$ and 1.41 ± 0.22 $\mu A \cdot cm^{-2}$. In addition to higher total viable counts in the catholyte, fluorescence microscopy and SEM images showed that this electrode had the thickest biofilm attached.

Table 1. Average and standard error of the different parameters related to MFCs performance obtained along the experiment recorded under continuous operation at 50 KΩ and from the IV curves made at different times. (OCV: Open Circuit Voltage, MCD: Maximum Current Density, MPD: Maximum Power Density).

	Oxygen-MFC	Nitrate-MFC	Fumarate-MFC
OCV (mV)	393.62 ± 4.08	95.55 ± 7.1	8.68 ± 4.7
MCD ($\mu A \cdot cm^{-2}$)	1.41 ± 0.22	0.165 ± 0.02	0.015 ± 0.007
MPD ($\mu W \cdot cm^{-2}$)	0.16 ± 0.02	$4.6e^{-3} \pm 1e^{-3}$	$7.2e^{-5} \pm 4.7e^{-5}$
Voltage (50 KΩ, mV)	276.76 ± 31.21	37.7 ± 9.7	12.48 ± 3.9

Polarization curve at day 7 of oxygen MFC showed practically no voltage drop at low currents indicating low activation losses. These losses were higher at the start of the experiment since bacteria need to develop structures or produce electron shuttles, which cost additional energy. After this, it has been observed that bacteria seem to decrease the overpotential for oxygen reduction at the cathode [4]. Additionally, in oxygen cathodes a higher oxygen concentration might decrease activation losses [14,15]. Nevertheless, a sharp drop at high current values occurred, likely due to mass transfer problems caused by a poor migration of protons across de PEM, as it has been reported in other studies [16] or low oxygen diffusion through the biofilm limiting the availability of the electron acceptor within the biofilm.

Although aerobic cathodes haven been well studied in the last years, anaerobic cathodes have the advantage of eliminating both, oxygen cross over through the PEM and the limitations imposed by the low stability of oxygen in water [17]. Nitrate has been reported as an alternative to oxygen when used as electron acceptor in the cathode compartment [3,18]. Nevertheless, these observations were produced after actively polarizing the cathode therefore, it was not clear whether denitrification could be carried out autonomously only with the electrons provided by bacteria in the anode. In 2007, Clauwaert and co-workers described a complete cathodic denitrification system sustained by biological acetate oxidation in a MFC using complex community [5].

It has been reported that *Shewanella* has the ability to reduce nitrate to ammonium or nitrogen [19,20]. Due to the fact that these reactions have standard potentials very close to those of oxygen reduction [13], a similar performance could be expected in both cases. However, in the case of nitrate reduction power output was much lower as can be observed in Table 1, with maximum power values of $4.6e^{-3} \pm 1e^{-3}$ $\mu W \cdot cm^{-2}$ (OCVs of 95.55 ± 7.1 mV, maximum currents of 0.165 ± 0.02 $\mu A \cdot cm^{-2}$). This poor performance when compared to oxygen MFCs, can be attributed to an incomplete reduction of nitrate to nitrite. The lower potential (+0.43 V) of this redox pair affects the cathode potential determining the energy gained by the microorganisms and therefore, the performance of the fuel cell. Additionally, the number of anode electrons consumed in the cathode reaction is also reduced to 2, compared to the 5 electrons required for the reduction of nitrate to nitrogen gas. The slower electron consumption in the cathode will result in a lower power output. This fact has been already reported in some *Geobacter* species, but the reason for the incomplete nitrate reduction remains unknown [3].

In the fumarate MFC, cathode bacteria should catalyze the electron transfer from the cathode to fumarate, with production of succinate. Polarization curves of MFC-fumarate showed a decrease of OCV values after the second day, obtaining the lowest potential (average of 8.68 ± 4.7 mV) (Table 1). The low redox potential of the fumarate/succinate pair (+0.033 V) could be the cause of the low OCV obtained by this MFC, making this final electron acceptor a poor choice for current generation. Power production was very low with a maximum of $1e^{-3}$ $\mu W \cdot cm^{-2}$ at the beginning of the

experiment. Later on this, values decreased to remain below $2e^{-4}$ $\mu W \cdot cm^{-2}$. Fumarate can be reduced to succinate by bacteria present in the cathode with the consumption of 2 electrons. However, incomplete reduction of fumarate has been reported in several studies, when it is used in the cathode of a MFC [3,12]. In these studies, less than half of the electrons needed for succinate production come from the anode. Therefore, fumarate could be depleted by vias not related to anaerobic respiration thus limiting electricity production. The low number of bacteria present in the cathode suspension of this MFC also indicated poor growth conditions for *Shewanella* in this cathode chamber, probably due to the fact that the proteins needed for electron uptake from the cathode have potentials very closed or higher than those of fumarate reductase.

Since an anode-adapted community has been shown to be able to turn into a biocathode changing the operation conditions [17], it is supposed that similar mechanisms, such as direct contact or mediated electron transfer, are the responsible for both oxidation and reduction of the electrodes [21]. However, the fact that *Shewanella* can use electrodes as either an electron donor or acceptor depends upon the potential of the electrode. So, electron transfer from the cathode to the organisms has to occur at potential higher than reverse process in the anode in order to allow the flux of electrons from the anode to the cathode. So, according to these differences in potential, it can be supposed different proteins are involved in the bacterial respiration in both anode and cathode chambers. So, a study performed with *Geobacter sulfurreducens* by cyclic voltammetry, in which electron transfer from electrode to the biofilm was studied, reported potentials more positive than those normally found in anode biofilms, indicating that different cytochromes could be involved in both process [22]. In the same way, the different electron acceptors used in the cathode with different redox potentials, could make that *Shewanella* changes the proteins used for the electron uptake to obtain more energy in the reduction process.

To study whether the presence of different electron acceptors had an effect in the redox characteristics of *Shewanella* cultures, the electrochemical profile of the cathode and the catholyte were checked by cyclic voltammetry.

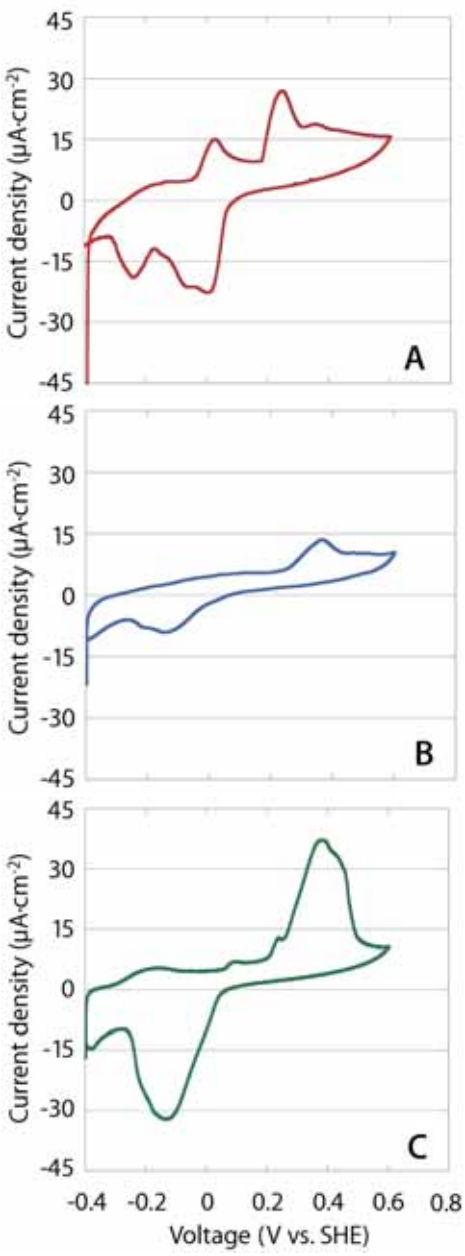

Figure 5. Cyclic voltammograms of the cathodes of oxygen-MFC (A), nitrate-MFC (B) and fumarate-MFC (C) at the end of the experiment.

Cyclic voltammetries of the cathodes have been represented in Figure 5. The voltammograms differ depending on the electron acceptor. Figure 5A shows the voltammetry of the MFC-oxygen cathode at the end of the experiment. Different oxidation and reduction peaks were observed centered at potentials of +0.22 and +0.03 V for the oxidation peaks, and-0.25, -0.16 and -0.03 V for the reduction peaks. In other studies using *Shewanella* as a catalyst for oxygen reduction, a catalytic wave with onset at about +0.2 mV vs. SHE was found in the cell suspension [11]. In this study this peak was related to membrane redox compounds with similar redox potentials as *Omc*A and *Mtr*C cytochromes [23].

The cathode of MFC-nitrate (Figure 5B) presented a voltammogram with an oxidation peak at +0.38 V, and a reduction peak at -0.1 V. Meanwhile the cathode biofilm grown with fumarate (Figure 5C) presented two major peaks at -0.21 and +0.38 V.

At the end of the experiment, 10 mL of the anolyte from each of the four cathode reactors were filtered and analyzed by cyclic voltammetry to check the presence of possible redox species in the catholyte. The results from catholyte voltammetries did not show peaks indicating that no electron mediators were present in cathode chamber and therefore, direct contact was the predominant electron transfer mechanism. *Shewanella oneidensis* MR-1 has been reported to produce flavins that contribute to electron transfer from the bacteria during anode respiration [24,25]. However, the very negative potential (-0.2/-0.25 mV vs. SHE [25]) of these redox species can be the reason for their absence from cathode chamber. Other electrochemical analyses performed in *Shewanella* catholytes showed peaks very similar to those obtained by the biofilm. However, this fact was attributed to heme-containing proteins present in the bulk solution due to the cell lysis since no typical reverse peaks of the flavins was observed [11].

Finally, although the different MFC architecture and lower biomass used in this work does not allow an in depth comparison, it is possible to observe that the power output obtained for oxygen abiotic reduction at platinum coated electrodes studied in Chapter 1 was close to the power output obtained using *Shewanella* as catalyst for oxygen reduction, indicating that *Shewanella*

constitutes an efficient alternative to expensive metal catalysts to catalyze the oxygen reduction in complete MFCs.

CONCLUSIONS

The use of bacteria as catalysts in the cathode of MFCs, has generated much interest in recent years. This is due to their sustainability and low cost in relation to commonly used catalysts like ferricyanide or platinum, thus allowing for a large number of applications in wastewater treatment or bioremediation. This study demonstrates the capacity of *Shewanella oneidensis* MR-1 to couple the oxidation of lactate to the reduction of different electron acceptors at the cathode. The results show a good performance of the *Shewanella* biocathodes when oxygen is used as an electron acceptor, with power outputs comparable to those obtained using platinum coated electrodes. Anaerobic biocathodes (nitrate and fumarate) had lower performances particularly in the case of fumarate, which it does not seem to be suitable for its use as electron acceptor in *Shewanella oneidensis* MR-1 biocathodes.

Acknowledgements

This work was supported by grants CSD2006-00044 TRAGUA (CONSOLIDER-INGENIO2010) and CTQ2009-14390-C02-02 from the Spanish Ministry of Education and Science to JM.

REFERENCES

(1) Logan, B.E.; Hameler, B.; Rozendal, R. Schröder, U.; Keller, J.; Freguia, S.; Aelterman, P.; Verstraete, W.; Rabaey, K. Microbial fuel cell: methodology and technology. *Environ. Sci. Technol*. 2006, 40, 5181-5192.

(2) Yu, E.H.; Cheng, S.; Scott, K.; Logan, B.E. Microbial fuel cell performance with non-Pt cathode catalysts. *J. Power Sources*. 2007, 171, 275-281.

(3) Gregory, K.B.; Bond, D.R.; Lovley, D.R. Graphite electrodes as electron donors for anaerobic respiration. *Environ. Microbiol*. 2004, 6(6), 596-604.

(4) Rabaey, K.; Read, S.T.; Clauwaert, P.; Freguia, S.; Bond, P.L., Blackall, L.L.; Keller, J. Cathodic oxygen reduction catalyzed by bacteria in microbial fuel cells. *ISME J*. 2008, 2, 519-527.

(5) Clauwaert, P.; Rabaey, K.; Aelterman, P.; De Schamphelaire, L.; Pham, T. H.; Boeckx, P.; Boon, N.; Verstraete, W. 2007. Biological denitrification in Microbial Fuel cells. *Environ. Sci. Technol*. 2007, 41,3354-3360.

(6) He, Z.; Largus, T.; Angenent, T. Application of bacterial biocathodes in microbial fuel cells. *Electroanal*. 2006, 18, 2009-2015.

(7) Heidelberg, J.F.; Paulsen, I.T.; Nelson, K.E.; Gaidos, E.J.; Nelson, W.C.; Read, T.D.; Eisen, J.A.; Seshadri, R.; Ward, N.; methe, B.; Clayton, R.A.; Meyer, T.; Tsapin, A.; Scott, J.; Beanan, M.; Brinkac, L.; Daugherty, S.; deBoy, R.T.; Dodson, R.J.; Scott Durkin, A.; Haft, D.H.; Kolonay, J.F.; Madupu, R.; Peterson, J.D.; Umayam, L.A.; White, O.; Wolf, A.M.; vamathevan, J.; Weidman, J.; Imprain, M.; Lee, K.; Berry, K.; Lee, C.; Mueller, J.; Khouri, H.; Gill, J.; Utterback, T.R.; McDonald, L.A.; Feldblyum, T.V.; Smith, H.O.; Craig venter, J.C.; Nealson, K.H.; Fraser, C.M. Genome sequence of the dissimilatory metal ion-reducing bacterium *Shewanella oneidensis*. *Nat. Biotechnol*. 2002, 20, 1118-1123.

(8) Myers, C.R.; Myers, J.M. Role of menaquinone in the reduction of fumarate, nitrate, iron(III) and manganese(IV) by *Shewanella putrefaciens* MR-1. FEMS *Microbiol. Lett*. 1993, 114, 215-222.

(9) Myers, C.R.; Myers, J.M. Cloning and sequence of cymA, a gene encoding a tetraheme cytochrome c required for reduction of iron(III), fumarate, and nitrate by *Shewanella putrefaciens* MR-1. *J. Bacteriol*. 1997, 179(4), 1143-1152.

(10) Myers, C.R.; Myers, J.M. Localization of cytochromes to the outer membrane of anaerobically grown *Shewanella putrefaciens* MR-1. *J. Bacteriol*. 1992, 174, 3429-3438.

(11) Freguia S.; Tsujimura, S.; Kano, K. Electron transfer pathways in microbial oxygen biocathodes. *Electrochim. Acta*. 2010, 55, 813-818.

(12) Hsu, L.; Masuda, S.A.; Nealson, K.H.; Pirbazari, M. 2012. Evaluation of microbial fuel cell *Shewanella* biocathodes for treatment of chromate contamination. RSC Advances (In press).

(13) He, Z.; Angenent, L.T. Application of bacterial biocathodes in microbial fuel cells. *Electroanal*. 2006. 18(29-30), 2009-2015.

(14) Sell, D.; Kramer, P.; Kreysa, G. Use of an oxygen gas diffusion cathode and three-dimensional packed-bed anode in a bioelectrochemical fuel cell. *Appl. Microbiol. Biotechnol*. 1989, 31, 211-213.

(15) Schröder, U.; et al. Electrochemical loses. In *Bioelectrochemical Systems: from extracellular electron transfer to biotechnological application;* Rabaey, K.; Angenent, L.; Schröer, U.; Keller, J., Eds.; IWA Publishing 2010; pp 119.

(16) Rozendal, R.A.; Hamelers, H.V.M.; Buisman, C.J.N. Effects of membrane cation transport on pH and microbial fuel cell performance. *Environ. Sci. Technol*. 2006, 40, 5206-5211.

(17) Huang, L.; Regan, J.M.; Quan, X. Electron transfer mechanisms, new applications, and performance of biocathode microbial fuel cells. *Bioresource Technol*. 2011, 102, 316-323.

(18) Park, H.I.; Kim, D.K.; Choi, Y.; Pak, D. Nitrate reduction using an electrode as direct electron donor in a biofilm-electrode reactor. *Process Biochem*. 2005, 40, 3383-3388.

(19) Samuelsson, M. Dissimilatory nitrate reduction to nitrite, nitrous oxide, and ammonium by *Pseudomonas putrefaciens*. *Appl. Environ. Microbiol*. 1985, 50, 812-815.

(20) Krause, B.; Nealson, K.H. Physiology and enzymology involved in denitrification by *Shewanella putrefaciens*. *Appl. Environ. Microbiol*. 1997, 63(7), 2613-2618.

(21) Cadena, A.; Texier, A.C.; Gonzalez, I.; Cervantes, F.J.; Gomez, J. Qualitative and quantitative determination of a humica model compound in microbial cultures by cyclic voltammetry. *Environ. Technol*. 2007, 28, 1035-1044.

(22) Dumas, C.; Basseguy, R.; Bergel, A. Microbial electrocatalysis with *Geobacter sulfurreducens* biofilm on stainless steel cathodes. *Electrochim. Acta*. 2008, 53(5), 2494-2500.

(23) Firer-Sherwood, M.; Pulcu, G.S.; Elliott, S.J. Electrochemical interrogations of the *Mtr* cytochromes from *Shewanella*: opening a potential window. *J. Biol. Inorg. Chem*. 2008,13, 849-854.

(24) von Canstein, H.; Ogawa, J.; Shimizu, S.; Lloyd, J.R. Secretion of flavins by *Shewanella* species and their role in extracellular electron transfer. *Appl. Environ. Microbiol.* 2008, *74* (3), 615-623.

(25) Marsili, E.; Baron, D.B.; Shikhare, I.D.; Coursolle, D.; Gralnick, J.A.; Bond, D.R. *Shewanella* secretes flavins that mediate extracellular electron transfer. *PNAS*. 2008, 105(10), 3968-3973.

(26) Uría, N.; Sánchez, D.; Mas, R.; Sánchez, O.; Muñoz, F.X.; Mas, J. Effect of the anode/cathode ratio and the choice of cathode catalyst on the performance of microbial fuel cell transducers for the determination of microbial activity. *Sensor. Actuator. B-Chem.* 2011 (In press)

Chapter 3

Transient storage of electrical charge in biofilms of *Shewanella oneidensis* MR-1 growing in microbial fuel cells.

Published in Environmental Science & Technology

CHAPTER 3.

TRANSIENT STORAGE OF ELECTRICAL CHARGE IN BIOFILMS OF ***Shewanella oneidensis*** MR-1 GROWING IN MICROBIAL FUEL CELLS

ABSTRACT

Current output of microbial fuel cells (MFCs) depends on a number of engineering variables mainly related to the design of the fuel cell reactor and the materials used. In most cases the engineering of MFCs relies on the premise that for a constant biomass, current output correlates well with the metabolic activity of the cells. In this study, we analyze to what extent, MFC output is also affected by the mode of operation, emphasizing how discontinuous operation can affect temporal patterns of current output.

The experimental work has been carried out with *Shewanella oneidensis* MR-1, grown in conventional two-chamber MFCs subject to periodic interruptions of the external circuit. Our results indicate that after closure of the external circuit, current intensity shows a peak that decays back to basal values. The result suggests that the MFC has the ability to store charge during open circuit situations. Further studies using chronoamperometric analyses were carried out using isolated biofilms of *Shewanella oneidensis* MR-1 developed in a MFC and placed in an electrochemistry chamber in the presence of an electron donor. The results of these studies indicate that the amount of excess current over the basal level released by the biofilm after periods of circuit disconnection is proportional to the duration of the disconnection period up to a maximum of approximately 60 minutes. The results indicate that biofilms of *Shewanella oneidensis* MR-1 have the ability to store charge when oxidizing organic substrates in the absence of an external acceptor.

INTRODUCTION

Power output of Microbial Fuel Cells (MFC) depends on a number of different factors, some of them related to the amount of microorganisms in the MFC and their level of activity, others related to the design and mode of operation of the fuel cell reactor. Design factors have been extensively studied. The area of the electrodes as well as the cathode/anode relative sizes should be properly dimensioned to avoid limitation in the current produced by the microorganisms [1,2,3]. The presence of a proton exchange membrane, the type of material used in the membrane, the concentration of substrate, internal resistance, type of cathode catalysts and others, have also been explored in an attempt to improve the performance of these devices. Bruce Logan in his excellent review published in 2008 [4] provides an in depth detailed review of the many contributions to this specific area.

However, other parameters related to MFC operation have been less studied despite their importance in current production. The potential of the anode can influence the capacity of the biocatalyst to transfer electrons to the electrode as well as the amount of metabolically useful energy that can be obtained in the process. This is due to the fact that extracellular electron transfer is influenced by the electric potential between the final electron carrier and the anode [5,6]. External resistance has been also reported to exert an effect. Higher resistances produce smaller current densities due to a limitation in the flow of electrons through the circuit. So, the transference of charge from bacteria to the electrode is reduced resulting in a decrease of bacterial growth and the performance of the system [7,8].

In all cases, MFCs are assumed to operate continuously, that is, without interruptions in the current flow. Some cases of MFCs operating discontinuously have been described in which a capacitor is included in the external circuit. In these cases the capacitors accumulate charge at low currents and high potentials, and release high intensity bursts during discharge. The discharge of the capacitor can be sent to the external circuit and to the cathode [9] or channelled back to the anode in such a way that the reactor acts as a MEC [10]. In both cases, during the time the capacitor takes to charge, there is no output from the MFC, but the organisms at the anode continuously produce

charge, which is stored in the capacitor. Changes at the anode potential during capacitor charge transiently improve electron transfer between bacteria and the anode. However, the organisms are never exposed to open circuit conditions.

Discontinuous operation seldom raises issues when chemical fuel cells (hydrogen or methanol) are involved. This is probably a consequence of the fact that these devices use simple inorganic catalysts for the oxidation reactions of the anode. In this type of system it is safely assumed that the fuel cell can be switched on or off at will without a penalty in performance. However, it is by no means clear how microorganisms in a MFC would behave under truly discontinuous operation (periodic exposure to open circuit conditions). Does electrogenesis stop when the anode is unable to accept the electrons? At least in the case of *Geobacter sulfurreducens* it has been shown that the organism can go on with its oxidative metabolism in the absence of external electron acceptors by using its extremely high amount of extracytoplasmic cytochromes as an electron sink. This ability was elegantly proved by Esteve-Núñez *et al*. [11] for cells in suspension using fluorescence to monitor the redox state of the cytochromes, and has been recently proved in biofilms of the same organisms by Schrott *et al.* [12] using electrochemical methods. Thus, while it is quite clear that *Geobacter sulfurreducens* can respond to periods of unavailability of external electron acceptor by storing charge, it is not clear whether this is also possible in other electrogenic microorganisms such as *Shewanella*. The existence of a capacity in cells of *Shewanella oneidensis* MR-1 has been recently suggested by Harris *et al.* [13] after observing a fast motility response to metal oxide particles that they call “electrokinesis”. After contacting the particle, the cells swim away and the authors relate this behaviour to the instantaneous transfer of electrons from bacteria to the metal oxide. Besides this indirect evidence, there is no actual study on how *Shewanella* responds when subject to periodic open circuit conditions in a MFC.

In this work we explore the behaviour of a MFC of *Shewanella oneidensis* MR-1 when subject to discontinuous operation. We first describe how discontinuous operation affects the behaviour of a MFC of this organism, and later on, we analyze whether and to what extent isolated biofilms of *Shewanella oneidensis* MR-1 developed on an electrode have the ability to store charge during periods of open circuit conditions.

EXPERIMENTAL PROCEDURE

Bacterial strains and growth conditions

Shewanella oneidensis strain MR-1 (ATCC 70050) was grown aerobically in 100 mL of Tripticase Soy Broth (TSB) during 36 hours. After this, the culture was centrifuged (10100 *g* x 15 min, 4ºC) using a 5804R Eppendorf centrifuge. The resulting pellet was resuspended in 1 L of AB minimal medium ($[NH_4]SO_4$ 2 g, Na_2HPO_4 7.31 g, KH_2PO_4 7.85 g, NaCl 3 g, Na_2SO_4 0.011 g, $MgCl_2{\cdot}6H_2O$ 0.2 g, CaCl 3.625 mg, $FeCl_3{\cdot}6H_2O$ 0.2 mg) [14] previously sparged with nitrogen gas to eliminate oxygen. Lactate (0.02 M) and fumarate (0.1 M) were added to the medium as electron donor and acceptor respectively. After 48 hours of incubation with agitation at room temperature, the cells were harvested again by centrifugation, resuspended in 100 mL of anolyte medium and transferred to the anode chamber under anoxic conditions. The composition of the anolyte medium depended on the experiment. Thus, for the experiments of circuit interruption in MFCs we used AB minimal medium. For the development of biofilms at the surface of the anode for later use in electrochemical analysis KNO_3 0.5 M was employed.

Microbial Fuel Cell set up and characterization

The type of MFC reactor used in this work has already been described in Chapter 1 [3]. Basically, two identical MFCs were constructed by joining two methacrylate blocks with a volume of 130 mL. The proton exchange membrane selected in this study was Nafion®117 (Ion power, Inc.) with a thickness of 183 μm and effective area of 38.46 cm^2.

Anode and cathode electrodes were connected to a source meter (Keithley®2612) controlled by a personal computer running a custom made program developed with LabView 8.5 to automate data collection.

Experimental measurements in Microbial Fuel Cell reactors

To study the effect of discontinuous operation in MFCs of *Shewanella oneidensis*, two identical reactors were used. The anode chambers were filled with AB minimal medium containing lactate (0.02 M) as the only electron donor and inoculated with *Shewanella oneidensis* MR-1 at a final concentration of $4.8x10^8$ cells·mL^{-1}. The anodes consisted of carbon paper electrodes (B2120 Toray Carbon Paper Designation TGPH-120, plain, no wet proofing; E-Tek, Inc.) with a thickness of 0.35 mm and an area of 3 cm^2.

The cathode chambers contained ferricyanide (0.05 M $K_3[Fe(CN)_6]$) in 0.1 M phosphate buffer. For the cathodes we used the same material used in the anodes but with a larger area (15 cm^2) to avoid cathodic limitations [3].

Both, anode and cathode chambers were continuously sparged with nitrogen and air respectively and stirred at 250 rpm using a magnetic stirrer.

After inoculation both reactors were connected to a Keithley source meter programmed as to measure maximum current output by setting the internal resistance of the meter to its minimal value (about 65-70 Ω).

When the fuel cells reached stable values of current output, the external circuit of the MFCs was periodically interrupted (open circuit) for different time periods, 10 min for the first MFC and 30 min for the second one. After each external circuit interruption, the circuit was closed again for a period of 1 h and values of current output were recorded.

The electric charge (Coulombs) stored during the 30 min of open circuit was calculated as the excess current produced after the interruption by integrating the area of the peak of current above the stable baseline.

Electrochemical analysis of isolated biofilm-covered anodes

In this part of the work, biofilms were allowed to develop at the surface of the anode using the MFC reactor described above. The biofilm-covered anode was then removed from the MFC and subject to electrochemical analyses.

Biofilm development

The anode compartment was filled with potassium nitrate (KNO_3) at a concentration of 0.5 M as anolyte and lactate (20 mM) as carbon source, and inoculated with *Shewanella oneidensis* MR-1 at a final concentration of approximately 10^8 cfu·mL^{-1}. KNO_3 was used in the anode instead of AB minimal medium to avoid the interference of iron from the medium during the electrochemical characterization of the anolyte. KNO_3 (0.5 M) was also used at the cathode compartment. Both, anode and cathode chambers were continuously sparged with nitrogen and air respectively and stirred at 250 rpm using a magnetic stirrer.

In this case, anode and cathode materials were not the same. Carbon paper with an area of 0.5 cm^2 was used as the anode. The cathode was a silicon wafer coated with platinum (13.55 cm^2), the same size and material that was later used as auxiliary electrode in the electrochemical analysis.

The biofilm was allowed to develop under conditions of low current output (1 nA) for a period of several days until a stable voltage of 0.150 V was reached. After that, both the anolyte and the biofilm-covered anode were removed and subject to electrochemical studies.

Electrochemical measurements

Cyclic voltammetric and chronoamperometric analyses were performed using a potentiostat/galvanostat model FRA2 Micro-Autolab Type II. An Ag/AgCl electrode (Methrom, Switzerland) and a platinised silicon wafer electrode were used as reference and auxiliary electrode

respectively. In the results section, all potentials have been adjusted to E vs. SHE (Standard Hydrogen Electrode). Before the measurements, the solution was flushed with nitrogen to remove oxygen traces. The electrochemical cell was kept in a Faraday cage to minimize external interferences.

Cyclic Voltammetric Analysis

Cyclic voltammetric analyses were run between -0.6 V and 0.4 V vs. Ag/AgCl (-0.8 to 0.2 vs. SHE) at a scan rate of 1 $mV \cdot s^{-1}$. The scan rate was chosen after performing a very large number of CV with both cell suspensions and biofilms of *Shewanella*. 1 $mV \cdot s^{-1}$ provided by far the best resolution.

In order to analyze the possible presence of redox shuttles in the anolyte, the anode solution (100 mL) was filtered using a sterile filter with a pore size of 0.22 µm (Millex®GP, Millipore) to remove bacteria, and introduced in an electrochemical cell. A carbon paper electrode with an area of 0.5 cm^2 was used as the working electrode.

For the cyclic voltammetric analysis of the biofilm, the anode of the MFC was removed from the reactor and washed several times in KNO_3 to remove the mediators from the biofilm. This electrode was then used as the working electrode in an electrochemical cell containing 100 mL of oxygen free KNO_3.

Chronoamperometric analysis

A biofilm-covered anode developed in a separate MFC reactor was rinsed and placed as the working electrode in an electrochemical cell containing oxygen-free phosphate buffer (0.1 M) supplemented with lactate (0.02 M). During the oxidation of lactate, protons could accumulate producing changes in pH and affecting bacterial activity. Phosphate buffer was used to avoid these changes.

Several chronoamperometric analyses of the electrode biofilm were run at a potential of 0.3 V vs. Ag/AgCl (0.1 V vs. SHE) during a time of 30 s, sufficient to reach a stationary current. Before each chronoamperometry, the electrochemical cell was switched off for different periods: 0, 2, 4, 8, 16, 32, 64, 90, 120 and 180 min. Five replicates of each time were made.

As a control, the same set of measurements was repeated using a carbon paper electrode without bacteria. This allowed us to observe and remove from our results the effect of overpotentials strictly related to interface phenomena at the surface of the electrode material and not due to the presence of the biofilm.

The amount of charge stored during switch off was calculated as previously described in the section 3 of Experimental Procedure.

Biofilm morphology and viability

Scanning Electron Microscopy (SEM) and Confocal laser scanning microscopy (CLSM) images were obtained from the biofilm. Before staining, the electrode was washed in phosphate buffer and cut in different fragments of 0.5 cm^2. Scanning electron micrographs were taken using an EVO®MA 10 microscope (Zeiss, Germany) after the electrode fragment was coated with gold.

For CLSM, the electrode sample was prepared with HOETSCH DNA stain that allows observation of bacterial cells, while exopolimers in the biofilm were visualized with Alexa Fluor®488 conjugated Concavalin A (ConA) and Alexa Fluor®594 conjugated wheat germ agglutinin (WGA). ConA selectively binds to α-mannopyranosyl and α-glucopyranosyl residues, while WGA binds to sialic and N-acetylglucosaminyl residues. Images were obtained with a confocal microscope Leica TCS SP2 AOBS (Leica, Germany).

RESULTS AND DISCUSSION

Experimental observations with MFC reactors

Two MFC were used to analyze the effect of intermittent operation on current output. After two days of close circuit operation, a stable current was reached. After this, the external circuit was periodically interrupted in both reactors. In one of the reactors, the open circuit intervals were 10 min followed by 60 min of closed circuit operation. In the second reactor, external circuit interruptions were 30 min followed also by 60 min of closed circuit operation.

Figure 1 shows the registered values of current output during the experiment. In the first reactor, which was subject to 10 minute interruptions, a stable current of 0.1 $mA \cdot cm^{-2}$ was observed corresponding to the current that the device was able to supply continuously (Figure 1A).

However, when the external circuit was interrupted for longer periods (30 min) a current peak was observed immediately after circuit closure that decayed slowly until reaching normal current output of 0.08 $mA\ cm^{-2}$ (Figure 1B).

Current levels after stabilization were different in both cases. We attribute this difference to the fact that data from Fig. 1A and 1B come from two separate completely independent MFCs. The differences observed can be the consequence of slight differences in the degree of development of the biofilms in the anodes. This differences might affect the stable current levels but no the existence of the peaks.

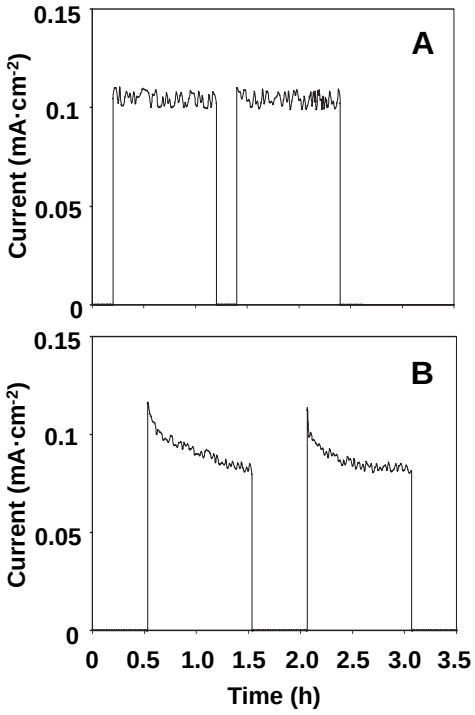

Figure 1. Current output of two independent MFCs of *Shewanella oneidensis* MR-1 during intermittent operation with different periods of circuit interruption (A) Periods of 10 min of circuit interruption are followed by 60 min of closed circuit operation. (B) Periods of 30 min of circuit interruption are followed by 60 min of closed circuit operation.

During circuit interruption, the increase in open circuit potential is due to the reduction of energy losses caused by the overpotentials of the anode and cathode that produced an increase in the cathode potential and a decrease in the anode potential [15,16]. The reasons behind these gradual changes are in fact quite diverse and include among others, factors such as an increase in the amount of reduced species in the anode chamber, both free (soluble redox mediators or fermentation products) and cell/biofilm bound (cytochromes and other redox proteins), changes in the proton gradient across the exchange membrane, or changes in the concentration of oxidized iron in the cathode chamber.

Calculations of the amount of charge stored during open circuit periods are summarized in Table 1. Approximately 0.1 C were accumulated during 30 min interruption.

Table 1. Amount of charge expressed both as Coulombs and moles of electrons stored after different times of circuit interruption.

OCT (min)	Stored charge	
	Coulombs	Electron mols
10	0	0
	0	0
30	0.126	1.3e-6
	0.072	7.47e-7

How the charge is stored in the anode of the MFC during periods of interruption is by no means straightforward. Since we used a defined minimal medium in the anode reactor, we have a precise idea of the chemical composition in the anode chamber. Iron, which is the only redox species that might act as a shuttle and temporarily store charge, was present at a concentration of 2.96 μM. In the unlikely event that all of the iron present in the 100 mL of medium was reduced during the 30 min interrupt and re-oxidized at the anode during the next 60 min close circuit period, this would only amount to 0.029 C, less than one third of the total charge stored. It is quite clear that although some charge could be stored as reduced iron, the bulk of the storage must occur either in *Shewanella* cells both, in suspension or forming the biofilm, or in soluble redox mediators secreted by the cells.

Therefore, the existence of a current peak when the circuit is interrupted suggests that the MFC was able to store charge and burst-release it as soon as the circuit was restored. This demonstrates

that discontinuous operation of a MFC can affect temporal patterns of current output influencing the performance of these devices. In order to find out whether biofilms of *Shewanella oneidensis* MR-1 could contribute to charge storage in the MFC we ran some electrochemical analysis.

Electrochemical analysis of isolated biofilm-covered anodes

In order to ascertain whether biofilms of *Shewanella oneidensis* MR-1 were able to store charge, we decided to run a set of chronoamperometric analyses after different time of exposure of the isolated biofilm to lactate in the absence of either soluble electron acceptors or an active electrode.

At the end of each incubation period the biofilm-covered electrode (Figure 2) was polarized and the current produced was followed for a period of 30 s. To confirm that the biofilm contained active redox compounds, and to determine the optimum polarization potential to be used in the chronoamperometric analyses, a cyclic voltammetric analysis of the biofilms was performed.

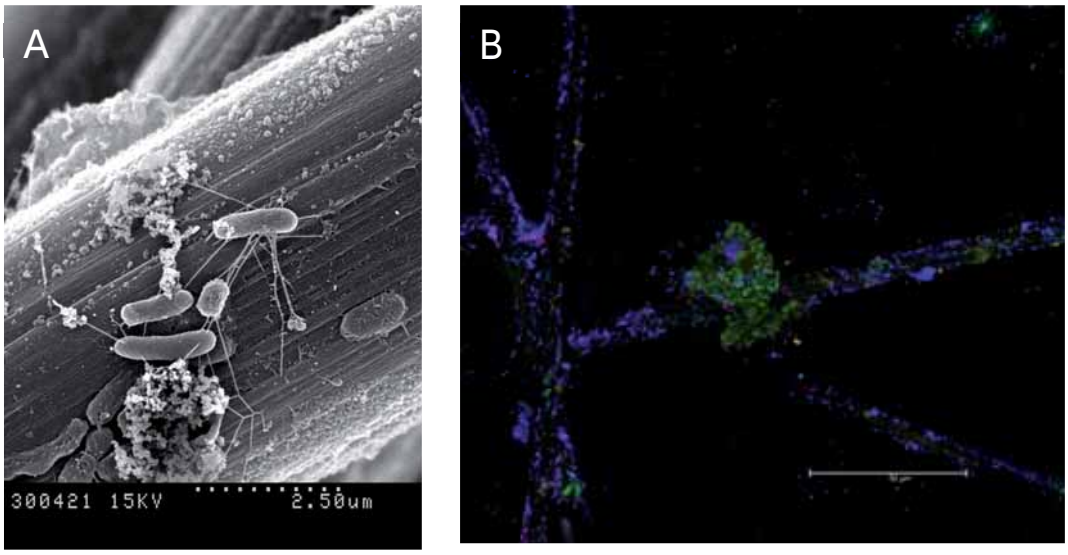

Figure 2. SEM (A) and CLSM (B) images of *Shewanella oneidensis* MR-1 attached to the electrode.

A cyclic voltammogram of the biofilm formed at the anode surface is showed in Figure 3A. The voltammogram indicates the existence of two reversible oxidation-reduction peaks. These peaks, with potential values of -0.16 and -0.10 V (vs. SHE), match closely with the values reported in the literature for *Omc*A [17] and *Mtr*C [18] respectively. The *c*-type cytochromes *Mtr*C and *Omc*A mediate the extracellular reduction of Fe(III) oxides in *Shewanella oneidensis* MR-1 [19,20]. Moreover, these cytochromes are capable of reducing Fe(III) oxides by indirectly transferring electrons to either flavin-chelated Fe(III) or oxidized flavins [21] that act as shuttles during electron transfer to external acceptors [22,23]. Another peak corresponding to a potential of 0.14 V (vs. SHE) also appeared in the biofilm voltammogram, however the potential of this peak is too high to be involved in the primary electron transfer process which usually occurs in the range of -0.25 to 0 V (vs. SHE) [23].

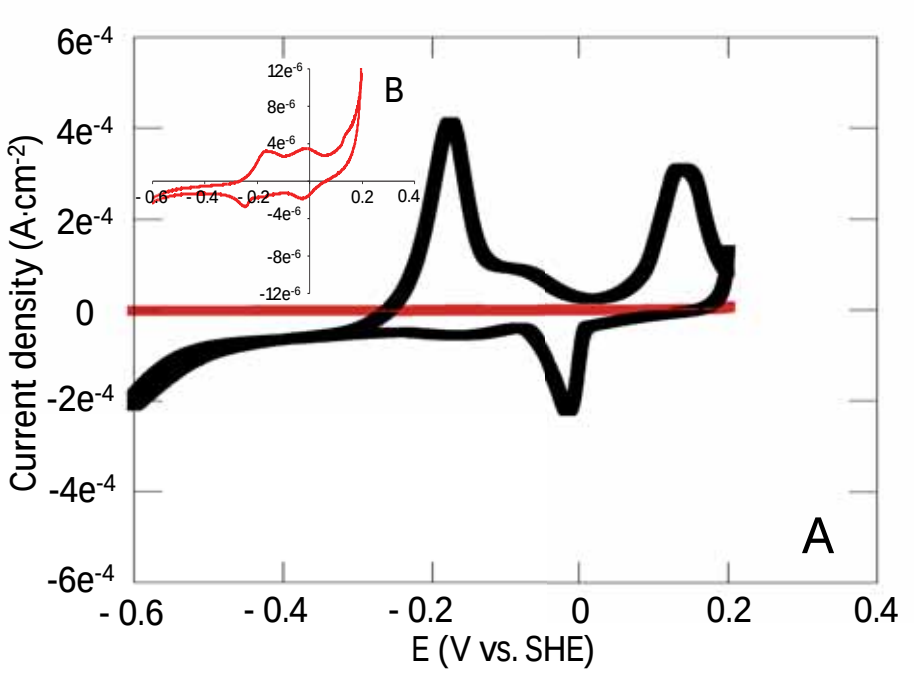

Figure 3. (A) Cyclic voltammetry at a scan rate of 1 mV·s^{-1} of *Shewanella oneidensis* MR-1 biofilm covered electrode (black line) and filtered MFC anolyte (red line). (B) Scaled up cyclic voltammogram of the anolyte from Figure 3a.

Additionally, cyclic voltammetry was also performed to analyze the anolyte of the MFC (Figure 3A and 3B). The results indicate the presence of some redox species but the currents involved in this case were two orders of magnitude lower suggesting that these compounds were present at a very low concentration. The reversible peaks were detected at potentials of -0.18 and -0.02 V (vs. SHE). The presence of a peak at −0.18 V (vs. SHE) agrees with the presence of extracellular flavins. It has been shown in some studies that the primary mediators excreted by *Shewanella oneidensis* MR-1 are riboflavin and flavin mononucleotide (FMN) [22,23]. Our cyclic voltammogram also shows a higher potential peak, between -0.1 and -0.01 V (vs. SHE), that suggests the presence of a second redox species not yet characterized.

In general, flavins have been reported to be present at very low concentrations, between 0.3 and 2 μM [24,25]. The results obtained by cyclic voltammetry in our MFC system suggest the same and indicate a much higher capacity for electron storage of the bacteria forming the biofilm than the mediators present in the anolyte.

Once the existence of oxidation/reduction peaks in the biofilm was confirmed and their potentials determined, we ran chronoamperometric analyses in an attempt to analyze the capacity of the biofilm to store charge. Chronoamperometric analyses of the biofilm-covered electrode were run in the presence of lactate as the carbon source. Prior to the beginning of the chronoamperometry, the biofilm was allowed to metabolize lactate for variable periods of time (0, 2, 4, 8, 16, 32, 64, 90, 120 and 180 min) with the circuit interrupted in such a way that electron transfer to the anode was not possible. During these periods, bacteria oxidized lactate potentially storing electrons intracellularly since no external acceptors were available and electron transfer to the anode was disabled. After these periods, a positive potential was applied and the kinetics of current production were recorded during a period of 30 s.

The choice of an adequate oxidation potential is critical. The percentage of the stored charge recovered during the chronoamperometric analysis depends to a large extent on whether the potential used is high enough to oxidize all the relevant redox compounds present in the system.

In a recent publication by Schrott *et a.l* [12], the percentage of charge recovered from biofilms of *Geobacter sulfurreducens* increases with the potential used in up to a value of 0 V (vs. SHE).

In our case, the oxidation potential of 0.1 V (vs. SHE) was selected taking into account the cyclic voltammetry data of our biofilms and selecting a potential high enough to oxidize all of the redox species present in the biofilm. In the study carried out by Carmona-Martinez *et al.* [26] using biofilms plus unattached cells of *Shewanella oneidensis* MR-1 two redox systems are identified, one of them attributed to mediated electron transfer (-0.2 V vs. Ag/AgCl/-0.4 V vs. SHE) and the other to direct electron transfer with a maximum catalytic activity at a potential of 0.1 V vs. Ag/AgCl (-0.1 V vs. SHE). The potential of these systems falls well below the 0.1 V (vs. SHE) used in our chronoamperometric analyses and confirms that the potential used is high enough to oxidize all the redox systems present in *Shewanella*.

The results of the chronoamperometric analyses corresponding to the 4, 32 and 90 min disconnection periods have been plotted in Figure 4.

In all three cases the current peaked at the beginning of the measurements right after the electrode was polarized. The current peaks observed can be related to a lower electrode potential produced during disconnection. After the initial peak, current decayed quickly suggesting that the charge stored in the biofilm during the interruption period was transferred to the electrode. After approximately 30 s virtually all of the stored charge had been released although more than 90% of the release occurred during the first 2 s.

The study of isolated biofilms in an electrochemical cell has several advantages as it allows discarding several of the mechanisms susceptible to cause overpotentials in a MFC. First, by removing most of the chemistry associated to the cathode chamber we avoid possible changes in the proportion of oxidized/reduced species in this compartment during the disconnection period. Second, since there is no PEM, the possible consequences of relaxing the concentration gradient of protons across the membrane during the interruption period are also avoided. Third, all cells and redox shuttles not bound to the biofilm/anode structure are removed, thus simplifying the

interpretation of the results and avoiding distortions in the kinetic behaviour of the system derived from the existence of diffusion limitation in the biological/chemical redox species that might be present in the anode chamber of the MFC.

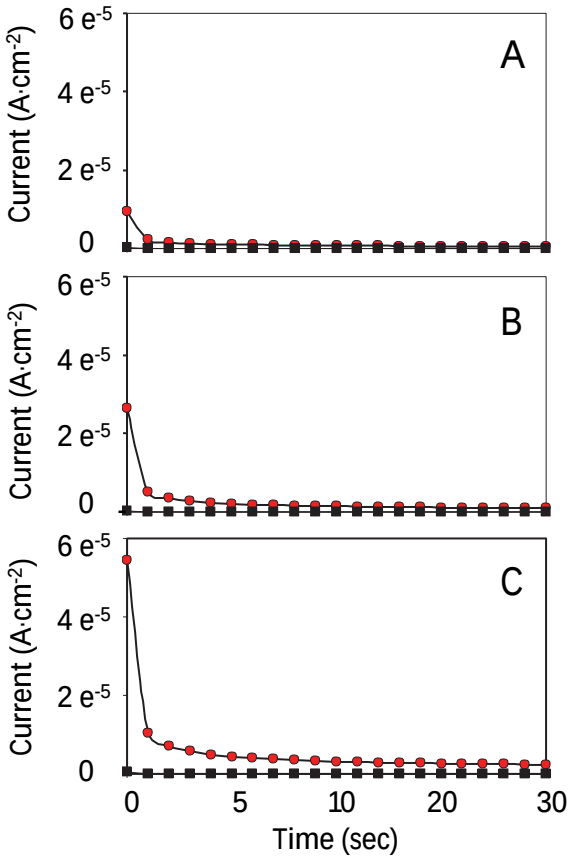

Figure 4. Current production of a biofilm-covered anode during polarization at 0.1 V (vs. SHE) after 4 (A), 32 (B), and 90 (C) minutes of exposure of the isolated biofilm to lactate in the absence of either soluble electron acceptors or an active electrode (●). An electrode without biofilm was used as control in all cases (■). Error bars (n=5) are smaller than the symbol size.

Even after getting rid of all this factors, the potential of the anode is likely to decrease during disconnection of the external circuit, mainly as a result of two mechanisms: the effect of

overpotentials related to interface phenomena at the surface of the electrode, and an increase in the amount of reduced cell/biofilm-bound redox species (cytochromes, other redox proteins, electron shuttles...). To assess the magnitude of the effect of these overpotentials at the electrode surface, we ran controls using naked carbon electrodes without biofilm. These values of current obtained with the controls, also included in Fig. 4 are much lower that those obtained with the biofilm-covered electrode.

The discharge times observed during the chronoamperometry are similar to those reported by Schrott *et al*. [12] in *Geobacter sulfurreducens* and suggest that although electron discharge is not instantaneous, the kinetics are fast enough as to indicate a rather conductive biofilm structure. Using the chronoamperometric data we calculated the magnitude of the stored charge as the area of the peak over the stable current at 30 s. When the stored charge was plotted against time of circuit interruption (Figure 5) a saturation relationship emerged with stored charge increasing as a function of disconnection time up to approximately 60 min.

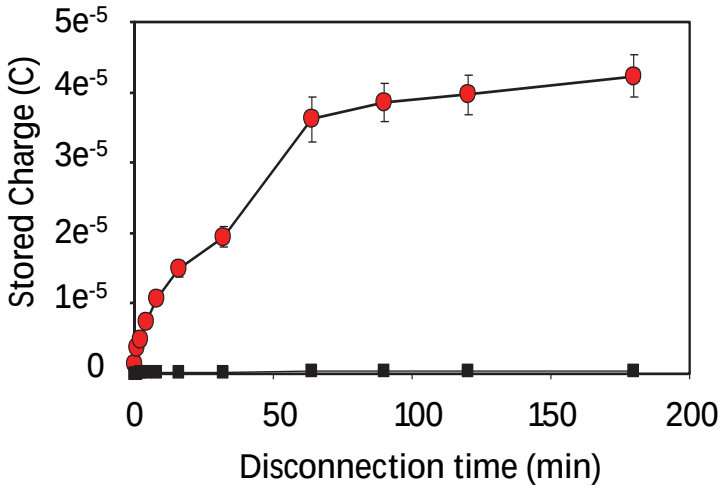

Figure 5. Magnitude of total charge released by the biofilm (●) during the chronoamperometry as a function of disconnection time. Control (■). Error bars (n=5).

Beyond that point the biofilm was apparently saturated and unable to store further electrons. In *Geobacter sulfurreducens* the results are quite similar [12] although saturation seems to occur earlier, after approximately 30 min. In a previous study by Esteve-Núñez *et al*. [11], also with *Geobacter*, charge storage stopped much earlier, after only 8 min but the difference might be related to the fact that work was not carried out with attached cells forming a biofilm, but with cells in suspension.

After normalizing the amount of stored charge to the surface area of the electrode, we obtain a maximum value of $8x10^{-10}$ moles of electrons per square cm, somewhat lower than the maximum of $1x10^{-9}$ obtained by Schrott *et al.* for *Geobacter sulfurreducens*. Attempts to further normalize stored charge per cell were not successful. In our experiment, due to the fact that the anode consists of carbon paper, which is a highly porous material, biomass determination was not straightforward. We attempted to assess biomass using epifluorescence microscopy of DAPI and Live Dead stained samples but only the cells at the surface of the carbon paper could be counted thus underestimating by an unknown factor the actual biomass present in the electrode. Confocal microscopy did not improve the results due to its inability to provide images within the graphite matrix of the carbon paper electrode. Given the impossibility to provide an accurate estimate of attached biomass we opted to include only the raw data as stored Coulombs, without normalizing to biomass. We strongly advice that further experimental work with biofilms attached to electrode surfaces, be carried out using polished non-porous electrode materials (see [27] as an example) in order to make quantification of attached biomass possible.

CONCLUSIONS

Our results report the ability of biofilms of *Shewanella oneidensis* MR-1 to store charge during periods in which an external acceptor is not available. The relevance of this storage capacity for future work with MFCs should be carefully assessed. Several papers dealing with the use of MFCs in activity and toxicity sensors [28,29,30] have been recently published. Use of MFCs for this type of

application should take into account the fact that current production does not only depend on the amount of bacteria and their activity levels, but also on the recent history of the organisms. Also, evaluation of power output curves in microbial fuel cells should take into account that current after disconnection events can be considerably higher that current produced under steady state conditions.

Acknowledgements

This work was supported by grants CSD2006-00044 TRAGUA (CONSOLIDER-INGENIO2010) and CTQ2009-14390-C02-02 from the Spanish Ministry of Education and Science to JM.

REFERENCES

(1) Oh, S.; Logan, B.E. Proton exchange membrane and electrode surface areas as factors that affect power generation in microbial fuel cells. *Appl. Microbiol. Biotechnol.* 2006, *70*, 162–169; DOI 10.1007/s00253-005-0066-y.

(2) Oh, S.; Min, B.; Logan, B.E. Cathode performance as a factor in electricity generation in microbial fuel cells. *Environ. Sci. Technol*. 2004, *38*, 4900–4904.

(3) Uría, N.; Sánchez, D.; Mas, R.; Sánchez, O.; Muñoz, F.X.; Mas, J. *Sensor. Actuat. B: Chem.* 2011 (In press)

(4) Logan, B.E. *Microbial Fuel Cells*; John Wiley & Sons: N.Y., 2008.

(5) Lee, H.; Torres, C.I.; Rittmann, B.E. Effects of substrate diffusion and anode potential on kinetic parameters for anode-respiring bacteria. *Environ. Sci. Technol*. 2009, *43*, 7571-7577.

(6) Aelterman, P.; Freguia, S.; Keller, J.; Verstraete, W.; Rabaey, K. The anode potencial regulates bacterial activity in microbiol fuel cells. Appl. *Microbiol. Biotechnol.* 2008, *78*, 409-418; DOI 10.1007/s00253-007-1327-8.

(7) Picioreanu, C.; Katuri, K.P.; Head, I.M.; van Loosdrecht, M.C.M.; Scott, K. Mathematical model for microbial fuel cells with anodic biofilms and anaerobic digestión. *Water Sci. Technol*. 2008, *57*, 965-971.

(8) Katuri, K.P.; Scott, K.; Head, I.M.; Picioreanu, C.; Curtis, T.P. Microbial fuel cells meet with external resistance. *Bioresource Technol*. 2011, *102*, 2758-2766.

(9) Dewan, A.; Beyenal, H.; Lewandowski, Z. Intermittent energy harvesting improves the performance of microbial fuel cells. *Environ. Sci. Technol*. 2009, *43*, 4600-4605.

(10) Liang, P.; Wu, W.; Wei, J.; Yuan, L.; Xia, X.; Huang, X. Alternate charging and discharging of capacitor to enhance the electron production of bioelectrochemical systems. *Environ. Sci. Technol*. 2011, *45*, 6647-6653.

(11) Esteve-Nuñez, A.; Sosnik, J.; Visconti, P.; Lovley, D.R. Fluorescent properties of *c*-type cytochromes reveal their potencial role as an extracytoplasmatic electron sink in *Geobacter sulfurreducens*. *Environ. Microbiol*. 2008, *10* (2), 497-505.

(12) Schrott, G.D.; Bonanni, P.S.; Robuschi, L.; Esteve-Nuñez, A.; Busalmen, J.P. Electrochemical insight into the mechanism of electron transport in biofilms of *Geobacter sulfurreducens*. *Electrochim. Acta.* 2011. (In Press)

(13) Harris, H.W.; El-Naggar, M.Y.; Bretschger, O.; Ward, M.J.; Romine, M.F.; Obraztsova, A.Y.; Nealson, K.H. Electrokinesis is a microbial behavior that requires extracellular electron transport. *PNAS*. 2010, *107* (1), 326-331.

(14) Clarck, D.J.; Maaøle, O. DNA replication and the division cycle in *Escherichia coli*. *J. Mol. Biol*. 1967, *23*, 99-112.

(15) Zhao, F.; Slade, R.C.T.; Varcoe, J.R. Techniques for the study and development of microbial fuel cells: an electrochemical perspective. *Chem. Soc. Rev*. 2009, *38*, 1926-1939.

(16) Logan, B.E.; Hamelers, B.; Rozendal, R.; Schröder, U.; Keller, J.; Freguia, S.; Aelterman, P.; Verstraete, W.; Rabaey, K. Microbial Fuel Cell: Methodology and Technology. *Environ. Sci. Technol.* 2006, *40* (17), 5181-5192.

(17) Firer-Sherwood, M.; Pulcu, G.S.; Elliot, S.J. Electrochemical interrogation of the Mtr cytochromes from *Shewanella*: opening a potential window. *J. Biol. Chem*. 2008, *13*, 849-854; DOI 10.1007-s00775-008-0398-z.

(18) Hartshore, R.S.; Jepson, B.N.; Clarke, T.A.; Field, S.J.; Fredrickson, J.; Zachara, J.; Shi, L.; Butt, J.N.; Richardson, D.J. Characterization of *Shewanella oneidensis* MtrC: a cell-surface decaheme cytochrome involved in respiratory electron transport to extracellular electron acceptors. *J. Biol. Inorg. Chem*. 2007, *12*, 1083-1094; DOI 10.1007-s00775-007-0278-y.

(19) Baron, D.; LaBelle, E.; Coursolle, D.; Gralnick, J.A.; Bond, D.R. Electrochemical measurement of electron transfer kinetics by *Shewanella oneidensis* MR-1. *J. Biol. Chem*. 2009, *284* (42), 28865-28873.

(20) Meitl, L.A.; Eggleston, C.M.; Colberg, P.J.S.; Khare, N.; Reardon, C.L.; Shi, L. Electrochemical interaction of *Shewanella oneidensis* MR-1 and its outer membrane cytochromes OmcA and MtrC with hematite electrodes. *Geochim. Cosmochim. Acta*. 2009, *73*, 5292-5307.

(21) Shi, L.; Richardson, D.J.; Wang, Z.; Kerisit, S.N.; Rosso, K.M.; Zachara, J.M.; Fredrickson, J.K. The roles of outer membrane cytochromes of *Shewanella* and *Geobacter* in extracellular electron transfer. *Environ. Microbiol. Reports*. 2009, *1*(4), 220-227.

(22) von Canstein, H.; Ogawa, J.; Shimizu, S.; Lloyd, J.R. Secretion of flavins by *Shewanella* species and their role in extracellular electron transfer. *Appl. Environ. Microbiol.* 2008, *74* (3), 615-623.

(23) Marsili, E.; Baron, D.B.; Shikhare, I.D.; Coursolle, D.; Gralnick, J.A.; Bond, D.R. *Shewanella* secretes flavins that mediate extracellular electron transfer. *PNAS*. 2008, *105*(10) 3968-3973.

(24) Covington, E.D.; Gelbmann, C.B.; Kotloski, N.J.; Gralnick, J.A. An essential role for UshA in processing of extracellular flavin electron shuttles by Shewanella oneidensis. *Molecular Microbiology*. 2010, DOI:10.1111/j.1365-2958.2010.07353.

(25) Gil, G.; Chang, I.; Kim, B.H.; Kim, M.; Jang, J.; Park, H.S.; Kim, H.J. Operational parameters affecting the performance of a mediator-less microbial fuel cell. *Biosens. Bioelectron*. 2003, *18*, 327-334.

(26) Carmona-Martinez, A.A.; Harnisch, F.; Fitzgerald, L.A.; Biffinger, J.C.; Ringeisen, B.R.; Schröder, U. Cyclic voltammetric analysis of the electron transfer of *Shewanella oneidensis* MR-1 and nanofilament and cytochrome knock-out mutants. *Bioelectrochemistry*. 2011, *81*, 74-80.

(27) McLean, J.S.; Wanger, G.; Gorby, Y.A.; Wainstein, M.; McQuaid, J.; Ishii, S.; Bretschger, O.; Beyenal, H.; Nealson, K.H. Quantification of electron transfer rates to a solid phase electron acceptor through the stages of biofilm formation from single cells to multicellular communities. *Environ. Sci. Technol*. 2010, *44*, 2721-2727.

(28) Davila, D., Esquivel, J.P.; Sabate, N.; Mas, J. Silicon-based microfabricated microbial fuel cell toxicity sensor. *Biosens. Bioelectron*. 2011, *26*, 2426-2430.

(29) Kim, M.; Hyun, M.S.; Gadd, G.M.; Kim, H.J. A novel biomonitoring system using microbial fuel cells. *Environ. Monit*. 2007, *9*, 1323-1328.

(30) Tront, J.M.; Fortner, J.D.; Plotze, M.; Hughes, J.B.; Puzrin, A.M. Microbial fuel cell biosensor for in situ assessment of microbial activity. *Biosens. Bioelectron*. 2008, *24*, 586-590.

Chapter 4

Electron transfer role of different microbial groups in microbial fuel cells harbouring complex microbial communities.

Submitted to Environmental Science & Technology

CHAPTER 4.

ELECTRON TRANSFER ROLE OF DIFFERENT MICROBIAL GROUPS IN MICROBIAL FUEL CELLS HARBOURING COMPLEX MICROBIAL COMMUNITIES

ABSTRACT

A large number of different microorganisms have been described able to grow forming complex microbial communities at the anode of Microbial Fuel Cells. However, the role of many of these organisms in current production is far from clear. In this work, we attempt to gain some insight into the actual electrogenic capacity of several of these organisms by using a very simple carbon source and a set of experimental MFC reactors with anode configurations that restrict the occurrence of some of the possible electron transfer mechanisms. By observing the different microbial communities formed in each of the reactors as well as their performance, we draw some conclusions on the relevance of the different electron transfer mechanisms under the conditions used. In the MFC1 operating with a naked anode only 30% of the power output was derived from mediated electron transfer while the biofilm at the anode surface was responsible for 70% of the current produced. In this MFC, bacteria with known capacity for direct electron transfer as *Shewanella*, *Clostridium, Dysgonomonas* or *Anaeromonas* were found. In MFC2, with an anode enclosed in a dialysis membrane, current production was only sustained by mediated electron transfer, explained by the presence of a number of different redox species dissolved in the anolyte. Genus as *Acinetobacter*, *Pseudomonas* or *Shewanella* among other reported electron shuttles producers, were present in this MFC. Last, MFC3, with an anode coated with nafion, did not allow the access of either cells or electron shuttles to the electrode. Under these conditions, current production was very low, but a community developed with the prevalence of the *Comamonas* and the archaea *Methanosaeta*. Since methane was not present in the reactor we speculate in the possibility that both *Comamonas* and *Methanosaeta* might be oxidizing acetate to H_2 and CO_2 using tetrahydrofolate and tetrahydromethanopterine cofactors respectively. Hydrogen produced would then cross the nafion barrier and be oxidized at the anode surface.

INTRODUCTION

In a Microbial Fuel Cell (MFC), microorganisms transform the energy available in a reduced substrate directly into electricity by using an anode as the electron acceptor. These bacteria are called electricigens due to their ability to transport electrons outside the cell.

Different mechanisms have been described for the transfer of electrons to the electrode. The most extended classification divides these mechanisms into two types depending on whether electron transfer to the electrode surface occurs through soluble compounds or through membrane-bound electron carriers.

Direct electron transfer (DET) proceeds via membrane bound redox proteins. It has been proved that redox active proteins, such as *c*-type cytochromes and iron sulphur proteins, are localized to the outer-membrane and produce the electron transfer to solid-phase electron acceptors [1].

Mediated electron transfer (MET) is carried out by organic redox species of microbial origin, secreted to the medium where they are able to accept electrons from the cellular electron transport chains, and diffuse to the electrode surface where they are reoxidized to their initial state, thus effectively acting as electron shuttles between cells and electrode [2,3,4,5]. These molecules are reversible and unspecific terminal electron acceptors, so that those excreted by one organism can be taken up and used for intracellular electron transfer by other organism [4] for a large number of redox cycles. Finally, some metabolic end products produced by fermentation can also be oxidized at the electrode surface producing electric current [3]. The fact that oxidation of these products is not reversible does not allow to consider them as shuttles. Nevertheless, current production by these compounds is very inefficient due to their slow reaction with electrodes [6].

Although DET is usually considered more energetically efficient with respect to endogenous soluble redox compounds, it has been demonstrated that mediated electron transfer is absolutely widespread among bacteria. External factors such as the type of substrate, anodic potential, external resistance or mode of reactors operation can have an effect on bacterial metabolism

[7,8,9,10,11,2] and, therefore, on the mechanism of electron transfer. Additionally, the use of microbial mixed cultures in MFC research, and the not unreasonable possibility that different electron transfer mechanisms may be used by the same organism, makes it extremely difficult to determinate or analyze the transfer processes [1].

A relative large number of papers describing the bacterial community in MFCs under different conditions have been published. However, although many of the bacteria described consistently appear in different studies, the complexity of the bacterial relations within de community makes it really difficult to determine their role in current production.

In this work, we attempt to gain some insight into the actual electrogenic capacity of several of the organisms present in complex communities, as well as into the mechanisms at work that allow electron transfer to the anode. By using acetate as the only carbon source, we also simplify the metabolic landscape that could emerge when using more complex carbon sources as glucose. The anode configuration in each MFC limited some of the mechanisms of electron transfer thus simplifying the microbial community developed as well as the amount of current produced. In the first MFC, all possible mechanisms of current production were allowed. In the second fuel cell, in which the anode was surrounded by a dialysis membrane, direct contact was not possible and thus, only redox shuttles or reduced metabolic end products could contribute to current production. The third fuel cell used a nafion-coated anode that only allowed movement of either gases or cations thus precluding a role for electron shuttles or reduced metabolic end products. The study of the microbial communities developed in each MFC together with the performance of each of these systems enables us to speculate about the role of some of these common anode bacteria in current production.

EXPERIMENTAL PROCEDURE

Microbial Fuel Cell Design and Set Up

In this study, three two-chamber fuel cells using different types of anode were used. The MFCs were formed by two cylindrical glass vessels (anode chamber and cathode chamber), both closed at the top by a lid with multiple holes to provide ports for inoculation and sampling as well as the entry of different electrodes (working, reference and auxiliary electrodes) and gases supply. The two reactor vessels were connected at the bottom (Figure 1). At the connecting point, Nafion®117 (Ion power, Inc.) proton exchange membrane (PEM) with a thickness of 183 μm and effective area of 11.34 cm^2 was clamped. This union was sealed using a stainless steel clamp.

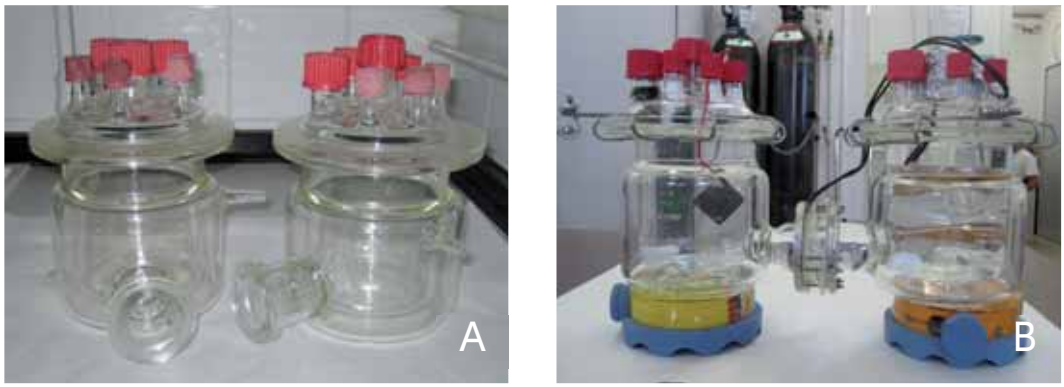

Figure 1. A. Cylindrical glass vessels. B. Microbial Fuel Cell reactor.

In all cases the cathode chamber contained 0.1 M phosphate buffer. Cathodes consisted of 75.91 cm^2 silicon wafers coated with platinum manufactured as previously described [12].

The anode chamber of the three MFCs was filled with 800 mL of AB minimal medium ($[NH_4]SO_4$ 2 g, Na_2HPO_4 7.31 g, KH_2PO_4 7.85 g, NaCl 3 g, Na_2SO_4 0.011 g, $MgCl_2 \cdot 6H_2O$ 0.2 g, CaCl 3.625 mg, $FeCl_3 \cdot$

$6H_2O$ 0.2 mg) [13], containing acetate (10 mM) as the any carbon source. 10 mL of sediment-water slurry obtained from a small creek running through the campus of the Autonomous University of Barcelona (Spain) was added to each reactor as inoculum. The anodes were made of carbon paper (B2120 Toray Carbon Paper Designation TGPH-120, plain, no wet proofing; E-Tek, Inc.) with a thickness of 0.35 mm and an area of 10 cm^2.

Figure 2 shows the different anode configuration used in this study. MFC1 had a naked carbon paper anode. This allows both soluble redox shuttles and bacteria to arrive at the electrode surface thus contributing to current production.

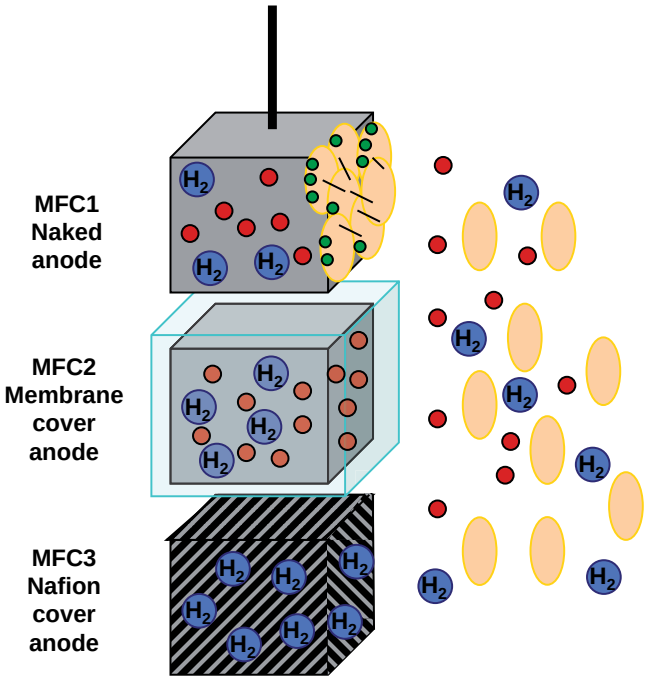

Figure 2. Diagram of the anode configurations used in each MFC.

In the case of MFC2, the carbon paper anode was enclosed in a dialysis bag previously autoclaved, and filled with AB minimal medium to permit the pass of soluble molecules to the anode. The dialysis membrane employed was a Spectra/Por®3 Regenerated Cellulose (RC) membrane (SpectrumLabs), which had a molecular weight cut off (MWCO) rating of 3.5 Daltons (Figure 3A). This membrane was sealed at one end with a Spectra/Por Closure, and pulled out of the bioreactor by one of the top holes. The intended use of second setup is to preclude direct electron transfer to the anode while allowing mediated electron transfer to proceed. This allows to observe the contribution of mediator-dependent processes to current generation and power output.

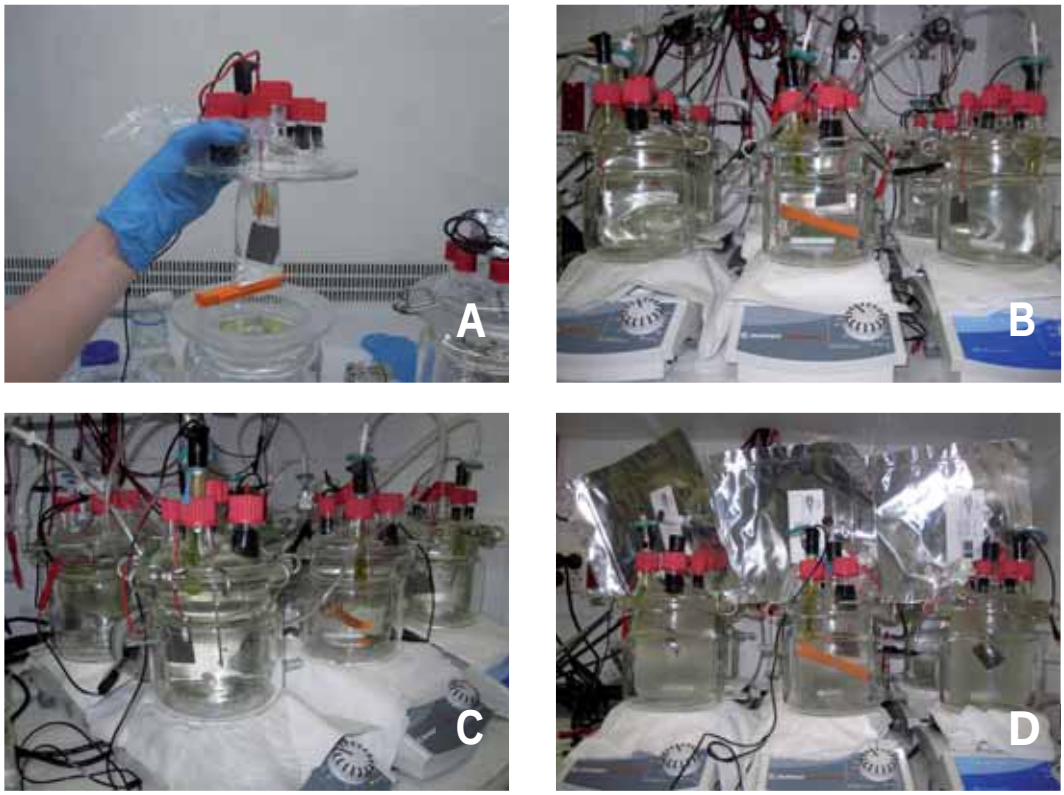

Figure 3. A. Anode covered by Spectra/Por®3 Regenerated Cellulose (RC) membrane (SpectrumLabs). B,C,D. Microbial Fuel Cells set up.

Finally, in MFC3 the carbon paper anode was coated with 4 layers of Nafion ion exchange resin (20 wt.% soln. in lower aliphatic alcohols/H_2O, Sigma-Aldrich Co.). Since nafion only allows cations and gases to reach the anode, we expect neither direct contact nor conventional redox shuttles to be operative thus severely limiting most of the usual electron transfer mechanisms.

The three MFCs were operated with gentle stirring in a temperature controlled room at 28°C. The cathode chambers were gently sparged with air. The anode chambers were sparged with nitrogen except during periods of headspace gas sampling (Figure 3).

Microbial Fuel Cell operation and characterization

The different MFCs were operated under an external load of 65 KΩ. Voltage across this load was continuously monitored, using a digital multimeter with data acquisition system (HP 34970A, Agilent, USA).

Daily, polarization curves were recorded using a source meter unit Keithley®2612 (Keithley Instruments Inc., USA) connected to a personal computer. Curves were performed by imposing different output current values during 3 min and, measuring the resulting voltage. The curve ended when the voltage reached 0, and power was calculated as the product of voltage and current. Power and current values were normalized to the anode area. Likewise, internal resistance (R_{int}) was calculated from the open circuit voltage (OCV) and the slope of the polarization curves using $V=OCV-I \cdot R_{int}$ [14,15].

Anode and cathode working potentials were measured during operation under the external resistance mentioned above. For this, anode and cathode electrodes were connected via a Fluke 112 True RMS Multimeter (Fulke Corporation, Everett, WA) to an Ag/AgCl reference electrode. All potential data have been expressed referring to a standard hydrogen electrode (SHE).

Electrochemical characterization of anolytes and anodes

Cyclic voltammetries of anolytes and anodes were performed using a potentiostat/galvanostat model FRA2 Micro-Autolab Type II. An Ag/AgCl electrode (Methrom, Switzerland) and a platinised silicon wafer electrode were used as reference and auxiliary electrode respectively. Cyclic voltammetries were run between -0.7 V and 0.4 V (vs. Ag/AgCl) at a scan rate of 1 $mV \cdot s^{-1}$. Before the measurements, the electrolyte solution was flushed with nitrogen to remove oxygen traces.

Analysis of the redox species present in the different anolytes was conducted at different times during the experiment. 10 mL of anode solution was filtered using a sterile filter with a pore size of 0.22 µm (Millex®GP, Millipore) to remove bacteria, and introduced in an electrochemical cell. A carbon paper electrode with an area of 0.5 cm^2 was used as working electrode.

In order to perform voltammetries of the biofilm, the anodes of the each MFC were removed from the reactor at the end of the experiment (day 31). After washing several times in phosphate buffer, these electrodes were then used as working electrodes submerged in 100 mL of oxygen free phosphate buffer (0.1 M).

For the sake of comparison, current values were normalized to the area of working electrodes used. Also, in this case, potentials were expressed vs. SHE.

Chemical Analyses

Approximately 4 times a week, 1 mL of anode solution of each MFC was collected and filtered, using a sterile filter with a pore size of 0.22 µm (Millex®GP, Millipore), to determine the concentration of acetate. Samples were analyzed by gas chromatography using a 7820A Agilent GC System (Agilent, USA) with helium as carrier gas and a flame ionization detector (FID). Detection limit was 25 $mg \cdot L^{-1}$.

Gas production in the reactors was monitored using 1 L polypropylene sample bags (245-2x Series Sample Bag, SKC Inc., USA) connected to the anode chambers headspaces (Figure 3D). The contents of the bags were analyzed weekly using a gas chromatograph with argon as carrier gas and a thermal conductivity detector (TCD).

Biomass determination

Concentration of bacteria in the anolyte chamber was monitored at different times using spectrophotometry and fluorescence microscopy.

Optical density at 550 nm was measured using a SmartSpecTMPlus spectrophotometer (BIO-RAD Laboratories, USA). AB minimal medium was employed as a blank.

For fluorescence microscopy counts, samples were fixed with formaldehyde (0.4% final concentration) (Sigma, USA) and filtered through 0.2 µm pore size GTBP filters (Millipore, USA). Bacteria were stained with 20 $\mu g \cdot mL^{-1}$ of 4'-6'-diamidino-2-phenylindole (DAPI) (Merk, Germany) for 5 min and then, rinsed in phosphate buffered saline (PBS) immediately prior to imaging. The filters were mounted on glass slides using immersion oil and were observed in a Zeiss AXIO Imager A1 fluorescence microscope (Zeiss, Germany).

Biofilm morphology and viability

Scanning Electron Microscopy (SEM) and Confocal laser scanning microscopy (CLSM) images were obtained from the biofilm formed on MFC1 anode. This allowed us to observe the biofilm morphology and to estimate the biofilm thickness. Before staining, the electrode was washed in phosphate buffer and cut in different fragments of 0.5 cm^2. Scanning electron micrographs were taken using an EVO®MA 10 microscope (Zeiss, Germany) after the electrode fragment was coated with gold.

For CSML, the electrode samples were prepared with HOETSCH DNA stain that allows observation of bacterial cells, while exopolimers in the biofilms were visualized with AlexaFluor®488 conjugated Concavalin A (ConA) and AlexaFluor®594 conjugated wheat germ agglutinin (WGA). ConA selectively binds to alfa-mannopyranosyl and alfa-glucopyranosyl residues, while WGA binds to sialic and N-acetylglucosaminyl residues. Images were obtained with a confocal microscope Leica TCS SP2 AOBS (Leica, Germany).

Viability of cells in the biofilm was also determined using the bacterial viability test Live/Dead®BacLight™ Bacterial Viability Kit (Invitrogen) by following the protocol detailed by the supplier. Images were acquired with a Zeiss AXIO Imager A1 fluorescence microscope (Zeiss, Germany).

DNA extraction and amplification of 16S rRNA gene

At 0, 8, 15, 29 and 31 days after start of operation, samples of 50 mL of each anolyte were filtered and stored at -20°C for further analyses. At the end of the experiments DNA was extracted from the samples using the UltraClean water kit MOBIO ref. 14880-25. After fuel cell disassembly, the anodes of MFC1 and 3 were subject to DNA extraction using PowerSoil kit MOBIO ref. 12888-50. DNA integrity was checked by agarose gel electrophoresis, and quantified using a low DNA mass ladder as a standard (Invitrogen, USA).

Bacterial 16S rRNA genes were amplified with primers 358F with a 40-bp GC clamp, and the universal primer 907RM [16]. Polymerase chain reaction (PCR) was carried out in a Biometra thermocycler using the following program: initial denaturation at 94ºC for 5 min; 10 touchdown cycles of denaturation (at 94ºC for 1 min), annealing (at temperatures between 62-52 and 65-55°C for 1 min, decreasing 1ºC each cycle), and extension (at 72ºC for 3 min); 20 standard cycles (annealing at 55.5ºC, 1 min) and a final extension at 72ºC for 5 min. PCR mixtures with a final volume of 50 µL contained 1-10 ng of template DNA, deoxynucleoside triphosphate (200 µM), 1.5 mM $MgCl_2$, each primer at a concentration of 0.3 µM, *Taq* DNA polymerase (2.5 U) (Invitrogen, USA)

and PCR buffer supplied by the manufacturer. BSA (Bovine Serum Albumin) at a final concentration of 600 $\mu g \cdot ml^{-1}$ was added to minimize the inhibitory effect of humic substances [17].

Anolyte and anode samples at the end of the experiment were checked for the presence of *Archaea*. Primers 344f-GC and 915R were used for archaeal 16S rRNA amplification [18]. The PCR protocol included an initial denaturation step at 94°C for 5 min, followed by 20 touchdown cycles of denaturation (at 94°C for 1 min), annealing (at 71°C to 61°C for 1 min, decreasing 1°C each cycle), and extension (at 72°C for 3 min); 20 standard cycles (annealing at 55°C, 1 min) and a final extension at 72°C for 5 min.

PCR products were verified and quantified by agarose gel electrophoresis with a low DNA mass ladder standard (Invitrogen, USA) using the Quantity One software package (Bio-Rad Laboratories, USA) for gel documentation and analysis.

Denaturing gradient gel electrophoresis

Three different DGGEs were performed using a DCode universal mutation detection system (Bio-Rad Laboratories, USA) as described by [19]. DGGE1 contained the anolyte samples of the three MFCs at different times as well as the inoculum. DGGE2 and 3 analyzed bacterial and *Archaea* communities respectively, of anolyte and anode at the end of the experiment.

For DGGE analyses approximately 700 ng of PCR product per lane were loaded onto 6% (wt/vol) polyacrylamide gels with gradients of 30-70% (DGGE1), 25-65% (DGGE2) and 40-80% (DGGE3). DNA-denaturant agent was cast by mixing solutions of 0% and 80% denaturant agent (100% denaturant agent is 7 M urea and 40% deionized formamide) using a gradient delivery system EP-1 Econo Pump (Bio-Rad Laboratories, USA). Electrophoresis was run at 100 V for 18 h at 60°C in 1xTAE buffer (40 mM Tris [pH 7.4], 20 mM sodium acetate, 1 mM EDTA). The gels were stained with SybrGold (Molecular Probes) for 45 min, rinsed with 1xTAE buffer, and visualized with UV in a Gel

Doc EQ (Bio-Rad Laboratories, USA). In addition to gel analysis by Quantity One software (Bio-Rad Laboratories, USA), prominent bands were excised.

After leaving overnight in milli-q water, excised bands were re-amplified. Products were purified and sequenced by Macrogen (Amsterdam) with primers 907RM (DGGE1 and 2) and 915R (DGGE3). Macrogen utilized the Big Dye Terminator version 3.1 sequencing kit and reactions were run in an automatic ABI 3730XL Analyzer-96 capillary type. Gene sequences were deposited in GenBank under accession numbers HE856389-HE856491. Sequences were subject to a BLAST search [19] to obtain an indication of the phylogenetic affiliation.

Statistical analysis

DGGE images were processed and converted into unweighted binary patterns using the Quantity One software package (Bio-Rad Laboratories, USA) (absent= 0, present= 1). Similarity metrics of the microbial community profiles were generated with SPSS 12.0 using Dice's similarity coefficient.

In order to obtain direct descriptors of the diversity in each sample, we calculated Simpson´s biodiversity richness index [20] at genus level. This index was obtained from the bands, according to the genus assigned to each band by BLAST search, and using the following expression:

$$D_{si} = \sum_{i}^{s} \frac{n_i \times (n_i - 1)}{n \times (n - 1)}$$

in which n_i = number of bands related to one genus, n = number total of bands, s = number of different genera. Higher values indicate lower richness.

RESULTS

Acetate consumption and community growth

MFCs containing 1L of AB minimal medium and acetate 10 mM were inoculated with 10 mL of sediment-water slurry obtained from a small creek. Following inoculation, the MFCs were operated in batch mode for a period of 31 days.

Figure 4 shows changes in biomass (cell·mL^{-1}), optical density (Abs 550 nm) and acetate concentration (mM) during this period.

After the first addition at the beginning of the experiment, acetate was fed twice to all reactors. The first time, at day 7, and the second time, at day 23, in each case, right after sampling and data acquisition.

Microbial biomass in the anolyte was monitored during the experiment by measuring optical density at 550 nm, and total cell counts by epifluorescence microscopy. Both variables showed a steady increase during the first 10 days of the experiment, stabilizing thereafter.

At the beginning of the experiment, cell densities in the anolyte of three MFCs averaged 1.16e^{7} ± 5.56e^{6} cell·mL^{-1}. During the first week cell numbers increased steadily up to a maximum values of 1.09e^{8}, 1.17e^{8} and 8.65e^{7} cell·mL^{-1} for MFCs 1, 2 and 3 respectively. This increase in cell density was paralleled by a decrease in acetate. Acetate was consumed quickly. Before the first addition 60% of the acetate had been consumed. For the second addition, acetate was fed when concentration fell below 5% of initial value. After adding acetate for a second time, cell concentration barely increased and acetate was not consumed, indicating that the stabilization of bacterial growth was not due to a limitation in the carbon source concentration but due to depletion of some other compound essential for growth.

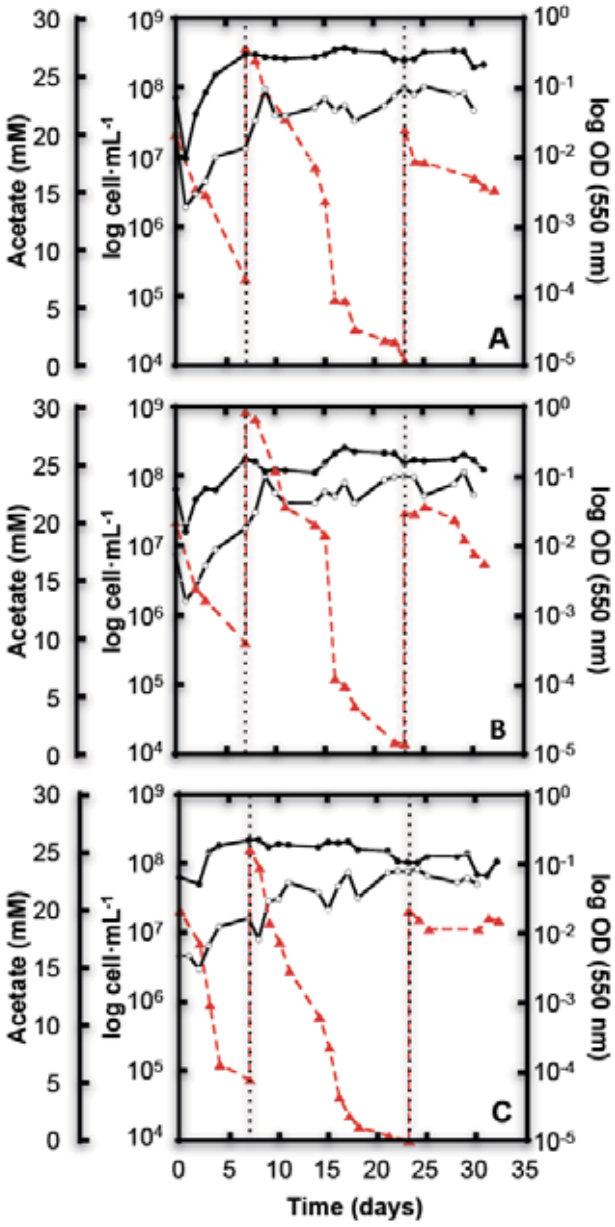

Figure 4. Evolution of acetate (▲), cell concentration (○) and optical density at 550 nm (●), during the experiment in MFC1 (A), MFC2 (B) and MFC3 (C). Vertical dotted lines show the different acetate feeds.

SEM (Figure 5A and 5B) and CSLM were used to visualize the biofilm structure and to determine the thickness of the biofilm formed on the anode of MFC1. CSML images of the electrode biofilm showed an average biofilm thickness of 55.6 ± 1 µm. Additionally, biofilms of electrode 1 and electrode 3 were also observed by fluorescence microscope after staining using Live/Dead® BacLight™ Bacterial Viability Kit demonstrating that most of the cells in the biofilm were alive (Figure 5C and 5D).

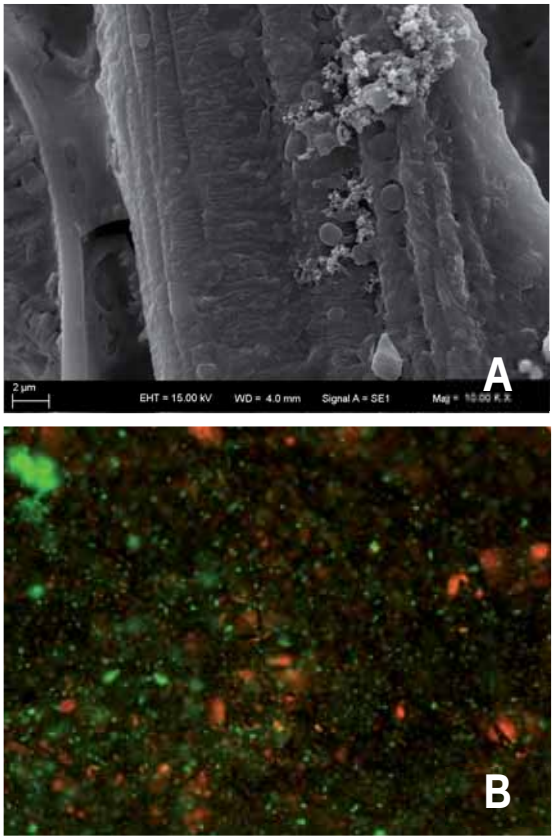

Figure 5 A. SEM images of MFC1 anode (naked anode). B. Fluorescence microscopy images of the MFC1 anode after staining using Live/Dead® BacLight™ Bacterial Viability Kit.

Methane and hydrogen production were measured weekly using the procedure outlined in material and methods by chromatography. Only during the first week traces of methane were found in MFC3. Hydrogen was not detected in any of the three MFCs.

Electrical Performance

MFCs were run under the same conditions for 4 weeks. Voltage was continuously recorded, and stable values were reached after 4-6 days in all three reactors. Additionally both anode and cathode potentials were measured under these conditions.

During this period average voltages of 86.55 ± 2.46, 59.81 ± 3.58 and 8.18 ± 2.67 mV were measured in MFCs 1, 2 and 3 respectively, showing a better performance of the MFC with non-coated anode. These voltage data have been represented in Figure 6 together with the anode and cathode potentials measured during operation.

From the start of the experiment, MFC1 showed the highest anode potentials with an average of -0.06 ± 0.01 V. At day 21, data showed a hard drop, recovering previous potential values after addition of acetate. Initial anode potentials of MFC2 and 3 started from more negative values as a result of the impossibility of certain redox species to reach the electrode. MFC2 with an anode potential average of -0.11 ± 0.016 V, suffered a slow increase during the first five days probably due to an increase in the oxidation of redox species at the anode, until reaching values very similar to those of the MFC1. MFC3 anode potential showed the lowest anode potentials of the three reactors (-0.21 ± 0.013 V), indicating a high resistance to electron transfer to the anode and the accumulation of even higher amounts of reduced compounds. Cathode potentials were stable and similar between MFCs. Values between 0.19 ± 0.004 V and 0.28 ± 0.02 V were registered.

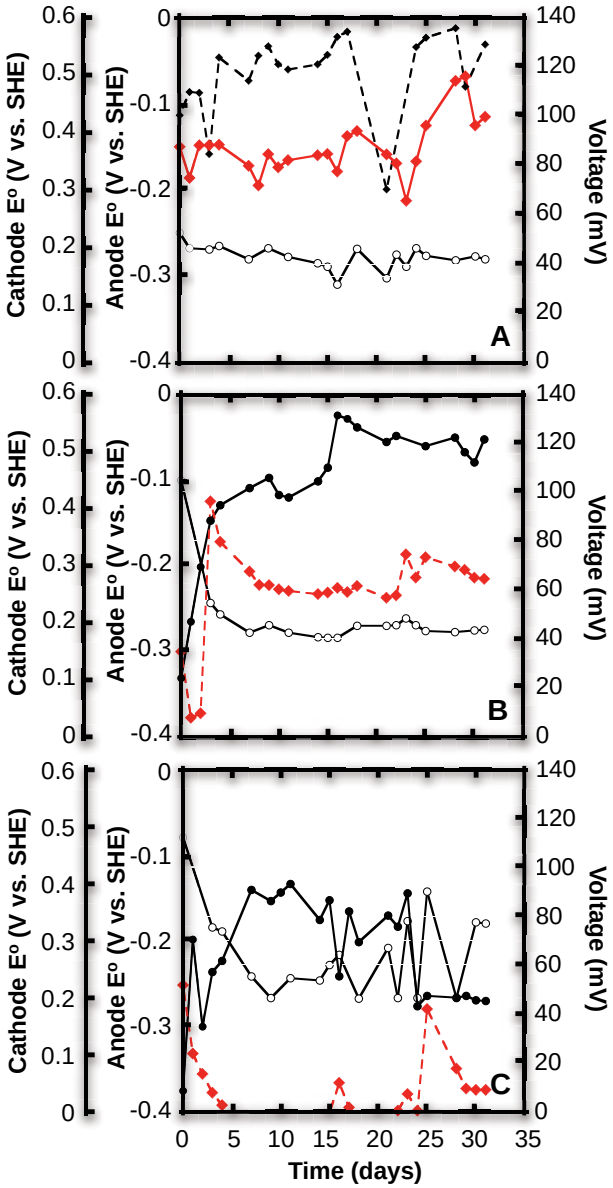

Figure 6. Evolution of cell voltage (◆), anode potential (◆) and cathode potential (○) under operational conditions (65 KΩ) along the experiment in MFC1 (A), MFC2 (B) and MFC3 (C).

Most detectable difference between cathode potentials of the three cells, were the high transient values observed in MFC2 and 3. This was likely due to a lower consumption of oxygen present in the cathode chamber since the current provided by these MFCs was much lower.

Polarization curves obtained daily showed that the three MFCs had different power output capacities. Table 1 shows an average of OCV and maximum current density (MCD) data obtained from polarization curves.

Table 1. Average and standard error of the different parameters related to MFCs performance obtained along the experiment recorded under continuous operation at 65 KΩ and from the polarization and power curves made at different times. [1]Maximum Current Density, [2].Maximum Power Density.

	MFC1	MFC2	MFC3
V at 65 KΩ (mV)	86.55 ± 2.46	59.81 ± 3.58	8.18 ± 2.67
OCV (mV)	136.75 ± 3.05	123.42 ± 6	26.79 ± 5.23
Rint (KΩ)	53.53 ± 4.69	106.43 ± 24.7	1577.37 ± 636.38
MCD[1] (μA/cm^2)	0.32 ± 0.02	0.15 ± 0.01	0.02 ± 0.005
MPD[2] (μW/cm^2)	$9.7e^{-3}$ ± $6.8e^{-4}$	$4.56e^{-3}$ ± $4.09e^{-4}$	$3.1e^{-4}$ ± $1.21e^{-4}$
E° Cathode (V vs SHE)	0.19 ± 0.001	0.21 ± 0.01	0.28 ± 0.017
E° Anode (V vs SHE)	-0.06 ± 0.01	-0.11 ± 0.016	-0.21 ± 0.013

As expected, the non-coated anode MFC, showed the best performance with higher OCV and maximum current density values (136.75 ± 3.05 mV, 0.32 ± 0.02 μA·cm^{-2}).

Although MFC2 showed similar OCV values, maximum current density, with an average of 0.15 ± 0.01 μA·cm^{-2}, was 50% lower than the obtained for the first MFC reactor. In general, large internal resistances were limiting the performance of our MFCs due to the employed H-shape fuel cells, as a

consequence of large distance between the anode and cathode, and the relatively small surface area of proton exchange membrane [21].

Internal resistance detected in MFC1 was about 53.53 ± 4.69 KΩ, meanwhile in MFC2, an average internal resistance of 106.43 ± 24.7 KΩ was measured along the experiment. The highest internal resistance of 1577.37 ± 636.38 KΩ was found in MFC3 and probably explained the poor performance observed (OCV values were the smallest, 26.79 mV, and maximum current density was very low, 0.02 ± 0.005 $\mu A \cdot cm^{-2}$).

Electrochemical Measurements

After eliminating cells in suspension by filtration, cyclic voltammetries of the anolytes were run at different times to check for soluble redox compounds that might contribute to current production in the different systems. Additionally, the anodes were also analyzed by cyclic voltammetry at the end of the experiment.

Table 2. Average and standard error of the peak potential of the species redox found along the experiment in the anolyte of the three MFCs by cyclic voltammetry. An average of the current and area (Coulombs) of the peaks has been also added.

	E Peak (V vs. SHE)	Peak current (A/cm^2)			Peak Area (C)		
		MFC 1	MFC 2	MFC 3	MFC 1	MFC 2	MFC 3
1	-0.207 ± 0.001	-3,39E-05	-3,89E-05	-1,20E-04	7,54E-04	6,31E-04	2,54E-03
2	-0.395 ± 0.011	-6,75E-05	-2,20E-05		3,01E-03	7,65E-04	
3	-0.215 ± 0.002	1,40E-05	-1,15E-04	-1,46E-04	9,64E-04	4,05E-03	4,04E-03
4	-0.037 ± 0.002	1,05E-05	2,01E-05	5,99E-05	1,79E-04	4,23E-04	1,26E-03
5	-0.694 ± 0.007	-1,13E-04		-1,45E-02	1,03E-02		9,53E-03
6	-0.287 ± 0.007		-2,39E-05	-1,18E-05		3,30E-04	2,30E-04
7	-0.248 ± 0.002		1,18E-05			3,00E-04	
8	-0.272 ± 0.007		-2,39E-05			3,30E-04	
9	0.028 ± 0.008		4,71E-05			1,79E-03	
10	-0.118 ± 0.002		7,40E-06			3,66E-04	
11	-0.297 ± 0.008		-1,18E-05			2,30E-04	

Table 2 indicates the potential at which the different redox peaks were observed during the experiment. Voltammograms of the anolytes showed three peaks in common at potentials of -0.207 ± 0.001, -0.215 ± 0.002 and -0.037 ± 0.002 V. All the redox species present in the anolyte of the MFC with the non-coated anode were also found in some of the other MFCs. In addition to the peaks mentioned above, two reduction peaks were detected. The first, at a potential of -0.395 ± 0.01 V, belonged with a redox species also present in MFC2. The last peak, detected in both non coated and nafion-coated anode MFCs (MFC1 and MFC3), was found at -0.694 ± 0.007 V. Voltammograms of MFC2 anolyte showed high number of exclusive peaks demonstrating the importance of electron shuttles in current production for this reactor.

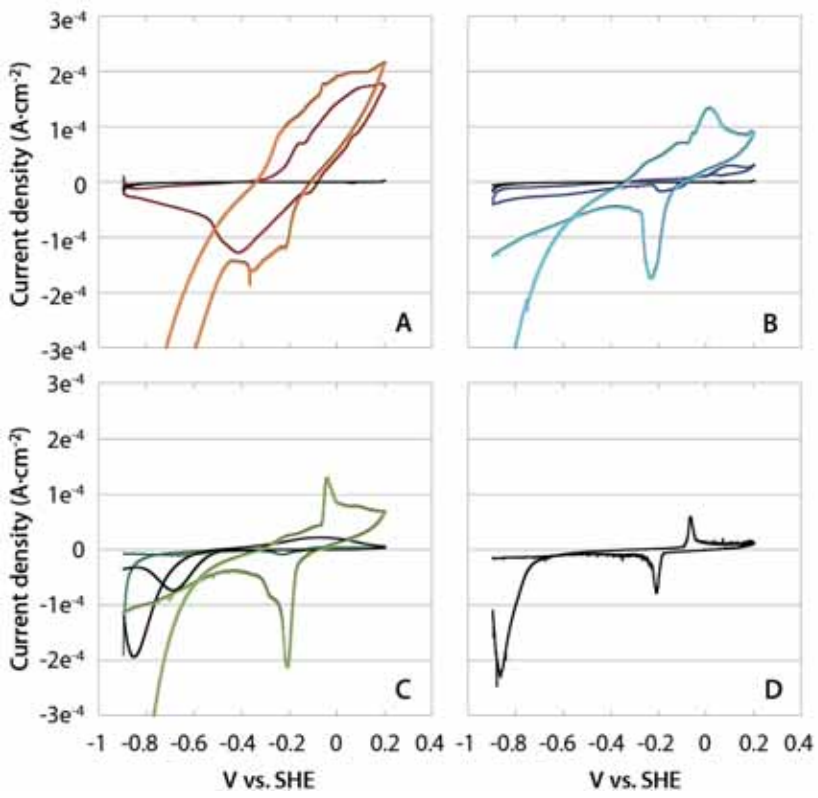

Figure 7. Cyclic voltammograms at a scan rate of 1 mV·sec^{-1} of anode electrodes (MFC1: red line, MFC2: dark blue, MFC3: dark green) and anolytes (MFC1: orange line, MFC2: light blue, MFC3: light green) obtained of the MFC1 (A), MFC2 (B) and MFC3 (C)

taken at the end of the experiment. The black line in each graphic correspond to the voltammogram of each electrode previously to MFC assembly as electrode blank. (D) Voltammogram of the minimal medium AB used as blank of the anolyte.

To analyze the biofilms attached to the electrodes, cyclic voltammetries were carried out in phosphate buffer (0.1M) using the anodes as working electrodes. The results are shown in Figure 7 together with the voltammogram of the anolyte performed at the end of the experiment. The voltammogram of the MFC1 anode, which had a biofilm attached, showed electrochemical activity. Three reversible peaks were detected at potentials of about 0.091, 0.014 and -0.134 V. In addition to these, two reduction peaks were observed at -0.427 and -0.504 V. Some of these peaks were also present in the anolyte voltammograms likely indicating the existence of electron shuttles attached to the biofilm matrix. The voltammogram for the anode taken from the second MFC reactor had a small peak (-0.2 V) coincident with a large peak found in the anolyte. The results suggest that a small quantity of soluble redox active compounds remained adsorbed to the graphite electrode. The voltammogram of the MFC3 anode, as expected, showed no peaks.

Microbial community succession and Diversity analysis

To analyze the diversity of the non-attached microbial community, samples of the anolyte of the three MFCs were taken after 0,7,15, 22, 29 and 31 days of operation. At the end of the experiment, small pieces of biofilm-coated carbon paper anode from MFCs 1 and 3, were also cut off for the analyses of the microbial diversity forming the biofilm. All samples were analyzed by denaturing gradient gel electrophoresis (DGGE). Image and informative sequences with a similarity higher than 95% of the three DGGEs are available as supplementary material (Images S1, S2 and S3, and Table S1, S2 and S3).

The band pattern observed in the different DGGE gels was recorded as a binary matrix that was later used to carry out an analysis of similarity using Dice coefficient. Dice index equal to 1 shows the maximum similarity. Table 3 shows the results of the analyses as the average of Dice similarity

coefficient between the different sample sets. So, all three MFCs showed very low similarities with the inoculum (0.08, 0.05 and 0.05 in MFC1, 2 and 3 respectively). On the contrary, higher similarities in band pattern were observed within sample sets taken during the experiment for each MFC (0.48 ± 0.03, 0.5 ± 0.04 and 0.64 ± 0.04 for MFC1, 2 and 3 respectively). As to the relation between the anolytes and electrodes, a coefficient of 0.9 was calculated in MFC1 indicating very small differences in bacterial community composition. However, MFC 3 showed more differences with a Dice coefficient of 0.48.

Table 3. Average and standard error of similarity index Dice obtained between the different sample sets.

Dice Index	Inoculum	MFC1	MFC1 Anode	MFC2	MFC3	MFC3 Anode
MFC1	0,08	0.48 ± 0.03	0.9			
MFC2	0,05	0.23 ± 0.02		0.50 ± 0.04		
MFC3	0,05	0.16 ± 0.01		0.24 ± 0.02	0.64 ± 0.04	0.483

Simpson Index was also calculated as a metric for richness of genera in the different samples. Richness (0.06) was slightly higher in the inoculum than in MFC1 and 2 (0.07 and 0.08). In the case of MFC3, genera richness was the lowest, with a Simpson Index of 0.17, in accordance with the overall characteristics of energy deprived MFCs.

In relation to phylogenetic composition, 20.7% of gel bands present in the inoculum sample were affiliated with the phylum *Bacteroidetes* with a large fraction of the clones, which were members of the order *Bacteroidales*. Whereas a 24.14% were associated with *Firmicutes,* completely belonging to the order *Clostridiales*. Results for anolyte and anodes of the three MFC reactors at the end of the experiment can be observed in Table 4. Additionally, an average of the percentage of presence of each genus during the experiment has also been included.

In the anolyte of MFC1 (Table 4, Figure 8A), *Bacteroidetes* was the most important group in reference to number of bands during all the experiment, with values of band percentage over 40%.

Uncultured bacterium clone ZL9 related to the genera *Flavobacterium*, was the most abundant, constituting the 21.05% of the genus found in the MFC1 anolyte. Bands related to *Dysgonomonas* (10.53%) and *Bacteroides* completed this group.

Table 4. Percentage of the bands related to each genus at the end of the experiment and as an average of the percentage obtaining along the experiment.

ORDER	GENUS	MFC1				MFC2			MFC3			
		Day 31	Average	SE	Anode	Day 31	Average	SE	Day 31	Average	SE	Anode
Rhodocyclales	***Azonexus***	0,00	0,62	0,62	0,00	0,00	1,55	0,98				
	Azovibrio	10,53	4,96	1,89	5,88							
Burkholderiales	***Hydrogenophaga***	0,00	0,62	0,62	5,88	26,67	16,47	3,40	16,67	9,84	3,21	26,67
	Comamonas	5,26	6,83	0,93	5,88	6,67	7,19	2,74	41,67	29,52	4,40	13,33
	Diaphorobacter					0,00	3,59	1,19	0,00	2,84	1,78	0,00
	Acidovorax					6,67	3,77	1,25	0,00	0,00	0,00	6,67
	Alicycliphillus	0,00	0,00	0,00	5,88				0,00	0,00	0,00	6,67
Pseudomonadales	***Pseudomonas***	0,00	4,20	1,98	0,00	0,00	6,93	3,10	0,00	2,61	1,61	0,00
	Acinetobacter	10,53	16,04	2,46	17,65	13,33	14,02	1,59	8,33	10,80	2,74	13,33
Alteramonadales	***Shewanella***	5,26	4,36	0,96	5,88	6,67	4,53	1,00	0,00	2,00	2,00	0,00
Aeromonadales	***Aeromonas***	5,26	5,60	1,45	0,00							
Clostridiales	***Clostridium***	0,00	1,73	1,16	11,76	6,67	4,08	1,94	0,00	1,18	1,18	0,00
	Anaerofilum	5,26	1,80	1,14	0,00	6,67	3,90	1,28				
Flavobacteriales	***Chryseobacterium***	0,00	1,11	1,11	0,00				8,33	7,94	0,69	6,67
	Flavobacterium	21,05	17,09	3,00	5,88	6,67	2,22	1,41	0,00	3,10	1,90	0,00
Bacteroidales	***Bacteroides***	15,79	8,50	2,15	5,88	13,33	17,22	1,47	0,00	2,35	2,35	6,67
	Dysgonomonas	10,53	8,51	2,05	5,88	6,67	6,84	1,46	8,33	6,76	1,75	0,00
Fusobacteriales	***Fusobacterium***								8,33	7,94	0,69	0,00
Actinomycetales	***Propionibacterium***	0,00	5,34	1,49	0,00							
Gemmatimonadales	***Gemmatinomas***								0,00	2,84	1,78	13,33
Campylobacterales	***Arcobacter***					0,00	3,23	1,03				
Others	***Others***	10,53	0,00	0,00	0,00				0,00	0,00	0,00	6,67
Unidentified	***Unidentified***	0,00	2,47	2,47	11,76	0,00	0,93	0,93	8,33	7,94	0,69	0,00

In the anode of MFC1 (Table 4, Table S2), *γ-proteobacteria* was the group with highest number of bands (29.41%) following by *β-proteobacteria* (23.53%). The order *Pseudomonadales*, and more specifically the genus *Acinetobacter* (17.65%), was the most abundant *γ-proteobacteria. Costridium* was also important in the anode sample (11.76%), although it was not present in the anolyte.

Bacterial clones obtained in the anolyte of MFC2 (Table 4, Figure 8B, Table S1) were affiliated mostly to *β-proteobacteria* (40%) and *Bacteroidetes* (26.67%). In this MFC a rise of *Burkholderiales* order was observed along the experiment. Clones related to *Hydrogenophaga* genus, covered the 26.67% of the bands of the sample. *Bacteroidetes* were represented by the same genera that dominated in the anolyte of MFC1 (*Flavobacterium, Dysgonomonas and Bacteroides*).

Regarding MFC3, the restrictions imposed by the use a nafion-coated anode, were reflected in its phylogenetic composition with large number of bands related to the same genera. MFC3 was clearly dominated by *β-proteobacteria*, in particular by *Burkholderiales* order (58.33%). An important feature of the MFC3 anolyte community was the marked abundance of bands related to *Comamonas* throughout the experiment. At the end, this genus represented the 41.67% of all the bands, while *Hydrogenophaga*, was present in a 16.67% (Table 4, Figure 8C).

Bacteria were also found attached to the nafion-coated electrode (Table 4, Figure S2). As in the anolyte, *Burkholderiales* order was the 53.33% of the bands. Within this group *Hydrogenophaga* was the most represented organism with 27% of the bands, followed by *Acidovorax* and *Alicycliphilus*.

Members of *Archaea* were also found in the anode chambers of MFC1 and MFC2, but a larger number of bands with higher intensity were observed in MFC3. Overall, 75% of the *Archaea* bands found could be sequenced and all belonged to the *Methanosarcinales,* specifically the genus, *Methanosaeta* (Table S3).

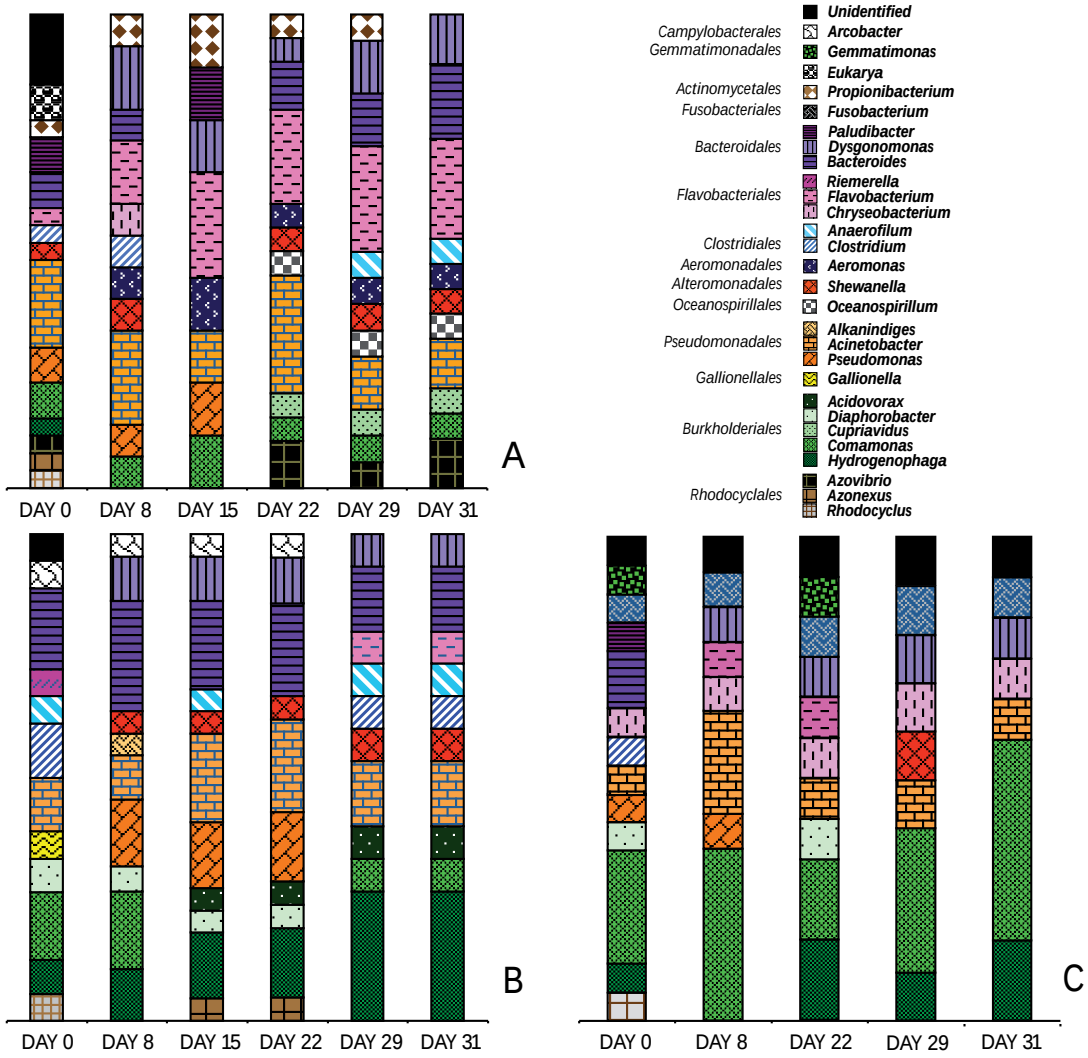

Figure 8. Percentage of the number of bands related to each genus in the anolyte of the MFC1 (A), MFC2 (B) and MFC3 (C) at different times.

DISCUSSION

In the three MFC designs studied, a decrease in taxonomic richness was observed in relation to the inoculum (Simpson Index 0.06 in comparison with the values between 0.07 and 0.17 obtained in the three MFCs) showing the selective capacity of MFC environments. Although differences between the communities selected in each reactor were observed, in general *Proteobacteria*, particularly *β-proteobacteria*, dominated in the three reactors. Phung and co-workers (2004)[22] also found a community dominated by this group in a MFC enriched with river water. Additionally, a high proportion of denitrifying bacteria appeared in our experiment. The prevalence of this group of bacteria in MFCs [23,22] has already been reported. The authors in these papers suggest that these bacteria play an important role in power production in exoelectrogenic communities in absence of dissimilatory metal reducing bacteria [22].

The formation of an exoelectrogenic biofilm in MFC1 resulted in power densities about 60% and 95% higher than in MFC2 and 3 respectively, which did not allow direct electron transfer to the anode. In general, acetate was consumed quickly, indicating an efficient degradation of the carbon source by the community found in the three reactors. DAPI counts of the anolyte showed that the number of bacteria present in the three MFCs was in the same range, and there were no significant differences between them related to acetate consumption and cell density after the first week. So, different performance and efficiency in the cells should be related to differences in diversity and the electron transfer mechanisms developed in the MFC reactors.

Bacteria forming the biofilm attached to the anode of MFC1 mostly belonged to *γ-proteobacteria*. This group can be usually found at higher numbers within electrode biofilms as consequence of their biofilm-forming capacities [24,25]. The fact that the biofilm contained an electrochemically active community was demonstrated by cyclic voltammetry. Reported electroactive bacteria as *Shewanella* [3] or *Clostridium* [26,27] were found in the composition of the biofilm. *Dysgonomonas* also formed part of the anode biofilm [28,29,30]. In fact, a specie of this genus, *Dysgonomonas wimpennyi* ANFA2, has been described as an electrochemically active Fe(III)-reducing bacterium,

which was isolated from an MFC with no mediator [31]. The exoelectrogenic activity of some species of the genus *Comamonas* in biofilm electrodes have been determined in some studies [22,32], although in our experiment and others [33], more bands related to this genus were detected in the anolyte than at the electrode surface [34]. The genus *Aeromonas* was also present in the anolyte of this MFC. Species of *Aeromonas* are able to reduce ferric iron Fe(III), nitrate and sulphate, expressing *c*-Type cytochromes when growth under anaerobic conditions with oxidation and reduction peaks at 50 and -350 mV (vs. Ag/AgCl) [35]. The potential of these reported peaks have a good coincidence with some of those found in our biofilm voltammetry.

Geobacter is a well-known exoelectrogenic bacteria, which is often found in anode biofilm of MFCs fed with acetate [8]. However, it did not show up in our MFCs, probably because the organism was absent from the inoculum [36].

However, the anode biofilm is a complex matrix in which mechanisms of electron transfer, other than direct contact cell membrane-bound proteins, can contribute to power generation. Thus, microbial species able to produce electron shuttles, whose presence was also found in the anolyte, were forming part of the biofilm. Other studies have demonstrated the importance of redox mediators embedded in the matrix on electron transfer rates [35]. In this way, power output is not only dependent of the cells in contact with the anode, but upper layers of the biofilm can contribute to electron transfer [35]. This is supported by the high similarity between the microbial community at the anode surface and in the anolyte (Dice index 0.9). Additionally, cyclic voltammetries of the anolyte showed redox species with potential peaks very similar to those found in biofilm voltammogram, suggesting the presence of mediators embedded in the biofilm.

The anolyte of MFC1 contained a microbial community formed by bacteria previously reported in the literature as able to produced electron shuttles. Between them, *Pseudomonas* produces pyocianine with a redox potential of -0.03 V [5] and other phenazine derivates [37], while *Propionibacterium* and *Shewanella* excrete quinoid compound, 2-amino-3-carboxy-1,4-naphtoquinone (ACNQ) [5] with a midpoint potential of -0.071 V [38] and flavins (redox potential between -0.2 and -0.25 V) [39], respectively. An important genus was *Acinetobacter*. Some species

of this genus have been reported to use a self-secreted redox compound with redox characteristics matching those of pyrroloquinoline quinone (redox potential -0.4 V [40]), a previously reported electron shuttle between a soluble enzyme and an electrode [41,42]. So, the high importance of the genus *Acinetobacter* in MFCs 1 and 2 and, its abundant presence in other studies with MFCs [34,43,44] suggest a role for this organism in electricity production although more experiments are needed for this affirmation. However, a high quantity of bands of the anolyte sample belonged to the genus *Flavobacterium*. This genus, which is formed by bacteria with a big variety of metabolic features, has been found in the anolyte community of a large number of papers related to BES systems [22,45], although the role of this bacterium in current production remains unknown.

The fact that a MFC, in which direct electron transfer is possible, has an abundant presence of organisms that rely on electron shuttles, it is related to the type of operation. Batch mode operation has been observed to favour the presence of organisms able to produce redox shuttles [46,47]. So, the anolytes of MFC1 and MFC2 had a large number of genera in common.

While the producers of electron shuttles found in the anolyte of MFC1 (*Pseudomonas, Shewanella,* and *Acinetobacter*) were also found in MFC2, the most important genus in terms of number of bands, was *Hydrogenophaga*, previously found in a microbial electrolysis cell system [48].

Cyclic voltammetries of the MFC1 and MFC2 anolytes showed several redox peaks, many of them compatible with some of the mediators described above, such as ACNQ, pyocianine, pyrroloquinoline quinone (PQQ) and flavins. In the anode chamber of MFC2, where conditions prevented the development of organisms dependent on direct electron transfer, the number of redox species was the highest. So, this anolyte presented peaks not found in other MFCs anolytes and that could be related to organisms selected only in this MFC. For example, electrochemical activity of *Arcobacter butzleri* ED-1 cultures has been found attached to the electrode of acetate-fed fuel cells although the mechanisms of electron transfer used by this microorganism has not been established [49]. In this way, its presence in this MFC could indicate a mediated mechanism for this bacterium. Additionally, two denitrifying bacteria belonging to the *Burkholderiales* order, *Diaphorobacter* and *Acidovorax,* were also found only in the anolyte only of this MFC. They are

genus frequently reported in MFC studies although their role in current production remains unknown [46,50,51].

At the end of the experiment, the anode from MFC1 with biofilm attached was removed and replaced by a new carbon paper electrode. This resulted in a 70% decrease in current and power density, providing values very close to those obtained in MFC2. This demonstrated that despite the presence of an important community of non attached electrogenic bacteria in suspension, the biofilm was responsible for most the current produced.

Finally, MFC3 in which access of either cells or organic shuttles to the electrode was restricted by a nafion coating showed the maximum differences in all parameters related to the other two MFCs. Very low values of current were detected in this reactor due to the fact that neither bacteria nor conventional electron shuttles could react with the electrode. Additionally, overpotentials due to ohmic losses and activation losses increased in this reactor as a consequence of the resistance imposed by the nafion layers coating the electrode.

The fact that the anode potential in MFC3 (-0.21 ± 0.013 V) was considerably lower than in MFC1 (-0.06 ± 0.01 V) and 2 (-0.11 ± 0.016 V) suggests the accumulation of reduced species that could not be oxidize at the electrode surface due to the presence of the nafion coating.

Normally, in MFCs inoculated with mixed cultures, anode respiring bacteria have to compete for the substrate with other groups such as fermenters or methanogens. The existence of anoxic conditions in the anode chamber, and the restriction imposed by the nafion coating not allowing direct or mediated electron transfer reduces the metabolic options available for organisms growing in the anolyte to only two: methanogenesis and syntrophic acetate oxidation.

In syntrophic acetate oxidation, acetate is oxidized to CO_2 in a series of reactions in which acetate is split and oxidized by a carbon monoxide dehydrogenase, which releases CO_2 and generates a corrinoid-linked methyl moiety. The methyl moiety is sequentially oxidized to CO_2 in a series of reactions in which the methyl group remains linked to a tetrahydrofolate (THF) carrier (Figure 9B)

[52,53]. Syntrophic acetate oxidation under anoxic condition requires the presence of a series of enzymes: methiltransferase, methylene-THF reductase, methylene-THF dehydrogenase, methenyl-THF cyclohydrolase and formyl-THF synthetase. A described syntrophic acetate oxidizing bacterium *Clostridium* [52] was found in this reactor. However, the organism prevalent in MFC3 was *Comamonas* (41.67%). Searching the complete genome of this bacterium, indicated that genes coding all of these enzymes were indeed present, strongly suggesting that *Comamonas* could be oxidizing acetate via this pathway. The complete genome of other genus of the same order as *Alicycliphilus* or *Acidovorax* was also checked for these enzymes observing their presence.

The only problem with a syntrophic acetate oxidation mechanism is the fact that it has to be "syntrophic" with an accompanying organism taking up the reducing power released to the medium as hydrogen. Most of the time the hydrogen-using companion is either a sulphate reducer or a hydrogenotrophic methanogen. Since neither organisms were present, nor methane and hydrogen sulphide were produced, we must assume that hydrogen was oxidized at the electrode surface. In this case, the ability of hydrogen to diffuse through the nafion and the possibility that H^+ produced during oxidation can also cross the membrane gives extra weight to this hypothesis. Electricity generation from biohydrogen has been demonstrated in MFCs [54], although better catalysts than carbon paper electrode are necessary for a good performance in current production.

The presence of methanogenic *Archaea* in the anode chamber suggests that methanogenesis might play a role, however methane could not be detected in the headspace of the anode chamber except at the beginning of the experiment and at very low values. All bands of *Archaea*, corresponding to different clones, were related to the same genus, *Methanosaeta*, an acetoclastic methanogen that converts acetate to CH_4 and CO_2 [55]. *Methanosaeta* was also found in the other reactors, even though in a smaller proportion probably as a consequence of competition with existing electricigens. It has been reported by several studies that most acetoclastic methanogens typically have larger half saturation constants than anode respiring bacteria, therefore, this last group can outcompete the acetoclastic methanogens when acetate concentration is low [56,57,58].

The presence and prevalence of an acetoclastic methanogen in MFC3 is indeed quite puzzling when taking into account that no methane production occurred. Although we can not prove it, we think that *Methanosaeta* could be performing a type of metabolism closely resembling syntrophic acetate oxidation as described above. Under regular methanogenic conditions *Methanosaeta* uses a carbon monoxide dehydrogenase to split acetate into CO_2 and a corrinoid-linked methyl group. The methyl group is later transferred to a Coenzyme M and reduced to free methane using the reducing equivalents released by the carbon monoxide dehydrogenase probably as hydrogen.

In the anode chamber of the MFC3, hydrogen oxidation at the anode surface might scavenge enough hydrogen as to prevent *Methanosaeta* from reducing methyl-CoM to methane. Under these conditions, sequential oxidations of this methyl group to CO_2 via the tetrahydromethanopterine (H_4MPT) pathway might occur (Figure 9A). This would require the presence of a number of enzymes: methyl-H_4MPT-CoM methyltransferase, methylene-H_4MPT reductase, H_4-forming methylene-H_4MPT dehydrogenase, methenyl-H_4MPT cyclohydrolase, formylmethanofuran: H_4MPT formyltransferase, formylmethanofuran dehydrogenase [53], that upon search of the genome sequence of *Methanosaeta concilii*, turn out to be present in their totality. Thus, under conditions of hydrogen removal from the reactor, *Methanosaeta* might shift to an acetate oxidizing mechanism with a structure similar to syntrophic acetate oxidation, but with H_4MPT instead of THF. The reducing equivalents obtained during acetate oxidation would end up being oxidized at the anode surface.

Huser *et al.* [59] characterized a strain, *Methanotrix soehngenni*, which was capable of splitting formate into H_2 and CO_2, although no more studies have been reported on the production of H_2 by the strain [60]. *Methanosaeta termophila*, has also been shown to produce hydrogen [61].

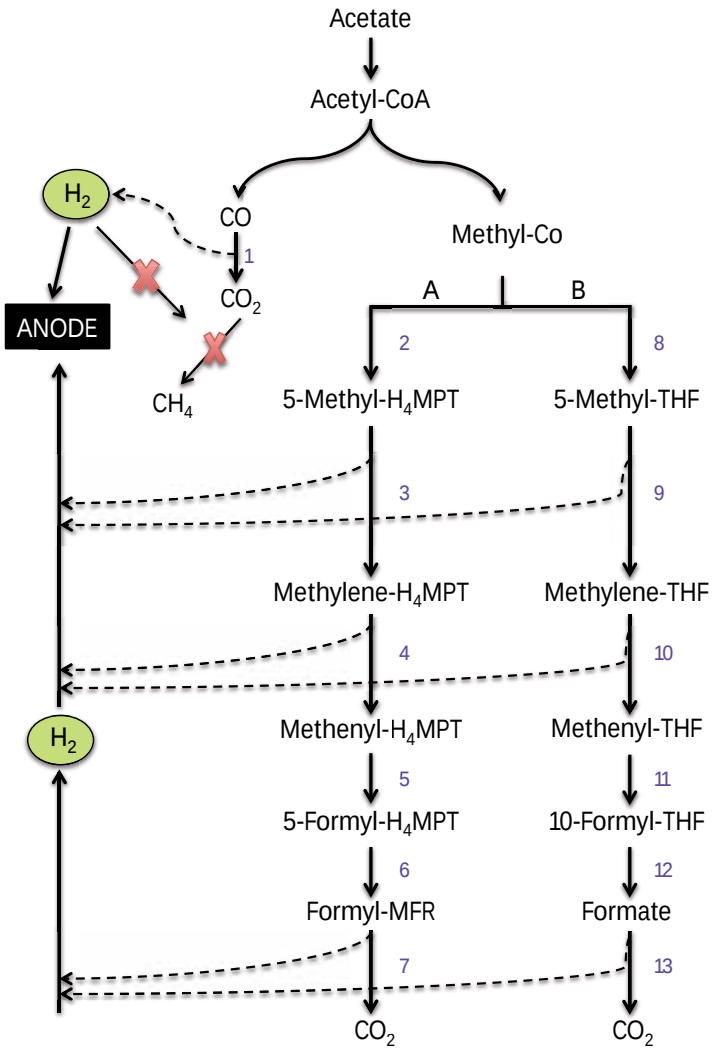

Figure 9. Diagram of acetate oxidation by syntrophic association with the anode using tetrahydromethanopterine (H_4MPT) (A) (Enzimes: 1. Carbon monoxide dehydrogenase, 2. Methyl-H_4MPT-CoM methyltransferase, 3. Methylene-H_4MPT reductase, 4. H_4-forming methylene-H_4MPT dehydrogenase, 5. Methenyl-H_4MPT cyclohydrolase, 6. Formylmethanofuran: H_4MPT formyltransferase, 7. Formylmethanofuran dehydrogenase) and tetrahydrofolate (THP) (B) pathways (Enzimes: 1. Carbon monoxide dehydrogenase, 8. methiltransferase, 9. Methylene-THF reductase, 10. Methylene-THF dehydrogenase, 11. Methenyl-THF cyclohydrolase, 12. Formyl-THF synthetase, 13. Formate dehydrogenase).

CONCLUSIONS

Summarizing, the different anode configurations used in our study allow us to exclude certain electron transfer mechanisms and, thus, compare the capacity of the remaining mechanisms for current production, as well as to analyze what type of microbial diversity develops associated to these mechanisms. MFC1 with an electrochemically active biofilm at the anode showed the best performance, with a biofilm responsible for 70% of current production. This demonstrates the higher efficiency of direct contact mechanisms in power output. In this MFC, bacteria with known capacity for direct electron transfer as *Shewanella*, *Clostridium, Dysgonomonas* or *Anaeromonas* were found. The production of current in MFC2 could only be derived from the oxidation of electron shuttles and fermentation end products. Genus as *Acinetobacter*, *Pseudomonas* or *Shewanella* among other reported electron shuttles producers, were present in this MFC. Finally, MFC3 not even reduced organic compounds could reach the anode. The power output obtained showed a poor performance of the MFC3 that obtained values of power output nearly 95% lower than the obtained by direct contact electron transfer. In this case, we speculate that hydrogen was produced by a community with the prevalence of *Comamonas* and *Methanosaeta* using tetrahydrofolate and tetrahydromethanopterine cofactors respectively. Hydrogen produced would then cross the nafion barrier and be oxidized at the anode surface.

Acknowledgements

This work was supported by grants CSD2006-00044 TRAGUA (CONSOLIDER-INGENIO2010) and CTQ2009-14390-C02-02 from the Spanish Ministry of Education and Science to JM. We thank to Èdgar Ribot and Albert Guisasola for their support in gas chromatography measurements.

REFERENCES

(1) Bretschger, O.; et al. A survey of direct electron transfer from microbes to electronically active surfaces. In *Bioelectrochemical Systems: from extracellular electron transfer to biotechnological application;* Rabaey, K.; Angenent, L.; Schröer, U.; Keller, J., Eds.; IWA Publishing 2010; pp 81.

(2) Rabaey, K.; Verstraete, W. Microbial fuel cells: novel biotechnology for energy generation. *TRENDS Biotechnol.* 2006, 23(6), 291-298.

(3) Schröder, U. Anodic electron transfer mechanisms in microbial fuel cells and their energy efficiency. *Phys. Chem. Chem. Phys*. 2007, 9, 2619-2629.

(4) Hernandez, M.E.; Newmann, D.K. Extracellular electron transfer. *Cell. Mol. Life Sci*. 2001, 58, 1562-1571.

(5) Newman, D.K.; Kolter, R.A. Role for excreted quinones in extracellular electron transfer. *Nature*. 2000, 405(6782), 94-97.

(6) Callies, E.; Manheim, W. Classification of the Flavobacterium-Cytophaga complex on the basis of respiratory quinones and fumarate respiration. *Int. J. Syst. Bacteriol.* 1978, 28(1), 14-19.

(7) Rabaey, K.; Boon, N.; Siciliano, S.D.; Verhaege, M.; Verstraete, W. Biofuel cells select for microbial consortia that self-mediate electron transfer. *Appl. Environ. Microbiol*. 2004, 70, 5373–5382.

(8) Lee, J.Y. ; Phung, N.T.; Chang, I.S.; Kim, B.H.; Sung, H.C. Use of acetate for enrichment of electrochemically active microorganisms and their 16S rDNA analyses. *FEMS Microbiol. Lett*. 2003, 223, 185–191 .

(9) Kim, B.H.; Park, H.S. Kim, H.J.; Kim, G.T,.; Chang, I.S.; Lee, J.; Phung, N.T. Enrichment of microbial community generating electricity using a fuel-cell-type electrochemical cell. *Appl. Microbiol. Biotechnol*. 2004, 63, 672–681.

(10) Champine, J.E.; Underhill, B.; Johnston, J.M.; Lilly, W.W.; Goodwin, S. Electron transfer in the dissimilatory iron-reducing bacterium *Geobacter metallireducens*. *Anaerobe.* 2000, 6, 187–196.

(11) Nevin, K.P.; Lovley, D.R. Mechanisms for accessing insoluble Fe(III) oxide during dissimilatory Fe(III) reduction by *Geothrix fermentans*. *Appl. Environ. Microbiol*. 2002, 68, 2294–2299.

(12) Uría, N.; Sánchez, D.; Mas, R.; Sánchez, O.; Muñoz, F.X.; Mas, J. Effect of the anode/cathode ratio and the choice of cathode catalyst on the performance of microbial fuel cell transducers for the determination of microbial activity. *Sensor. Actuat. B: Chem.* 2011 (In press)

(13) Clarck, D. J.; Maaøle, O.. DNA replication and the division cycle in *Escherichia coli*. *J. Mol. Biol*. 1967, 23, 99–112.

(14) Cheng, S.; Liu, H.; Logan, B.E. Increased power generation in a continuous flow MFC with advective flow through the porous anode and reduced electrode spacing. *Environ. Sci. Technol*. 2006, 40(7), 2426-2432.

(15) Jung, S.; Regan, J.M. Comparison of anode bacterial communities and performance in microbial fuel cells with different electron donors. *Appl Microbiol. Biotechnol.* 2007, 77, 393-402.

(16) Sánchez, O., Gasol, J.M., Massana, R., Mas, J., Pedrós-Alió, C. Comparison of different denaturing gradient gel electrophoresis primer sets for the study of marine bacterioplankton communities. *Appl. Environ. Microb*. 2007, 73, 5962-5967.

(17) Kreader, C.A. Relief of amplification inhibition in PCR with bovine serum albumin or T4 gene 32 protein. *Appl. Environ. Microb*. 1996, 62, 1102-1106.

(18) Casamayor, E.O., Massana, R., Benlloch, S., Øvreás, L., Díez, B., Goddard, V.J., Gasol, J.L.; Joint, I.; Rodríguez-Valera, F.; Pedrós-Alió, C. Changes in archaeal, bacterial and eukaryal assemblages along a salinity gradient by comparison of genetic fingerprinting methods in a multipond solar saltern. *Environ. Microbiol.* 2002, 4: 338–348.

(19) Muyzer, G.; et al. Denaturing gradient gel electrophoresis (DGGE) in microbial ecology. *In Microbial Ecology Manual*. Akkermans, A.D.L.; van Elsas, J.D.; Bruijn, F.J., Eds.; Molecular Dordrecht, Netherlans: Kluwer Academic Publishers 1998; pp 1-27.

(20) Simpson, E.H. Measurement of diversity. *Nature*. 1949, 163, 688.

(21) Logan, B.E.; Hamelers, B.; Rozendal, R.; Schröder, U.; Keller, J.; Freguia, S.; Aelterman, P.; Verstraete, W.; Rabaey, K. Microbial Fuel Cells: Methodology and technology. *Environ. Sci. Technol*. 2006, 40(17), 5181-5192.

(22) Phung, N.T.; Lee, J.; Kang, K.H.; Chang, I.S.; Gadd, G.M.; Kim, B.H. Analysis of microbial diversity in oligotrophic microbial fuel cells using 16S rDNA sequences. *FEMS* Microbiol. Lett. 2004, 233, 77-82.

(23) Xing, D.; Cheng, S.; Logan, B.E.; Regan, J.M. Isolation of the exoelectrogenic denitrifying bacterium *Comamonas denitrificans* based on dilution to extinction. *Appl. Microbiol. Biotechnol*. 2010, 85, 1575-1587.

(24) Sutherland, I.W. The biofilm matrix-an immobilized but dynamic microbial environment. *Trends Microbiol*. 2001, 9, 222-227.

(25) Aelterman, P.; et al. Microbial Fuel Cells as an engineered ecosystem. In *Bioenergy*; Wall, J.D., Harwood, C.S., Demain, A. Eds.; ASM Press: Washington, DC 2008; pp 307.

(26) Kostka, J.E.; Dalton, D.D.; Skelton, H.; Dollhopf, S.; Sucki, J.W. Growth of iron(III)-reducing bacteria on clay minerals as the sole electron acceptor and comparison of growth yields on a variety of oxidized iron forms. *Appl. Environ. Microbiol*. 2002, 68, 6256-6262.

(27) Park, H.S.; Kim, B.H.; Kim, H.S.; Kim, H.J.; Kim, G.T.; Kim, M. Chang, I.S. A novel electrochemically active and Fe(III)-reducing bacterium phylogenetically related to *Clostridium butyricum* isolated from a microbial fuel cell. *Anaerobe*. 2001, 7, 297-306.

(28) Parameswaran, P.; Torres, C.I.; Lee, H.; Rittmann, B.E.; Krajmalnik-Brown, R. Hydrogen consumption in microbial electrochemical systems (MXCs): The role of homo-acetogenic bacteria. *Bioresource Technol*. 2011, 102, 263-271.

(29) Torres, C.I; Krajmalnik-Grown, R.; Parameswaran, P.; Marcus, A.K.; Wanger, G.; Gorby, Y.A.; Rittmann, B.E. Selecting anode-respiring bacteria based on anode potential: phylogenetic, electrochemical, and microscopic characterization. *Environ. Sci. Technol*. 2009, 43(24), 9519-9524.

(30) Xing, D.F.; Cheng, S.; Regan, J.M.; Logan, B.E. Change in microbial communities in acetate-and glucose-fed microbial fuel cells in the presence of light. *Biosens. Bioelectron.* 2009, 25(1),105-112.

(31) Zhang, Y.; Min, B.; Huang, L.; Angelidaki, I. Generation of electricity and analysis of microbial communities in wheat straw biomass-powered microbial fuel cell. *Appl. Environ. Microbiol*. 2009, 75(1), 3389-3395.

(32) Sun, Y.; Zuo, J.; Cui, L.; Deng, K.; Dan, Y. Diversity of microbes and potential exoelectrogenic bacteria on anode surface in microbial fuel cells. *J. Gen. Appl. Microbiol.* 2010, 56, 19-29.

(33) Rismani-Yazi, H.; Christy, A.D.; Dehority, B.A.; Morrison, M.; Yu, Z.; Tuovinen, O.H. Electricity generation from cellulose by rumen microorganisms in Microbial Fuel Cells. *Biotechnol. Bioeng*. 2007, 97(6), 1398-1407.

(34) Sun, M.; Tong, Z.; Sheng, G.; Chen, Y.; Zhang, F.; Mu, Z.; Wang, H.; Zeng, R.J.; Liu, X.; Yu, H.; Wei, L.; Ma, F. Microbial communities involved in electricity generation from sulfide oxidation in a microbial fuel cell. *Biosens. Bioelectron.* 2010, 26(2), 470-476.

(35) Pham, A.C.; Jung, S.J.; Phung, N.T.; Lee, J.; Chang, I.S.; Kim, B.H.; Yi, H.; Chun, J. A novel electrochemically active and Fe(III)-reducing bacterium phylogenetically related to *Aeromonas hydrophila*, isolated from a microbial fuel cell. *FEMS Microbiol. Lett.* 2003, 223, 129-134.

(36) Patil, S.A.; Suraski, V.P.; Koul, S.; Ijmulwar, S.; Vivek, A.; Shouche, Y.S.; Kapadnis, B.P. Electricity generation using chocolate industry wastewater and its treatment in activated sludge. *Bioresource Technol*. 2009, 100(21), 5132-5139.

(37) Rabaey, K.; Boon, N.; Höfte, M.; Verstratete, W. Microbial phenazine production enhances electron transfer in biofuel cells. *Environ, Sci, Technol*. 2005, 39, 3401-3408.

(38) Yamazaki, S.; Taketomo, N.; Kano, K.; Ikeda, T. Electrochemical and end-product analysis of quinone-induced modification of metabolic pathways in Bifidobacteria and Lactic Acid bacteria. *Anal. Sci*. 2001, 17 (Supplement), 1019-1021.

(39) Marsili, E.; Baron, D.B.; Shikhare, I.D.; Coursolle, D.; Gralnick, J.A.; Bond, D.R. *Shewanella* secretes flavins that mediate extracellular electron transfer. *PNAS*. 2008, 105(10),3968-3973.

(40) Willner, I.; Arad, G.; Katz, E. A biofuel cell based on pyrroloquinoline quinone and microperoxidase-11 monolayer-functionalized electrodes. *Bioelectroch. Bioener*. 1998, 44, 209-214.

(41) Laurinavicius, V.; Razumiene, J.; Ramanavicius, A.; Ryabov, A.D. Wiring of PQQ-dehydrogenases. *Biosens. Bioelectron.* 2004, 20, 1217-1222.

(42) Huang, L.; Regan, J.M.; Quan, X. Electron transfer mechanisms, new applications, and performance of biocathode microbial fuel cells. *Bioresource Technol.* 2011, 102, 316-323.

(43) Park, H.I.; Sanchez, D.; Cho, S.K.; Yun, M. Bacteria communities on electron-beam Pt-deposited electrodes in a mediator-less microbial fuel cell. *Environ. Sci. Technol.* 2008, 42, 6243-6249.

(44) Choo, Y. F.; Lee, J.; Chang, I. S.; Kim, B. H. Bacterial communities in microbial fuel cells enriched with high concentrations of glucose and glutamate. *J. Microbiol. Biotechnol.* 2006, 16, 1481–1484.

(45) Wang, A.; Liu, W.; Ren, N.; Zhou, J.; Cheng, S. Key factors affecting microbial anode potential in a microbial electrolysis cell for H2 production. *Int. J. Hydrogen Energ.* 2010, 35, 13481-13487.

(46) Borole, A.P.; Hamilton, C.Y.; Vishnivetskaya, T.; Leak, D.; Andras, C. Improving power production in acetate-fed microbial fuel cells via enrichment of exoelectrogenic organisms in flow-through systems. *Biochem. Eng. J.* 2009, 48, 71-80.

(47) Huang, L.P.; Logan, B.E. Electricity production from xylose in fed-batch and continuous-flow microbial fuel cells. *Appl. Microbiol. Biotechnol.* 2008, 80, 655-664.

(48) Kim, Y.; Kim, M.K.; Weon, H.; Kim, H.; Yang, D. *Hydrogenophaga temperata* sp. nov., a betaproteobacterium isolated from compost in Korea. *J. Gen. Appl. Microbiol.* 2010, 56, 419-425.

(49) Fedorovich, V.; Knighton, M.C.; Pagaling, E.; Ward, F.B.; Free, A.; Goryanin, I. A novel electrochemically active bacterium phylogenetically related to *Arcobacter butzleri* isolated from a Microbial Fuel Cell. *App. Environ. Microbiol.* 2009, 75(23), 7326-7334.

(50) He, Z.; Kan, J.; Wang, Y.; Huang, Y.; Mansfeld, F.; Nealson, K.H. Electricity production coupled to ammonium in a microbial fuel cell. *Environ. Sci. Technol.* 2009, 43, 3391-3397.

(51) Kiely, P.D.; Rader, G.; Regan, J.M.; Logan, B.E. Long-term cathode performance and the microbial communities that develop in microbial fuel cells fed different fermentation end products. *Bioresource Technol.* 2011, 102, 361-366.

(52) Hattori, S. Syntrophic acetate-oxidizing microbes in methanogenic environments. *Microbes Environ.* 2008, 23(2), 118-127.

(53) Edward, B.; Maden, H. Tetrahydrofolate and tetrahydromethanopterin compared: functionally distinct carriers in C_1 metabolism. *Biochem. J.* 2000, 350,609-629.

(54) Oh, S.; Logan, B.E. Hydrogen and electricity production from a food processing wastewater using fermentation and microbial fuel cell technologies. *Water Res.* 2005, 39, 4673-4682.

(55) Kendall, M.M.; et al. The Order Methanosarcinales. In *Prokaryotes*; Dworkin, M., Falkow, S., Rosenberg, E., Schleifer, K., Eds.; Springer: 2006; pp 244-256.

(56) Parameswaran, P.; Torres, C.I.; Lee, H.; Krajmalnik-Brown, R.; Rittmann, B.E. Syntrophic interactions among anode respiring bacteria (ARB) and non-ARB in biofilm anode: electron balances. *Biotechnol. Bioeng*. 2009, 103(3), 513-523.

(57) Zinder SH. Physiological ecology of methanogens. In *Methanogenesis—Ecology, physiology, biochemistry & genetics*. Ferry, J.G., Eds.; New York, NY: Chapman & Hall 1993; pp 128–206.

(58) Esteve-Nuñez A, Rothermich M, Sharma M, Lovley DR. Growth of *Geobacter sulfurreducens* under nutrient limiting conditions in continuous culture. *Environ. Microbiol*. 2005, 7(5), 641–648.

(59) Huser, B.H.; Wuhrmann, K.; Zehnder, A.J.B. *Methanothrix soehngenii gen. nov.* sp. *nov*., a new acetotrophic non hydrogen oxidizing methane bacterium. *Arch. Microbiol*. 1982, 132, 1.

(60) Nandi, R.; Sengupta, S. Microbial production of hydrogen: An overview. *Crit. Rev. Microbiol*. 1998, 24(1), 61-84.

(61) Valentine, D.L.; Blanton, D.C.; Reeburgh, W.S. Hydrogen production by methanogens under low-hydrogen conditions. *Arch. Microbiol*. 2000, 174, 415-421.

SUPPLEMENTARY MATERIAL

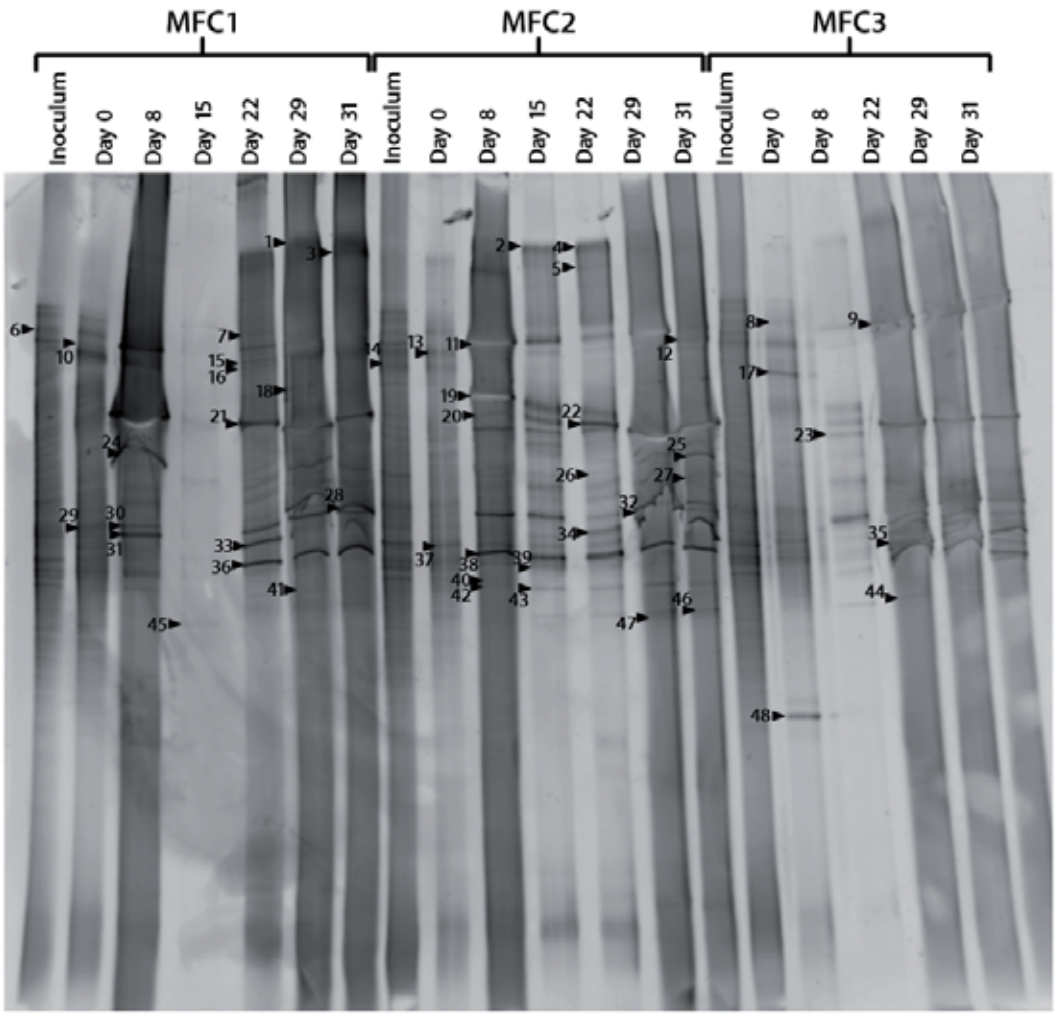

Figure S1. Negative images of DGGE gel 1 with PCR products amplified with bacterial primer sets from anolyte samples of each MFC during the experiment samples. Band excised and sequenced are numbered and their affiliations are shown in Table S1.

Table S1. Phylogenetic affiliation of sequences obtained from DGGE1 bands, with closest uncultured and cultured matches. (I: inoculum, 1: MFC1, 2: MFC2, 3: MFC3

Band	Closest match	% similarity (nº bases)[a]	Taxonomic group	Accession nº (Gen Bank)	Cultured closest match (% similarity)	MFC
1	Uncultured bacterium clone ZL29	99 (521)	*Bacteroidetes*	JF733662.1	*Flavobacterium* sp. DR2 (97)	1,3
2	Uncultured bacterium clone MFC4P_365	100 (523)	*Bacteroidetes*	JF309196.1	*Bacteroides graminisolvens* strain JCM 15093 (100)	2
3	Uncultured bacterium clone ZL29	100 (520)	*Bacteroidetes*	JF733662.1	*Flavobacterium* sp. DR2 (98)	1
4	Uncultured bacterium clone AcL_A02	99 (516)	*Bacteroidetes*	HE583107.1	*Dysgonomonas* sp. A1(2011) (99)	2
5	*Arcobacter butzleri* ED-1	100 (508)	*ε-proteobacteria*	AP012047.1		2
6	Uncultured bacterium clone M0111_66	97 (480)	*Bacteroidetes*	EU104063.1	*Paludibacter propionicigenes* WB4 (97)	I,1
7	Uncultured bacterium clone ZL29	99 (519)	*Bacteroidetes*	JF733662.1	*Flavobacterium* sp. DR2 (97)	1
8	Uncultured Bacteroidales bacterium clone HI6	99 (518)	*Bacteroidetes*	EU573844.1	*Bacteroides caccae* strain: JCM 9498 (93)	1,3
9	*Chryseobacterium taeanense* strain: NBRC 100863	97 (482)	*Bacteroidetes*	AB681269.1		3
10	Uncultured bacterium clone: B0618R003_G03	98 (513)	*Bacteroidetes*	AB658255.1	*Paludibacter propionicigenes* WB4 (97)	I,1
11	Uncultured bacterium clone MFC4P_365	100 (505)	*Bacteroidetes*	JF309196.1	*Bacteroides graminisolvens* strain: JCM 15093 (100)	1,2
12	Uncultured bacterium clone AcL_A02	100 (522)	*Bacteroidetes*	HE583107.1	*Dysgonomonas* sp. A1(2011) (100)	1,2,3
13	Uncultured Bacteroidales bacterium clone HI6	100 (502)	*Bacteroidetes*	EU573844.1	*Bacteroides* sp. 253c (94)	1,2,3
14	Uncultured bacterium clone MR2.1.25M.26	99 (510)	*Bacteroidetes*	AY209435.1	*Bacteroides* sp. enrichment culture clone CS3 (93)	I,1,2
15	Uncultured bacterium clone AcL_A02	99 (512)	*Bacteroidetes*	HE583107.1	*Dysgonomonas* sp. A1(2011) (99)	I,1
16	Uncultured bacterium clone ncd897g10c1	98 (525)	*γ-proteobacteria*	HM298798.1	*Acinetobacter* sp. DNPA10 (98)	I,1,2
17	Uncultured Fusobacteria bacterium	99 (502)	*Fusobacteria*	AY193168.1	*Fusobacterium varium* strain: JCM 6320 (91)	3
18	Uncultured bacterium clone ZL29	100 (488)	*Bacteroidetes*	JF733662.1	*Flavobacterium* sp. DR2 (97)	I,1
19	*Acinetobacter* sp. M1T8B5	99 (521)	*γ-proteobacteria*	GQ246681.1		2,3
20	Uncultured bacterium clone MFC4P_365	99 (525)	*Bacteroidetes*	JF309196.1	*Bacteroides graminisolvens* strain: JCM 15093 (99)	2
21	*Acinetobacter* sp. M1T8B5	99 (527)	*γ-proteobacteria*	GQ246681.1		1
22	*Acinetobacter* sp. TDIW13 clone B05	100 (528)	*γ-proteobacteria*	GU003823.1		2,3
23	*Acinetobacter baumanni*i str. SDF	97 (474)	*γ-proteobacteria*	CU468230.2		2,3
24	Uncultured *Acinetobacter* sp. clone W4S19	97 (514)	*γ-proteobacteria*	GU560165.1	*Acinetobacter* sp. WJ07 (97)	1,2
25	Uncultured bacterium clone: HNB-10	99 (498)	*Firmicutes*	AB509215.1	*Anaerofilum agile* strain F (99)	1,2
26	Uncultured bacterium clone ncd2066a03c1	99 (518)	*γ-proteobacteria*	JF168585.1	*Pseudomonas* sp. RM12W (99)	1,2
27	Uncultured bacterium clone BicL_E08	99 (525)	*β-proteobacteria*	HE583075.1	*Hydrogenophaga* sp. TR7-01 (98)	2
28	Uncultured bacterium clone R_G06	99 (530)	*β-proteobacteria*	HE589858.1	*Azovibrio restrictus* strain S5b2 (99)	1
29	Uncultured bacterium clone MR2.1.25M.26	99 (516)	*Bacteroidetes*	AY209435.1	*Bacteroides graminisolvens* strain: JCM 15093 (93)	I,1,2
30	Uncultured bacterium clone BicS_D07	99 (514)	*Firmicutes*	HE582905.1	*Clostridium* sp. NML 04A032 (96)	1
31	*Shewanella putrefaciens* strain: NBRC 3910	98 (513)	*γ-proteobacteria*	AB680169.1		1,2
32	Uncultured bacterium clone BicL_E08	99 (534)	*β-proteobacteria*	HE583075.1	*Hydrogenophaga* sp. TR7-01 (99)	2,3
33	Uncultured beta proteobacterium isolate DGGE band AMFC 5-1	99 (519)	*β-proteobacteria*	EF506582.1	*Azovibrio restrictus* strain S5b2 (99)	1
34	Uncultured Betaproteobacteria clone QEDN6BE11	98 (512)	*β-proteobacteria*	CU925083.1	*Azonexus caeni* strain Slu-05 (95)	2
35	Uncultured bacterium clone B1_58	99 (49)	*Gemmatimonadetes*	HM228610.1	*Gemmatimonas* sp. clone AOCRB-EC-6 (86)	3
36	Uncultured bacterium clone nbw112f02c1	99 (519)	*β-proteobacteria*	GQ008024.1	*Comamonas nitrativorans* strain 23310 (99)	1,2,3
37	Uncultured bacterium clone ncd389g12c1	99 (533)	*β-proteobacteria*	HM321911.1	*Diaphorobacter* sp. QH-6 (99)	I,2,3
38	Uncultured bacterium clone BicL_E08	100 (527)	*β-proteobacteria*	HE583075.1	*Hydrogenophaga* sp. TR7-01 (99)	I,1,2,3
39	Uncultured bacterium clone BicL_E08	100 (527)	*β-proteobacteria*	HE583075.1	*Hydrogenophaga* sp. TR7-01 (99)	2
40	*Comamonas terrigena* strain: NBRC 13299	98 (521)	*β-proteobacteria*	AB680400.1		1,2,3
41	Uncultured bacterium clone ZL29	97 (509)	*Bacteroidetes*	JF733662.1	*Flavobacterium* sp. DR2 (95)	1
42	*Comamonas terrigena* strain IMI 359870	97 (503)	*β-proteobacteria*	NR_028719.1		2
43	Uncultured bacterium clone ABRB56	100 (531)	*β-proteobacteria*	HQ224844.1	*Acidovorax caeni* strain R-24607 (100)	2
44	*Comamonas* sp. enrichment culture clone JXS-02-02	99 (501)	*β-proteobacteria*	JN873181.1		3
45	Uncultured organism clone ELU0035-T194-S-NIPCRAMgANb_00026	100 (506)	*Actinobacteria*	HQ753914.1	*Propionibacterium acnes* strain M_1503_10 (99)	1
46	Uncultured bacterium clone BicL_E08	98 (516)	*β-proteobacteria*	HE583075.1	*Hydrogenophaga* sp. TR7-01 (97)	2
47	Uncultured bacterium clone ZL29	98 (488)	*Bacteroidetes*	JF733662.1	*Flavobacterium* sp. DR2 (96)	2
48	Uncultured bacterium clone B1_58	99 (505)	*Gemmatimonadetes*	HM228610.1	*Gemmatimonas* sp. clone AOCRB-EC-6 (86)	3

a. Number of bases used to calculate the levels od sequence similarity.

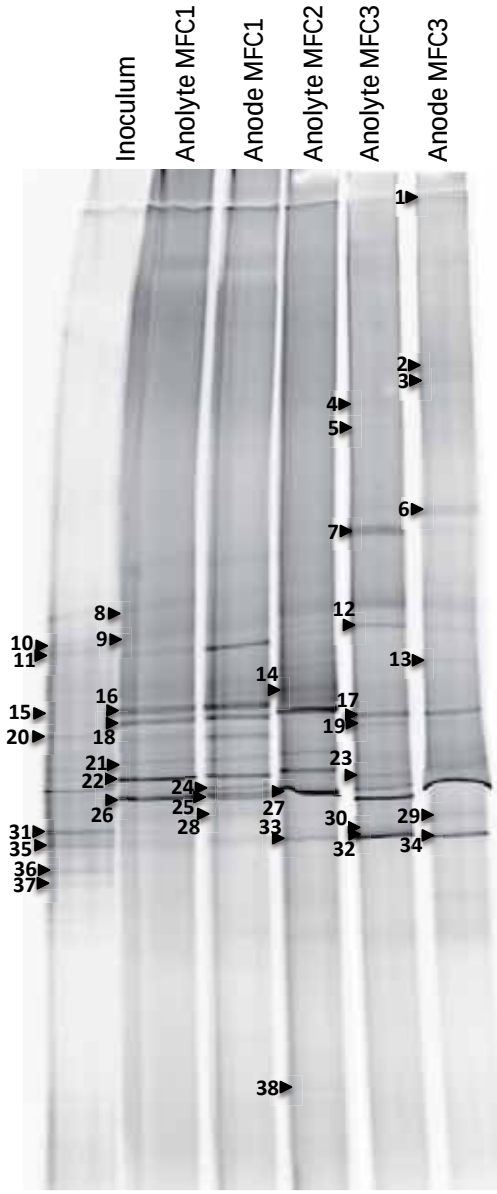

Image S2. Negative images of DGGE gel 2 with PCR products amplified with bacterial primer sets from samples of MFC anolytes and the anodes of MFC1 and MFC3 at the end of the experiment. Band excised and sequenced are numbered and their affiliations are shown in Table S2.

Table S2. Phylogenetic affiliation of sequences obtained from DGGE2 bands, with closest uncultured and cultured matches. (I: inoculum, Ay: anolyte, A: anode).

Band	Closest match	% similarity (nº bases)[a]	Taxonomic group	Accession nº (Gen Bank)	Cultured closest match (% similarity)	MFC
1	Uncultured *Hydrogenophaga* sp. Clone W5S29	99 (539)	*β-proteobacteria*	GU560177.1	*Hydrogenophaga* sp. TR-7 (98)	I,1,2,3
2	Uncultured bacterium clone MFC4P_81	93 (406)	*ε-proteobacteria*	JF309167.1	*Arcobacter butzleri* ED-1 (93)	A3
3	Uncultured *ε-proteobacterium* clone PFC_3_peak_H07	94 (382)	*ε-proteobacteria*	FJ664785.1	*Arcobacter butzleri* ED-1 (93)	A3
4	*Comamonas terrigena* strain NBRC 13299	94 (511)	*β-proteobacteria*	AB680400.1		Ay3
5	*Comamonas terrigena* strain IMI 359870	97 (522)	*β-proteobacteria*	NR028719.1		Ay3
6	Uncultured *Hydrogenophaga* sp. Clone W5S29	98 (529)	*β-proteobacteria*	GU560177.1	*Hydrogenophaga flava* strain NBRC 102514 (97)	A3
7	*Chryseobacterium* sp. HNR12	99 (527)	*Bacteroidetes*	EU373367.1		Ay3,A3
8	Uncultured bacterium clone BIfciii21	95 (487)	*Bacteroidetes*	AJ318124.1	*Bacteroides* sp. D-2 (95)	I,1,2
9	*Dysgonomonas* sp. A1 (2011)	99 (528)	*Bacteroidetes*	HQ659694.1		1,2,3
10	Uncultured Bacteroidales bacterium clone HI6	97 (510)	*Bacteroidetes*	EU573844.1	*Bacteroides graminisolvens* (92)	I
11	Uncultured Bacteroidales bacterium clone HI6	97 (500)	*Bacteroidetes*	EU573844.1	*Bacteroides graminisolvens* (92)	I
12	*Flavobacterium* sp. IICDBZ3	99 (530)	*Bacteroidetes*	UN836920.1		1,2,3
13	Uncultured *β-proteobacterium* isolate DGGE gel band B1-A	91 (479)	*β-proteobacteria*	HQ836420.1	*Hydrogenophaga flava* strain NBRC 102514 (88)	2,A3
14	*Acinetobacter* sp. TDIW13	99 (528)	*γ-proteobacteria*	GU003823.1		1,Ay2
15	Uncultured bacterium clone F_HeJ1_D14	93 (384)	*Firmicutes*	JF837889.1	*Clostridium populeti* strain 743A (92)	I
16	*Acinetobacter* sp. M1T8B5	99 (533)	*γ-proteobacteria*	GQ246681.1		1,Ay2,A3
17	*Comamonas terrigena* strain NBRC 13299	95 (510)	*β-proteobacteria*	AB680400.1		Ay3
18	*Acinetobacter* sp. PRM8	99 (522)	*γ-proteobacteria*	JN544148.1		1,2,A3
19	Uncultured *γ-proteobacterium* clone DG-KL-G2	98 (525)	*β-proteobacteria*	AB635955.1	*Comamonas aquatica* strain NBRC 14918 (98)	AY3,A3
20	Uncultured bacterium clone ncd2092c07c1	93 (377)	*Firmicutes*	JF169102.1	*Clostridium clariflavum* DSM 19732 (92)	I
21	Uncultured Clostridia bacterium clone XDC04	98 (498)	*Firmicutes*	FJ938125.1	*Clostridium celerecrescens* strain N2 (97)	I,1,Ay2
22	Uncultured bacterium clone R_G06	98 (526)	*β-proteobacteria*	HE589858.1	*Azovibrio restrictus* strain S5b2 (98)	I,1,2
23	Comamonas terrigena strain NBRC 13299	99 (531)	*β-proteobacteria*	AB680400.1		Ay3,A3
24	Uncultured Clostridiales bacterium clone MFC-B162-F04	97 (495)	*Firmicutes*	FJ393118.1	*Clostridium* sp. NML04A032 (96)	I,A1
25	Uncultured *Shewanella* sp. Clone SFC1G121	92 (499)	*γ-proteobacteria*	AM981330.1	*Shewanella putrefaciens* (92)	A1
26	Uncultured bacterium clone nbw112f02c01	99 (537)	*β-proteobacteria*	GQ008024.1	*Alicycliphylus denitrificans* strain C11 (98)	I,1,2,3
27	Uncultured *Hydrogenophaga* sp. Clone W5S29	99 (537)	*β-proteobacteria*	GU560177.1	*Hydrogenophaga* sp. TR-7 (99)	Ay3
28	*Stenotrophomonas* sp. enrichment culture clone CW-4Y	97 (518)	*γ-proteobacteria*	JN995250.1		Ay1,A1
29	*Hydrogenophaga flava* strain NBRC 102514	99 (535)	*β-proteobacteria*	AB681848.1		A3
30	*Comamonas aquatica* strain DNPA9	99 (534)	*β-proteobacteria*	FJ404812.1		Ay3
31	Uncultured bacterium clone nbw432h05c1	94 (504)	*β-proteobacteria*	GQ094975.1	*Diaphorobacter* sp. MC-pb1 (94)	I
32	Uncultured *γ-proteobacterium* clone DG-KL-G2	99 (533)	*β-proteobacteria*	AB635955.1	*Comamonas* sp. CHb (99)	Ay3
33	*Comamonas* sp. enrichment culture clone JXS-02-02	99 (510)	*β-proteobacteria*	JN873181.1		1,Ay2,Ay3
34	Uncultured bacterium clone ncd474d12c1	99 (535)	*β-proteobacteria*	JF042097.1	*Acidovorax caeni* strain R-24607 (99)	A3
35	Uncultured bacterium clone B0423R001_B06	91 (363)	*Firmicutes*	AB656092.1	*Bacillus* sp. PCWCS6 (84)	I
36	Uncultured bacterium clone PW185	99 (510)	*Firmicutes*	GQ402678.1	*Clostridium* sp. 6-31 (97)	I
37	Uncultured bacterium clone D23L8C05 isolate D23L8	91 (444)	*Firmicutes*	FN643508.1	*Clostridium* sp. 6-31 (91)	I
38	Uncultured bacterium clone nby578g05c1	90 (488)	*γ-proteobacteria*	HM840591.1	*Acinetobacter* sp. A56 (2011) (90)	Ay2

a. Number of bases used to calculate the levels od sequence similarity.

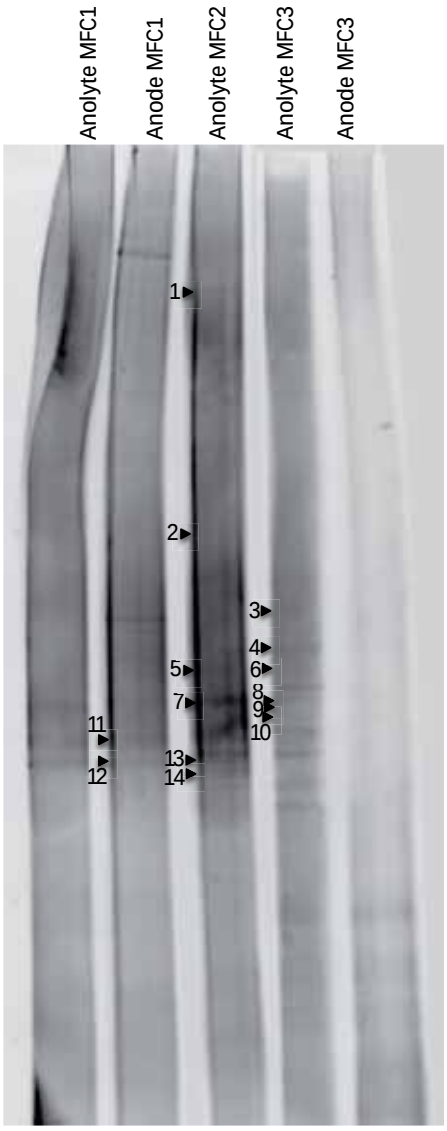

Image S3. Negative images of DGGE gel 3 with PCR products amplified with archaeal primer sets from samples of MFC anolytes and the anodes of MFC1 and MFC3 at the end of the experiment. Band excised and sequenced are numbered and their affiliations are shown in Table S3.

Table S3. Phylogenetic affiliation of sequences obtained from DGGE3 bands, with closest uncultured and cultured matches.

Band	Closest match	% similarity (nº bases)[a]	Taxonomic group	Accession nº (Gen Bank)	Cultured closest match (% similarity)	MFC
1	Uncultured archaeon clone A1001R003 P03	98 (416)	*Euryarchaeota, Methanomicrobia*	AB6546911	*Methanosaeta* sp. clone A2287 (97)	2
2	Uncultured *Methanosaeta* sp. clone M0AR73_25m	99 (418)	*Euryarchaeota, Methanomicrobia*	JQ0799141	*Methanosaeta concilii* GP-6 (97)	2
3	Uncultured archaeon clone Sp1-44	99 (426)	*Euryarchaeota, Methanomicrobia*	JN6174421	*Methanosaeta concilii* strain NBRC 103675 (98)	2,3
4	Uncultured *Methanosaeta* sp. clone M0AR73_25m	94 (402)	*Euryarchaeota, Methanomicrobia*	JQ0799141		2,3
5	Uncultured archaeon clone MBS_A1	91 (360)	*Euryarchaeota, Methanomicrobia*	AB6890791	*Methanosaeta* sp. clone A1492 (90)	2
6	Uncultured archaeon clone R6aA6	97 (111)	*Euryarchaeota, Methanomicrobia*	HQ2705431	*Methanosaeta* sp. clone A14138 (96)	2,3
7	Uncultured Methanosaetaceae archaeon clone LrhA36	95 (312)	*Euryarchaeota, Methanomicrobia*	AJ8790191	*Methanosaeta* sp. clone A1492 (94)	1,2
8	Uncultured archaeon clone SWA0201-09	99 (416)	*Euryarchaeota, Methanomicrobia*	JN3980111	*Methanosaeta concilii* strain NBRC 103675 (98)	3
9	Uncultured archaeon clone MH_E2A	94 (348)	*Euryarchaeota, Methanomicrobia*	JN6491591	*Methanosaeta* sp. clone A1492 (93)	2,3
10	Uncultured archaeon clone A0610D003_B10	98 (431)	*Euryarchaeota, Methanomicrobia*	AB6558151	*Methanosaeta concilii* strain NBRC 103675 (97)	2,3
11	Uncultured archaeon clone SWA0201-09	98 (410)	*Euryarchaeota, Methanomicrobia*	JN3980111	*Methanosaeta* sp. clone A1492 (97)	1
12	Uncultured archaeon clone MH_E2A	95 (315)	*Euryarchaeota, Methanomicrobia*	JN6491591	*Methanosaeta* sp. clone A14110 (91)	1,2
13	Uncultured archaeon clone LB6A	97 (315)	*Euryarchaeota, Methanomicrobia*	AB154430	*Methanosaeta* sp. clone A1492 (96)	2,3
14	Uncultured archaeon clone A0423R001_F07	95 (398)	*Euryarchaeota, Methanomicrobia*	AB6516391	Uncultured *Methanosaeta*	2

a. Number of bases used to calculate the levels od sequence similarity.

Discussion

DISCUSSION

Optimization of Microbial Fuel Cell design and operation for each different application is important if maximum performance must be extracted from these systems. A great diversity of studies about the variable performance of MFCs, have been carried out indicating the high number of different factors that can affect power output [1]. In this work we attempt to study some of these factors. Between them, design factors such as the area ratio cathode/anode and the type of catalyst are studied in Chapter 1, while the possible use of electrogenic bacteria as alternative catalyst is developed in Chapter 2. The effect of discontinuous operation is studied in Chapter 3 as a new operational factor of great relevance for some applications. All these studies have been performed using the electrogenic model organism *Shewanella oneidensis* MR-1. Pure cultures, however, are usually ill suited for real world applications and complex communities normally tend to show the best long term performance. The need for a better understanding of the factors shaping the microbial communities that develop in complex MFCs led us in Chapter 4 to study how different experimental conditions related to the accessibility of the anode affect the performance of the MFC, the microbial community and the metabolisms that develop, and the different electron transfer pathways and mechanisms that can be found under each set of conditions.

Cathode performance

Design factors as the architecture of reactors, type of material used for the electrodes or the effect of the proton exchange membrane have been widely studied [2,3,4]. Although the results found in the literature are useful, they are often optimized for one type of MFC and cannot always be extrapolated to other types of MFC, since other parts of the system have a direct effect on the performance [5].

In many studies, data obtained are normalized to the area of the anode. This seems to indicate a general agreement about considering the anode as the factor limiting power output in a MFC. Nevertheless, the use of different catalysts in the cathode often shows considerable increases in

power output [6,7] thus indicating the existence of a limitation in the cathode reaction. Avoiding this limitation is of the utmost importance if we want to optimize MFC operation and avoid an incorrect interpretation of the results obtained.

Improvement of oxygen reduction at the cathode is still one of the great challenges for successful use of MFCs. The low catalytic activity of the cathode can be improved by modifying the electrode with metals, surfactants and organic materials [8,9] or by using soluble mediators [10], although they are not practical for all applications.

Despite their excellent performance, platinum electrodes are not practical for large-scale applications due to their high cost. Different metals (copper, gold and molybdenum) have been studied as cheaper alternatives to platinum cathodes. However, most of them are not as effective as platinum cathodes [11]. In this work, platinum foil together with other more economical platinum-based cathodes (platinum-covered silicon oxide and black platinum-covered silicon oxide) were tested as surface catalysts for oxygen reduction at the cathode. In general, the surface catalysts tested showed low but sustained power outputs. Platinum-covered silicon oxide was unable to reach the power obtained by the platinum foil. However, the increase of roughness by the deposition of black platinum on a silicon oxide wafer allowed the increase of power until values close to these obtained with platinum foil. Additional voltammetric analyses confirmed black platinum as a viable alternative for the cathode of our MFCs.

Soluble Fe catalysts used in combination with carbon paper anodes, particularly the extensively studied ferricyanide, achieved much higher power output than platinum cathodes. The causes of the performance enhancement observed in soluble catalysts can be diverse. For example, lower activation energy or higher mass transfer efficiency [2,12,13] as well as the possibility of iron acting as an electron acceptor rather than as a shuttle and catalyst for oxygen reduction [10], could be the reasons. Despite their low cost and high performance, they are not considered as sustainable as iron. Iron reduction at the cathode surface usually proceeds at a higher rate than iron oxidation by oxygen. As a consequence, reduced iron becomes the predominant form after some time. Besides,

iron being a cation tends to cross over to the anode compartment through the cation-selective nafion membrane thus disrupting normal anode operation.

Regarding size, the dimensions of the cathode must be large enough as to avoid limitation of the activity developing at the anode. Our results indicate that the minimal ratio cathode/anode necessary to avoid cathodic limitation depends to a large extent on the type of electrode and catalyst used. Thus ratios above 3-4 are enough to ensure a full performance of the anode when a soluble iron catalyst is used in combination with carbon paper, while much higher ratios, above 27 are required when using surface platinum catalysts.

Summarizing right now there is no perfect solution in terms of materials and design for the cathode of a microbial fuel cell. Our results show that while soluble iron catalysts provide the best performance per unit area of the cathode, but at the expense of a limited life span. On the other hand, platinum catalysts show a stable behaviour over extended periods of operation but with a much lower power output per unit area of the cathode.

Given the limitations of the different abiotic cathodes available, serious thought has been given to the possibility of using biological components to catalyze oxygen reduction at the cathode. Thus, conventional catalysts, either soluble or surface-bound can be eliminated by the use of microorganisms able to take up electrons from the cathode and efficiently transfer them to oxygen, therefore increasing the environmentally sustainability and the economic viability, by reducing construction and operating costs of the MFC systems [14]. Additionally, microbial metabolisms in biocathodes may be used to produce useful products or remove unwanted compounds. However, limited information about them is available and the mechanisms used by bacteria to oxidize the electrode remain still unclear.

We employed the electrogenic bacterium *Shewanella oneidensis* MR-1 to test the power sustainability of our MFC by biological cathode reaction. This electrogenic bacterium was selected due to its known capacity to transfer electrons to an anode through any of several pathways [15,16] and its versatility for anaerobic respiration [17], which allows it to use a wealth of different

electron acceptors in the cathode. So, three MFCs with an aerobic cathode, and two anaerobic cathodes using nitrate and fumarate as electron acceptors were compared.

Although *Shewanella oneidensis* has been reported as able to transfer electrons to an anode using both direct and mediator-dependent pathways, cyclic voltammograms showed that mediators were not present in the cathode solution. On the other hand, voltammograms performed on cathode biofilms grown under different electron acceptors showed a diverse electrochemical response. Thus, the presence of an electron acceptor with a certain redox potential seems to lead *Shewanella* to use a certain set of proteins to take up electrons from the cathode, which is not surprising due to the great number of electron transport components that have been described in this bacterium and the need to maximize the redox gap between electron source and electron sink.

In terms of performance, as expected, the aerobic biocathode showed the highest power output, 75% higher than the anaerobic biocathodes. Higher values could probably be obtained, but mass transfer limitations related to insufficient proton migration through the membrane or to limited oxygen diffusion within the biofilm prevent them [18,19]. Although anaerobic cathodes have the advantage of eliminating oxygen diffusion to the anode as well as supply problems to the anode caused by the low solubility of oxygen [20], poor performances were observed. These low power outputs, above all in the case of the MFC with fumarate in the cathode, were related to incomplete reduction of these electron acceptors although the reasons remain unknown.

When compared to conventional cathodes using either soluble or solid phase catalysts, biocathodes show a relatively good performance. While not achieving the high power densities observed with soluble catalysts as ferricyanide, biocathodes provide power densities comparable and as good as those observed when using solid platinum or platinum-coated electrodes. This indicates that *Shewanella oneidensis* MR-1 constitutes a good alternative to noble metals for the catalysis of oxygen reduction in the cathode compartment of MFCs.

Discontinuous operation

While design factors have been studied to a great extent in the literature, not much attention has been paid to operational factors. As a rule, optimizing MFC performance requires extensive exploration of the operational parameters involved. For example, the potential of the anode or the magnitude of the external resistance has been demonstrated to have an effect in the capacity of biocatalysts to transfer electrons resulting in reduced power output [21,22].

One operating component not commonly taken into account is the effect of interruptions in the normal cycle of operation of the MFC. Several papers [23] provide evidence that current production in a MFC can be successfully improved by introducing a capacity in the MFC circuit. In this type of reactor, current production by bacteria is continuous, but current output from the cell is conditioned by the discharge of the capacitors. In this study, we attempted to explore the opposite, the consequences of discontinuous operation on the behaviour of the organisms present in the MFC. To that end we have followed two MFCs that used *Shewanella oneidensis* MR-1 in the anode when periods of circuit disconnection were applied.

Rather surprisingly, restoring the MFC circuit after a period of interruption resulted in a current peak of remarkable intensity that decayed slowly until reaching normal current output. This temporary effect in current was caused by an increase of the MFC potential (OCV) during the disconnection period due to the reduction of anode and cathode overpotentials [24,25]. These results demonstrate the effect of a discontinuous operation in temporal patterns of current output and thus suggest the charge storage by the MFC, releasing it as soon as the circuit is restored. However, the factors causing this effect are diverse due to the complexity of the MFC systems.

To determine the contribution of *Shewanella oneidensis* MR-1 biofilm in the charge storage, several electrochemical analyses were run. Analysis of the isolated biofilm in an electrochemical cells has the advantage of eliminating all the abiotic factors that produce overpotentials in a MFC. So, at first the electrochemical capacity of the biofilm attached to the anode was probed by cyclic voltammetry. After this, charge accumulation by the biofilm was studied by running different

chronoamperometric analyses at 0.1 V during 30 sec. Prior to each chronoamperometry, the circuit was disconnected for variable times until a maximum of 180 min during which bacteria oxidized lactate potentially storing electrons intracellularly since electrode was disabled. The results showed again a current peak right after restoring the current flow. The charge accumulated increased with the disconnection time up to approximately 60 min when the biofilm seemed to be saturated. These results demonstrate the capacity of *Shewanella oneidensis* MR-1 to store charge in absence of electron acceptors and as a consequence the necessity for future works to take this into account for different applications such as sensors.

Complex Microbial Communities

Despite all the efforts put into the improvement of the MFCs output, it is known that these devices do not operate to the full capability of the anodic microbial metabolism. New advances in design and operation at conditions require a better understanding of how electricigens transfer electrons to anodes. With this information, it may be possible to optimize practical applications and improve our modelling of natural processes [26]. Besides *Shewanella*, MFC research has achieved the isolation of a wide range of organisms that can produce power individually in a MFC [27]. Studies with pure isolates allow the understanding of the basic microbiology involved in biological current generation by reducing the complexity of multiple species interaction on the anode [27].

However, for many practical applications MFC technology uses natural complex communities and, thus, requires an understanding of the interaction between the different species involved [27]. MFCs operated with complex communities are usually able to reach a much higher power output than those using pure cultures [3,25]. Many bacteria enriched from MFCs cannot grow as pure culture in a MFC. This is likely due to a number of synergistic interactions that occur in the original mixed cultures and that cannot be reproduced in the pure culture [27,28]. Community analyses performed in MFCs have also shown a great diversity in composition [3,25,29,30], indicating that microorganisms that are not electricigens can contribute to current production or even to be essential for current production [31].

In the case of MFCs based on electrochemically enriched bacterial mixed cultures the combination and interaction of different electron transfer mechanisms and redox species can lead to a rather complex electrochemical behaviour [32]. The finally goal of this work was to shed some light on the possible electron transfer pathways that develop in a MFC and to estimate the extent of their contribution to power output, while analyzing the diversity profile of the microbial community responsible for these processes.

Three different coated anode configurations were used to restrict different pathways of electron transfer. So, in contrast to the first MFC, which had a naked anode, the second configuration in which the anode was enclosed in a dialysis membrane prevented direct electron transfer. In the third MFC, the anode was coated with nafion and transfer of electrons to the anode surface could only be sustained by bacterial hydrogen production.

After 4 weeks of operation, the selective environment of the MFCs resulted in a decrease in taxonomic richness. The MFC with a naked electrode developed a biofilm attached to the anode and showed the best performance, with a power output 60 and 95% higher that electron shuttle and hydrogen sustained MFCs respectively. In order to favour their growth, electricigens must reduce potential losses due to extracellular electron transfer. Direct contact provides the most efficient mechanism because electrons do not need to travel long distance to reach the anode and therefore, a solid conductive matrix is needed to achieve high current densities and low anode potentials in MFCs [33].

The electrochemical activity of the anode biofilm developed in MFC1 was demonstrated by cyclic voltammetry. In addition to the electrochemical measurements, several bacteria with known capacity for direct electron transfer such as *Shewanella*, *Dysgonomonas* or *Aeromonas* were detected in the community profile of this MFC. At the end of the experiment, replacement of the anode by a fresh carbon paper electrode resulted in a considerable decrease in current output. However, 30% of the current was maintained showing that power output was not only dependent on the anode biofilm, but also, that bacteria in the anolyte were able to contribute substantially to the activity of the MFC. The microbial community in the anolyte was formed by bacteria with

capacity for electron transfer via electron shuttle production, among them for example *Pseudomonas*, *Propionibacterium* or *Acinetobacter* were detected.

These very same shuttle-producing organisms were also found in MFC2 in which the anode was enclosed by a dialysis membrane only allowed mediated electron transfer. Electrochemical analysis of the anolyte indicated the presence of several dissolved redox species, many of them compatible with mediators produced by the organisms mentioned above. 16S rRNA analyses of the microbial community allowed the detection of microorganisms not found in MFC1 but frequently reported in MFC studies as *Arcobacter*, *Diaphorobacter* or *Acidovorax*. The electron transfer mechanism for these bacteria has not been established, but their presence in this reactor indicates that they use an indirect electron transfer using self-secreted redox shuttles or compounds produced by other members of the community.

Finally, in MFC3 the anode was coated with nafion and did not allow the access of either cells or electron shuttles to the electrode. Under these conditions, current production was very low. Actually power output was 95% lower than in MFC1 where direct electron transfer was allowed.

The microbial community developed in this MFC was mainly composed by members of the genus *Comamonas* and by the archaea *Methanosaeta*. However, the mechanism of current production in this MFC was far from clear. The existence of anoxic conditions and the restrictions imposed by the nafion coating reduce the metabolic options available for organisms growing in the anolyte to only two: syntrophic acetogenesis and methanogenesis. During syntrophic acetate oxidation, microorganisms oxidize acetate to CO_2 in a series of reactions that use tetrahydrofolate as a cofactor. Since no hydrogenotrophic methanogens were detected, we postulate that the role of hydrogenotrophic methanogens was fulfilled by the anode, which thanks to the capacity of hydrogen to diffuse through nafion, would be taking up the reducing power released to the medium as hydrogen. As mentioned above, oxidation of organic matter while channelling reducing equivalents to hydrogen requires a rather specific metabolic pathway that includes a series of reactions, which include tetrahydrofolate as the cofactor [34,35]. Searching the available genomic sequences of several of the organisms found, between them *Comamonas*, showed that

the genes coding for all the proteins in the pathway were present, strongly supporting the likelihood of this type of metabolism.

The *Archaea* found was *Methanosaeta*, an acetoclastic methanogen that converts acetate to CO_2 and methane. Although its presence first led us to think that electrons were channelled into methane production, no methane was found during the experiment. So, a route similar to syntrophic acetate oxidation but using tetrahydromethanopterine cofactor was hypothesized. In this case, the presence of the anode in a MFC could prevent production of methane by oxidizing hydrogen released during acetate oxidation. Under these conditions acetate would be converted into CO_2 via the tetrahydromethanopterine pathway in a sequence of reactions closely resembling those occurring in the tetrahydrofolate pathway [35]. Once again, all the enzyme necessary for this route were found coded in the genome of *Methanosaeta* thus supporting our theory.

In summary, the different anode configurations used in our study allowed us to exclude certain electron transfer mechanisms and, thus, compare the capacity of the remaining mechanisms for current production, as well as to analyze what type of microbial diversity develops associated to these mechanisms. Our results confirm that while direct contact electron transfer wears the weight of electrogenesis in MFC reactors, contact independent mechanisms seem to be important too, in our case accounting for about 30% of the total current produced. Finally, the experimental data obtained with nafion-coated anodes evidence that although hydrogen mediated electron transfer may indeed play a role as a contact-independent mechanism, its contribution is probably marginal.

REFERENCES

(1) Davis, F.; Higson, S.P.J. Biofuel cells: recent advances and applications. Biosens. Bioelectron. 2007, 22(7), 1224-1235.

(2) Oh, S.E.; Min, B.; Logan, B.E. Cathode performance as a factor in electricity generation in microbial fuel cells. *Environ. Sci. Technol*. 2004, 38, 4900-4904.

(3) Logan, B.E.; Hamelers, B.; Rozendal, R.; Schröder, U.; Keller, J.; Freguia, S.; Aelterman, P.; Verstraete, W.; Rabaey, K. *Microbial Fuel Cells: methodology and technology*. 2006, 40(17), 5181-5192.

(4) Oh, S.E.; Logan, B.E. Proton exchange membrane and electrode surface areas as a factor that affect power generation in microbial fuel cells, *Appl. Microbiol. Biotechnol*. 2006, 70, 162-169.

(5) Watanabe, K. Recent developments in microbial fuel cell technologies for sustainable bioenergy. *Journal of Bioscience and Bioengineering*. 2008, 106(6), 528-536.

(6) Aelterman, P.; Versichele, M.; Genettello, E.; Verbeken, K.; Verstraete, W. Microbial fuel cells operated with iron-chelated air cathodes. *Electrochim. Acta*. 2009, 54, 5754-5760.

(7) You, S.; Zhao, Q.; Zhang, J.; Jiang, J.; Zhao, S. A microbial fuel cell using permanganate as the cathodic electron acceptor. *J. Power Sources*. 2006, 162, 1409-1415.

(8) Chen, P.; Fryling, M.A.; McCreery, R.L. Electron transfer kinetics at modified carbon electrode surfaces: The role of specific surface sites. *Anal. Chem*. 1995, 67, 3115-3122.

(9) DuVall, S.H.; McCreery, R.L. Control of catechol and hydroquinone electron-transfer kinetics on native and modified glassy carbon electrodes. *Anal. Chem*. 1999, 71, 4594-4602.

(10) Zhao, F.; Harnisch, F.; Schröder, U.; Scholz, F.; Bogdanoff, P.; Herrmann, I. Challenges and constraints of using oxygen cathodes in microbial fuel cells. *Environ. Sci. Technol*. 2006, 40(17), 5193-5199.

(11) Kim, B.H.; Chang, I.S.; Gadd, G.M. Challenges in microbial fuel cell development and operation. *Appl. Microbiol. Biotechnol*. 2007, 76, 485-494.

(12) Zhuwei, D.; Li, H.; Gu, T. A state of the art review on microbial fuel cells: a promising technology for wastewater treatment and bioenergy. *Biotechnology Advances.* 2007, 25, 464-482.

(13) Rismani-Yazdi, H.; Carver, S.M.; Christy, A.D.; Tuovinen, O.H. Cathodic limitations inmicrobial fuel cells: an overview. *Journal of Power Sources*. 2008, 180, 683-694.

(14) Huang, L.; Regan, J.M.; Quan, X. Electron transfer mechanisms, new applications, and performance of biocathode microbial fuel cells. *Bioresource technology*. 2011, 102, 316-323.

(15) Myers, C.R.; Myers, J.M. Role of menaquinone in the reduction of fumarate, nitrate, iron(III) and manganese(IV) by *Shewanella putrefaciens* MR-1. FEMS *Microbiol. Lett*. 1993, 114, 215-222.

(16) Myers, C.R.; Myers, J.M. Localization of cytochromes to the outer membrane of anaerobically grown *Shewanella putrefaciens* MR-1. *J. Bacteriol*. 1992, 174, 3429-3438.

(17) Heidelberg, J.F.; Paulsen, I.T.; Nelson, K.E.; Gaidos, E.J.; Nelson, W.C.; Read, T.D.; Eisen, J.A.; Seshadri, R.; Ward, N.; methe, B.; Clayton, R.A.; Meyer, T.; Tsapin, A.; Scott, J.; Beanan, M.; Brinkac, L.; Daugherty, S.; deBoy, R.T.; Dodson, R.J.; Scott Durkin, A.; Haft, D.H.; Kolonay, J.F.; Madupu, R.; Peterson, J.D.; Umayam, L.A.; White, O.; Wolf, A.M.; vamathevan, J.; Weidman, J.; Imprain, M.; Lee, K.; Berry, K.; Lee, C.; Mueller, J.; Khouri, H.; Gill, J.; Utterback, T.R.; McDonald, L.A.; Feldblyum, T.V.; Smith, H.O.; Craig venter, J.C.; Nealson, K.H.; Fraser, C.M. Genome sequence of the dissimilatory metal ion-reducing bacterium *Shewanella oneidensis*. *Nature biotechnology*. 2002, 20, 1118-1123.

(18) Rozendal, R.A.; Hamelers, H.V.M.; Buisman, C.J.N. Effects of membrane cation transport on pH and microbial fuel cell performance. *Environ. Sci. Technol*. 2006, 40, 5206-5211.

(19) Behera, M.; Jana, P.S.; Ghangrekar, J.M.M. Performance evaluation of low cost microbiol fuel cell fabricated using earthen pot with biotic and abiotic cathode. *Bioresource Technol.* 2010, 101, 1183-1189.

(20) Huang, L.; Regan, J.M.; Quan, X. Electron transfer mechanisms, new applications, and performance of biocathode microbial fuel cells. *Bioresource Technology*. 2011, 102, 316-323.

(21) Aelterman, P.; Freguia, S.; Keller, J.; Verstraete, W.; Rabaey, K. The anode potential regulates bacterial activity in microbial fuel cells. Appl. *Microbiol. Biotechnol.* 2008, *78*, 409-418; DOI 10.1007/s00253-007-1327-8.

(22) Katuri, K.P.; Scott, K.; Head, I.M.; Picioreanu, C.; Curtis, T.P. Microbial fuel cells meet with external resistance. *Bioresource Technol*. 2011, *102*, 2758-2766.

(23) Dewan, A.; Beyenal, H.; Lewandowski, Z. Intermittent energy harvesting improves the performance of microbial fuel cells. *Environ. Sci. Technol*. 2009, *43*, 4600-4605.

(24) Zhao, F.; Slade, R.C.T.; Varcoe, J.R. Techniques for the study and development of microbial fuel cells: an electrochemical perspective. *Chem. Soc. Rev*. 2009, *38*, 1926-1939.

(25) Logan, B.E.; Hamelers, B.; Rozendal, R.; Schröder, U.; Keller, J.; Freguia, S.; Aelterman, P.; Verstraete, W.; Rabaey, K. Microbial Fuel Cell: Methodology and Technology. *Environ. Sci. Technol*. 2006, *40* (17), 5181-5192.

(26) Lovley, D.R. Bug juice: harvesting electricity with microorganisms. *Nature Reviews, Microbiology*. 2006, 4, 497-508.

(27) Franks, A.E.; Malvankar, N.; Nevin, K.P. Bacterial biofilms: the powerhouse of a microbial fuel cell. *Biofuels*. 2010, 1(4), 589-604.

(28) Kim, B.H.; Park, H.S.; Kim, H.J.; Kim, G.T.; Chang, I.S.; Lee, J.; Phung, N.T. Enrichment of microbial community generating electricity using a fuel-cell-type electrochemical cell. *Appl. Microbiol. Biotechnol.* 2004, 63(6), 672-681.

(29) Bond, D.R.; Holmes, D.E.; Tender, L.M.; Lovley, D.R. Electrode-reducing microorganisms that harvest energy from marine sediments. *Science.* 2002, 295, 483-485.

(30) Phung, N.T.; Lee, J.; Kang, K.H.; Chang, I.S.; Gadd, G.M.; Kim, B.H. Analysis of microbial diversity in oligotrophic microbial fuel cells using 16S rDNA sequences. *FEMS Microbiol. Lett*. 2004, 233, 77-82.

(31) Lovley, D.R.; et al. Electricity production by electricigens. In *Bioenergy*; Wall, J.D., Harwood, C.S., Demain, A. Eds.; ASM Press: Washington, DC 2008; pp 295.

(32) Schröder, U. Anodic electron transfer mechanisms in microbial fuel cells and their energy efficiency. *Physical Chemistry Chemical Physics.* 2007, 9, 2619-2629.

(33) Torres, C.I.; Marcus, A.K.; Lee, H-S.; Parameswaran, P.; Krajmalnik-Brown, R.; Rittmann, B.E. A kinetic perspective on extracellular electron transfer by anode-respiring bacteria. *FEMS Microbiol. Rev*. 2010, 34, 3-17.

(34) Hattori, S. Syntrophic acetate-oxidizing microbes in methanogenic environments. *Microbes Environ*. 2008, 23(2), 118-127.

(35) Edward, B.; Maden, H. Tetrahydrofolate and tetrahydromethanopterin compared: functionally distinct carriers in C_1 metabolism. *Biochem. J.* 2000, 350,609-629.

Conclusions

CONCLUSIONS

The main conclusions drawn from this research are presented in this section.

1. Maximum current values obtained in a MFC increase with increasing anode surface. However, normalization of the results to the anode surface indicates that above a certain anode size, power output is limited by the capacity of the cathode to channel electrons to oxygen. The area ratio cathode/anode in which the cathode ceases to be limiting depends on the catalyst used in the cathode. So in our MFC configurations, ratios cathode/anode of 4 are enough to avoid cathode limitations when soluble catalysts are used. However, a higher ratio of about 27 is needed in the case of oxygen reduction with platinum-based electrodes.

2. Current generation by a MFC is dependent on the catalyst used. Fe-based soluble catalysts coupled to carbon paper cathodes reach between 10 and 20 times higher power output than platinum-based cathodes with the same area. These findings are associated to lower activation energy and higher mass transfer efficiency of soluble catalysts.

3. Fe-based soluble catalysts are suitable for applications requiring high power output, but with a limited operation span due to the appearance of problems related to poor kinetics of iron reoxidation, or crossover of iron through the PEM into the anode. Platinum-based cathodes provide a relatively low but stable signal making them suitable for applications requiring extended operations.

4. The power values obtained using black platinum coated silicon, are close to those obtained using platinum foil, making it a viable alternative for its use in MFCs.

5. The electrogenic bacterium *Shewanella oneidensis* MR-1 is able to catalyze electron transfer from a graphite cathode to external electron acceptors in the cathode compartment of a MFC. Values of power output under aerobic conditions are comparable to those obtained using

platinum-based catalysts, indicating that aerobic biocathodes constitute a cheap and viable alternative to nobel metal electrodes.

6. Biofilms of *Shewanella oneidensis* MR-1 are able to store charge during periods in which an external acceptor is not available. Moreover, charge storage increases as a function of the disconnection time up to about 60 min, when the biofilm seems to be saturated and unable to store further electrons. Thus, current production is not only related to bacterial concentration or their activity levels but also to the recent history of the organisms.

7. Electrical charge stored in the biofilm is discharged fast enough (90% of the release occur during the first 2 sec), indicating a rather conductive biofilm structure.

8. MFCs with exposed anodes select bacteria with known capacity for direct electron transfer such as *Shewanella*, *Aeromonas* or *Dysgonomonas*. Direct electron transfer provides the best performance, with values of power output 60% above the values provided by other mechanisms.

9. The similarity between anolyte and anode voltammograms of direct contact MFC suggests that mediated electron transfer also occurs inside the biofilm. Actually, bacteria related to production of electron shuttles (*Pseudomonas, Acinetobacter, Propionibacterium*) were detected in the community profile of this MFC.

10. Enclosing of the anode of a MFC in a dialysis membrane results in low but sustainable power, indicating that mediated electron transfer is sufficient to sustain a MFC. Under these conditions, the anolyte solution presents a great variety of redox species not reported in MFC literature suggesting the presence in this MFC of bacteria with not yet described capacity for current production using soluble redox shuttles.

11. Coating of the anode of a MFC with nafion causes a 95% decrease in current production. Given that the only reduced chemical species that could sustain current production across a nafion

membrane is hydrogen, this result indicates that hydrogen dependent current generation may play a role in MFCs harbouring complex communities.

12. Oxidation of acetate in MFCs can be produced by “syntrophic” association between the bacteria and the anode, which consumes the reducing equivalents produced and released as hydrogen. This contributes to select bacteria able to use the tetrahydrofolate pathway of acetate oxidation. The presence of all the enzymes needed to carry it out suggests that the genus *Comamonas, Alicycliphilus* or *Acidovorax* are active factors in current generation.

13. The absence of methane indicates that the archaea *Methanosaeta,* found in MFCs with nafion coated anodes, is not using a methanogenic metabolism. We suggest that this organism oxidizes acetate to CO_2 following a mechanism similar to tetrahydrofolate pathway, but using tetrahydromethanopterine cofactor. The presence in its genome of all the enzymes necessary gives credibility to this hypothesis.

Annex

Annex I

Procedia Engineering 2010, 5:790-795

Annex II

Sensors and Actuators B: Chemical 2011 (In Press)

Annex III

Environmental Science & Technology 2011, 45(23):10250-10256

Available online at www.sciencedirect.com

ScienceDirect

Procedia Engineering 5 (2010) 790–795

Procedia Engineering

www.elsevier.com/locate/procedia

Proc. Eurosensors XXIV, September 5-8, 2010, Linz, Austria

Performance of different cathode catalysts in microbial fuel cell transducers for the determination of microbial activity

Naroa Uria[1*], David Sánchez[2], Roser Mas[2], Olga Sánchez[1], Francesc Xavier Muñoz[2], Jordi Mas[1*]

[1]*Group of Environmental Microbiology, Universitat Autònoma de Barcelona, Bellaterra, Spain*
[2]*National Centre for Microelectronics (CNM-IMB) CSIC, Spain*

Abstract

Microbial activity can be measured using sensors based on microbial fuel cell technology. In these sensors, the strength and stability of the signal depend among others on the type of catalyst used at the cathode since different power outputs can be reached depending on the catalyst. For this reason, it is necessary to know the efficiency of different catalysts, and thus, to use the best in terms of its application. Our results show that liquid phase catalysts provide much higher power output than solid phase catalysts, but at the expense of a reduced life span which limits their use for applications requiring extended operations.

Keywords: microbial fuel cell; microbial activity; biosensors

1. Introduction

Microbial fuel cell (MFC) based sensors can detect and quantify microbial activity. Fuel cell output depends on the flow of electrons to the anode which acts as a sink for the respiratory processes of bacteria growing in the anode compartment. At the cathode, these electrons recombine with protons and oxygen to produce water. For these processes to be conducted efficiently, the electrodes must possess certain characteristics that minimize both activation and ohmic losses. This can be achieved by adding suitable catalysts to the electrode and/or increasing the available surface and roughness of the electrode.

Due to the poor kinetics of oxygen reduction reaction in a neutral pH medium [1,2,3], the choice of the cathode material greatly affects performance, and it is changed depending on application [4]. Platinum is the best known oxygen reduction catalyst [5]. Platinum based oxygen electrodes are not practical for large-scale applications due to their high cost, but they provide useful benchmarks on the performance of the system [6]. Additionally, platinum is

* Corresponding author. Tel.: +34 935813011; fax: +34 935812387.
E-mail address: naroa.uria@uab.es.

1877-7058 © 2010 Published by Elsevier Ltd.
doi:10.1016/j.proeng.2010.09.227

prone to poisoning [4,7] because its activity is reduced by the formation of a PtO layer at the electrode surface at positive potentials [8]. Moreover, precious metal catalysts are highly sensitive to biological and chemical fouling [9,10]. Instead, non-noble metal catalysts such as pyrolysed iron (II) phathalocyanine (Pyr-FePc) and cobalttetramethoxyphenylporphyn (CoTMPP) applied on graphite cathodes have been proposed as a cheaper alternative to catalyze the oxygen reduction [11,7].

Carbon paper or graphite can also be used but, due to the kinetically limitation of oxygen reduction especially on these electrode materials, a liquid catalyst is usually required. The couple ferric/ferrous iron is a good electron mediator for oxygen reduction for three reasons: it is known for its fast reaction at carbon electrodes [12,13], it has a high standard potential [+0.77 V vs NHE (normal hydrogen electrode)] for equal concentrations of Fe^{3+} and Fe^{2+} at low pH), and ferrous iron can be biologically oxidized to ferric iron with oxygen as the electron acceptor up to high potentials of +850 to +950 mV vs NHE [14,13]. The most commonly used chemical catholyte in MFC next to oxygen is ferricyanide. It has a standard potential of 0.361 V, it is highly soluble in water, and it does not require a precious metal on the cathode such as platinum. Tests using ferricyanide show much greater power generation than those with oxygen due to the fact that there is little polarization of the cathode and the cathode potential achieved is quite close to that calculated for standard conditions [13,15,16]. Thus, while oxygen is predicted to have a higher cathode potential than ferricyanide, in practice the potentials achieved using oxygen are much lower than the theoretical values [16]. Ferricyanide, however, has some disadvantages. Kinetics of ferrocyanide oxidation by oxygen in the cathode are very slow and as a result, most of the catholyte ends up entirely reduced [4,7]. Besides, the system ferricyanide-ferrocyanide is not stable over long periods due to its slow conversion into Prussian Blue. In addition to ferricyanide, other ferric iron solution such as iron sulphite or iron chloride can be used as an intermediate electron acceptor as long as iron remains in solution [7]. In order to prevent the precipitation of iron at a neutral pH, the addition of a chelating agent is required. Ethylenediaminetetraacetic acid (EDTA) is well known for its iron-chelating properties [17]. Moreover, the reactivity of a Fe-EDTA couple towards the oxygen reduction reaction has been reported [18,7], which makes it a possible catalyst for the oxygen reduction reaction in MFCs [7].

In this study we want to compare different types of catalysts to determine their efficiency when used in the cathode compartment of MFC transducers.

2. Experimental Procedure

2.1. Bacterial strains and their cultivation

Shewanella oneidensis strain MR1 (ATCC 7005500) was grown aerobically in Trypticase Soy Broth (TSB) at 27ºC. After 36 hours of aerobic growth, the cells were harvested by centrifugation (10100gx15min,4ºC) and the resulting pellet was resuspended in 1 liter of AB minimal medium. The inoculated medium, supplemented with lactate (0.02M) as carbon source and fumarate (0.1M) as electron acceptor, was incubated with agitation at 22ºC for 48 hours.

2.2. Microbial Fuel Cell design and operation

In this study we used a two-chamber methacrylate reactor (Fig. 1) with a volume of 260 mL. The two chambers, separated by a proton exchange membrane (PEM), were held together by steel screws. The tightness of the piece was secured thanks to a round rubber gasket (76x3 mm) which exerted pressure on the membrane.

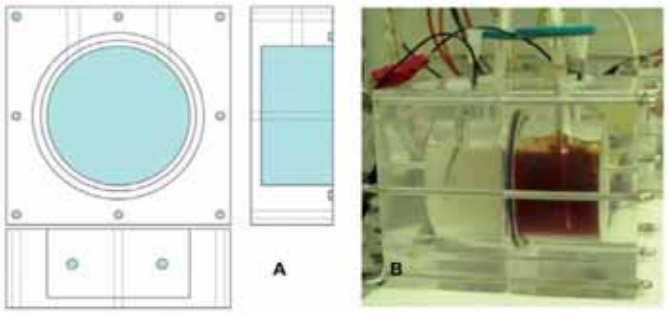

Fig. 1. Microbial Fuel Cell used in the experiments. (A) Reactor design. (B) Assembled reactor.

Five MFCs were constructed with different cathodes in order to compare solid catalysts, such as a platinum electrode and silicon wafer-based platinum, and liquid catalysts such as ferricyanide, EDTA chelated iron sulphate and EDTA chelated iron chloride. For the anode, carbon paper electrodes [16] (B2120 Toray Carbon Paper Designation TGPH-120, plain, no wet proofing; E-Tek, Inc.) with a thickness of 0.35mm, and a size of 3 cm^2 was used in all cases. In the cathodic chamber, different electrode materials were employed. On the one hand, solid catalysts were used, such as a platinum foil and a silicon wafer platinized on both sides. Platinum foil (Goodfellow Cambridge Limited), with a purity of 99.95%, had dimensions of 6.25cm^2 and thickness of 0.1mm. Silicon wafer-based platinum cathodes had a size of 6.022cm^2. On the other hand, carbon paper electrode with a size of 12cm^2 was used. The main difference when this material is employed for the cathode is that a catalyst is usually necessary in order to accelerate the reduction of oxygen. In our case, we used three different liquid catalysts: ferricyanide (0.05M $K_3[Fe(CN)_6]$ in a 0.1M phosphate buffer), EDTA chelated iron sulphate (0.5M $Fe_2(SO_4)_3$, 0.1M EDTA) and EDTA chelated iron chloride (0.5M $FeCl_3$, 0.1M EDTA). Electrodes were welded to their respective wires using silver loaded epoxy (RS Components). The weldings were covered with a non corrosive silicone rubber (RS Components). As a PEM we used Nafion®117 (Ion power, Inc.) with a thickness of 183μm and effective area of 38.46cm^2.

The anode composition was the same in all MFCs, a culture of *Shewanella oneidensis* MR1 with a concentration of 10^8 ufc·ml^{-1} in AB minimal medium, supplemented with 0.02M lactate. In the MFCs with solid catalyst, the catholyte was phosphate buffer (0.1M). Both, anode and cathode were stirred slowly (250 rpm). The cathode was pumped with air and, nitrogen was injected into the anode headspace to avoid oxygen inputs.

2.3. Microbial Fuel Cell characterization

Current (I) and voltage (V) measurements were carried put using a source meter unit (Keithley®2612) connected to a personal computer. Data were collected using a custom made program developed with LabView 8.5 (Nationals Instruments). For MFC characterization, I-V curves were built at selected times. I-V curves were performed by imposing different output current values between the cell electrodes. Current initially set to 0, was increased stepwise with an interval of time between steps of 3 minutes. At the end of each step, voltage was recorded. The procedure was repeated until voltage readings reached zero. Power density was calculated as the product between voltage and current.

3. Results and Discusion

Power generation of a MFC transducer is affected by many factors, including the choice of cathode catalyst. Thus, if the cathode catalyst performs poorly it becomes a bottle neck for the whole system, precluding the expression of high biological activities in the anode compartment. To compare solid and liquid catalysts, five MFC, using *Shewanella oneidensis* MR1 at a concentration of 10^8 ufc·ml^{-1}, were monitored over time.

When solid catalysts were used (Fig 2) (Pt and Pt silicon wafer) we measured maximum voltages of 531.5mV and 446.2mV. In this case, maximum values were reached in the early hours of the experiment and did not change significantly over time. The maximum power generated using platinum was 0.07 μW·cm^{-2}, with a maximum current density of 1.12 μA·cm^{-2}, while the maximum power reached by silicon wafer-based platinum was 0.09 μW·cm^{-2} with a maximum current of 1.27 μA·cm^{-2}.

In Figure 3 we can see the data obtained using liquid catalysts during the 130 hours of the study. The data collected in this experiment, showed much higher values of power density than those obtained using solid catalysts. The increase in power when using liquid catalysts, such as ferricyanide or iron-chelating catholytes, versus oxygen is both a function of the different potentials of the chemicals (lower activation energy) as well as the mass transfer efficiency [19]. Activation losses at the cathode have been identified as the dominant limitation in MFCs [9,10], particularly due to low proton availability [8,10]. Concentration overpotentials are associated with the concentration gradient of the reagents and products in the proximity of the electrode. Inefficient mass transfer through diffusion and convection of substrate or removal of products may limit the maximal current production at an electrode [20].

Besides, the formation of mixed potentials and the flow of internal currents have been reported in the case of platinum based electrodes, due to the permeation of fuel from the anode. Fuel crossover through the separator membrane into the cathode compartment may considerably decrease the electrode performance due to the formation of mixed potentials and the flow of internal currents causing a depolarization even at open circuit [21,22].

In all three cases, the open circuit voltage reached was very similar, around 400mV, as shown in Figures 3B, 3C y 3D. The maximum power values were obtained with ferricyanide (2.24 $\mu W \cdot cm^{-2}$), followed by EDTA chelated iron sulphate (0.83 $\mu W \cdot cm^{-2}$) and EDTA chelated iron chloride (0.38 $\mu W \cdot cm^{-2}$).

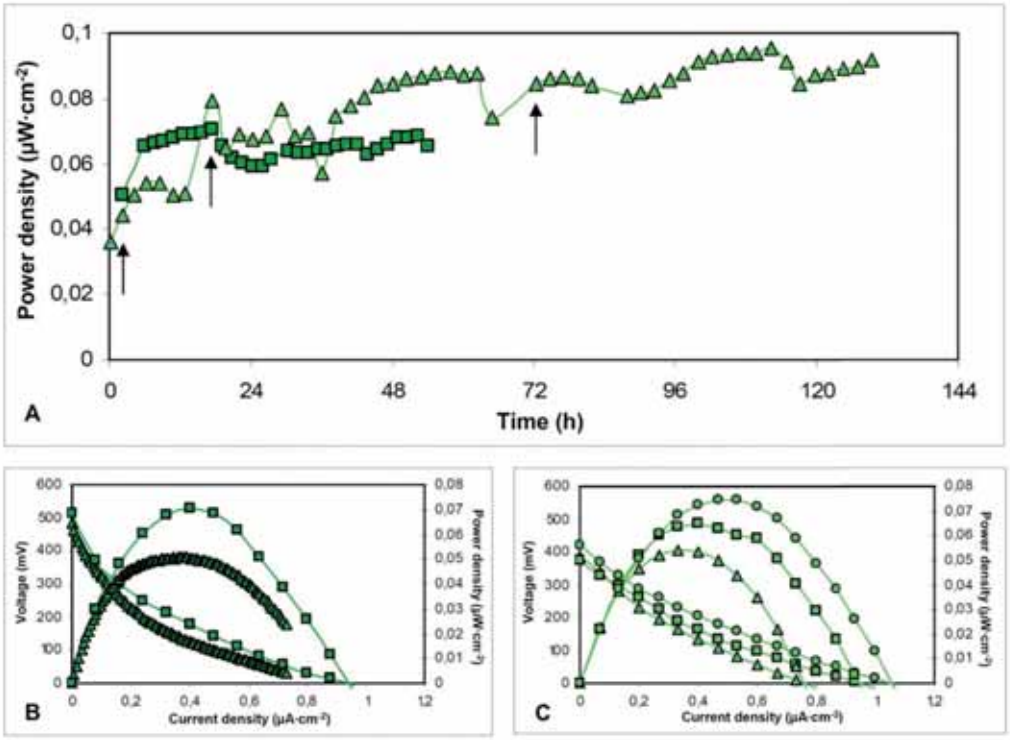

Fig. 2. (A) Evolution of the maximum power density in MFC transducers using platinum (■) and Silicon wafer-based platinum (▲) as the cathode catalysts. (B) I-V characteristic curves and power density curves taken after 2 (▲) and 18 hours (■) of operation in the MFC with platinum cathode. (C) I-V characteristic curves and power density curves taken after 2 (▲), 18 (■) and 72 (●) hours of operation in the MFC with platinised wafer cathode. Arrows indicate the times when the curves were constructed.

Clearly visible is the major disadvantage of oxygen when compared to ferricyanide. Whereas the latter reaction and thus its redox potential are independent of the proton concentration, the oxygen reduction reactions involve the consumption of one proton per transferred electron, independently if the reaction proceeds to water or to hydrogen peroxide. The consequence is a thermodynamically controlled shift of the polarization curve toward more negative values, which, depending on the nature and thus pH dependence of the anodic reaction, significantly reduces the MFC potential and power output [5].

The values obtained by liquid catalysts, however, were not as stable, as in the case of solid catalysts. In all cases, liquid catalysts showed a progressive increase in power and current density that probably reflects the development of the biological population in the anode compartment. This rapid increase could not be observed in the solid catalyst experiments because maximum power output was about one order of magnitude lower, and thus, did not allow the bacteria to fully express their maximum power output.

The increase in power output observed when using liquid catalysts was followed by quick drop. The drop could be related to a lowering of the Fe^{3+}/Fe^{2+} ratio due to an insufficient reoxidation of these iron chelates by oxygen. For this reason, the drop occurred first in the cells with higher current values.

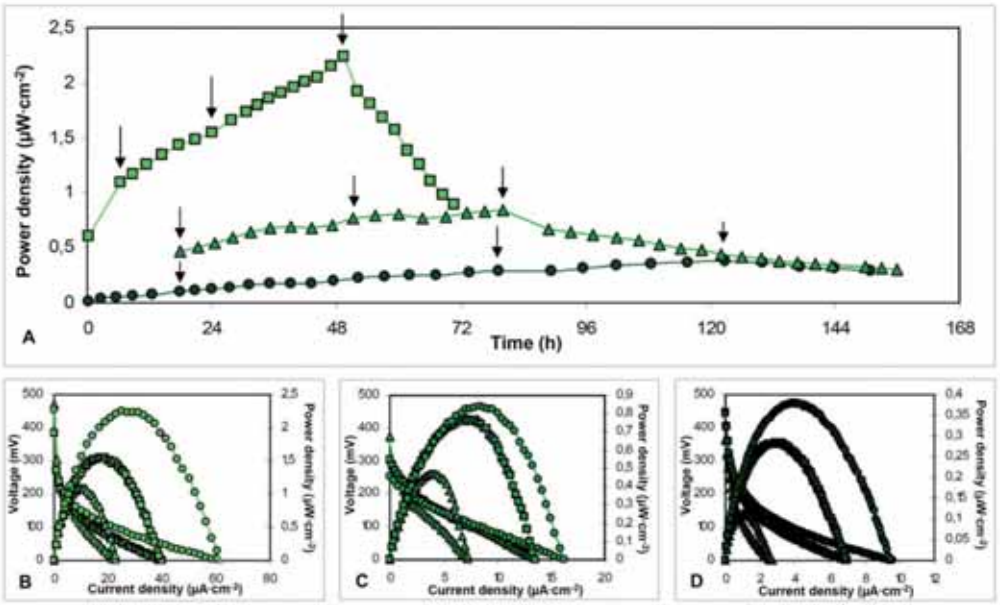

Fig. 3. (A) Evolution of the maximum power density in MFC transducers using liquid catalysts: Ferricyanide (■), EDTA-iron sulphate (▲) and EDTA-iron chloride (●). (B) I-V characteristic curves and power density curves taken after 10 (▲), 24 (■) and 50 hours (●) of operation in the MFC with ferricyanide catalyst. (C) I-V characteristic curves and power density curves taken after 22 (▲), 70 (■) and 80 hours (●) of operation in the MFC with EDTA-iron sulphate catalyst. (D) I-V characteristic curves and power density curves taken after 22 (▲), 80 (■) and 125 hours (●) of operation in the MFC with EDTA-iron chloride catalyst. Arrows indicate the times when the curves were constructed.

However, the fall in maximum power density coincided with the onset of iron diffusion through the proton exchange membrane. The cation exchange membrane could not maintain the low catholyte pH required to keep ferric iron soluble. Also, cation exchange membranes transport other cations besides protons, which can cause a pH rise in the cathodic compartment [23,13]. This pH rise caused extensive iron precipitation that damaged the membrane [13]. Diffusion of iron through the membrane can also cause a decrease in fuel cell performance because bacteria use this iron as electron acceptor instead of the anode.

4. Conclusions

The data collected in this experiment showed that, in general, fuel cells with liquid catalysts in the cathode provided much higher power densities than cells using solid surface catalysts.

The results indicate that solid surface catalysts provide a relatively low but very stable signal making them suitable for applications requiring extended operation, but in which high sensitivity is not needed. Transducers using liquid catalysts provide an alternative when higher output is required, but at the expense of a limited operation span.

Acknowledgements

Part of the work was supported by grants CSD2006-00044 TRAGUA (CONSOLIDER-INGENIO2010) and CTQ2009-14390-C02-02 from the Spanish Ministry of Education and Science.

References

[1] Gil GC, Chang IS, Kim BH, Kim M, Jang JK, Park HS, Kim HJ. Operational parameters affecting the performance of a mediator-less microbial fuel cell. *Biosens Bioelectron* 2003 **18**:327-334.

[2] Pham HT, Jang JK, Chang, IS, Kim BH. Improvement of cathode reaction of a mediatorless microbial fuel cell. *Microbio Biotechnol* 2004 **14**(2):324-329.

[3] Cheng S, Liu H, Logan BE. Increased performance of single-chamber microbial fuel cells using an improved cathode structure. *Electrochemistry Communications* 2006 **8**:489-494.
[4] Logan BE, Hamelers B, Rozendal R, Schröder U, Keller J, Freguia S, Aelterman P, Verstraete W, Rabaey K. Microbial Fuel Cell: Methodology and Technology. *Environmental Science & Technology 2006* **40**(17):5181-5192.
[5] Zhao F, Harnisch F, Schröder U, Scholz F, Bogdanoff P, Herrmann I. Challenges and constraints of using oxygen cathodes in microbial fuel cells. *Environmental Science & Technology* 2006 **40**(17): 5193-5199.
[6] Yu EH, Cheng S, Scott K, Logan BE. Microbial fuel cell performance with non-Pt cathode catalysts. *Journal of Power Sources* 2007 **171**: 275-281.
[7] Aelterman P, Versichele M, Genettello E, Verbeken K, Verstraete W. Microbial fuel cells operated with iron-chelated air cathodes. *Electrochimica Acta* 2009 **54**:5754-5760.
[8] Zhuwei D, Li H, Gu T. A state of the art review on microbial fuel cells: a promising technology for wastewater treatment and bioenergy. *Biotechnology Advances* 2007 **25**:464-482.
[9] Rismani-Yazdi H, Carver SM, Christy AD, Tuovinen OH. Cathodic limitations in microbial fuel cells: An overview. *J Power Sources* 2008 **180**:683-694.
[10] Erable B, Etcheverry L, Bergel A. Increased power from a two-chamber microbial fuel cell with a low-pH air-cathode compartment. *Electrochemistry Communications* 2009 **11**:619-622.
[11] Zhao F, Harnisch F, Schroder U, Scholz F, Bogdanoff P, Herrmann I. Application of pyrolysed iron (II)phthalocyanine and CoTMPP based oxygen reduction catalysts as cathode materials in microbial fuel cells. *Electrochem Commun* 2005 **7:**1405–10.
[12] Taylor RJ, Humffray AA. Electrochemical studies on glassy carbon electrodes. I. Electron transfer kinetics. J Electroanal Chem 1973 **42**:347-354.
[13] ter Heijne A, Hamelers HV.M, de Wilde V, Rozendal RR, Buisman CJN. A bipolar membrane combined with ferric iron reduction as an efficien cathode system in microbial fuel cells. *Environ Sci Technol* 2006 **40**:5200-5205.
[14] Rohwerder T, Gehrke T, Kinzler K, Sand W. Bioleaching review part A: Progress in bioleaching: fundamentals and mechanisms of bacterial metal sulfide oxidation. *Appl Microbiol Biotechnol* 2003 **63:**239-248.
[15] You S, Zhao Q, Zhang J, Jiang J, Zhao S. A microbial fuel cell using permanganate as the cathodic electron acceptor. *J Power Sour* 2007 **162**:1409-1415.
[16] Logan BE. *Microbial Fuel Cells*. New York: John Wiley & Sons; 2008.
[17] Zumdahl SS. *Chemical Principles*. Boston: Houghton Mifflin Company; 1998.
[18] Santana-Casiano M, González-Dávila M, Rodríguez MJ, Millero FJ. The effect of organic compounds in the oxidation kinetics of Fe(II). *Mar Chem* 2000 **70:**211-222.
[19] Oh SE, Min B, Logan BE. Cathode performance as a factor in electricity generation in microbial fuel cells. *Environ Sci Technol* 2004 **38**:4900-4904.
[20] Clauwaert P, Aelterman P, Pham TH, De Schamphelaire L, Carballa M, Rabaey K, Verstraete W. Minimizing losses in bio-electrochemical systems: the road to applications. *Appl Microbial Biotechnol* 2008 **79**:901-913.
[21] Bockris JOM, Khan UM. *Surface Electrochemistry, A Molecular Level Approach*. New York, London: Plenum Press; 1993.
[22] Harnisch F, Wirth S, Schröder U. Effects of substrate and metabolite crossover on the cathodic oxygen reduction reaction in microbial fuel cells: Platinum vs. iron(II) phthalocyanine based electrodes. *Electrochemistry Communications* 2009 **11**:2253-2256.
[23] Rozendal RA, Hamelers HVM, Buisman CJM. Effects of membrane cation transport on pH and microbial fuel cell performance. *Environ Sci Technol* 2006 **40**:5206-5211.

G Model
SNB-12903; No. of Pages 7
ARTICLE IN PRESS

Sensors and Actuators B xxx (2011) xxx–xxx

Contents lists available at ScienceDirect

Sensors and Actuators B: Chemical

journal homepage: www.elsevier.com/locate/snb

Effect of the cathode/anode ratio and the choice of cathode catalyst on the performance of microbial fuel cell transducers for the determination of microbial activity

Naroa Uría[a,*], David Sánchez[b], Roser Mas[b], Olga Sánchez[a], Francesc Xavier Muñoz[b], Jordi Mas[a]

[a] Group of Environmental Microbiology, Universitat Autónoma de Barcelona, Bellaterra, Spain
[b] Centro Nacional de Microelectrónica (CNM-IMB) CSIC, Spain

ARTICLE INFO

Article history:
Received 30 September 2010
Received in revised form 1 February 2011
Accepted 12 February 2011
Available online xxx

Keywords:
Microbial fuel cell
Microbial activity
Biosensor

ABSTRACT

Microbial activity can be measured using sensors based on microbial fuel cell technology. In these sensors, microorganisms in contact with the anode generate a current proportional to their metabolic activity. Proper operation of such a device requires that activity at the anode is not impaired by the ability of the cathode to transfer current to the cathodic electron acceptor. Therefore, we have determined the minimum cathode to anode ratio required for unhindered performance of the microbial fuel cell. Our results indicate that for the same level of biological activity, the optimal cathode/anode ratios depend on the type of cathode being used. Thus, while carbon paper/ferricyanide cathodes require ratios of 4, platinum cathodes need much higher ratios of about 27. Cyclic voltammetry measurements indicate that platinum cathodes have a much slower dynamic behaviour than cathodes based on carbon paper/ferricyanide. While these results indicate that carbon paper/ferricyanide cathodes provide the most current for the same cathode area, extended experiments carried over a period of several days indicate a progressive degradation of fuel cell performance in cells using iron catalysts. Overall, our conclusion is that soluble iron-based catalysts provide much higher power output than solid phase platinum catalysts, but at the expense of a reduced life span which limits their use for applications requiring extended operation.

1. Introduction

During recent years, a number of different sensor types using impedance spectroscopy, fluorescence or optical density have been proposed for the detection and quantification of microbial biomass in liquid samples. In some instances, the models proposed have actually been commercialized. However, efficient systems for the quantification of bacterial activity have not yet been described.

Microbial fuel cells (MFCs) provide a viable transducing mechanism for the determination of microbial activity in liquid samples. In some specific instances, the principle has been used for specific applications such as detection of toxicity [1–3]. Utilization of MFCs as sensing devices requires however their ability to respond to changes in the level of biological activity present in the anode compartment. The problem is that power output, and therefore signal output of a MFC is also dependent on several other factors. Between them, the surface area of the proton exchange membrane (PEM) and the relative sizes of the anode and cathode seem to play an important role [4]. The power values obtained are usually normalized in order to make the efficiency of power production by different MFCs comparable. In many studies, this normalization is carried using the surface area of the anode, assuming that bacterial activity limits power output. However, recent reports demonstrating that tripling the surface area of the cathode increased power density by 22% [4,5] indicate otherwise.

Additionally, the choice of the cathode material is another factor to consider depending on the application [6]. For oxygen reduction different cathode materials have been proposed. Platinum is the best known [7]. However, due to its high cost [8], tendency to poisoning by the formation of a platinum oxide layer at the surface [6,9,10], and sensitivity to biological and chemical fouling [11,12], platinum based electrodes are not useful for all applications. For this reason, different and cheaper alternatives to noble metal catalyst have been studied such as pyrolysed iron (II) phthalocyanine (Pyr-FePc) and cobalt tetramethoxyphenylporphyrin (CoTMPP) applied on graphite cathodes [9,13].

Other materials such as carbon paper or graphite can also be used with a soluble catalyst which accelerates the poor oxygen reaction on these electrode materials. The couple ferric/ferrous iron is a good electron mediator for oxygen reduction for three reasons:

* Corresponding author at: Department of Genetics and Microbiology, Autonomous University of Barcelona, 08193 Bellaterra, Spain.
Tel.: +34 935 813 011, fax: +34 935 812 387.
E-mail address: naroa.uria@uab.cat (N. Uría).

0925-4005/$ – see front matter © 2011 Elsevier B.V. All rights reserved.
doi:10.1016/j.snb.2011.02.030

fast reaction at carbon electrodes [14,15], high standard potential ([+0.77 V vs. NHE (normal hydrogen electrode)], and possible biological oxidation of ferrous iron to ferric iron with oxygen as the electron acceptor up [15,16].

Ferricyanide is the catalyst most extensively used due to its highly solubility in water and the fact that replaces the use of precious metal in the cathode. Moreover it has a standard potential of 0.361 V that, due to the short polarization of the cathode, is quite close to the real potential achieved [15,17,18]. So, despite the fact that oxygen reduction has a standard potential supposedly higher than ferricyanide reduction [18] in practice this is not true and a higher energy yield is obtained with ferricyanide. Nevertheless, ferricyanide has some disadvantages that have drawn the attention to the use of alternative ferric iron catalysts such as sulphate or iron chloride [9]. Ferricyanide is commonly used as a catalyst in MFC cathodes, but due to the very slow re-oxidation rate by oxygen, it is not regarded as sustainable [6,9]. On the other hand, other ferric iron sources precipitate at neutral pH. To avoid this precipitation the use of chelating agents is required such as ethylenediaminetetraacetic acid (EDTA) [9,19,20].

In this study, we attempt to determine the optimal anode/cathode ratio for both solid surface and soluble catalysts as well as to compare the performance and stability of different types of catalysts when used in the cathode compartment of MFC transducers for prolonged periods of several days.

2. Experimental procedure

2.1. Bacterial strains and their cultivation

Shewanella oneidensis strain MR1 (ATCC 7005500) was grown aerobically in 100 ml of Trypticase Soy Broth (TSB) at 27 °C. After 36 h of aerobic growth, the cells were harvested by centrifugation (10,100 *g* × 15 min, 4 °C) using a 5804R Eppendorf centrifuge. For subsequent adaptation to anaerobic conditions, the resulting pellet was resuspended in 1 l of AB minimal medium. After inoculation the medium was supplemented with lactate (0.02 M) as the carbon source and fumarate (0.1 M) as electron acceptor, and further incubated with agitation at room temperature for 48 h. After this period the culture was centrifuged and inoculated in AB minimal medium with lactate (0.02 M), so the culture was ready for inoculation into a fuel cell.

2.2. Microbial fuel cell design and measurements

2.2.1. Fuel cell architecture and assembly

In this study, a two-chamber fuel cell was used. The cell was built using two solid (4 cm × 11 cm × 11 cm) methacrylate blocks. The interior of each block had been machined to form an inner cylindrical reactor with a volume of 130 ml. The top of the blocks was drilled to provide ports for inoculation and sampling as well as electrical connections for both the anode and the cathode. The two methacrylate blocks were assembled around a proton exchange membrane (PEM) and held in place by means of stainless steel screws. The membrane employed was Nafion®117 (Ion power, Inc.) with a thickness of 183 μm and effective area of 38.46 cm^2. The reactor was made watertight using a rubber gasket (76 mm × 3 mm) between both methacrylate blocks which exerted pressure on the membrane.

2.2.2. Electrodes

In the anode chamber, carbon paper electrodes (B2120 Toray Carbon Paper Designation TGPH-120, plain, no wet proofing; E-Tek, Inc.) with a thickness of 0.35 mm were used in all cases. This material is very common in MFC because it has a high conductivity (electrical resistivity of 80 mΩ·cm through plane) and is well suited for bacterial growth [18].

In the cathode chamber, different electrode materials were employed. On the one hand, four metal or metal coated cathodes were used: commercial platinum foil, silicon wafers coated with platinum and black platinum, and a heavy duty commercial stainless steel scourer woven from a single strand of stainless steel. Platinum foil was obtained from a commercial source (Goodfellow Cambridge Limited), with a purity of 99.95% and a thickness of 0.1 mm. The silicon wafers with platinum were produced by thin-film technology using 4" double side polished silicon wafers. A first titanium layer of 150 Å was deposited as adhesion promoter, followed by 1500 Å platinum layer deposited in both sides. The metallization was performed in a single process using electron beam evaporation. Black platinum was obtained using the same procedure but modifying parameters that provide a metal layer with higher rugosity.

On the other hand, carbon paper electrode with a size of 12 cm^2 was used. The main difference when this material is employed for the cathode is that a catalyst is usually necessary in order to accelerate the reduction of oxygen. In our case, we used three different liquid catalysts: ferricyanide (0.05 M $K_3[Fe(CN)_6]$ in a 0.1 M phosphate buffer), EDTA chelated iron sulphate (0.5 M $Fe_2(SO_4)_3$, 0.1 M EDTA) and EDTA chelated iron chloride (0.5 M $FeCl_3$, 0.1 M EDTA).

Each electrode was welded to the wire using conducting silver loaded epoxy (RS Components) with all exposed surfaces of the wire covered with epoxy as well. The weldings were covered with a noncorrosive silicone rubber coating (RS Components).

2.2.3. Microbial fuel cell operation and characterization

Once the fuel cells were assembled the two chambers were filled through the sampling ports. Inoculation of the fuel cells was made at a final concentration of approximately 10^8 cells ml^{-1} in AB minimal medium. Lactate (0.02 M), used as the carbon source was added only once right before inoculation. Both, anode and cathode were stirred slowly (250 rpm). The cathode was pumped with air and nitrogen was injected into the anode headspace to avoid oxygen inputs. After inoculation the electrodes were connected to a source meter and current output was monitored. The measurements were made with 2 source meter units (Keithley®2612) connected to a personal computer that allow simultaneous monitoring of up to 4 independent fuel cells. Data collection was automatized using a custom made program developed with LabView 8.5 (Nationals Instruments).

For MFC characterization, IV curves were built at selected times. IV curves were performed by imposing different output current values between the cell electrodes and measuring the resulting voltage. So, current initially set to 0 μA, was increased stepwise with an interval of time between steps of 3 min. For each current step, the device measured the output voltage. The curve ended when the voltage reached 0. The power was calculated as the product of the values of voltage and current.

2.2.4. Electrochemical characterization of the cathodes

Cyclic voltammetries were performed on a potentiostat/galvanostat model FRA2 Micro-Autolab Type II. The electrochemical cell was kept at 25 °C and maintained in a Faraday cage to avoid external noise. An Ag/AgCl electrode (Metrohm, Switzerland), and a platinum-ring electrode (Metrohm, Switzerland) were used as reference and auxiliar electrode respectively. The system was operated through a PC using GPES software.

Platinum/oxygen and carbon paper/ferricyanide electrodes were compared by cyclic voltammetry at a scan rate of 20 mV s^{-1}. For the platinum-oxygen system, the electrochemical cell was filled with oxygen saturated 0.5 M potassium nitrate and using a pla-

Please cite this article in press as: N. Uría, et al., Effect of the cathode/anode ratio and the choice of cathode catalyst on the performance of microbial fuel cell transducers for the determination of microbial activity, Sens. Actuators B: Chem. (2011), doi:10.1016/j.snb.2011.02.030

tinized silicon wafer as the working electrode. In the case of carbon paper-Fe system, a working electrode of carbon paper was submerged in 1 mM potassium hexacyanoferrate (II) dissolved in the 0.5 M potassium nitrate.

Cyclic voltammetries of the platinum and black platinum silicon wafer cathodes were performed at different scan rates (2–500 mV s^{-1}) in 1 mM potassium hexacyanoferrate (II) dissolved in 0.5 M potassium nitrate, Before performing the voltammetry, the solution was flushed with nitrogen to remove the oxygen.

2.3. Experimental design

2.3.1. Impact of the ratio cathode/anode on the power output of MFCs with soluble and solid catalysts

To study the effect of the ratio anode/cathode four identical fuel cells were inoculated with *S. oneidensis* MR1 at a final concentration of 10^8 ufc ml^{-1} in AB minimal medium, supplemented with 0.02 M lactate as anolyte.

As a model of soluble catalyst, ferricyanide was used to study the influence of cathode/anode relation. We compared four different anode sizes (1.5 cm^2, 3 cm^2, 6 cm^2 and 12 cm^2) while maintaining a constant cathode of 12 cm^2. The cathode had phosphate buffer (0.1 M) with 0.05 M ferricyanide.

For solid catalysts the experiment was repeated using a 13.55 cm^2 platinum-coated silicon wafer as the cathode in all cells while using 0.1 M buffer phosphate as catholyte. Four reactors were assembled with different anode sizes of 0.25, 0.5, 0.75 and 1 cm^2. The anode sizes were much smaller than in the previous experiment as preliminary trials indicated that solid catalysts used at the cathode surface reach power densities an order of magnitude lower than soluble catalysts.

Characterization of the MFCs was executed at start up, before detectable growth occurred, by means of one initial ($t = 0$) IV curve. At the time of inoculation, since all the MFCs shared the same inoculum, differences between them could be only attributed to the ratios cathode/anode used. The maximum power density obtained for each cathode/anode ratio in this curve, was represented as a function of the ratio.

Our experimental set up allows the simultaneous study of 4 microbial fuel cells. In this experiment we decided to use the 4 cells to study 4 different cathode/anode ratios instead of running replicate experiments. The variability of the experimental results was thus determined in separate experiments in which identical fuel cells were inoculated with the same culture giving relative standard errors inferior to 10%. The relative standard errors increased up to 40–50% when fuel cells were filled with different inocula. Therefore, whenever possible we have attempted to run comparison experiments using the same inoculum.

2.3.2. Long term performance of different solid and soluble catalysts

To analyze the extent to what long term performance of the cathode was affected by the type of material being used we constructed several MFCs with different solid catalysts such as a commercial platinum foil (6.25 cm^2), platinum-coated silicon (13.55 cm^2), black platinum silicon (13.55 cm^2), and stainless steel (529.5 cm^2), and liquid catalysts such as ferricyanide, EDTA chelated iron sulphate and EDTA chelated iron chloride.

As in the previous experiment, the anode composition was the same in all MFCs and contained a culture of *S. oneidensis* MR1 at a concentration of about 10^8 ufc ml^{-1} in AB minimal medium, supplemented with 0.02 M lactate. The anode size was 0.5 cm^2 in the case of MFC with solid catalysts, and 3 cm^2 in the case of MFCs with liquid catalysts.

In the MFCs with solid catalyst, the cathode contained 0.1 M phosphate buffer and one of the electrodes mentioned above. Fuel cells with carbon paper electrode had ferricyanide, EDTA chelated iron sulphate and EDTA chelated iron chloride as soluble catalysts, all at a concentration of 0.05 M. Both, anode and cathode were stirred slowly (250 rpm). The cathode was pumped with air and, nitrogen was injected into the anode headspace to avoid oxygen inputs.

The fuel cells were run for 5–7 days. During this period they were monitored by carrying out IV curves preceded by a 1 h stabilization period during which the cell circuit was open and voltage was allowed to stabilize.

3. Results and discussion

3.1. Impact of the ratio cathode/anode on the power output with solid and soluble catalysts

Power output in microbial fuel cells depends on the properties of the anode as electron acceptor for the microbial populations as well as on the properties of the cathode as a catalyst for oxygen reduction. But it also depends to a rather large extent on the abundance and level of activity of the microbial components. It turns out that when comparing different electrode materials, growth of the biological components is strongly affected by the material used. Thus in fuel cells containing cathodes of different sizes or catalytic performances, growth can range from virtually nonexistent to exuberant. When comparing these cells, the bulk of the differences observed would be caused by the large difference in biomass found between both cells despite the fact that both used exactly the same inoculum. In order to avoid this problem, only the results corresponding to the IV curve obtained right after the inoculation were used in this experiment. That way it is sure that biomass concentration is the same and that the results obtained depends only on the cathode/anode ratio.

3.1.1. Soluble catalysts

In the study carried out using soluble iron ferricyanide as a catalyst the IV curves (Fig. 1A) indicate very similar values of open circuit voltage (OCV), between 300 and 400 mV with a maximum difference of about 76 mV. The observed voltage drop when increasing current output was more pronounced the smaller was the anode surface. The IV plots also indicate that maximum current and power values increased when increasing the anode area (0.125 mA and 5.35 μW for 1.5 cm^2 anode, 0.27 mA and 10.32 μW for 3 cm^2 anode, 0.4 mA and 17.45 μW for 6 cm^2 anode and, 0.68 mA and 28.82 μW for 12 cm^2 anode). Normalizing power and current values to the area of the anode (Fig. 1B) shows that the MFCs with the highest performance (higher current and power output per surface unit) are those with smaller anodes. Increasing the anode size to ratios cathode/anode below 4 causes a clear decrease in the normalized power and current values. Plotting normalized maximum power density against the ratio cathode/anode (Fig. 2) again indicates this fact. The results show that attempts to increase power output by maximizing power production in the anode (through increasing the size of the anode or the concentration of bacteria) in fuel cells that use soluble mediators are severely hampered by the performance of the cathode. This can be attributed to the appearance of mass transfer problems at the surface of the cathode [21].

3.1.2. Solid catalysts

When the study was performed using platinum as a cathode catalyst the IV curves (Fig. 3) showed open circuit voltages between 200 and 300 mV in the four cells. As in the previous experiment maximum current and power outputs tended to increase when increasing anode size (Fig. 3A). Also as in the previous experiment, current and power values normalized to the anode surface show that maximum values are obtained with the small anode areas

Please cite this article in press as: N. Uría, et al., Effect of the cathode/anode ratio and the choice of cathode catalyst on the performance of microbial fuel cell transducers for the determination of microbial activity, Sens. Actuators B: Chem. (2011), doi:10.1016/j.snb.2011.02.030

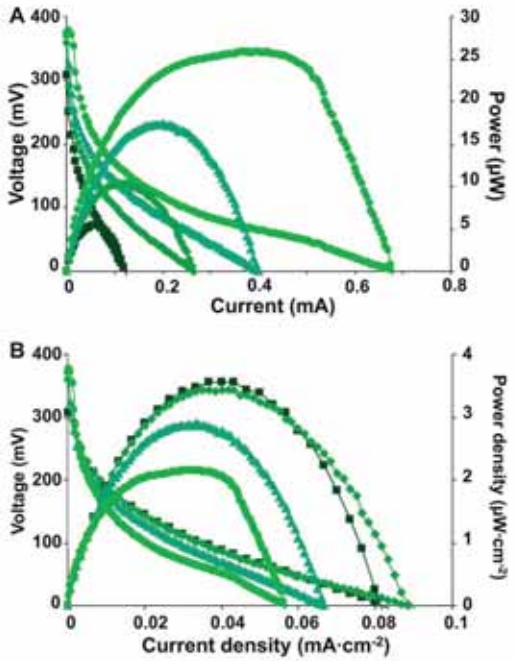

Fig. 1. Initial IV curves made at the time of inoculation (A) without normalized values and (B) with values normalized by the anode area (ratios cathode/anode, ■:8, ♦:4, ▲:2, ●:1).

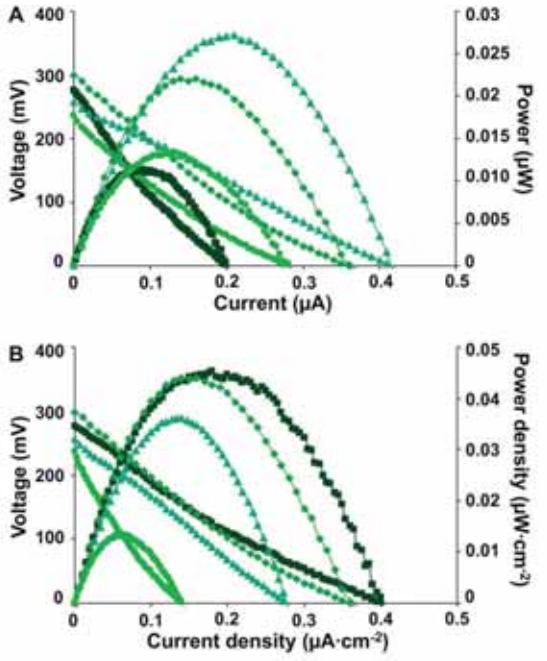

Fig. 3. Initial IV curves made at the time of inoculation (A) without normalized values and (B) with values normalized by the anode area (ratios cathode/anode, ■:54.6, ♦:27.3, ▲:18.2, ●:13.65).

(Fig. 3B). However, plotting maximum values of normalized power output against the ratio cathode/anode (Fig. 4) indicates that the cathode becomes limiting at ratios below 30.

3.2. Long term performance of different solid and soluble catalysts

Once we established the optimal cathode/anode ratio for both solid and soluble catalysts, we proceeded to evaluate the ability of different soluble and solid catalysts to operate at the cathode of a microbial fuel cell for extended periods of time.

As stated in materials and methods, several solid (solid platinum, silicon oxide covered with platinum and black platinum, and stainless steel) as well as soluble (ferricyanide, EDTA chelated iron sulphate and EDTA chelated iron chloride) catalysts were used.

For each catalyst, after inoculating the fuel cells, maximum power output as a function of time was estimated from individual IV curves taken at different times. Maximum power was then normalized to the area of the cathode and the results, expressed as maximum power densities, have been plotted in Figs 5 and 7.

Fig. 5 shows the variation with time of maximum power output in fuel cells containing 4 different solid catalysts. The results indicate that, except for the case of the platinum covered silicon wafer that seems to increase with time, the rest of the materials (black platinum covered silicon, solid platinum and stainless steel) are quite stable, being able to provide a low but sustained power output at values that range between a maximum average of 0.065 $\mu W\,cm^{-2}$ in the case of solid platinum, and a minimum average of 0.0001 $\mu W\,cm^{-2}$ in the case of stainless steel. Also, the

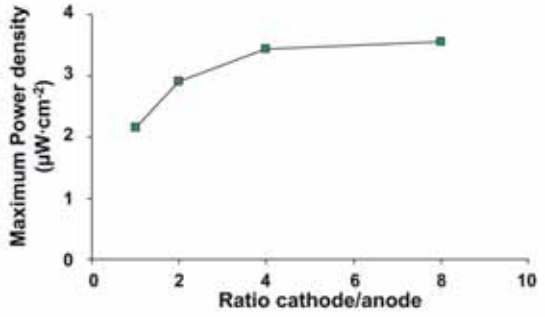

Fig. 2. Relation between maximum power density values of initial IV curves obtained for the different anode sizes MFCs with liquid catalyst and the ratio cathode/anode.

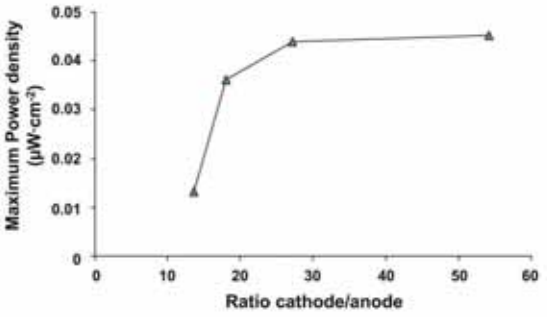

Fig. 4. Relation between maximum power density values of initial IV curves obtained for the different anode sizes MFCs with solid catalyst, and the ratio cathode/anode.

Please cite this article in press as: N. Uría, et al., Effect of the cathode/anode ratio and the choice of cathode catalyst on the performance of microbial fuel cell transducers for the determination of microbial activity, Sens. Actuators B: Chem. (2011), doi:10.1016/j.snb.2011.02.030

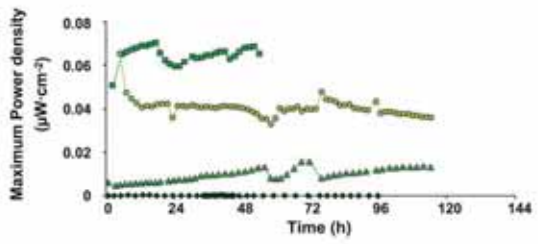

Fig. 5. Evolution of the maximum power density, obtained in the IV curves made all along the experiment, in MFC transducers using platinum (■), black platinum (●), silicon wafer-based platinum (▲), and stainless steel (♦) as cathode catalysts.

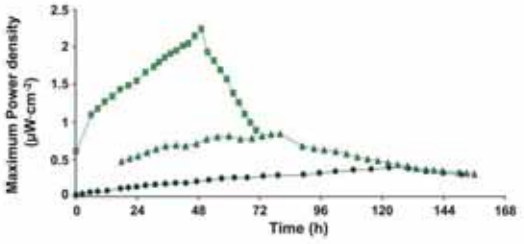

Fig. 7. Evolution of the maximum power density, obtained in the IV curves made all along the experiment, in MFC transducers using liquid catalysts: ferricyanide (■), EDTA-iron sulphate (▲) and EDTA-iron chloride (●).

power densities obtained were extremely dependent on the type of material used. The highest power density was obtained with solid platinum foil. Because platinum foil is prohibitively expensive for mass production, other materials were tested. Thin layers of platinum deposited on top of wafers of silicon oxide might provide an inexpensive alternative. As a control we used stainless steel. Not surprisingly, stainless steel provided the lowest, by far, power density. Platinum-covered silicon oxide wafers were unable to match the power output of solid platinum, a fact for which we have no clear cut answer but which might be related to the extreme smoothness of the silicon chip surface. To increase the roughness of the electrode, some of the silicon oxide wafers were coated with a thin layer of black platinum, in which the coating metal surface presents a much higher roughness. Black platinum coated electrodes had a power density much higher than smooth surface platinum. In an attempt to explain the different behaviour of platinum and black platinum we ran cyclic voltammetries of both electrode types. Voltammetry can be used for testing the performance of the electrodes. By analysing the variation of peak position as a function of scan rate it is possible to gain an estimate for the electron transfer rate constants [22]. So, Fig. 6A shows the separation of cathodic and anodic peak potential of each voltammogram, made at different scan rates in the range between 2 mV s^{-1} and 500 mV s^{-1} for black platinum and silicon wafer-based platinum electrodes in ferrocyanide. The difference between redox peaks with the increase of scan rate is very stable in both cases. However, this distance is smaller for black platinum indicating improved catalytic activity. Additionally, as seen in the voltammograms obtained with a scan rate equal to 50 mV s^{-1} (Fig. 6B), black platinum obtained higher redox peak currents and higher graphic amplitude due to their higher capacitance. It should be noted that many electrode materials used in MFCs cannot produce reversible electrochemical reactions even for the classic reversible redox couple $Fe(CN)_6^{-3}/Fe(CN)_6^{-4}$. The main reason for this is that the heterogeneous processes of electrode reactions can be significantly affected by the microstructure, roughness and function groups present on the electrode surface [23]. Thus, these voltammetries confirm black platinum as a viable alternative in the cathode of MFCs due to its higher roughness and better catalytic and charge-transfer capacity.

When long term experiments were attempted using soluble catalysts, the observations were quite different. Fig. 7 shows the results obtained during 7 days of continuous operation. A common pattern observed in the three soluble catalysts used was a progressive increase in power density that probably reflects the development of biological populations in the anode compartment. This rapid increase could not be observed in the solid catalyst experiments because maximum power output was about one order of magni-

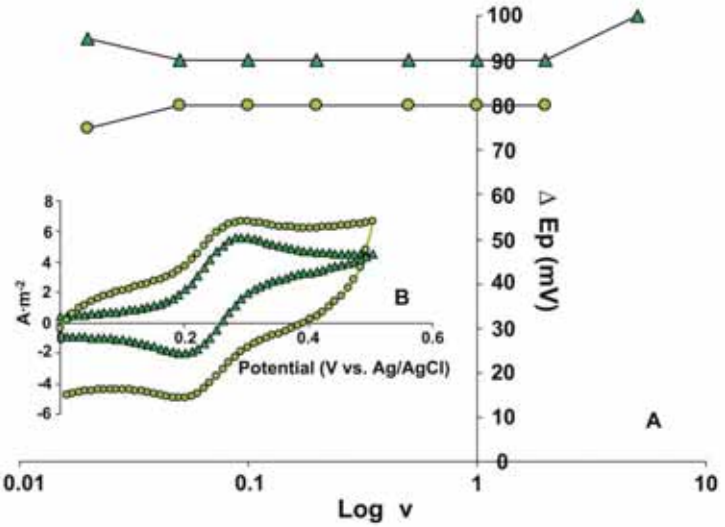

Fig. 6. (A) Variation of oxidation and reduction peak separation of silicon wafer-based platinum (▲) and black platinum (●) cyclic voltammograms at different potential scan rates. (B) Cyclic voltammograms of silicon wafer-based platinum (▲) and black platinum (●) at potential scan rate of 0.5 V s^{-1}.

Please cite this article in press as: N. Uría, et al., Effect of the cathode/anode ratio and the choice of cathode catalyst on the performance of microbial fuel cell transducers for the determination of microbial activity, Sens. Actuators B: Chem. (2011), doi:10.1016/j.snb.2011.02.030

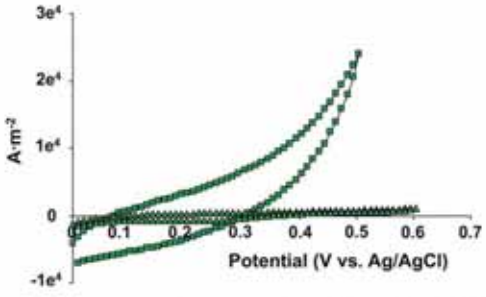

Fig. 8. Cyclic voltammograms of oxygen reduction on silicon wafer based platinum (▲) and ferric reduction (■) on carbon paper electrode at a potential scan rate of 0.2 V s^{-1}.

tude lower, and thus, did not allow the bacteria to fully express their maximum power production.

The increase in power output observed when using soluble catalysts was followed by a progressive decrease, above all in the case of the ferricyanide cell. We first attributed this decrease to lactate depletion. However, a quick calculation shows a coulombic yield of 1003 C from the oxidation of 0.02 M lactate to acetate (4 mol e$^-$/mol lactate). If we take into account a coulombic efficiency of 50% as reported for pure cultures of *S. oneidensis* MR1 [24], the amount of charge released should be about 500 C. The amount of charge produced by our cells up to the inflection point is only 64 C, much less than the amount released if all lactate had been consumed.

The drop could also be related to a lowering of the Fe^{3+}/Fe^{2+} ratio due to an insufficient reoxidation of these iron chelates by oxygen. For this reason, the drop would occur first in the cells with higher current values, but again the amount of oxidized iron available is more than sufficient to accept all the electrons released during the oxidation of 0.02 M lactate.

We observed that the fall in maximum power density coincided with the onset of iron diffusion through the proton exchange membrane. The cation exchange membrane could not maintain the low catholyte pH required to keep ferric iron soluble. Cation exchange membranes transport cations other than protons, which can cause a pH rise in the cathodic compartment [15,25]. This pH rise caused extensive iron precipitation that damaged the membrane [15]. Diffusion of iron through the membrane can also cause a decrease in fuel cell performance because bacteria use this iron as electron acceptor instead of electrode.

The data collected in this experiment, show maximum power densities (0.38, 0.83 and 2.24 μW cm^{-2}) much higher than the maximum obtained with solid platinum foil (0.07 μW cm^{-2}). This difference of 10–20 times in power output when changing from a Pt-oxygen cathode (solid platinum, silicon oxide covered with platinum and black platinum) to a carbon paper-Fe (ferricyanide, EDTA chelated iron sulphate and EDTA chelated iron chloride) is much higher than reported increases of 1.5–1.8 times in similar experiments [4,5]. To confirm this data, we carried out a separate electrochemical study running cyclic voltammetries of Pt-oxygen and carbon paper-Fe systems. The results confirm the experimental observations made in the MFCs. So, in Fig. 8 is possible to observe the maximum values obtained by the carbon paper-Fe system are on the order of 20 fold higher (2.4e^4 A m^{-2}) than the obtained by the Pt-oxygen system (2.4e^3 A m^{-2}).

The discrepancy between our 10–20 fold increase and the 1.5–1.8 fold increase reported by Oh et al. [4,5] is probably related to the fact that this authors use platinized carbon paper instead a platinum. It is likely that platinized carbon paper has a much higher roughness and therefore, a much higher effective area than our platinum electrodes. The large difference observed, thus, is not a result of much higher electron transfer efficiency when using ferricyanide, but of a much lower transfer rate of our solid catalysts due to their smooth surface.

The higher power values observed when using soluble catalysts, such as ferricyanide or iron-chelating catholytes, vs solid surface catalysts is both a function of the different potentials of the chemicals (lower activation energy) as well as the higher mass transfer efficiency [5]. Activation losses at the cathode have been identified as the dominant limitation in MFCs [11,12], particularly due to low proton availability [10,12]. Concentration overpotentials are associated with the concentration gradient of the reagents and products in the proximity of the electrode. Inefficient mass transfer through diffusion and convection of substrate or removal of products may limit the maximal current production at an electrode [26].

Besides, the formation of mixed potentials and the flow of internal currents have been reported in the case of platinum based electrodes, due to the permeation of fuel from the anode. Fuel crossover through the separator membrane into the cathode compartment may considerably decrease the electrode performance due to the formation of mixed potentials and the flow of internal currents causing a depolarization even at open circuit [27,28].

Another factor that may play a role in the order of magnitude difference observed between solid surface catalysts and soluble catalysts might be related to the fact that during the first part of the experiment, iron acts as an electron acceptor rather than as a shuttle/catalyser for oxygen reduction. As soon as the pool of oxidized iron falls below a certain level, the cathode reaction becomes limited by the kinetics of oxygen reduction by iron which is clearly slower than the kinetics of iron reduction at the cathode surface [7]. As soon as the MFC shifts from iron reduction to oxygen reduction, an additional factor comes into play. Whereas iron reduction and thus its redox potential are independent of the proton concentration, the oxygen reduction reactions involve the consumption of one proton per transferred electron, no matter whether the reaction proceeds to water or to hydrogen peroxide. The consequence is a thermodynamically controlled shift of the polarization curve toward more negative values, which, depending on the nature and thus pH dependence of the anodic reaction, significantly reduces the MFC potential and power output [7].

4. Conclusions

In order for the anode to provide its full signal range when used as a sensing element, the performance of the device cannot be limited by the cathode. The area ratio cathode/anode above which the cathode ceases to be limiting depends on the type of catalyst used. For soluble cathode catalyst, ratios above 3–4 are enough to guarantee full performance of the anode. When solid cathode catalysts are used ratios above 27 must be used to ensure the same performance.

As a rule, fuel cells with liquid catalysts in the cathode provide much higher power densities than cells using solid surface catalysts. Our results seem to indicate that this is probably related to the fact that during the first days of operation of the MFC, iron acts as an electron acceptor rather than as a mediator for oxygen reduction.

The different solid surface catalysts tested provide a relatively low but very stable signal making them suitable for applications requiring extended operation, but in which high sensitivity is not needed. Transducers using liquid catalysts provide an alternative when higher output is required, but at the expense of a limited operation span.

Please cite this article in press as: N. Uría, et al., Effect of the cathode/anode ratio and the choice of cathode catalyst on the performance of microbial fuel cell transducers for the determination of microbial activity, Sens. Actuators B: Chem. (2011), doi:10.1016/j.snb.2011.02.030

Acknowledgements

This work was supported by grants CSD2006-00044 TRAGUA (CONSOLIDER-INGENIO2010) and CTQ2009-14390-C02-02 from the Spanish Ministry of Education and Science to JM.

References

[1] D. Dávila, J.P. Esquivel, N. Sabaté, J. Mas, Silicon-based microfabricated microbial fuel cell toxicity sensor, Biosens. Bioelectron. 26 (2011) 2426–2430.
[2] M. Kim, M.S. Hyun, G.M. Gadd, H.J. Kim, A novel biomonitoring system using microbial fuel cell, Environ. Monit. 9 (2007) 1323–1328.
[3] J.M. Tront, J.D. Fortner, M. Plötze, J.B. Hughes, A.M. Puzrin, Microbial fuel cell biosensor for in situ assessment of microbial activity, Biosens. Bioelectron. 24 (2008) 586–590.
[4] S.E. Oh, B.E. Logan, Proton exchange membrane and electrode surface areas as a factor that affect power generation in microbial fuel cells, Appl. Microbiol. Biotechnol. 70 (2006) 162–169.
[5] S.E. Oh, B. Min, B.E. Logan, Cathode performance as a factor in electricity generation in microbial fuel cells, Environ. Sci. Technol. 38 (2004) 4900–4904.
[6] B.E. Logan, B. Hamelers, R. Rozendal, U. Schröder, J. Keller, S. Freguia, P. Aelterman, W. Verstraete, K. Rabaey, Microbial fuel cell: methodology and technology, Environ. Sci. Technol. 40 (2006) 5181–5192.
[7] F. Zhao, F. Harnisch, U. Schröder, F. Scholz, P. Bogdanoff, I. Herrmann, Challenges and constraints of using oxygen cathodes in microbial fuel cells, Environ. Sci. Technol. 40 (2006) 5193–5199.
[8] E.H. Yu, S. Cheng, K. Scott, B.E. Logan, Microbial fuel cell performance with non-Pt cathode catalysts, J. Power Sources 171 (2007) 275–281.
[9] P. Aelterman, M. Versichele, E. Genettello, K. Verbeken, W. Verstraete, Microbial fuel cells operated with iron-chelated air cathodes, Electrochim. Acta 54 (2009) 5754–5760.
[10] D. Zhuwei, H. Li, T. Gu, A state of the art review on microbial fuel cells: a promising technology for wastewater treatment and bioenergy, Biotechnol. Adv. (2007) 464–482.
[11] H. Rismani-Yazdi, S.M. Carver, A.D. Christy, O.H. Tuovinen, Cathodic limitations in microbial fuel cells: an overview, J. Power Sources 180 (2008) 683–694.
[12] B. Erable, L. Etcheverry, A. Bergel, Increased power from a two-chamber microbial fuel cell with a low-pH air-cathode compartment, Electrochem. Commun. 11 (2009) 619–622.
[13] F. Zhao, F. Harnisch, U. Schroder, F. Scholz, P. Bogdanoff, I. Herrmann, Application of pyrolysed iron (II) phthalocyanine and CoTMPP based oxygen reduction catalysts as cathode materials in microbial fuel cells, Electrochem. Commun. 7 (2005) 1405–1410.
[14] R.J. Taylor, A.A. Humffray, Electrochemical studies on glassy carbon electrodes. I. Electron transfer kinetics, J. Electroanal. Chem. 42 (1973) 347–354.
[15] A. ter Heijne, H.V.M. Hamelers, V. de Wilde, R.R. Rozendal, C.J.N. Buisman, A bipolar membrane combined with ferric iron reduction as an efficient cathode system in microbial fuel cells, Environ. Sci. Technol. 40 (2006) 5200–5205.
[16] T. Rohwerder, T. Gehrke, K. Kinzler, W. Sand, Bioleaching review part A: progress in bioleaching: fundamentals and mechanisms of bacterial metal sulfide oxidation, Appl. Microbiol. Biotechnol. 63 (2003) 239–248.
[17] S. You, Q. Zhao, J. Zhang, J. Jiang, S. Zhao, A microbial fuel cell using permanganate as the cathodic electron acceptor, J. Power Sources 162 (2007) 1409–1415.
[18] B.E. Logan, Microbial Fuel Cells, John Wiley & Sons, New York, 2008.
[19] S.S. Zumdahl, Chemical Principles, Houghton Mifflin Company, Boston, 1998.
[20] M. Santana-Casiano, M. González-Dávila, M.J. Rodríguez, F.J. Millero, The effect of organic compounds in the oxidation kinetics of Fe(II), Mar. Chem. 70 (2000) 211–222.
[21] D. Dávila, J.P. Esquivel, N. Vigués, O. Sánchez, L. Garrido, N. Tomás, N. Sabaté, F.J. del Campo, F.J. Muñoz, J. Mas, Development and optimization of microbial fuel cells, J. Mater. Electrochem. Syst. 11 (2008) 99–103.
[22] D. Andrienko, Cyclic Voltammetry, 2008.
[23] F. Zhao, R.C.T. Slade, J.R. Varcoe, Techniques for the study and development of microbial fuel cells: and electrochemical perspective, Chem. Soc. Rev. 38 (2009) 1926–1939.
[24] M. Lanthier, K.B. Gregory, D.R. Lovley, Growth with high planktonic biomass in *Shewanella oneidensis* fuel cell, FEMS Microbiol. Lett. 278 (2008) 29–35.
[25] R.A. Rozendal, H.V.M. Hamelers, C.J.M. Buisman, Effects of membrane cation transport on pH and microbial fuel cell performance, Environ. Sci. Technol. 40 (2006) 5206–5211.
[26] P. Clauwaert, P. Aelterman, T.H. Pham, L. de Schamphelaire, M. Carballa, K. Rabaey, W. Verstraete, Minimizing losses in bio-electrochemical systems: the road to applications, Appl. Microbiol. Biotechnol. 79 (2008) 901–913.
[27] J.O.M. Bockris, U.M. Khan, Surface Electrochemistry, A Molecular Level Approach, Plenum Press, New York, London, 1993.
[28] F. Harnisch, S. Wirth, U. Schröder, Effects of substrate and metabolite crossover on the cathodic oxygen reduction reaction in microbial fuel cells: platinum vs. iron (II) phthalocyanine based electrodes, Electrochem. Commun. 11 (2009) 2253–2256.

Biographies

Naroa Uría has a degree in Biology by the Basque Country University. In 2009 she obtained her M.S. degree in Microbiology at the Universitat Autònoma de Barcelona. She is currently engaged in her Ph.D. project at the Department of Genetics and Microbiology of the Autonomous University of Barcelona, Spain. Her research includes the development of sensors for the detection of microbial activity, based on biological fuel cells.

David Sánchez received his B.S. in electronic engineering and a M.S. degree in micro and nano electronic engineering from Autonomous University of Barcelona, in 2008 and 2009 respectively. He is currently working toward the Ph.D. degree in the department of BioMEMS at the National Centre for Microelectronics (CNM-CSIC) in Barcelona, Spain. His current research includes design and fabrication of microbial fuel cell transducers for the determination of microbial activity.

Roser Mas, MSc in Chemistry Sciences in the Autonomous University of Barcelona, 1998. She is currently working in the Micro- and Nanosystems Department at the National Centre for Microelectronics (CNM-CSIC). Her main area of activity is focused on dry etch and new materials.

Olga Sánchez is an aggregate teacher at the Autonomous University of Barcelona (Spain). Her research began with the study of photosynthetic bacteria and derived to the utilization of complex microbial biofilms in packed reactors for the treatment of contaminated effluents. Presently, her investigation focuses on the development of molecular techniques for the characterization of the diversity of natural microbial communities. These methodologies include clone libraries, FISH (Fluorescence in situ hybridization), and fingerprinting techniques such as DGGE (Denaturing Gradient Gel Electrophoresis), which allow the identification of microorganisms in a culture-independent way.

Xavier Muñoz received his Ph.D. degree in physical chemistry from the National Centre for Microelectronics in 1990. During 1990–1992 he performed postdoctoral research work in the Biosensors Group of the MESA Institute at the University of Twente. In 1992 he joined the National Centre for Microelectronics of Barcelona (CNM-CSIC), where he has been working in the development of new chemical and biochemical microsensors for industrial applications. In 1997 he joined the CNM's Department of Microsystems as an associated researcher scientist. His areas of interest are silicon micromachining technologies, polymer micro-fabrication and their application to integrated chemical microsensors and biosensors.

Jordi Mas received his Ph.D. in biology in 1985 from the Autonomous University of Barcelona. During 1988 and 1989 he was a postdoctoral fellow in the Microbial Ecology group at the Biology Centre of the University of Groningen in the Netherlands. In 1989 he got a professorship at the Department of Genetics and Microbiology of the Autonomous University of Barcelona where he currently holds a Chair in Microbiology. His group carries out research in Environmental Microbiology on the role of microbial biofilms in water treatment and distribution systems. His research focuses in the development of advanced sensors for the monitorization of microbial biomass and activity in aquatic environments.

Please cite this article in press as: N. Uría, et al., Effect of the cathode/anode ratio and the choice of cathode catalyst on the performance of microbial fuel cell transducers for the determination of microbial activity, Sens. Actuators B: Chem. (2011), doi:10.1016/j.snb.2011.02.030

ENVIRONMENTAL Science & Technology

ARTICLE

pubs.acs.org/est

Transient Storage of Electrical Charge in Biofilms of *Shewanella oneidensis* MR-1 Growing in a Microbial Fuel Cell

Naroa Uría,[†,*] Xavier Muñoz Berbel,[‡] Olga Sánchez,[†] Francesc Xavier Muñoz,[‡] and Jordi Mas[†]

[†]Group of Environmental Microbiology, Universitat Autònoma de Barcelona, Bellaterra, Spain

[‡]Centro Nacional de Microelectrónica (CNM-IMB) CSIC, Spain

ABSTRACT: Current output of microbial fuel cells (MFCs) depends on a number of engineering variables mainly related to the design of the fuel cell reactor and the materials used. In most cases the engineering of MFCs relies on the premise that for a constant biomass, current output correlates well with the metabolic activity of the cells. In this study we analyze to what extent, MFC output is also affected by the mode of operation, emphasizing how discontinuous operation can affect temporal patterns of current output.

The experimental work has been carried out with *Shewanella oneidensis* MR-1, grown in conventional two-chamber MFCs subject to periodic interruptions of the external circuit. Our results indicate that after closure of the external circuit, current intensity shows a peak that decays back to basal values. The result suggests that the MFC has the ability to store charge during open circuit situations. Further studies using chronoamperometric analyses were carried out using isolated biofilms of *Shewanella oneidensis* MR-1 developed in a MFC and placed in an electrochemistry chamber in the presence of an electron donor. The results of these studies indicate that the amount of excess current over the basal level released by the biofilm after periods of circuit disconnection is proportional to the duration of the disconnection period up to a maximum of approximately 60 min. The results indicate that biofilms of *Shewanella oneidensis* MR-1 have the ability to store charge when oxidizing organic substrates in the absence of an external acceptor.

INTRODUCTION

Power output of microbial fuel cells (MFC) depends on a number of different factors, some of them related to the amount of microorganisms in the MFC and their level of activity, others related to the design and mode of operation of the fuel cell reactor. Design factors have been extensively studied. The area of the electrodes as well as the cathode/anode relative sizes should be properly dimensioned to avoid limitation in the current produced by the microorganisms.[1−3] The presence of a proton exchange membrane, the type of material used in the membrane, the concentration of substrate, internal resistance, type of cathode catalysts and others, have also been explored in an attempt to improve the performance of these devices. Bruce Logan in his excellent review published in 2008[4] provides an in depth detailed description of the many contributions to this specific area.

However, other parameters related to MFC operation have been less studied despite their importance in current production. The potential of the anode can influence the capacity of the biocatalyst to transfer electrons to the electrode as well as the amount of metabolically useful energy that can be obtained in the process. This is due to the fact that extracellular electron transfer is influenced by the electric potential between the final electron carrier and the anode.[5,6] External resistance has been also reported to exert an effect. Higher resistances produce smaller current densities due to a limitation in the flow of electrons through the circuit. So, the transference of charge from bacteria to the electrode is reduced resulting in a decrease of bacterial growth and the performance of the system.[7,8]

In all cases, MFCs are assumed to operate continuously, that is, without interruptions in the current flow. Some cases of MFCs operating discontinuously have been described in which a capacitor is included in the external circuit. In these cases the capacitors accumulate charge at low currents and high potentials, and release high intensity bursts during discharge. The discharge of the capacitor can be sent to the external circuit and to the cathode[9] or channeled back to the anode in such a way that the reactor acts as a MEC.[10] In both cases, during the time the capacitor takes to charge, there is no output from the MFC, but the organisms at the anode continuously produce charge which is stored in the capacitor. Changes at the anode potential during capacitor charge transiently improve electron transfer between bacteria and the anode. However, the organisms are never exposed to open circuit conditions.

Discontinuous operation seldom raises issues when chemical fuel cells (hydrogen or methanol) are involved. This is probably a consequence of the fact that these devices use simple inorganic catalysts for the oxidation reactions of the anode. In this type of system it is safely assumed that the fuel cell can be switched on or off at will without a penalty in performance. However, it is by no means clear how microorganisms in a MFC would behave under truly discontinuous operation (periodic exposure to open circuit

Received: July 26, 2011
Accepted: October 7, 2011
Revised: September 30, 2011
Published: October 07, 2011

conditions). Does electrogenesis stop when the anode is unable to accept the electrons? At least in the case of *Geobacter sulfurreducens* it has been shown that the organism can go on with its oxidative metabolism in the absence of external electron acceptors by using its extremely high amount of extracytoplasmic cytochromes as an electron sink. This ability was elegantly proved by Esteve-Núñez et al.[11] for cells in suspension using fluorescence to monitor the redox state of the cytochromes, and has been recently proved in biofilms of the same organisms by Schrott et al.[12] using electrochemical methods. Thus, while it is quite clear that *Geobacter sulfurreducens* can respond to periods of unavailability of external electron acceptor by storing charge, it is not clear whether this is also possible in other electrogenic microorganisms such as *Shewanella*. The existence of a capacity in cells of *Shewanella oneidensis* MR-1 has been recently suggested by Harris et al.[13] after observing a fast motility response to metal oxide particles that they call "electrokinesis". After contacting the particle, the cells swim away and the authors relate this behavior to the instantaneous transfer of electrons from bacteria to the metal oxide. Besides this indirect evidence, there is no actual study on how *Shewanella* responds when subject to periodic open circuit conditions in a MFC.

In this work we explore the behavior of a MFC of *Shewanella oneidensis* MR-1 when subject to discontinuous operation. We first describe how discontinuous operation affects the behavior of a MFC of this organism, and later on, we analyze whether and to what extent isolated biofilms of *Shewanella oneidensis* MR-1 developed on an electrode have the ability to store charge during periods of open circuit conditions.

EXPERIMENTAL PROCEDURE

1. Bacterial Strains and Growth Conditions. *Shewanella oneidensis* strain MR-1 (ATCC 70050) was grown aerobically in 100 mL of Tripticase Soy Broth (TSB) during 36 h. After this, the culture was centrifuged (10 100*g* × 15 min, 4 °C) using a 5804R Eppendorf centrifuge. The resulting pellet was resuspended in 1 L of AB minimal medium ($[NH_4]SO_4$ 2 g, Na_2HPO_4 7.31 g, KH_2PO_4 7.85 g, NaCl 3 g, Na_2SO_4 0.011 g, $MgCl_2 \cdot 6H_2O$ 0.2 g, CaCl 3.625 mg, $FeCl_3 \cdot 6H_2O$ 0.2 mg)[14] previously sparged with nitrogen gas to eliminate oxygen. Lactate (0.02 M) and fumarate (0.1 M) were added to the medium as electron donor and acceptor respectively. After 48 h of incubation with agitation at room temperature, the cells were harvested again by centrifugation, resuspended in 100 mL of anolyte medium and transferred to the anode chamber under anoxic conditions. The composition of the anolyte medium depended on the experiment. Thus, for the experiments of circuit interruption in MFCs we used AB minimal medium. For the development of biofilms at the surface of the anode for later use in electrochemical analysis KNO_3 0.5 M was employed.

2. Microbial Fuel Cell Set Up and Characterization. The type of MFC reactor used in this work has already been described in a previous paper.[3] Basically, two identical MFCs were constructed by joining two methacrylate blocks with a volume of 130 mL. The proton exchange membrane selected in this study was Nafion117 (Ion power, Inc.) with a thickness of 183 μm and effective area of 38.46 cm^2.

Anode and cathode electrodes were connected to a source meter (Keithley2612) controlled by a personal computer running a custom-made program developed with LabView 8.5 to automate data collection.

3. Experimental Measurements in Microbial Fuel Cell Reactors. To study the effect of discontinuous operation in MFCs of *Shewanella oneidensis*, two identical reactors were used. The anode chambers were filled with AB minimal medium containing lactate (0.02 M) as the only electron donor and inoculated with *Shewanella oneidensis* MR-1 at a final concentration of 4.8×10^9 cells mL^{-1}. The anodes consisted of carbon paper electrodes (B2120 Toray Carbon Paper Designation TGPH-120, plain, no wet proofing; E-Tek, Inc.) with a thickness of 0.35 mm and an area of 3 cm^2.

The cathode chambers contained ferricyanide (0.05 M $K^3[Fe(CN)_6]$) in 0.1 M phosphate buffer. For the cathodes we used the same material used in the anodes but with a larger area (15 cm^2) to avoid cathodic limitations.[3]

Both, anode and cathode chambers were continuously sparged with nitrogen and air respectively and stirred at 250 rpm using a magnetic stirrer.

After inoculation both reactors were connected to a Keithley source meter programmed as to measure maximum current output by setting the internal resistance of the meter to its minimal value (about 65−70 Ω).

When the fuel cells reached stable values of current output, the external circuit of the MFCs was periodically interrupted (open circuit) for different time periods, 10 min for the first MFC and 30 min for the second one. After each external circuit interruption, the circuit was closed again for a period of 1 h and values of current output were recorded.

The electric charge (Coulombs) stored during the 30 min of open circuit was calculated as the excess current produced after the interruption by integrating the area of the peak of current above the stable baseline.

4. Electrochemical Analysis of Isolated Biofilm-Covered Anodes. In this part of the work, biofilms were allowed to develop at the surface of the anode using the MFC reactor described above. The biofilm-covered anode was then removed from the MFC and subject to electrochemical analyses.

Biofilm Development. The anode compartment was filled with potassium nitrate (KNO_3) at a concentration of 0.5 M as anolyte and lactate (20 mM) as carbon source, and inoculated with *Shewanella oneidensis* MR-1 at a final concentration of approximately 10^8 cfu mL^{-1}. KNO_3 was used in the anode instead of AB minimal medium to avoid the interference of iron from the medium during the electrochemical characterization of the anolyte. KNO_3 (0.5 M) was also used at the cathode compartment. Both, anode and cathode chambers were continuously sparged with nitrogen and air, respectively, and stirred at 250 rpm using a magnetic stirrer.

In this case, anode and cathode materials were not the same. Carbon paper with an area of 0.5 cm^2 was used as the anode. The cathode was a silicon wafer coated with platinum (13.55 cm^2), the same size and material that was later on used as auxiliary electrode in the electrochemical analysis.

The biofilm was allowed to develop under conditions of low current output (1 nA) for a period of several days until a stable voltage of 0.150 V was reached. After that, both the anolyte and the biofilm-covered anode were removed and subject to electrochemical studies.

Electrochemical Measurements. Cyclic voltammetric and chronoamperometric analyses were performed using a potentiostat/galvanostat model FRA2Micro-Autolab Type II. An Ag/AgCl electrode (Methrom, Switzerland) and a platinized silicon wafer electrode were used as reference and auxiliary electrode

respectively. In the Results section, all potentials have been adjusted to E vs SHE (standard hydrogen electrode). Before the measurements, the solution was flushed with nitrogen to remove oxygen traces. The electrochemical cell was kept in a Faraday cage to minimize external interferences.

Cyclic Voltammetric Analysis. Cyclic voltammetric analyses were run between −0.6 and 0.4 V vs Ag/AgCl (−0.8 to 0.2 vs SHE) at a scan rate of 1 mV s^{-1}. The scan rate was chosen after performing a very large number of CV with both cell suspensions and biofilms of *Shewanella*. One mV s^{-1} provided by far the best resolution.

In order to analyze the possible presence of redox shuttles in the anolyte, the anode solution (100 mL) was filtered using a sterile filter with a pore size of 0.22 μm (MillexGP, Millipore) to remove bacteria, and introduced in an electrochemical cell. A carbon paper electrode with an area of 0.5 cm^2 was used as the working electrode.

For the cyclic voltammetric analysis of the biofilm, the anode of the MFC was removed from the reactor and washed several times in KNO_3 to remove the mediators from the biofilm. This electrode was then used as the working electrode in an electrochemical cell containing 100 mL of oxygen-free KNO_3.

Chronoamperometric Analysis. A biofilm-covered anode developed in a separate MFC reactor was rinsed and placed as the working electrode in an electrochemical cell containing oxygen-free phosphate buffer (0.1 M) supplemented with lactate (0.02 M). During the oxidation of lactate, protons could accumulate producing changes in pH and affecting bacterial activity. Phosphate buffer was used to avoid these changes.

Several chronoamperometric analyses of the electrode biofilm were run at a potential of 0.3 V vs Ag/AgCl (0.1 V vs SHE) during a time of 30 s, sufficient to reach a stationary current. Before each chronoamperometry, the electrochemical cell was switched off for different periods: 0, 2, 4, 8, 16, 32, 64, 90, 120, and 180 min. Five replicates of each time were made.

As a control, the same set of measurements was repeated using a carbon paper electrode without bacteria. This allowed us to observe and remove from our results the effect of overpotentials strictly related to interface phenomena at the surface of the electrode material and not due to the presence of the biofilm.

The amount of charge stored during switch off was calculated as previously described in the Section 3 of the Experimental Procedure section.

■ RESULTS AND DISCUSSION

1. Experimental Observations with MFC Reactors. Two MFC were used to analyze the effect of intermittent operation on current output. After two days of close circuit operation, a stable current was reached. After this, the external circuit was periodically interrupted in both reactors. In one of the reactors, the open circuit intervals were 10 min followed by 60 min of closed circuit operation. In the second reactor, external circuit interruptions were 30 min followed also by 60 min of closed circuit operation.

Figure 1 shows the registered values of current output during the experiment. In the first reactor, which was subject to 10 min interruptions, a stable current of 0.1 mA cm^{-2} was observed corresponding to the current that the device was able to supply continuously (Figure 1a). However, when the external circuit was interrupted for longer periods (30 min) (Figure 1b) a current peak was observed immediately after circuit closure that decayed slowly until reaching normal current output of 0.08 mA cm^{-2}.

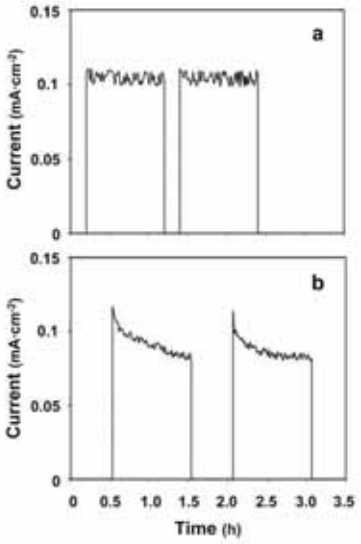

Figure 1. Current output of two independent MFCs of *Shewanella oneidensis* MR-1 during intermittent operation with different periods of circuit interruption (a) Periods of 10 min of circuit interruption are followed by 60 min of closed circuit operation. (b) Periods of 30 min of circuit interruption are followed by 60 min of closed circuit operation.

Table 1. Amount of Charge Expressed Both As Coulombs and Electron Mols Stored after Different times of Open Circuit (OCT)

OCT (min)	stored charge	
	coulombs	electron mols
10	0	0
	0	0
30	0.126	$1.3\,e^{-6}$
	0.072	$7.47\,e^{-7}$

Current levels after stabilization were different in both cases. We attribute this difference to the fact that data from Figure 1 come from two separate completely independent MFCs. The differences observed can be the consequence of slight differences in the degree of development of the biofilms in the anodes. This differences might affect the stable current levels but no the existence of the peaks.

Recorded values of voltage during circuit interruption showed a voltage increase of about 45 mV (from an average of 273.2−318.7 mV) during 10 min of current interruption in contrast to the 200 mV (from an average of 294.45−504 mV) of increase observed in the second MFC in which interruption length was 30 min

During circuit interruption, the increase in open circuit potential is due to the reduction of energy losses caused by the overpotentials of the anode and cathode that produced an increase in the cathode potential and a decrease in the anode potential.[15,16] The reasons behind these gradual changes are in fact quite diverse and include among others, factors such as an increase in the amount of reduced species in the anode chamber, both free (soluble redox mediators or fermentation products)

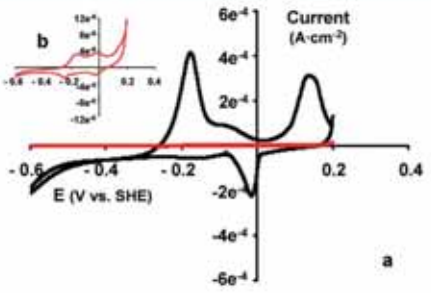

Figure 2. (a) Cyclic voltammetry at a scan rate of 1 mV sec^{-1} of *Shewanella oneidensis* MR-1 biofilm covered electrode (black line) and filtered MFC anolyte (red line). (b). Scaled up cyclic voltammogram of the anolyte from Figure 2a.

and cell/biofilm bound (cytochromes and other redox proteins), changes in the proton gradient across the exchange membrane, or changes in the concentration of oxidized iron in the cathode chamber.

Calculations of the amount of charge stored during open circuit periods are summarized in Table 1. Approximately 0.1 C were accumulated during 30 min interruption.

How the charge is stored in the anode of the MFC during periods of interruption is by no means straightforward. Since we used a defined minimal medium in the anode reactor, we have a precise idea of the chemical composition in the anode chamber. Iron, which is the only redox species that might act as a shuttle and temporarily store charge, was present at a concentration of 2.96 μM. In the unlikely event that all of the iron present in the 100 mL of medium was reduced during the 30 min interrupt and reoxidized at the anode during the next 60 min close circuit period, this would only amount to 0.029 C, less than one-third of the total charge stored. It is quite clear that although some charge could be stored as reduced iron, the bulk of the storage must occur either in *Shewanella* cells both, in suspension or forming the biofilm, or in soluble redox mediators secreted by the cells.

Therefore, the existence of a current peak when the circuit is interrupted suggests that the MFC was able to store charge and burst-release it as soon as the circuit was restored. This demonstrates that discontinuous operation of a MFC can affect temporal patterns of current output influencing the performance of these devices. In order to find out whether biofilms of *Shewanella oneidensis* MR-1 could contribute to charge storage in the MFC we ran some electrochemical analysis.

2. Electrochemical Analysis of Isolated Biofilm-Covered Anodes. In order to ascertain whether biofilms of *Shewanella oneidensis* MR-1 were able to store charge, we decided to run a set of chronoamperometric analyses after different time of exposure of the isolated biofilm to lactate in the absence of either soluble electron acceptors or an active electrode. At the end of each incubation period the biofilm-covered electrode was polarized and the current produced was followed for a period of 30 s. To confirm that the biofilm contained active redox compounds, and to determine the optimum polarization potential to be used in the chronoamperometric analyses, a cyclic voltammetric analysis of the biofilms was performed.

A cyclic voltammogram of the biofilm formed at the anode surface is showed in Figure 2a. The voltammogram indicates the existence of two reversible oxidation−reduction peaks. These peaks, with potential values of −0.16 and −0.10 V (vs SHE), match closely with the values reported in the literature for OmcA[17] and MtrC[18], respectively. The *c*-type cytochromes MtrC and OmcA mediate the extracellular reduction of Fe(III) oxides in *Shewanella oneidensis* MR-1.[19,20] Moreover, these cytochromes are capable of reducing Fe(III) oxides by indirectly transferring electrons to either flavin-chelated Fe(III) or oxidized flavins[21] that act as shuttles during electron transfer to external acceptors.[22,23] Another peak corresponding to a potential of 0.14 V (vs SHE) also appeared in the biofilm voltammogram, however the potential of this peak is too high to be involved in the primary electron transfer process which usually occurs in the range of −0.25 to 0 V (vs SHE).[23]

Additionally, cyclic voltammetry was also performed to analyze the anolyte of the MFC (Figure 2a and b). The results indicate the presence of some redox species but the currents involved in this case were 2 orders of magnitude lower suggesting that these compounds were present at a very low concentration. The reversible peaks were detected at potentials of −0.18 and −0.02 V (vs SHE). The presence of a peak at −0.18 V (vs SHE) agrees with the presence of extracellular flavins. It has been shown in some studies that the primary mediators excreted by *Shewanella oneidensis* MR-1 are riboflavin and flavin mononucleotide (FMN).[22,23] Our cyclic voltammogram also shows a higher potential peak, between −0.1 and −0.01 V (vs SHE), that suggests the presence of a second redox species not yet characterized.

In general, flavins have been reported to be present at very low concentrations, between 0.3 and 2 μM.[24,25] The results obtained by cyclic voltammetry in our MFC system suggest the same and indicate a much higher capacity for electron storage of the bacteria forming the biofilm than the mediators present in the anolyte.

Once the existence of oxidation/reduction peaks in the biofilm was confirmed and their potentials determined, we ran chronoamperometric analyses in an attempt to analyze the capacity of the biofilm to store charge. Chronoamperometric analyses of the biofilm-covered electrode were run in the presence of lactate as the carbon source. Prior to the beginning of the chronoamperometry, the biofilm was allowed to metabolize lactate for variable periods of time (0, 2, 4, 8, 16, 32, 64, 90, 120, and 180 min) with the circuit interrupted in such a way that electron transfer to the anode was not possible. During these periods, bacteria oxidized lactate potentially storing electrons intracellularly since no external acceptors were available and electron transfer to the anode was disabled. After these periods, a positive potential was applied and the kinetics of current production were recorded during a period of 30 s.

The choice of an adequate oxidation potential is critical. The percentage of the stored charge recovered during the chronoamperometric analysis depends to a large extent on whether the potential used is high enough to oxidize all the relevant redox compounds present in the system. In a recent publication by Schrott et al,[12] the percentage of charge recovered from biofilms of *Geobacter sulfurreducens* increases with the potential used in up to a value of 0 V (vs SHE).

In our case, the oxidation potential of 0.1 V (vs SHE) was selected taking into account the cyclic voltammetry data of our biofilms and selecting a potential high enough to oxidize all of the redox species present in the biofilm. In the study carried out by Carmona-Martinez et al.[26] using biofilms plus unattached cells of *Shewanella oneidensis* MR-1 et al. two redox systems are identified, one of them attributed to mediated electron transfer (−0.2 V vs Ag/AgCl/-0.4 V vs SHE) and the other to direct electron transfer

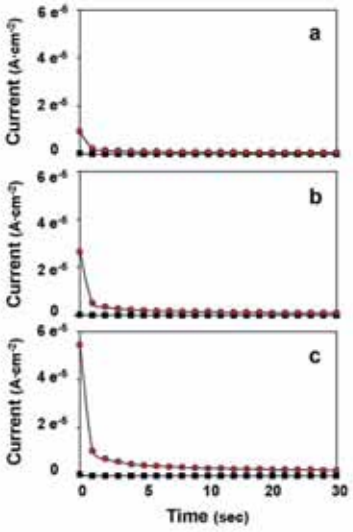

Figure 3. Current production of a biofilm-covered anode during polarization at 0.1 V (vs SHE) after 4 (A), 32 (B), and 90 (C) minutes of exposure of the isolated biofilm to lactate in the absence of either soluble electron acceptors or an active electrode (red circle). An electrode without biofilm was used as control in all cases (black square). Error bars ($n = 5$) are smaller than the symbol size.

with a maximum catalytic activity at a potential of 0.1 V vs Ag/AgCl (−0.1 V vs SHE). The potential of these systems falls well below the 0.1 V (vs SHE) used in our chronoamperometric analyses and confirms that the potential we used is high enough to oxidize all the redox systems present in *Shewanella*.

The results of the chronoamperometric analyses corresponding to the 4, 32, and 90 min disconnection periods have been plotted in Figure 3.

In all three cases the current peaked at the beginning of the measurements right after the electrode was polarized. The current peaks observed can be related to a lower electrode potential produced during disconnection. After the initial peak, current decayed quickly suggesting that the charge stored in the biofilm during the interruption period was transferred to the electrode. After approximately 30 s virtually all of the stored charge had been released although more than 90% of the release occurred during the first 2 s.

The study of isolated biofilms in an electrochemical cell has several advantages as it allows discarding several of the mechanisms susceptible to cause overpotentials in a MFC. First, by removing most of the chemistry associated to the cathode chamber we avoid possible changes in the proportion of oxidized/reduced species in this compartment during the disconnection period. Second, since there is no PEM, the possible consequences of relaxing the concentration gradient of protons across the membrane during the interruption period are also avoided. Third, all cells and redox shuttles not bound to the biofilm/anode structure are removed, thus simplifying the interpretation of the results and avoiding distortions in the kinetic behavior of the system derived from the existence of diffusion limitation in the biological/chemical redox species that might be present in the anode chamber of the MFC.

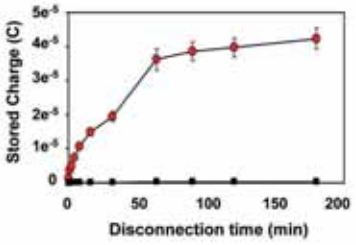

Figure 4. Magnitude of total charge released by the biofilm (red circle) during the chronoamperometry as a function of disconnection time. Control (black square). Error bars ($n = 5$).

Even after getting rid of all this factors, the potential of the anode is likely to decrease during disconnection of the external circuit, mainly as a result of two mechanisms: the effect of overpotentials related to interface phenomena at the surface of the electrode, and an increase in the amount of reduced cell/biofilm-bound redox species (cytochromes, other redox proteins, tethered electron shuttles...). To assess the magnitude of the effect of these overpotentials at the electrode surface, we ran controls using naked carbon electrodes without biofilm. The values of current obtained with the controls, also included in Figure 3 are much lower that those obtained with the biofilm-covered electrode.

The discharge times observed during the chronoamperometry are similar to those reported by Schrott et al.[12] in *Geobacter sulfurreducens* and suggest that although electron discharge is not instantaneous, the kinetics are fast enough as to indicate a rather conductive biofilm structure. Using the chronoamperometric data we calculated the magnitude of the stored charge as the area of the peak over the stable current at 30 s. When the stored charge was plotted against time of circuit interruption (Figure 4) a saturation relationship emerged with stored charge increasing as a function of disconnection time up to approximately 60 min. Beyond that point the biofilm was apparently saturated and unable to store further electrons. In *Geobacter sulfurreducens* the results are quite similar[12] although saturation seems to occur earlier, after approximately 30 min. In a previous study by Esteve-Núñez et al.,[11] also with *Geobacter*, charge storage stopped much earlier, after only 8 min but the difference might be related to the fact that work was not carried out with attached cells forming a biofilm, but with cells in suspension.

After normalizing the amount of stored charge to the surface area of the electrode, we obtain a maximum value of 8×10^{-10} moles of electrons per square cm, somewhat lower than the maximum of 1×10^{-9} obtained by Schrott et al. for *Geobacter sulfurreducens*. Attempts to further normalize stored charge per cell were not successful. In our experiment, due to the fact that the anode consists of carbon paper, which is a highly porous material, biomass determination was not straightforward. We attempted to assess biomass using epifluorescence microscopy of DAPI and Live Dead stained samples but only the cells at the surface of the carbon paper could be counted thus underestimating by an unknown factor the actual biomass present in the electrode. Confocal microscopy did not improve the results due to its inability to provide images within the graphite matrix of the carbon paper electrode. Given the impossibility to provide an accurate estimate of attached biomass we opted to include only the raw data as stored Coulombs, without normalizing to biomass.

We strongly advise that further experimental work with biofilms attached to electrode surfaces, be carried out using polished nonporous electrode materials (see ref 27 as an example) in order to make quantification of attached biomass possible.

Summarizing, our results report the ability of biofilms of *Shewanella oneidensis* MR-1 to store charge during periods in which an external acceptor is not available. The relevance of this storage capacity for future work with MFCs should be carefully assessed. Several papers dealing with the use of MFCs in activity and toxicity sensors[28−30] have been recently published. Use of MFCs for this type of application should take into account the fact that current production does not only depend on the amount of bacteria and their activity levels, but also on the recent history of the organisms. Also, evaluation of power output curves in microbial fuel cells should take into account that current after disconnection events can be considerably higher that current produced under steady state conditions.

AUTHOR INFORMATION

Corresponding Author

*Phone: (+34) 935 813 011; fax (+34) 935 812 387; e-mail: naroa.uria@uab.cat.

ACKNOWLEDGMENT

This work was supported by grants CSD2006-00044 TRAGUA (CONSOLIDER-INGENIO2010) and CTQ2009-14390-C02-02 from the Spanish Ministry of Education and Science to JM.

REFERENCES

(1) Oh, S.; Logan, B. E. Proton exchange membrane and electrode surface areas as factors that affect power generation in microbial fuel cells. *Appl. Microbiol. Biotechnol.* **2006**, *70*, 162−169; DOI: 10.1007/s00253-005-0066-y.

(2) Oh, S.; Min, B.; Logan, B. E. Cathode performance as a factor in electricity generation in microbial fuel cells. *Environ. Sci. Technol.* **2004**, *38*, 4900–4904.

(3) Uría, N.; Sánchez, D.; Mas, R.; Sánchez, O.; Muñoz, F. X.; Mas, J. *Sens. Actuators, B* **2011**In Press.

(4) Logan, B. E. *Microbial Fuel Cells*; John Wiley & Sons: N.Y., 2008.

(5) Lee, H.; Torres, C. I.; Rittmann, B. E. Effects of substrate diffusion and anode potential on kinetic parameters for anode-respiring bacteria. *Environ. Sci. Technol.* **2009**, *43*, 7571–7577.

(6) Aelterman, P.; Freguia, S.; Keller, J.; Verstraete, W.; Rabaey, K. The anode potencial regulates bacterial activity in microbiol fuel cells. *Appl. Microbiol. Biotechnol.* **2008**, *78*, 409-418; DOI: 10.1007/s00253-007-1327-8.

(7) Picioreanu, C.; Katuri, K. P.; Head, I. M.; van Loosdrecht, M. C. M.; Scott, K. Mathematical model for microbial fuel cells with anodic biofilms and anaerobic digestión. *Water Sci. Technol.* **2008**, *57*, 965–971.

(8) Katuri, K. P.; Scott, K.; Head, I. M.; Picioreanu, C.; Curtis, T. P. Microbial fuel cells meet with external resistance. *Bioresour. Technol.* **2011**, *102*, 2758–2766.

(9) Dewan, A.; Beyenal, H.; Lewandowski, Z. Intermittent energy harvesting improves the performance of microbial fuel cells. *Environ. Sci. Technol.* **2009**, *43*, 4600–4605.

(10) Liang, P.; Wu, W.; Wei, J.; Yuan, L.; Xia, X.; Huang, X. Alternate charging and discharging of capacitor to enhance the electron production of bioelectrochemical systems. *Environ. Sci. Technol.* **2011**, *45*, 6647–6653.

(11) Esteve-Nuñez, A.; Sosnik, J.; Visconti, P.; Lovley, D. R. Fluorescent properties of c-type cytochromes reveal their potencial role as an extracytoplasmatic electron sink in *Geobacter sulfurreducens*. *Environ. Microbiol.* **2008**, *10* (2), 497–505.

(12) Schrott, G. D.; Bonanni, P. S.; Robuschi, L.; Esteve-Nuñez, A.; Busalmen, J. P. Electrochemical insight into the mechanism of electron transport in biofilms of *Geobacter sulfurreducens*. *Electrochim. Acta* **2011**(In Press).

(13) Harris, H. W.; El-Naggar, M. Y.; Bretschger, O.; Ward, M. J.; Romine, M. F.; Obraztsova, A. Y.; Nealson, K. H. Electrokinesis is a microbial behavior that requires extracellular electron transport. *Proc. Natl. Acad. Sci. U. S. A.* **2010**, *107* (1), 326–331.

(14) Clarck, D. J.; Maaøle, O. DNA replication and the division cycle in *Escherichia coli*. *J. Mol. Biol.* **1967**, *23*, 99–112.

(15) Zhao, F.; Slade, R. C. T.; Varcoe, J. R. Techniques for the study and development of microbial fuel cells: an electrochemical perspective. *Chem. Soc. Rev.* **2009**, *38*, 1926–1939.

(16) Logan, B. E.; Hamelers, B.; Rozendal, R.; Schröder, U.; Keller, J.; Freguia, S.; Aelterman, P.; Verstraete, W.; Rabaey, K. Microbial fuel cell: Methodology and technology. *Environ. Sci. Technol.* **2006**, *40* (17), 5181–5192.

(17) Firer-Sherwood, M.; Pulcu, G. S.; Elliot, S. J. Electrochemical interrogation of the Mtr cytochromes from *Shewanella*: Opening a potential window. *J. Biol. Chem.* **2008**, *13*, 849-854; DOI: 10.1007-s00775-008-0398-z.

(18) Hartshore, R. S.; Jepson, B. N.; Clarke, T. A.; Field, S. J.; Fredrickson, J.; Zachara, J.; Shi, L.; Butt, J. N.; Richardson, D. J. Characterization of *Shewanella oneidensis* MtrC: a cell-surface decaheme cytochrome involved in respiratory electron transport to extracellular electron acceptors. *J. Biol. Inorg. Chem.* **2007**, *12*, 1083-1094; DOI: 10.1007-s00775-007-0278-y.

(19) Baron, D.; LaBelle, E.; Coursolle, D.; Gralnick, J. A.; Bond, D. R. Electrochemical measurement of electron transfer kinetics by *Shewanella oneidensis* MR-1. *J. Biol. Chem.* **2009**, *284* (42), 28865–28873.

(20) Meitl, L. A.; Eggleston, C. M.; Colberg, P. J. S.; Khare, N.; Reardon, C. L.; Shi, L. Electrochemical interaction of *Shewanella oneidensis* MR-1 and its outer membrane cytochromes OmcA and MtrC with hematite electrodes. *Geochim. Cosmochim. Acta* **2009**, *73*, 5292–5307.

(21) Shi, L.; Richardson, D. J.; Wang, Z.; Kerisit, S. N.; Rosso, K. M.; Zachara, J. M.; Fredrickson, J. K. The roles of outer membrane cytochromes of *Shewanella* and *Geobacter* in extracellular electron transfer. *Environ. Microbiol. Reports.* **2009**, *1* (4), 220–227.

(22) von Canstein, H.; Ogawa, J.; Shimizu, S.; Lloyd, J. R. Secretion of flavins by *Shewanella* species and their role in extracellular electron transfer. *Appl. Environ. Microbiol.* **2008**, *74* (3), 615–623.

(23) Marsili, E.; Baron, D. B.; Shikhare, I. D.; Coursolle, D.; Gralnick, J. A.; Bond, D. R. *Shewanella* secretes flavins that mediate extracellular electron transfer. *PNAS.* **2008**, *105* (10), 3968–3973.

(24) Covington, E. D.; Gelbmann, C. B.; Kotloski, N. J.; Gralnick, J. A. An essential role for UshA in processing of extracellular flavin electron shuttles by *Shewanella oneidensis*. *Mol. Microbiol.* **2010**, DOI: 10.1111/j.1365-2958.2010.07353.

(25) Gil, G.; Chang, I.; Kim, B. H.; Kim, M.; Jang, J.; Park, H. S.; Kim, H. J. Operational parameters affecting the performance of a mediator-less microbial fuel cell. *Biosens. Bioelectron.* **2003**, *18*, 327–334.

(26) Carmona-Martinez, A. A.; Harnisch, F.; Fitzgerald, L. A.; Biffinger, J. C.; Ringeisen, B. R.; Schröder, U. Cyclic voltammetric analysis of the electron transfer of *Shewanella oneidensis* MR-1 and nanofilament and cytochrome knock-out mutants. *Bioelectrochemistry.* **2011**, *81*, 74–80.

(27) McLean, J. S.; Wanger, G.; Gorby, Y. A.; Wainstein, M.; McQuaid, J.; Ishii, S.; Bretschger, O.; Beyenal, H.; Nealson, K. H. Quantification of electron transfer rates to a solid phase electron acceptor through the stages of biofilm formation from single cells to multicellular communities. *Environ. Sci. Technol.* **2010**, *44*, 2721–2727.

(28) Davila, D.; Esquivel, J. P.; Sabate, N.; Mas, J. Silicon-based microfabricated microbial fuel cell toxicity sensor. *Biosens. Bioelectron.* **2011**, *26*, 2426–2430.

(29) Kim, M.; Hyun, M. S.; Gadd, G. M.; Kim, H. J. A novel biomonitoring system using microbial fuel cells. *Environ. Monit.* **2007**, *9*, 1323–1328.

(30) Tront, J. M.; Fortner, J. D.; Plotze, M.; Hughes, J. B.; Puzrin, A. M. Microbial fuel cell biosensor for in situ assessment of microbial activity. *Biosens. Bioelectron.* **2008**, *24*, 586–590.